

INFORMATION TO USERS

This manuscript has been reproduced from the microfilm master. UMI films the text directly from the original or copy submitted. Thus, some thesis and dissertation copies are in typewriter face, while others may be from any type of computer printer.

The quality of this reproduction is dependent upon the quality of the copy submitted. Broken or indistinct print, colored or poor quality illustrations and photographs, print bleedthrough, substandard margins, and improper alignment can adversely affect reproduction.

In the unlikely event that the author did not send UMI a complete manuscript and there are missing pages, these will be noted. Also, if unauthorized copyright material had to be removed, a note will indicate the deletion.

Oversize materials (e.g., maps, drawings, charts) are reproduced by sectioning the original, beginning at the upper left-hand corner and continuing from left to right in equal sections with small overlaps.

ProQuest Information and Learning
300 North Zeeb Road, Ann Arbor, MI 48106-1346 USA
800-521-0600

UMI[®]

University of Alberta

HPLC Methodology Development and
De Novo Design of Antimicrobial Peptides

by

Yuxin Chen



A thesis submitted to the Faculty of Graduate Studies and Research in partial fulfillment
of the requirements for the degree of Doctor of Philosophy

Department of Biochemistry

Edmonton, Alberta

Spring 2005



Library and
Archives Canada

Bibliothèque et
Archives Canada

0-494-08215-1

Published Heritage
Branch

Direction du
Patrimoine de l'édition

395 Wellington Street
Ottawa ON K1A 0N4
Canada

395, rue Wellington
Ottawa ON K1A 0N4
Canada

Your file *Votre référence*

ISBN:

Our file *Notre référence*

ISBN:

NOTICE:

The author has granted a non-exclusive license allowing Library and Archives Canada to reproduce, publish, archive, preserve, conserve, communicate to the public by telecommunication or on the Internet, loan, distribute and sell theses worldwide, for commercial or non-commercial purposes, in microform, paper, electronic and/or any other formats.

The author retains copyright ownership and moral rights in this thesis. Neither the thesis nor substantial extracts from it may be printed or otherwise reproduced without the author's permission.

AVIS:

L'auteur a accordé une licence non exclusive permettant à la Bibliothèque et Archives Canada de reproduire, publier, archiver, sauvegarder, conserver, transmettre au public par télécommunication ou par l'Internet, prêter, distribuer et vendre des thèses partout dans le monde, à des fins commerciales ou autres, sur support microforme, papier, électronique et/ou autres formats.

L'auteur conserve la propriété du droit d'auteur et des droits moraux qui protègent cette thèse. Ni la thèse ni des extraits substantiels de celle-ci ne doivent être imprimés ou autrement reproduits sans son autorisation.

In compliance with the Canadian Privacy Act some supporting forms may have been removed from this thesis.

Conformément à la loi canadienne sur la protection de la vie privée, quelques formulaires secondaires ont été enlevés de cette thèse.

While these forms may be included in the document page count, their removal does not represent any loss of content from the thesis.

Bien que ces formulaires aient inclus dans la pagination, il n'y aura aucun contenu manquant.


Canada

Abstract

Our laboratory has made considerable efforts to develop new HPLC methods for peptide separation/optimization and subsequently applied them to study the structure and function of peptides. Using a series of 18-residue α -helical synthetic model peptides, we have been able to understand the dramatic effects of varying RP-HPLC parameters (mobile phase conditions, column packing and temperature) on the retention behavior of peptides. Temperature was shown to have a complex influence on peptide selectivity due to varying effects on peptide conformation. We developed a new method called "temperature profiling" in RP-HPLC to monitor the association of amphipathic molecules. We also demonstrated hydrophilic interaction/cation-exchange chromatography (HILIC/CEX) as an important complement of RP-HPLC to monitor the hydrophobicity/hydrophilicity variations on the polar and non-polar faces of amphipathic helices.

We revisited the optimum concentration of TFA for RP-HPLC of peptides. For efficient resolution of peptide mixtures, particularly those containing peptides with multiple positive charges, our results show that 0.2-0.25%TFA in the mobile phase will achieve optimum resolution, instead of the traditional concentration range of 0.05-0.1%TFA. In addition, the use of high temperature as a complement to such TFA concentration levels is also effective in maximizing peptide resolution.

To understand more clearly the effects of different amino acid substitutions, especially for D-amino acid substitutions, on α -helical structure and peptide stability, a systematic study was carried out on a series of amphipathic α -helical model peptides. L-

/D-amino acid substitutions showed a wide range of helix-destabilizing effects. A series of helix stability coefficients was subsequently determined.

Utilizing the peptide stability knowledge obtained from the model peptide study, we designed *de novo* a series of α -helical antimicrobial peptides, based on the framework of a potent biologically active α -helical antimicrobial peptide, V₆₈₁. By altering the peptide hydrophobicity/hydrophilicity, amphipathicity and stability via D- or L-amino acid substitutions, we obtained an analog (peptide NK_L) with a 3-fold increase in antimicrobial activity, a 32-fold decrease in hemolytic activity and thus a 100-fold improvement of therapeutic index against Gram-negative bacteria, and another peptide analog (NA_D) with broad spectrum activity including a 16-fold reduction in hemolytic activity coupled with a 45-fold and 16-fold increase in the therapeutic index against Gram-negative and Gram-positive bacteria, respectively, compared with the native peptide V₆₈₁.

Acknowledgements

First, I wish to thank my supervisor, Dr. Robert S. Hodges who gave me the opportunity to study in his laboratory. I thank him for his inspiration, advice, supervision and knowledge on sciences.

I would like to thank the members of the Hodges lab from both the University of Colorado Health Sciences Center, and the University of Alberta and its associated institutions, PENCE and the Alberta Peptide Institute. I thank Colin Mant for scientific suggestions and tremendous efforts on the preparation of my manuscripts. I thank Brian Tripet for so many invaluable suggestions on sciences and stimulating discussions, Kurt Wagschal for introducing me to peptide chemistry, Marc Genest and Jason Moses for peptide synthesis. Mike Carpenter for amino acid analysis and sequencing, Bob Luty for CD spectroscopy. Traian Popa for understanding capillary electrophoresis, and Paul Cachia, Darin Lee, Jennifer Litowski, Daniel Kao, James Kovacs, Stanley Kwok, Janine Mills, Mitsukuni Shibue, Zhe Yan, Eunice York, Bruce Yu and David Zoetewey for their expertise and technical supports.

I also would like to acknowledge our collaborators in the Bob Hancock laboratory (University of British Columbia) and the Michael Vasil laboratory (University of Colorado Health Sciences Center) for the efforts in this research.

Last but not the least, I would like to pay a special thank to my parents, my brothers and my wife, for their continued encouragement, support and love.

Table of Contents

Chapter I	Introduction.....	1
	A. Introduction to HPLC.....	1
	IA-1. General Information.....	1
	IA-2 Reversed-Phase Chromatography.....	7
	IA-2-1 General Background.....	7
	IA-2-2 Stationary Phases for RP-HPLC.....	8
	IA-2-3 Mobile Phases and Mobile Phase Additives for RP- HPLC.....	10
	IA-2-4 Peptide Retention Behavior during RP-HPLC.....	17
	IA-2-5 Temperature Effect on Peptide Retention Behavior.....	21
	IA-2-6 Temperature Profiling during RP-HPLC.....	22
	IA-3 Hydrophilic Interaction/Cation-Exchange Chromatography.....	24
	IA-3-1 General Background.....	24
	IA-3-2 Stationary Phases for HILIC/CEX	28
	IA-3-3 Mobile Phases and Mobile Phase Additives for HILIC/CEX	29
	IA-2-4 Peptide Retention Behavior during HILIC/CEX.....	30
	IA-3-5 Comparison of HILIC/CEX and RP-HPLC.....	31
	B. Introduction to Antimicrobial Peptides.....	35
	IB-1 Traditional Antibiotics.....	35
	IB-2 The Development of Antibiotic Resistance.....	37
	IB-3 Discovery of Antimicrobial Peptides.....	38
	IB-4 Structural and Physical Characteristics of Antimicrobial Peptides.....	39
	IB-5 Proposed Mechanisms of Action.....	41
	IB-6 Drawbacks of Antimicrobial Peptides as Therapeutics.....	46
	IB-7 Peptide V ₆₈₁	46
	IB-8 <i>De Novo</i> Peptide Design.....	47
Chapter II	Objectives, Hypotheses and Overview.....	49

Chapter III	General Methods and Materials.....	54
	III-1 Materials.....	54
	III-2 Solid Phase Peptide Synthesis (SPPS)	55
	III-3 Peptide Purification by Preparative RP-HPLC.....	61
	III-4 Analytical RP-HPLC.....	63
	III-5 Amino Acid Analysis.....	65
	III-6 Mass Spectroscopy.....	65
	III-7 Circular Dichroism Spectroscopy.....	65
	III-8 Trifluoroethanol Titration.....	68
	III-9 CD Temperature Denaturation.....	69
	III-10 Calculation of Resolution (R_s) during RP-HPLC.....	70
Chapter IV	Selectivity Differences in the Separation of Amphipathic α -Helical Peptides During Reversed-Phase Chromatography at pH 2.0 and pH 7.0: Effects of Different Packings, Mobile Phase Conditions and Temperature.....	73
	IV-1 Abstract.....	73
	IV-2 Introduction.....	74
	IV-3 Experimental.....	76
	IV-3-1 Columns and HPLC Conditions.....	76
	IV-4 Results and Discussion.....	77
	IV-4-1 Amphipathic α -Helical Model Peptides.....	77
	IV-4-1-1 Design of Model Peptides.....	77
	IV-4-1-2 CD Spectroscopy Studies.....	80
	IV-4-1-3 RP-HPLC Elution Behavior of Amphipathic α -Helical Peptides.....	83
	IV-4-2 HPLC Run Parameters Investigated in This Study.....	84
	IV-4-2-1 Anionic Ion-Pairing Reagents.....	84
	IV-4-2-2 Salt Additives to Mobile Phase.....	85
	IV-4-2-3 RP-HPLC Stationary Phases.....	85
	IV-4-2-4 Temperature.....	87

	IV-4-3 Effect of Run Parameters on RP-HPLC of Amphipathic α -Helical Peptides.....	87
	IV-4-3-1 Effect of Salt on RP-HPLC of Model Peptides at pH 2.0 and pH 7.0.....	87
	IV-4-3-2 Effect of Column Packing on RP-HPLC of Model Peptides at pH 2.0 and pH 7.0.....	97
	IV-4-3-3 Effect of Temperature on RP-HPLC of Model Peptides at pH 2.0 and pH 7.0.....	100
	IV-5 Conclusions.....	105
Chapter V	Temperature Selectivity Effects in Reserved-Phase Chromatography due to Conformation Differences between Helical and Non-Helical Peptides	107
	V-1 Abstract.....	107
	V-2 Introduction.....	108
	V-3 Experimental.....	111
	V-3-1 Columns and HPLC Conditions.....	111
	V-4 Results	111
	V-4-1 Peptide Design and Designation.....	111
	V-4-2 Conformation of Model Peptides.....	114
	V-4-3 Temperature Effect on RP-HPLC Selectivity of Amphipathic α -Helical Peptides.....	116
	V-4-4 Temperature Effect on RP-HPLC Selectivity for Random Coil Peptides.....	120
	V-4-5 Comparison of Temperature Effect on L- or D-Helical and Random Coil Model Peptides	120
	V-4-6 Optimum Separation of Peptide Mixtures of α -Helical and Random Coil Peptides.....	124
	V-5 Discussion.....	126
	V-6 Conclusions.....	134
Chapter VI	Optimum Concentration of Trifluoroacetic Acid (TFA) for Reversed-Phase Chromatography of Peptides Revisited.....	136
	VI-1 Abstract.....	136
	VI-2 Introduction.....	137

	VI-3 Experimental.....	139
	VI-3-1 Column and HPLC Conditions.....	139
	VI-4 Results and Discussion.....	139
	VI-4-1 Design of Synthetic Model Peptides.....	139
	VI-4-2 RP-HPLC Stationary Phase.....	141
	VI-4-3 Effect of TFA Concentration on Elution Behavior of Model Peptide Mixtures.....	142
	VI-4-4 Effect of Temperature on Elution Behavior of Model Peptide Mixtures.....	146
	VI-4-5 Effect of Nearest-Neighbor Effects on Elution Behavior of Model Peptide Mixtures.....	148
	VI-4-6 Effect of TFA Concentration and Temperature on Elution Characteristics of Model Peptide	150
	VI-5 Conclusions.....	158
Chapter VII	Temperature Profiling of Polypeptides in Reversed-Phase Chromatography: Monitoring of Dimerization and Unfolding of Amphipathic α-Helical Peptides.....	159
	VII-1 Abstract.....	159
	VII-2 Introduction.....	160
	VII-3 Experimental.....	162
	VII-3-1 Columns.....	162
	VII-4 Results.....	162
	VII-4-1 Synthetic Model Peptides Used in This Study.....	162
	VII-4-2 Retention Behavior of Model Peptides during RP- HPLC.....	168
	VII-4-3 Effect of Temperature on RP-HPLC of α -Helical Peptides.....	172
	VII-5 Discussion.....	178
	VII-5-1 Hypothesis for Monitoring Dimerization and Unfolding of α -Helical Peptides by Temperature Profiling in RP- HPLC.....	178
	VII-5-2 Monitoring Dimerization and Unfolding of α -Helical Peptide during RP-HPLC.....	181
	VII-6 Conclusions.....	187
Chapter VIII	Determination of Stereochemistry Stability Coefficients of Amino Acid Side-Chains in an Amphipathic α-Helix.....	189

	VIII-1 Abstract.....	189
	VIII-2 Introduction.....	190
	VIII-3 Experimental.....	192
	VIII-3-1 Reversed-Phase Chromatography (RP-HPLC) of Peptides.....	192
	VIII-4 Results and Discussion.....	193
	VIII-4-1 Design of Model Peptides.....	193
	VIII-4-2 Effect of D-Amino Acid Substitutions on RP-HPLC Retention Behavior of Peptides.....	195
	VIII-4-3 Relative Hydrophobicity of L- and D-Amino Acid Side-Chains.....	202
	VIII-4-4 CD Spectroscopy Studies.....	211
	VIII-4-5 Temperature Denaturation Studies.....	215
	VIII-4-6 Amino Acid Helix Stability and Stereochemistry Coefficients.....	223
	VIII-5 Conclusions.....	226
Chapter IX	Rational Design of α-Helical Antimicrobial Peptides with Enhanced Activities and Specificity/Therapeutic Index.....	227
	IX-1 Abstract.....	227
	IX-2 Introduction.....	228
	IX-3 Experimental.....	232
	IX-3-1 Analytical RP-HPLC of Peptides.....	232
	IX-3-2 CD Temperature Denaturation Study of Peptide V ₆₈₁	232
	IX-3-3 Determination of Peptide Amphipathicity.....	233
	IX-3-4 Measurement of Antibacterial Activity.....	233
	IX-3-5 Measurement of Hemolytic Activity.....	234
	IX-4 Results and Discussion.....	234
	IX-4-1 Peptide Design.....	234
	IX-4-2 Structure of Peptide Diastereomers.....	238
	IX-4-3 Helix Stability of Peptide V ₆₈₁ in a Hydrophobic Environment.....	243
	IX-4-4 Effect of L-/D-Amino Acid Substitutions on RP-HPLC Retention Behavior of Peptides.....	245
	IX-4-5 Relative Hydrophobicity.....	248

IX-4-6 Determination of Peptide Self-Association Parameter by RP-HPLC Temperature Profiling.....	250
IX-4-7 Amphipathicity.....	255
IX-4-8 Relationships between Peptide Self-Association and Hydrophobicity, Amphipathicity and Helicity.....	257
IX-4-9 Hemolytic Activity.....	257
IX-4-10 Antimicrobial Activity Against Gram-Negative Microorganisms.....	260
IX-4-11 Antimicrobial Activity Against Gram-Positive Microorganisms.....	261
IX-4-12 Therapeutic Index.....	264
IX-4-13 Proposed Mechanism of Action of Antimicrobial Peptides in Biomembranes.....	265
IX-5 Conclusions.....	268

Chapter X

Comparison of Reversed-Phase Chromatography and Hydrophilic Interaction/Cation-Exchange Chromatography for the Separation of Amphipathic α -Helical Peptides with L- and D-Amino Acid Substitutions in the Hydrophilic Face.....	270
X-1 Abstract.....	270
X-2 Introduction.....	271
X-3 Experimental.....	272
X-3-1 Columns.....	272
X-4 Results and Discussion.....	273
X-4-1 RP-HPLC versus HILIC/CEX: General Principles.....	273
X-4-2 Synthetic Model Peptides Used in This Study.....	274
X-4-3 RP-HPLC of Amphipathic α -Helical Diastereomeric Peptides.....	277
X-4-4 HILIC/CEX of Amphipathic α -Helical Diastereomeric Peptides.....	280
X-4-5 Comparison of RP-HPLC and HILIC/CEX of Amphipathic α -Helical Diastereomeric Peptides at 25°C and 65°C.....	282
X-4-6 Comparison of Selectivity of RP-HPLC and HILIC/CEX Separation of Amphipathic α -Helical Diastereomeric Peptides.....	290
X-5 Conclusions.....	290

Chapter XI	Monitoring the Hydrophilicity/Hydrophobicity of Amino Acid Side-Chains in the Non-Polar and Polar Faces of Amphipathic α -Helices by Reversed-Phase and Mixed-Mode Hydrophilic Interaction/Cation-Exchange Chromatography.....	292
	XI-1 Abstract.....	292
	XI-2 Introduction.....	293
	XI-3 Experimental.....	295
	XI-3-1 Analytical HPLC Columns and Instrumentation.....	295
	XI-3-2 HPLC Run Conditions.....	296
	XI-4 Results and Discussion.....	296
	XI-4-1 RP-HPLC versus HILIC/CEX of Amphipathic α -Helical Peptides.....	296
	XI-4-2 Synthetic Peptide Analogs Based on V ₆₈₁	299
	XI-4-3 RP-HPLC of Amphipathic α -Helical Peptide analogs of V ₆₈₁	304
	XI-4-4 HILIC/CEX of Amphipathic α -Helical Peptide Analogues of V ₆₈₁	312
	XI-4-5 RP-HPLC and HILIC/CEX as Monitors of Hydrophilicity/Hydrophobicity of Amphipathic α -Helical Peptides.....	319
	XI-5 Conclusions.....	325
Chapter XII	Future Studies.....	327
Bibliography	331
Appendix I	Capillary Zone Electrophoresis (CZE) of α -Helical Diastereomeric Peptide Pairs Using Anionic Ion-pairing Reagents.....	354

List of Tables

Table		Page
I-1	Comparisons of HILIC/CEX and RP-HPLC.....	33
III-1	List of materials.....	54
IV-1	Effect of NaClO ₄ on peptide retention time and peak width during RP-HPLC at pH 7.0.....	90
IV-2	Effect of NaClO ₄ on peptide resolution during RP-HPLC at pH 7.0.....	91
IV-3	Effect of eluent system on peptide resolution during RP-HPLC at pH 2.0.....	94
IV-4	Effect of temperature on peptide resolution during RP-HPLC at pH 2.0.....	102
IV-5	Effect of temperature on peptide resolution during RP-HPLC at pH 7.0.....	104
VI-1	Sequences and names of the peptides in this study.....	140
VI-2	Retention times of +1, +3 and +5 peptides in different TFA concentrations.....	145
VI-3	Difference in retention times of +1, +3 and +5 peptides between 8 and 32 mM TFA.....	153
VI-4	Difference of peak width at half height of +1, +3 and +5 peptides between 8 and 32 mM TFA.....	155
VI-5	Relative increase in peptide resolution (<i>R_s</i>) between 2 and 32 mM TFA.....	156
VII-1	Synthetic peptides used in this study.....	163
VIII-1	RP-HPLC retention data of model peptide analogs at pH 7.0.....	198
VIII-2	RP-HPLC retention data of model peptide analogs at pH 2.0.....	199
VIII-3	Relative hydrophobicity of amino acid side-chains.....	204
VIII-4	CD data of model peptide analogs.....	210

VIII-5	Amino acid helix stability coefficients.....	221
VIII-6	Helix stereochemistry stability coefficients.....	222
IX-1	Circular dichroism data of V ₆₈₁ peptide analogs.....	242
IX-2	Relative hydrophobicity and association ability of peptide analogs during RP-HPLC temperature profiling.....	247
IX-3	Amphipathicity of peptide analogs.....	256
IX-4	Antimicrobial (MIC) and hemolytic (MHC) activities of peptide analogs against gram-negative bacteria and human red blood cells.....	258
IX-5	Antimicrobial (MIC) and hemolytic (MHC) activities of peptide analogs against gram-positive bacteria and human red blood cells.....	262
IX-6	Effect of amino acid substitutions on the biological activity of V ₆₈₁	263
X-1	Effect of temperature on peptide retention behavior in RP-HPLC and HILIC/CEX.....	283
X-2	Effect of temperature on separation of diastereomeric peptide pairs by RP-HPLC and HILIC/CEX.....	288
XI-1	RP-HPLC and HILIC/CEX retention data in the polar face of amphipathic α -helical peptides.....	307
XI-2	RP-HPLC and HILIC/CEX retention data in the non-polar face of amphipathic α -helical peptides.....	308
XI-3	Effect of amino acid substitutions on the retention behavior of peptide V ₆₈₁	320
XI-4	Monitoring of effects of the same substitutions on the non-polar versus the polar face by RP-HPLC and HILIC/CEX.....	321

List of Figures

Figure		Page
I-1	General outline of HPLC techniques.....	4
I-2	Relationship of resolution, speed and capacity.....	12
I-3	Effect of varying flow-rate or gradient-rate on separation of peptides in RP-HPLC.....	15
I-4	Comparison of peptide separation by RP-HPLC and HILIC ...:.....	25
I-5	Effect of acetonitrile concentration on column selectivity during HILIC/CEX of peptides.....	27
I-6	Comparison of peptide separation by CEC, HILIC/CEX and RP-HPLC.....	34
I-7	Examples of classical antibiotics.....	36
I-8	Antimicrobial peptides with different secondary structures.....	40
I-9	Representation of the “barrel-stave” and the “carpet” models for membrane permeation.....	43
II-1	Schematic diagram of the research in this thesis.....	50
III-1	Schematic diagram of solid-phase peptide synthesis.....	56
III-2	TFA catalyzed removal of the <i>t</i> -Boc group.....	58
III-3	(a) HBTU activation and (b) amino acid coupling during SPPS.....	59
III-4	RP-HPLC analysis comparison of the crude peptide and the peptide after purification.....	64
III-5	CD spectra of peptides with representative varying secondary structures.....	67
III-6	Illustration of relationship among resolution, column efficiency and column selectivity.....	72
IV-1	Sequences and representations of α -helical and random coil peptides....	78
IV-2	Circular dichroism (CD) spectra of synthetic model peptides.....	81

IV-3	Effect of salt on RP-HPLC elution profile of model peptides at pH 7.0...	88
IV-4	Effect of mobile phase conditions on RP-HPLC elution profile of model peptides at pH 2.0.....	95
IV-5	Effect of concentration of anionic ion-pairing reagents on the retention time of model peptides at pHs 2.0 and 7.0.....	98
IV-6	Comparison of RP-HPLC retention behavior on XDB and SB-C ₈ columns at pH 2.0 and pH 7.0.....	99
IV-7	Effect of temperature on RP-HPLC elution profile of model peptides at pH 2.0.....	101
IV-8	Effect of temperature on RP-HPLC elution profile of model peptides at pH 7.0.....	103
V-1	Model synthetic peptides with conformational differences.....	112
V-2	Circular dichroism (CD) spectra of helical and random coil L _L and L _D peptides.....	115
V-3	Effect for temperature on RP-HPLC selectivity for model α -helical peptides with L- or D-amino acid substitutions.....	117
V-4	Effect of temperature on RP-HPLC selectivity for random coil and α -helical peptides.....	121
V-5	Effect of temperature on RP-HPLC retention time of helical and random coil peptides.....	123
V-6	RP-HPLC separation of random coil and helical L- or D-peptides around the optimum temperatures	125
V-7	Comparison of temperature effect on RP-HPLC of L- and D-helical peptides.....	129
V-8	Comparison of temperature effect on RP-HPLC of random coil peptides.	131
V-9	Effect of temperature on RP-HPLC of helical and random coil peptides: normalization to retention behavior of the random coil Gly peptide.....	133
VI-1	Effect of TFA concentration on RP-HPLC retention behavior of positively charged model peptide mixtures.....	144
VI-2	Effect of temperature on RP-HPLC retention behavior of positively charged model peptide mixtures.....	147

VI-3	Effect of TFA concentration on retention characteristics of model positively charge peptides at 25 and 70 °C.....	151
VII-1	Representation of synthetic α -helical peptides as α -helical nets.....	164
VII-2	Circular dichroism spectra of synthetic peptide analogs.....	167
VII-3	RP-HPLC of synthetic amphipathic and non-amphipathic α -helical peptides.....	170
VII-4	RP-HPLC of diastereomeric peptide pairs.....	171
VII-5	RP-HPLC of α -helical peptides at 5 °C, 45 °C and 80 °C.....	173
VII-6	Effect of temperature on RP-HPLC of α -helical peptides.....	175
VII-7	Effect of temperature on RP-HPLC of L- and D-diastereomeric α -helical peptides.....	177
VII-8	Effect of temperature on RP-HPLC of monomeric α -helical peptides....	179
VII-9	Hypothesis for monitoring peptide dimerization and unfolding of monomeric α -helices by temperature profiling in RP-HPLC.....	180
VII-10	Effect of temperature on RP-HPLC of α -helical peptides: normalization to retention behavior of random coil peptide.....	183
VIII-1	Helical net and helical wheel of the “host” peptide used in this study....	194
VIII-2	Reversed-phase HPLC of D- and L-amino acid substituted peptides at pH 7.0.....	196
VIII-3	Plot of the difference in reversed-phase HPLC retention times between D- and L-diastereomeric peptide pairs ($\Delta t_R(X_L-X_D)$) at pH 7.0 versus pH 2.0.....	203
VIII-4	Histogram illustrating relative hydrophobicity of L- and D-diastereomeric peptides at pH 7.0.....	206
VIII-5	Plot of relative hydrophobicity of D-peptides or L-peptides at pH 2.0 versus pH 7.0.....	209
VIII-6	Circular dichroism (CD) spectra of Arg and Pro peptides at pH 7.0 and 5 °C.....	213
VIII-7	Comparison of molar ellipticity of D- and L-peptide analogs in benign buffer (50 mM aqueous $PO_4/100$ mM KCl) at 5 °C, pH 7.0.....	214

VIII-8	TFE titration of representative peptide analogs at 5 °C, pH 7.0.....	217
VIII-9	Temperature denaturation profiles of representative peptide analogs.....	218
VIII-10	Histograms illustrating relative contribution of L- and D-amino acid side-chains to helix stability at pH 7.0.....	220
IX-1	Representation of the "host" peptide V ₆₈₁ as helical wheel and the sequences of the synthetic peptide analogs used in this work.....	235
IX-2	Circular dichroism (CD) spectra of peptides NL _D and NL _L and peptides NK _D and NK _L at pH 7 and 25°C, in 50mM <i>aq.</i> PO ₄ containing 100mM KCl.....	241
IX-3	CD Temperature denaturation of peptide V ₆₈₁	244
IX-4	RP-HPLC temperature profiles of peptide V ₆₈₁ and its analogs.....	249
IX-5	Normalized RP-HPLC temperature profiles of peptide V ₆₈₁ and its analogs.....	254
X-1	Model synthetic amphipathic α -helical peptides.....	275
X-2	RP-HPLC of diastereomeric amphipathic α -helical peptides.....	278
X-3	HILIC/CEX of diastereomeric amphipathic α -helical peptides.....	281
X-4	Effect of temperature on retention behavior of diastereomeric amphipathic α -helical peptides in RP-HPLC and HILIC/CEX.....	286
X-5	Comparison of selectivity changes in the separation of diastereomeric amphipathic α -helical peptides by RP-HPLC and HILIC/CEX at 25 °C and 65 °C.....	289
XI-1	Synthetic amphipathic α -helical peptides.....	301
XI-2	RP-HPLC of amphipathic α -helical peptides.....	305
XI-3	HILIC/CEX of amphipathic α -helical peptides	313
XI-4	Effect of temperature on HILIC/CEX of amphipathic α -helical peptides, where substitutions are made in the polar face of the α -helix.....	316
XI-5	Effect of temperature on HILIC/CEX of amphipathic α -helical peptides, where substitutions are made in the non-polar face of the α -helix.....	317

XI-6	Selectivity of RP-HPLC versus HILIC/CEX of amphipathic α -helical peptides.....	322
-------------	--	-----

Abbreviation List

Ac-	Acetylated N-terminus
-amide	Amidated C-terminus
<i>t</i> -Boc	N ^α <i>tert</i> -butyloxycarbonyl
CD	Circular dichroism
CE	Capillary electrophoresis
CEX	Cation-exchange chromatography
DCM	dichloromethane
DIEA	<i>N,N</i> -diisopropylethylamine
DMF	dimethylformamide
DTT	Dithiothreitol
EDT	1,2-ethanedithiol
HBTU	<i>o</i> -benzotriazol-1-yl- <i>N,N,N',N'</i> -tetramethyluronium hexafluorophosphate
HF	Hydrofluoric acid
HIC	Hydrophobic interaction chromatography
HILIC/CEX	Hydrophilic interaction/cation-exchange chromatography
HOBt	<i>N</i> -hydroxybenzotriazole
HPLC	High performance liquid chromatography
I.D.	Internal diameter
IEC	Ion-exchange chromatography
LB	Luria-Bertani
MALDI-MS	Matrix assisted laser desorption ionization mass spectrometry
MBHA	4-methylbenzhydrylamine resin hydrochloride salt
MHC	Minimal hemolytic concentration
MIC	Minimal inhibitory concentration
MW	Molecular weight
NaClO ₄	Sodium perchlorate
NH ₂ -	Free amino terminus
NPN	1- <i>N</i> -phenyl <i>naphthyl</i> amine
<i>P</i> _A	Parameter of association
RBC	Red blood cell

RP-HPLC	Reversed-phase high performance liquid chromatography
R_s	Resolution
SB	StableBond
SEC	Size-exclusion chromatography
SPPS	Solid phase peptide synthesis
TFA	Trifluoroacetic acid
TFE	Trifluoroethanol
T_m	Melting temperature
t_R	Retention time
UV	Ultraviolet
$W_{1/2}$	Peak width at half height
XDB	Extra dense bonding

Amino acid nomenclature:

Ala, A	Alanine
Arg, R	Arginine
Asn, N	Asparagine
Asp, D	Aspartic acid
Cys, C	Cysteine
Gln, Q	Glutamine
Glu, E	Glutamic acid
Gly, G	Glycine
His, H	Histidine
Ile, I	Isoleucine
Leu, L	Leucine
Lys, K	Lysine
Met, M	Methionine
Phe, F	Phenylalanine
Pro, P	Proline
Ser, S	Serine
Thr, T	Threonine

Trp, W	Tryptophan
Tyr, Y	Tyrosine
Val, V	Valine

CHAPTER I

Introduction

A. Introduction to HPLC

IA-1. General information

The term chromatography refers to a group of separation techniques which are characterized by a distribution of the molecules to be separated between two phases, the stationary phase and mobile phase. Traditional column chromatography (so-called open column chromatography) is characterized by the stationary phase being packed into a column (usually a glass or a polymer column), through which the mobile phase is passed by gravity or pumped and the various sample components are eluted with different velocities through the column. Two types of gels are used in traditional chromatography: xerogels (such as cross-linked dextran gels and cross-linked polyacrylamide gels) and aerogels (such as glass, silica and organic polymer gels). Traditionally, three types of column chromatography were mainly utilized for peptide/protein purification and characterization: gel-exclusion chromatography (also called gel-permeation or, more commonly, size-exclusion chromatography), ion-exchange chromatography, and affinity chromatography. During the application of traditional chromatography to peptide/protein separations, there are some intrinsic drawbacks, including the low elution speed, poor resolution and relatively large volumes of eluent required for sample separation.

The need for highly-purified peptide/protein samples remains a significant issue for researchers during peptide and protein structure and function studies. Since its introduction about four decades ago, high-performance liquid chromatography (HPLC) has rapidly become a highly efficient, widely-used separation technology especially for

peptides and proteins. Compared with traditional chromatographic techniques, HPLC is not so much a type of chromatography as a new way of utilizing traditional chromatographic techniques in a much more efficient manner. In traditional column techniques, materials with large particle size are packed into glass columns. Since these materials are not resistant to high pressure, only slow flow-rates are able to be applied, producing long separation times, and resolution tends to be poor. In contrast, in HPLC, the same principles are involved, but the column support materials consist of more stable particles made of physically stronger materials (with smaller particle size) in a sealed stainless steel column instead of an open glass or plastic column, which can withstand high pressure without changing their structure. Such small particles are much more efficient than those employed in traditional chromatography, but require high-performance pumping systems, due to the high back pressures involved. Much better separations can be achieved with dramatically less amount of sample in a much shorter time with the proper applications of HPLC compared to traditional chromatography. In addition, during HPLC, the amount of eluent used is in orders of magnitude less than traditional chromatography (milliliters compared to liters).

Silica gel and silica gel-derivatized stationary phases are by far the most used in HPLC at present. Polymer-based column packings can be good complements to silica-based materials in HPLC, due to their stability in alkaline conditions. Based on the column packing materials and applications, HPLC techniques can be categorized as several types of chromatography, *i.e.*, reversed-phase chromatography (RP-HPLC), size-exclusion chromatography (SEC), ion-exchange chromatography (IEC), hydrophobic interaction chromatography (HIC), hydrophilic interaction/cation-exchange

chromatography (HILIC/CEX) and affinity/immunoaffinity chromatography (Figure I-1). Packing materials today are characterized by a trend of becoming smaller (3.5 and 5.0 μm particles are commonly used). Smaller packing materials lead to higher chromatographic efficiency.

HPLC can be applied to many different kinds of biological molecules, such as peptides/proteins, DNA, lipids and carbohydrates (Clejan, 1998; Imanari *et al.*, 1996; Koizumi, 1996; Loft *et al.*, 1998; Mant *et al.*, 1991; Patton *et al.*, 1998), with HPLC being the most frequently employed for peptides and proteins (Mant *et al.*, 1991). Based on the UV absorbance of peptide bonds, peptide or protein samples can be detected at the wavelength of 210 nm qualitatively and quantitatively (for the peptide bond, strong absorption range is in the 200 to 230 nm region and wavelength maximum is about 188 nm (Donovan, 1969)). Although the wavelength of 210 nm is not at the wavelength maximum, it is the practical wavelength of the detection system due to the UV cutoff of the mobile phase used in the HPLC of peptides and proteins. Peptides and proteins can also be detected at higher wavelength depending on the presence of aromatic amino acids. The aromatic amino acids (phenylalanine, tyrosine and tryptophan) have their own unique near UV spectra between 240 and 300 nm.

Ideal SEC separates peptides by a mechanism based solely on peptide size; however, most modern SEC columns are weakly anionic and slightly hydrophobic, resulting in either hydrophobic interactions or electrostatic interactions between the negatively charged column matrix and any positively charged character of solute (Engelhardt *et al.*, 1981a; Engelhardt *et al.*, 1981b; Kopaciewicz *et al.*, 1982; Pfannkoch *et al.*, 1980; Regnier, 1983b); in IEC, although the ideal separation mechanism is based

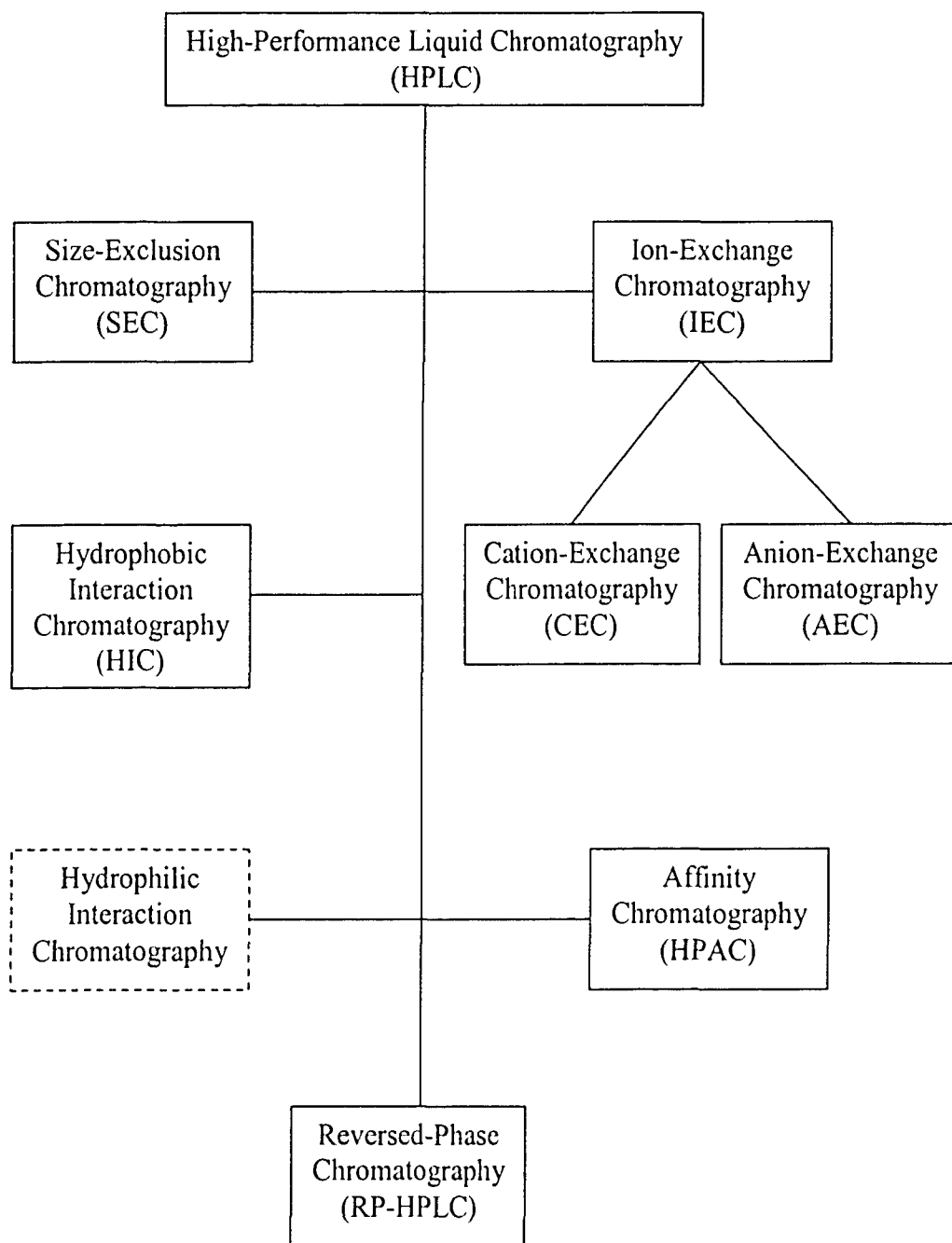


Figure I-1 General outline of HPLC techniques (adapted from Mant, C. T. *et al.* 1991).

on the electrostatic attraction between the column matrix and peptides, ion-exchange packing may also often exhibit significant hydrophobic characteristics, giving rise to mixed-mode contributions to solute separation (Kennedy *et al.*, 1986; Kopaciewicz *et al.*, 1983; Rounds *et al.*, 1987); and in RP-HPLC, residual, negatively-charged silanol groups present on the surface of silanized silica can influence the reserved-phase chromatographic behavior of peptide solutes with positively charged amino acid residues, producing undesirable effects such as peak tailing and non-reproducible peptide retention times (Bij *et al.*, 1981; Mant *et al.*, 1987b). In addition, extensive use of a silica-based reserved-phase column, due to the gradual removal of hydrophobic ligands from the silica, results in an increased concentration of underivatized silanols (Mant *et al.*, 1987c; Mant *et al.*, 1986), which further increases the non-ideal behaviors of peptides or proteins. However, all such non-ideal behaviors may be suppressed through manipulation of the mobile phase. For example, the non-ideal behavior of peptides/proteins in SEC may be suppressed by the addition of organic modifier acetonitrile or salt in the mobile phase; the non-ideal behavior of peptides in RP-HPLC may be suppressed by the addition of salt such as sodium perchlorate; and the non-ideal behavior of peptides/proteins in IEC may be suppressed by the addition of an organic modifier such as acetonitrile (Burke *et al.*, 1989; Mant *et al.*, 1991).

It is important in HPLC to achieve good reproducibility of peptide separations. The need for standards to monitor column chromatography is well established. Peptide standards designed in this laboratory have demonstrated their versatility in monitoring both ideal and non-ideal column performance for peptide separations during various modes of HPLC (Mant *et al.*, 1987b; Mant *et al.*, 1987c; Mant *et al.*, 1987d; Mant *et al.*,

1986). It is necessary to utilize peptide standards to assess column performance, as well as to determine mobile phase effects on peptide retention behavior and/or the column packing, prior to an application of the sample of interest.

In the last few years, there has been an increased effort into the separation, quantification and identification of all proteins in a cell or tissue, so-called proteomics. Entering the age of proteomics from the genomics era, we expect to see high-resolution, multidimensional bioanalytical techniques being used in an integrated and automated fashion, to solve separation problems and enable high performance analysis of complex mixtures of biomedical interest in the pharmaceutical and biotechnology industry (Guttman *et al.*, 2004; Issaq, 2001). At present, the most successful separation chemistries are gel electrophoresis and HPLC. However, the flexibility in selecting from a variety of separation chemistries improves the success rate for recovering classes of proteins that are difficult to handle in gel electrophoresis. Multidimensional HPLC has been utilized to separate and analyze samples of large numbers of proteins and peptides (Guttman *et al.*, 2004; Issaq, 2001; Liu *et al.*, 2002; Wehr, 2002). For example, coupling ion-exchange and reversed-phase chromatography as the first and second dimensions, respectively, has three appealing advantages (Wehr, 2002): (1) the two modes have complementary selectivity; (2) solvent used in IEC can be compatible with the second dimension of RP-HPLC; and (3) for further post-HPLC analysis, the solvent used in RP-HPLC is also compatible with electrospray ionization (ESI) and matrix-assisted laser-desorption ionization (MALDI) systems. Multidimensional HPLC has become a powerful approach for researchers to achieve comprehensive separations of the extremely complex peptide and/or protein mixtures characteristic of proteomics.

IA-2 Reversed-phase chromatography

IA-2-1 General background

Reversed-phase HPLC (RP-HPLC) is the most commonly-used and well-established technique in the analysis and isolation of peptides and proteins and it has revolutionized efficient peptide separations compared to traditional chromatography (Aguilar, 2004; Mant *et al.*, 1991). Indeed, it is noteworthy that RP-HPLC has no equivalent in classical column chromatography. The major reasons for the continuing dominance of RP-HPLC for solute separations of all types (Majors, 2004) are the speed and efficiency of RP-HPLC plus an almost unlimited degree of freedom in choice of mobile phase (buffer, organic modifier) as well as stationary phase. In this thesis, RP-HPLC was the major technique used in the studies of HPLC methodology and peptide structure and function. RP-HPLC is characterized by a non-polar column matrix and elution of solutes based on their hydrophobicity due to the hydrophobic interactions between solutes and the hydrophobic stationary phase. Solute are eluted from this hydrophobic stationary phase in order of increasing solute hydrophobicity by subsequent of an organic modifier to the mobile phase. It is noteworthy that, similar to RP-HPLC, hydrophobic interaction chromatography (HIC) is a mode of HPLC also relying on hydrophobic interactions between solutes and the stationary phase to effect separation. The separation is based on hydrophobic interactions of the surface of the folded proteins with the hydrophobic matrix. The mobile phase and the relatively weak hydrophobic matrix characteristic of HIC usually would not destabilize protein tertiary and quaternary structure. Whereas, in RP-HPLC, the conditions of chromatography (organic modifier

and high ligand density of the hydrophobic matrix) result in denaturation or unfolding of proteins (Lau *et al.*, 1984). HIC is not a commonly-used approach for the separations of peptides compared with RP-HPLC; however, HIC can separate proteins without, in general, causing denaturation and loss of enzymatic or other activity (Fausnaugh *et al.*, 1984a; Fausnaugh *et al.*, 1984b). In summary, there are three main differences between RP-HPLC and HIC: (1) mobile phase solvent utilized; (2) ligand density on the column support; and (3) hydrophobicity of the column matrix. In HIC, high salt concentrations are used to promote binding of proteins to stationary phase. Proteins adsorb to the stationary phase due to the hydrophobic interactions between the non-polar matrix and the non-polar areas on the polypeptide surface. Samples are eluted in order of increasing surface hydrophobicity either isocratically or by a descending salt gradient which weakens hydrophobic interactions and causes the solute to be released from the column.

IA-2-2 Stationary phases

In HPLC, the stationary phase can be a solid, a bonded or a coated phase on a solid support, or a wall-coated phase. As mentioned previously, the stationary phase used often characterizes the HPLC mode. For example, silica gel is used in adsorption chromatography; an octylsilane bonded phase is used in reversed-phase chromatography, *etc.* Supports can be naked or coated or can have a chemically bonded phase in HPLC. Packing materials can generally be divided into two major types: silica gel and silica-gel derivatized phases, organic polymers and derivatized materials. Most commercial reversed-phase columns for peptide and protein separations are silica-based, due to the excellent mechanical stability and high separation efficiencies offered by silica-based

packings. Reversed-phase packings based on silica are generally manufactured by reacting free hydroxyl groups on the surface of silica with a silane that contains a hydrophobic ligand, *e.g.*, alkyl, phenyl. However, it is well-known that silica-based reversed-phase columns are not stable at basic pH, due to dissolution of the silica; in addition, some reports have shown that in the acidic conditions typically used for peptide and protein separations, the silica-based bonded-phase is slowly degraded. Such acidic conditions were known to promote the cleavage of the silane from the silica (*i.e.*, cleavage of the siloxane bond) in bonded-phase columns, especially for monomeric stationary phases (Glajch *et al.*, 1987; Sagliano *et al.*, 1988). However, silica-based packings with excellent thermal and chemical stability have been developed in recent years. For example, SB (denoting stable-bond) packings were originally designed to protect the siloxane bond from acid hydrolysis at low pH; in contrast, XDB (denoting extra dense bonding) packings were designed to shield the silica support from dissolution at pH values at neutrality and higher (Barry *et al.*, 1995; Boyes *et al.*, 1993; Glajch *et al.*, 1990; Kirkland *et al.*, 1989; Kirkland *et al.*, 1997; Kirkland *et al.*, 1998). In addition, both packings were also designed to exhibit thermal stability over a wide temperature range.

Compared with silica-based columns, polymer-based columns have been developed which are stable from pH 1 to pH 14, making them more widely applicable and easier to clean than silica-based supports (Maa *et al.*, 1988; Williams *et al.*, 1986). However, silica-based columns are still generally superior to polymer-based counterparts in terms of mechanical strength, selectivity and efficiency (Nugent, 1991).

A wide variety of bonded phases exist for separation of peptides and proteins by RP-HPLC but the most commonly used columns are C₄, C₈ and C₁₈ (bonded-silane with alkyl chain length of 4, 8, 18 methylene groups, respectively). In RP-HPLC, a pore size of 300 Å has become the most popular; generally, peptides or proteins smaller than 100 kDa are well resolved on columns of 300 Å pore size (Burton *et al.*, 1988). For peptide separations, 100 Å pore size packings can be used. For very large proteins, columns with 1000 and 4000 Å pores may offer better performance (Burton *et al.*, 1988). Another parameter important to peptides/proteins separations is the particle size. Theory predicts that performance of separations goes up as particle size decreases. For analytical separations, most columns have particle size of 5 to 8 microns. Some manufacturers are offering columns with particles of 2 to 3 microns; however, small gains in efficiency with smaller particles may quickly be outweighed by higher column back pressures, greater susceptibility to plugging and shorter column life (Nugent, 1991).

Based on above considerations, in this thesis, silica-based C₈ reversed-phase columns with pore size of 300 Å and a particle size of 5 µm were utilized to study the retention behavior of peptides under different circumstances.

IA-2-3 Mobile phases and mobile phase additives in RP-HPLC

Mobile phase refers to the solvent that moves the solute through the column. Various mobile phase parameters can have dramatic effects on peptide/protein separations, including solvent, pH, flow rate, gradient rate and mobile phase additives. The selection of optimal conditions may be critical in establishing an analytical method. This selection really depends on the individual researcher's requirements and is a

compromise of run time (speed), resolution (see Chapter III for details), sensitivity (detector response) and sample capacity. The relationships among speed, resolution and capacity are shown in Figure I-2. The figure illustrates that, within limits, it is possible to alter the experimental conditions of a separation to improve one of these qualities at the expense of the other two. Generally, the search for optimum conditions for a separation should be done by varying one parameter at a time. For RP-HPLC with silica-based columns, although excellent resolution of peptide mixtures can be obtained at acidic or neutral pH, the majority of researchers have carried out RP-HPLC at pH < 3.0, since apart from the suppression of silanol ionization under acidic conditions, *i.e.*, suppressing undesirable ionic interactions with basic residues, silica-based columns are more stable at low pH (Mant *et al.*, 1990; Mant *et al.*, 2002). Flow rate (F) (the volumetric rate of flow of mobile phase through an HPLC column) is one of the most widely used parameters in HPLC (expressed as ml/min or μ l/min). Another related parameter is linear velocity (v), which refers to the velocity of the mobile phase moving through the column (expressed as cm/min). Linear velocity can be calculated by the equation:

$$v = F(l)/v_0$$

where l is the column length and v_0 is the void column;

$$v_0 = t_0 F$$

where t_0 is the time for unretained compounds to reach the detector from the point of injection.

In RP-HPLC, solutes bound or partition on the stationary phase by hydrophobic interactions are eluted in order of increasing solute hydrophobicity from the non-polar stationary phase as the mobile phase becomes more non-polar through the addition of

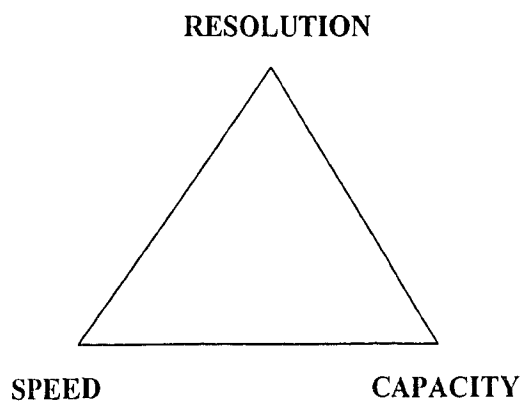


Figure I-2 Relationship of resolution, speed and capacity.

water-miscible organic modifiers. The modes of elution during RP-HPLC can be mainly divided as isocratic elution and gradient elution. Isocratic elution is achieved by keeping the same composition and concentration of eluents during the entire elution procedure; in contrast, in gradient elution, concentration of one or more eluents are increased or decreased in order to improve the resolution. Due to the varying hydrophobicity of different peptides in a peptide (or protein) mixture, it is usually very difficult to apply isocratic elution to obtain a good separation in RP-HPLC. The partitioning range of peptides and proteins is very narrow compared with that of small organic molecules, making the task of optimizing isocratic conditions difficult. For example, the small organic molecules (alkylphenones) can be separated isocratically over a wide range of acetonitrile concentrations; in contrast, peptides can be separated isocratically only over a very narrow range of acetonitrile concentrations due to their much narrower partitioning “windows” (Mant *et al.*, 1987a). Experiments also proved that the peptide peaks not only broaden in lower isocratic acetonitrile concentrations but also tail severely (Mant *et al.*, 1987a). Hence, optimization of peptide/protein separations in analytical and preparative reversed-phase chromatography generally involves the manipulation of gradient rate rather than isocratic elution conditions. In the beginning of a gradient run, a lower concentration of the organic modifier is chosen, then, the components which are most loosely bound to the adsorption sites will be eluted under favorable conditions. Other more strongly held compounds will be successively eluted as the concentration of the organic modifier is increased. The result is usually an increased resolution over a wide range of sample compounds, compared with isocratic elution. In gradient elution, the change in mobile phase composition with time is denoted as gradient rate. In practice, the

selection of gradient rate to improve one aspect of a separation (*e.g.*, resolution or speed) may be at the expense of others. For example, as shown in Figure I-3, at constant flow rate, there is a general improvement in peptide resolution with decreasing gradient rate; in contrast, at constant gradient rate, there is a general improvement in peptide resolution with increasing flow rate. Optimum conditions for a peptide separation will depend on the particular peptide mixture under investigation and the requirements of the separation.

During the application of HPLC to peptides/proteins, the critical part of maintaining efficient instrument and column performance lies in the careful preparation of the mobile phase. In addition, column life time will be extended through proper cleaning and storage procedures. Since several liters of a mobile phase may pass through a column in daily use, any impurities in the mobile phase may have an adverse effect on column performance unless care is taken to minimize their presence. The mobile solvents in RP-HPLC usually consist of water, non-polar solvent and mobile phase additives. Non-polar solvents refer to the organic modifier in RP-HPLC, *e.g.*, acetonitrile, methanol and isopropanol. Mobile phase additives refer to ion-pairing reagents, buffer components and salts. Trifluoroacetic acid (TFA) is by far the most extensively used mobile phase additive in RP-HPLC. Its efficacy in this role lies in its volatility and UV transparency, coupled with the hydrophobic, negatively charged trifluoroacetate ion (TFA^-) which is able to interact with basic, positively charged amino acid side-chains (Arg, Lys, His), as well as free N^α -amino groups, resulting in the improved solute resolution (Cunico *et al.*, 1998; Guo *et al.*, 1987; Mant *et al.*, 1991; Mant *et al.*, 2002). In addition, at low pH values (*e.g.*, pH 2), protonation of acidic residues enhances the interaction of peptides with the reversed-phase packing, concomitant with the suppression of free silanol

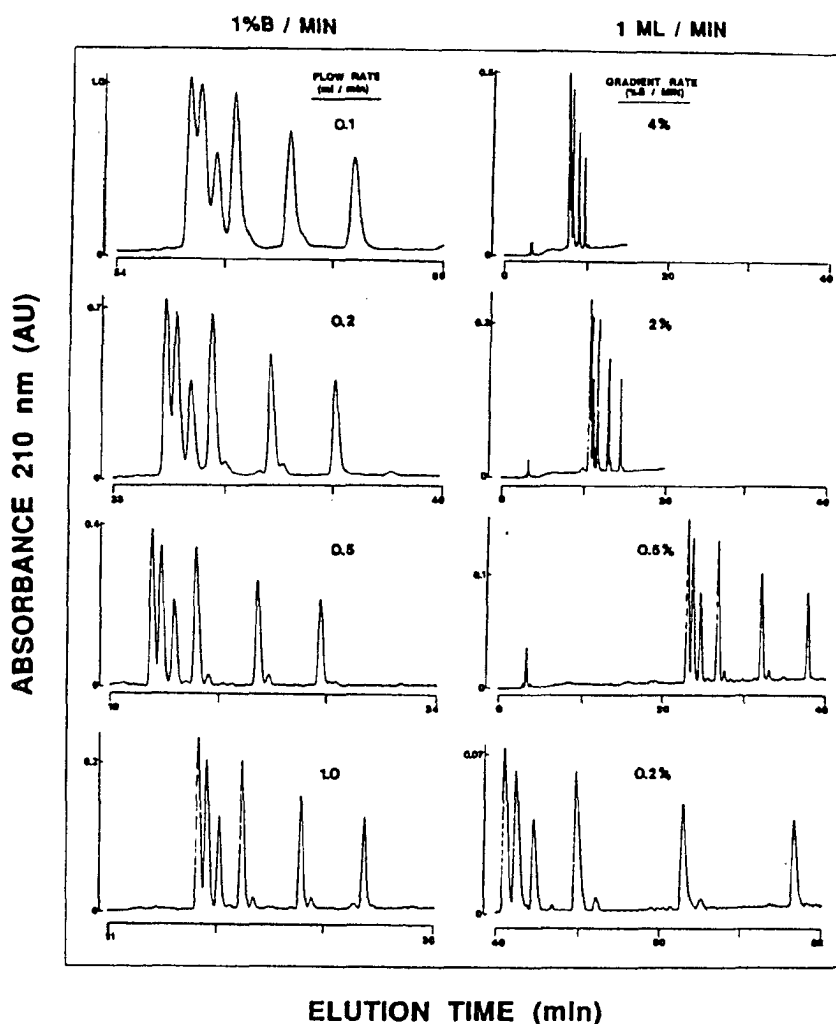


Figure I-3 Effect of varying flow-rate or gradient-rate on separation of peptides in RP-HPLC (adapted from Mant *et al.* 1991, pp314). Conditions: SynChropak RP-P (C₁₈) column (250x4.6 mm I.D., 6.5 μ m particle size, 300 Å pore size); eluent A was 0.1% *aq.* TFA and eluent B was 0.1% TFA in acetonitrile; flow-rates and linear AB gradients as shown. Left profiles: effect of varying flow-rate (0.1, 0.2, 0.5, and 1.0 ml/min) at constant gradient rate (1% B/min). Right profiles: effect of varying gradient-rate (4, 2, 0.5, and 0.2% B/min) at constant flow-rate (1 ml/min). Sequences of the six peptide standards are: Ac-RGGGGIGIGK-amide (I1), Ac-RGGGGIGLIGK-amide (I2), Ac-RGGGGLGLIGK-amide (S2), Ac-RGAGGLGLIGK-amide (S3), Ac-RGVGGLGLIGK-amide (S4), Ac-RGVVGLGLIGK-amide (S5).

ionization, thereby avoiding undesirable ionic interactions with positively charged peptide solutes (Mant *et al.*, 1987b; Mant *et al.*, 2002; Regnier, 1983a).

Favored models for the mechanism of such ion-pair separations involve either formation of ion-pairs with the sample solute in solution followed by retention of the solute molecules on a reversed-phase packing (Horvath *et al.*, 1976; Horvath *et al.*, 1977) or a dynamic ion-exchange event whereby the ion-pairing reagent is first retained by the reversed-phase column and then solute molecules exchange ions with the counterion associated with the sorbed ion-pair reagent (Kissinger, 1977; Kraak *et al.*, 1977; Van de Venne *et al.*, 1978). Whatever the mechanism, the resolving power of ion-pairing reagents is effected by their interactions with the ionized groups of a peptide. For example, hydrophobic anions such as trifluoroacetate form hydrophobic ion-pairs with the basic side-chains. The resulting complex tends to mask the positive charges and tends also to increase the affinity of the peptide or protein for the column. This, in turn, increases retention time. The actual effect on retention time of a peptide will depend strongly on the hydrophobicity of the ion-pairing reagent and the number of oppositely charged groups on the peptides.

Addition of salts to mobile phases over a pH range of approximately 4-7 is traditionally designed to suppress negatively charged silanol interactions (pK_a of charged silanol ~ 4) with positively charged solutes (Gaertner *et al.*, 1985; Guo *et al.*, 1986a; Mant *et al.*, 1987b; Mant *et al.*, 1991; Mant *et al.*, 2002; Meek, 1980; Sereda *et al.*, 1997; Snider *et al.*, 1988). However, the potentially beneficial effect of salt, specifically NaClO₄, on peptide separations at low pH has also been demonstrated (Sereda *et al.*, 1997). Indeed, the negatively charged perchlorate (ClO₄⁻) ion acts as a hydrophilic

anionic ion-pairing reagent and, thus, interacts with positively charged groups of solutes in a similar manner to H_2PO_4^- and TFA^- . Recently our laboratory has shown that the perchlorate anion is more effective than the trifluoroacetate anion as an ion-pairing reagent for RP-HPLC of peptides (Shibue *et al.*, 2005). NaClO_4 is also particularly useful as the salt additive to a RP-HPLC mobile phase since it is highly soluble in aqueous acetonitrile eluents, even at relatively high concentrations of this organic modifier (Zhu *et al.*, 1992).

IA-2-4 Peptide retention behavior during RP-HPLC

The excellent resolving power of RP-HPLC has made it the predominant HPLC technique for peptide separations and its ability to separate peptides of closely related structures makes it extremely useful for high-speed preparative and analytical applications. Many and varied influences will have an impact on the way a particular peptide interacts with a reversed-phase column, not least of which include characteristics of the peptide itself, *e.g.* amino acid composition (Guo *et al.*, 1986a; Zhou *et al.*, 1990), residue sequence (Houghten *et al.*, 1987; Zhou *et al.*, 1990), peptide length (Mant *et al.*, 1988; Mant *et al.*, 1989), and the presence of any secondary structure (α -helix or β -sheet) (Blondelle *et al.*, 1992; Heinitz *et al.*, 1988; Steer *et al.*, 1998; Steiner *et al.*, 1991; Zhou *et al.*, 1990). Compared to β -sheet peptides, the peptide retention behavior of α -helical peptides (both amphipathic and non-amphipathic) during RP-HPLC has been extensively studied. Indeed, peptide fragments from chemical or proteolytic digests of proteins typically contain peptides with α -helical potential. During RP-HPLC, such peptides will be induced into α -helical structure by the non-polar environment characteristic of this

technique (hydrophobic matrix and non-polar eluting solvent) (Blondelle *et al.*, 1995; Purcell *et al.*, 1995c; Steer *et al.*, 1998; Zhou *et al.*, 1990).

The study of α -helical peptides, especially amphipathic helices, is very relevant to native peptides and proteins (Mant *et al.*, 1993), since the amphipathic feature of helices is generally observed in biologically active peptides and proteins (Segrest *et al.*, 1990) and approximately 50% of all helices in proteins are amphipathic (Cornette *et al.*, 1987). A previous study from our laboratory (Zhou *et al.*, 1990) has shown that peptides with the same amino acid composition but different sequence have different α -helical contents. Zhou *et al.* (Zhou *et al.*, 1990) clearly demonstrated that if the hydrophobic residues of a peptide are well distributed around the α -helical structure of a peptide, the α -helical conformation of the peptide *per se* does not have a significant effect on peptide retention behavior in RP-HPLC. On the other hand, peptides which are induced into an amphipathic α -helix on interaction with a hydrophobic RP-HPLC stationary phase will exhibit preferred binding of their non-polar face with the stationary phase. Indeed, because of this preferred binding domain, amphipathic α -helical peptides are considerably more retentive than non-amphipathic peptides of the same amino acid composition (Zhou *et al.*, 1990). Due to the different retention behavior of peptides with different conformations, such as random coil peptides, amphipathic α -helical peptides, non-amphipathic α -helical peptides and β -sheet peptides, it is possible to use RP-HPLC to separate peptide mixtures with varying secondary structures.

One of the major applications of RP-HPLC to peptides/proteins is to separate large amounts of peptides/proteins in a short period with high efficiency, which means to improve the capacity (the amount of sample that can be injected onto a RP-HPLC column

without overload), speed and resolution of chromatography. However, as discussed in Section IA-2-3, the selection of optimum conditions for a peptide separation may be at the expense of one or more other parameters. That is, increasing the sample capacity during a run may cause worse resolution; in contrast, to obtain a fast elution of peptides, one has to sacrifice the capacity and resolution; in addition, good resolution is a result of well-resolved peaks and narrow peak widths, generally coupled with lower sample capacity and elution speed (Figure I-2).

For many RP-HPLC analyses, one tries to minimize the use of valuable peptide samples while maintaining excellent peptide resolution. Indeed, resolution can be affected by many chromatographic parameters, such as gradient rate, flow rate, pH, temperature, column packing, *etc.* Moreover, peptides derived from various sources differ widely in size, net charge and hydrophobicity, and purification of a single peptide from a complex mixture will require an approach different from a separation of all components of a mixture. Although a desired peptide separation may be obtained by trial and error, this may take many attempts, with subsequent loss of time and valuable peptide samples in cases where only limited quantities are available. Thus, prediction of peptide retention times has become a useful practical tool. Several groups have determined sets of coefficients for predicting peptide retention on reversed-phase columns, based on computer-calculated regression analyses of the retention times of a wide range of peptides of varying compositions (Browne *et al.*, 1982; Eng *et al.*, 1987; Mabuchi *et al.*, 1981; Meek, 1980; Meek *et al.*, 1981; Sakamoto *et al.*, 1988; Sasagawa *et al.*, 1982; Wilson *et al.*, 1981). A more precise method for determining the contribution of individual amino acid residues was developed by Guo *et al.* (Guo *et al.*, 1986a; Guo *et al.*,

1986b) on a series of model synthetic peptides. When the method was applied to retention time predictions for 58 peptides, the high correlation of predicted and observed retention times indicated good predictive accuracy for the range of peptides studied (2-16 residues) (Guo *et al.*, 1986b). In addition, combined with Guo's coefficients (Guo *et al.*, 1986a), Mant *et al.* (Mant *et al.*, 1988) demonstrated that there was a linear relationship between chain length and peptide retention behavior in addition to peptide hydrophobicity. Using this relationship, the retention behavior of peptides up to 50 residues in length can be accurately predicted. During the application of a prediction method, an internal peptide standard should be always run with the peptide samples, since the use of an internal standard allows the researcher to correct for any variation in HPLC apparatus, temperature, reversed-phase packings, and reversed-phase columns of any length or diameter (Guo *et al.*, 1986a; Guo *et al.*, 1986b). In fact, our laboratory has shown that the order of elution of proteins can be predicted in RP-HPLC using the sum of retention (hydrophobicity/hydrophilicity) coefficients (Mant *et al.*, 1989).

Denaturation of a peptide or a protein can be defined as a change in conformation from that which exists under benign, *i.e.*, non-denaturing, conditions. Thus, separation by RP-HPLC can cause denaturation because of the non-polar environment (non-polar mobile phase and non-polar sorbent) as well as the low pH utilized for most of separations. For example, RP-HPLC induces the protein to unfold to expose its more hydrophobic interior in order to bind the hydrophobic stationary phase. Spectroscopic studies have shown that some proteins undergo tertiary structure perturbations while bound to the reversed-phase sorbent and regain their original tertiary structure after elution (Lu *et al.*, 1988). This denaturing effect may lead to the formation of two peaks;

an earlier peak of native conformation and a latter eluted peak of denatured conformation (Benedek *et al.*, 1984). Although some proteins show a loss of biological activity (irreversible denaturation) during RP-HPLC, others retain full biological activity. In this thesis, peptides which have a potential to form dimers, will still be bound to the reversed-phase stationary phase as monomers; and peptides which have potential to be α -helical, will be induced as α -helices during RP-HPLC.

IA-2-5 Temperature effects on peptide retention behavior in RP-HPLC

Considering the complexity of proteomics applications of liquid chromatography, where the separation of hundreds or even thousands of peptides may be required, *e.g.* from simultaneous digest of a multi-protein mixture, optimization of the separation protocol is of prime importance. The introduction in recent years of stationary phases stable to high temperatures has added to the arsenal of RP-HPLC approaches for optimization of the resolution of peptide mixtures (Barry *et al.*, 1995; Boyes *et al.*, 1993; Chloupek *et al.*, 1994; Glajch *et al.*, 1990; Hancock *et al.*, 1994; Kirkland *et al.*, 1993; Kirkland *et al.*, 1989; Kirkland *et al.*, 1997; Lee *et al.*, 2003b; Mant *et al.*, 2003a; Mant *et al.*, 1997; Mant *et al.*, 2003b; McNeff *et al.*, 2000; Zhu *et al.*, 1996a; Zhu *et al.*, 1996b). In addition, RP-HPLC of peptides at varying temperature has also allowed an insight into the role of conformation in the retention behavior of peptides and proteins (Lee *et al.*, 2003b; Mant *et al.*, 2003a; Mant *et al.*, 2003b; Mant *et al.*, 1989; Purcell *et al.*, 1993; Purcell *et al.*, 1995a; Purcell *et al.*, 1995b; Purcell *et al.*, 1995c; Richards *et al.*, 1994). Indeed, peptides with the presence of different secondary structure (α -helix, β -sheet or random coil) interact in different ways with a reversed-phase matrix. For example, α -

helical peptides (amphipathic, non-amphipathic) and peptides that have a random coil structure in benign conditions but have α -helical potential will be present as α -helices during RP-HPLC; in contrast, β -sheet peptides and random coil peptides without α -helical potential will keep their original conformation during RP-HPLC. However, temperature has particular effects on induced amphipathic α -helical structure during RP-HPLC, *i.e.*, an increase in temperature may denature peptide amphipathic α -helical structure, resulting in faster elution of α -helical peptides due to the disruption of the non-polar face of the helices.

In addition to the effect on peptide conformation during RP-HPLC, temperature also exhibits a dramatic influence on the resolution and peak width of peptides, which may be due to the general effects of increasing temperature resulting in increased solubility of the solute in the mobile phase as the temperature rises (Cohen *et al.*, 1984; Guo *et al.*, 1986b; Hancock *et al.*, 1986; Ingraham *et al.*, 1985) as well as causing a decrease in solvent viscosity and an increase in mass transfer between the mobile and stationary phase (Dolan, 2002). We believe that studying temperature effects on peptide selectivity will be valuable for both the rational development of peptide separation optimization protocols and a probe to distinguish between peptide conformations.

IA-2-6 Temperature profiling during RP-HPLC

One of the most interesting developments of liquid chromatography in recent years has been the emergence of RP-HPLC as a physicochemical probe of peptide and protein structure. Such studies are based on the premise that the hydrophobic interactions between peptides and the non-polar stationary phase characteristic of RP-HPLC (Mant *et*

al., 1991; Mant *et al.*, 1996; Mant *et al.*, 2002) mimic the hydrophobicity and interactions between non-polar residues which are the major driving forces for protein folding and stability. Many studies have demonstrated the correlation between RP-HPLC retention behavior of peptides/proteins and their conformational stability (Aguilar *et al.*, 1993; Blondelle *et al.*, 1996; Heinitz *et al.*, 1988; Henderson *et al.*, 1990; Lazoura *et al.*, 1997; Lee *et al.*, 1997; Lork *et al.*, 1989; Purcell *et al.*, 1989; Purcell *et al.*, 1995a; Purcell *et al.*, 1995b; Purcell *et al.*, 1995c; Steer *et al.*, 1998; Steiner *et al.*, 1991; Zhou *et al.*, 1990). In addition, self-association of molecules is a critical factor in explaining biological activity, folding and stability of peptides/proteins. During RP-HPLC, temperature-induced unfolding of peptides can be considered as a probe to monitor the change of the hydrophobic interaction between peptides and the non-polar matrix which, in turn, may reflect the ability of peptide to self-associate. Thus, we believe that the conformation-dependent response of peptides to RP-HPLC under changing temperature (temperature profiling) has implications, not only for the approach to general analysis and purification of peptides, but also for the *de novo* design of peptides and proteins, since the contribution of different amino acid side-chains to the stability of α -helical/ β -sheet structure and oligomerization may be rapidly ascertained through this RP-HPLC approach. Up to date, temperature profiling has been utilized on peptides with different conformations, including α -helical, β -sheet, coiled-coil and random coil peptides (Lee *et al.*, 2003b; Mant *et al.*, 2003a; Mant *et al.*, 2003b), demonstrating its sensitivity, reliability and reproducibility in monitoring peptide self-association. In addition, this peptide self-associating ability is also important during the design of antimicrobial

peptides, which interact with biomembranes and lyse target cells in a channel/pore forming mechanism or a detergent-like wrapping mechanism.

IA-3 Hydrophilic interaction/cation-exchange chromatography

IA-3-1 General background

Although RP-HPLC has been established as the most commonly used method for separating peptides and proteins, the application of this technique may be limited when a low selectivity or the presence of complex solute mixtures does not permit satisfactory separation of individual components. Hydrophilic interaction chromatography (HILIC) has been promoted as an alternative chromatographic mode for applications to the separation of a wide range of solutes (Alpert, 1990). It is characterized by its use of polar stationary phases and decreasing gradients of high concentrations of organic solvents as the mobile phase. Separation by HILIC, in a manner similar to normal-phase chromatography, depends on hydrophilic interactions between the solutes and the hydrophilic stationary phase, *i.e.*, solutes are eluted from a HILIC column in order of increasing hydrophilicity (decreasing hydrophobicity). Under typical HILIC conditions, elution of solutes is in an order of increasing solute hydrophilicity, a behavior which is the opposite of that observed in RP-HPLC (Figure I-4). However, in a previous study in our laboratory, we noted that a HILIC column also possessed some ion-exchange characteristics (Zhu *et al.*, 1991). For example, a peptide mixture run on a HILIC column (polyhydroxyethylaspartamide) showed a similar profile to that obtained on a strong cation-exchange column (polysulfoethylaspartamide) (Zhu *et al.*, 1991). Indeed, in our hands, the hydrophilic sorbent of the polysulfoethylaspartamide strong cation-exchange

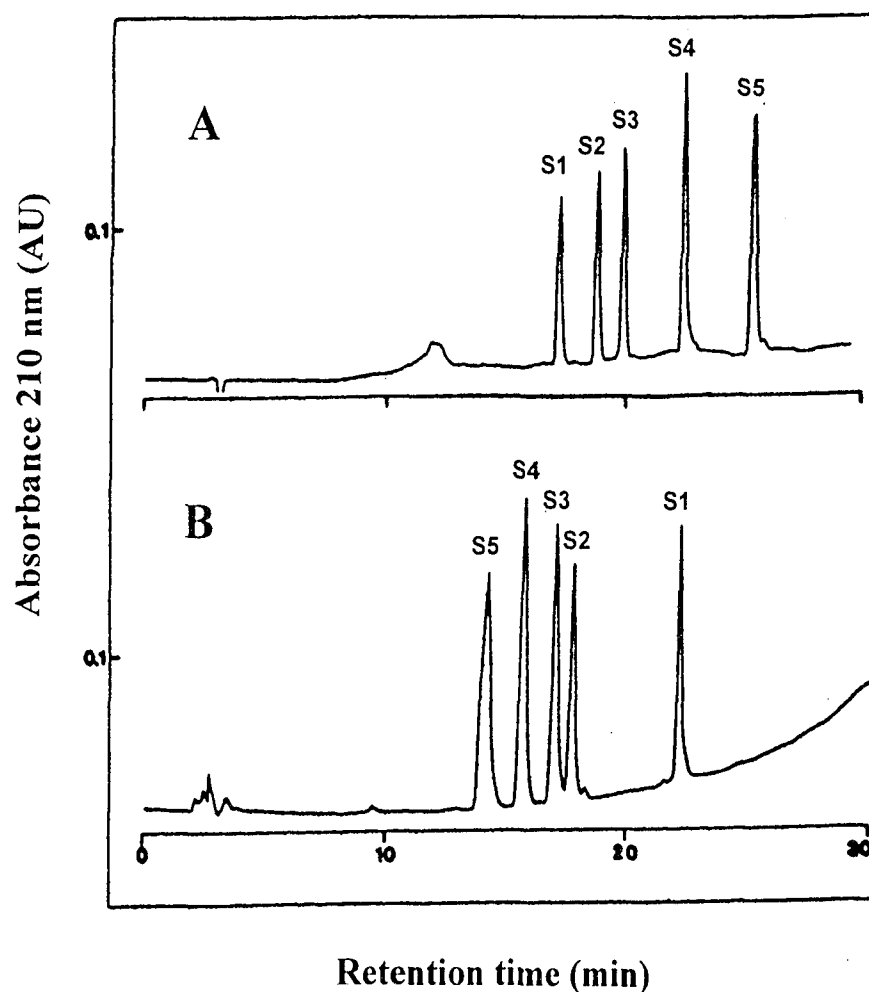


Figure I-4 Comparison of peptide separation by RP-HPLC (panel A) and HILIC (panel B) (adapted from Zhu. B. Y., *et al.* 1991). Panel A: column, SynChropak RP-P (C_{18}) (250x4.6 mm I.D.); mobile phase, linear AB increasing gradient (1%B/min) at a flow-rate of 1 ml/min, where A is 0.05% aqueous TFA and B is 0.05% TFA in acetonitrile; panel B: column, polyhydroxyethylaspartamide HILIC column (200x4.6 mm I.D.); mobile phase, linear AB decreasing gradient (1%B/min) at a flow-rate of 1 ml/min, where A is 0.2% orthophosphoric acid in acetonitrile and B is 0.2% aqueous orthophosphoric acid (starting conditions were 85% A–15% B). The sequence of peptide is NH₂-RGAGGLGLGK-amide S1, the sequences of peptides S2–S5 are same as in Figure I-3.

column provided much better selectivity than the ideal HILIC column (Zhu *et al.*, 1991; Zhu *et al.*, 1992). Our laboratory subsequently took advantage of the inherent hydrophilic character of ion-exchange packings, specifically strong cation-exchange (CEX) columns, by subjecting peptide mixtures to linear salt gradients in the presence of high levels of organic modifier, specifically acetonitrile (Litowski *et al.*, 1999; Mant *et al.*, 1998a; Mant *et al.*, 1998b; Mant *et al.*, 2000; Zhu *et al.*, 1992). Thus, we developed HILIC/CEX as a complementary HPLC mode to RP-HPLC. It is known that ion-exchange packings generally exhibit some hydrophobic character, perhaps producing undesirable peak broadening and organic solvents are frequently added to the mobile phase buffers at low concentration to suppress any such hydrophobic characteristics (Burke *et al.*, 1989; Mant *et al.*, 1991). At lower levels of acetonitrile, with hydrophobic interactions suppressed, peptides are separated on a cation-exchange column by an ionic mechanism only. However, as the level of acetonitrile is raised, the presence of high levels of organic modifier not only suppresses any undesirable hydrophobic interactions between the peptides and the cation-exchange matrix (Burke *et al.*, 1989), but also promotes hydrophilic interactions between the peptides and packing (Zhu *et al.*, 1991; Zhu *et al.*, 1992). Separations based on hydrophilicity are thus superimposed on top of those based on charge, resulting in mixed-mode HILIC/CEX, *i.e.*, such an approach takes simultaneous advantage of both the charged character of peptides as well as any hydrophilic/hydrophobic properties they possess. As shown in Figure I-5, in Panel B, at a relatively low concentration of acetonitrile (20%), peptides were eluted in order of increasing positive charge of the peptides; in contrast, in Panel A, when raising the concentration of acetonitrile to 90%, the peptides were separated not only by charge

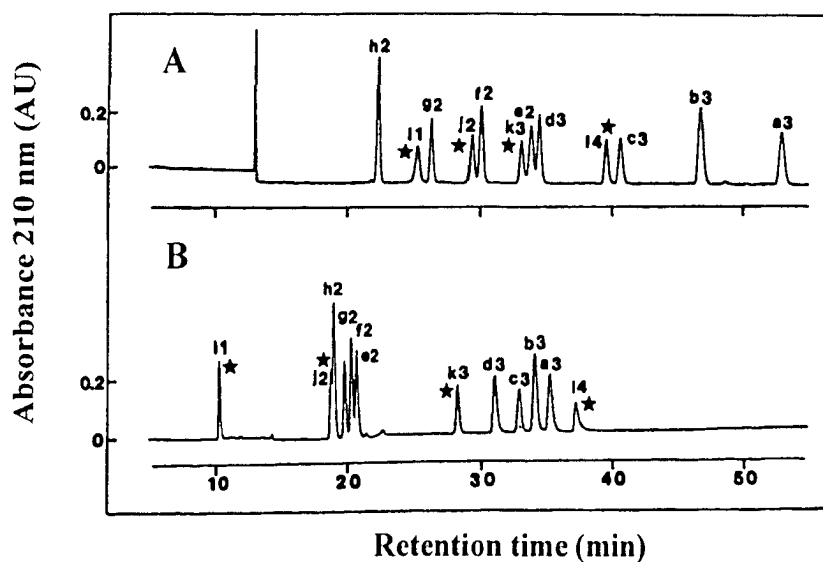


Figure I-5 Effect of acetonitrile concentration on column selectivity during HILIC/CEX of peptides (adapted from Zhu. B. Y., *et al.* 1992). Column, PolySulfoethyl A strong cation-exchange column (200×4.6 mm I.D.). Mobile phase: panels A and B, linear AB increasing salt gradient (2% B/min, equivalent to 5 mM NaClO₄/min, starting at 100% A) at a flow-rate of 1 ml/min, where A is 5 mM aqueous TEAP, pH 7, and B is A plus 0.25 M NaClO₄, pH 7, both A and B containing 90% (panel A) acetonitrile or 20% acetonitrile (panel B). The designation of peptides represents the number of positive charges on the peptides.

difference but also by peptide hydrophobicity, *e.g.*, peptide h2 (with 2 positive charges) was eluted faster than peptide i1 (with 1 positive charge) and peptide l4 (with 4 positive charges) was eluted faster than peptide c3 (with 3 positive charges) (Zhu *et al.*, 1992). This mixed-mode mechanism, with a balance of hydrophilic and ionic interactions, offers an excellent alternative to RP-HPLC for both peptide (Hartmann *et al.*, 2003; Litowski *et al.*, 1999; Mant *et al.*, 1998a; Mant *et al.*, 1998b; Oyler *et al.*, 1996) and protein separation (Lindner *et al.*, 1996; Lindner *et al.*, 1997; Lindner *et al.*, 1998; Lindner *et al.*, 1999; Mizzen *et al.*, 2000), including posttranslationally modified proteins, *e.g.*, various acetylated (Lindner *et al.*, 1996), phosphorylated (Lindner *et al.*, 1997), glycosylated (Mizzen *et al.*, 2000), and deamidated (Lindner *et al.*, 1998) proteins. Indeed, apart from its use as a complementary HPLC mode to RP-HPLC, HILIC/CEX has occasionally proven more effective as a separation technique than RP-HPLC for specific peptide separations (Hartmann *et al.*, 2003; Hodges *et al.*, 2004).

IA-3-2 Stationary phases for HILIC/CEX

Separation of peptide and protein mixtures by means of hydrophilic interaction chromatography is usually performed with packing materials having average diameters of 5-10 μm and a pore size between 300 and 1500 \AA (Lindner *et al.*, 2004). The stationary phases employed are by definition polar and usually include silica modified by chemical bonding of suitable functional groups. Generally, silica-based packings supplied by many manufacturers include weak and strong cation and anion exchangers, amino-, diol-, polyol-, amide- and amino-cyano-phases (Lindner *et al.*, 2004). Since soluble silicate

anions are formed under alkaline conditions, similar to that in RP-HPLC, silica materials used in HILIC are normally not suited for use at basic pH values.

A polypeptide coating with a strong cation exchanger poly(2-sulfoethylaspartamide) (PolySulfoethyl A, PolyLC) has been well used as a hydrophilic matrix in our laboratory (HILIC/CEX mode) (Hartmann *et al.*, 2003; Litowski *et al.*, 1999; Mant *et al.*, 1998a; Mant *et al.*, 1998b; Mant *et al.*, 2000; Zhu *et al.*, 1991; Zhu *et al.*, 1992). This material, synthesized by the reaction of taurine with polysuccinimide covalently bonded to silica (Alpert *et al.*, 1988), favors electrostatic interactions in lower organic solvent levels and hydrophilic interactions in higher organic solvent levels.

IA-3-3 Mobile phases and mobile phase additives for HILIC/CEX

Elution of peptides and proteins in HILIC/CEX is accomplished by an increasing salt gradient in the presence of a high concentration of organic modifier. This high concentration of organic solvent in the elution system is necessary to promote the favored hydrophilic interactions between the eluents and the polar column matrix. Selection of mobile phases during HILIC/CEX can dramatically alter the results of peptide elution. To date, acetonitrile has been the organic solvent of choice for peptide separations during HILIC/CEX, at concentrations of up to 90%, due to its excellent UV transparency at wavelengths around 210 nm and low viscosity. In addition to organic solvents, salts are also important to obtain good results in HILIC/CEX. Considering the UV transparency and good solubility in high concentrations of organic solvents, sodium perchlorate has proved to be particularly suitable for peptide separations during HILIC/CEX (Hartmann *et al.*, 2003; Litowski *et al.*, 1999; Mant *et al.*, 1998a; Mant *et al.*, 1998b; Mant *et al.*,

2000). In practice, the selection of the mobile phases, buffer ions, pH and even the stationary phases is case-dependent, and all these parameters can be powerful tools for high-resolution separations of peptides and proteins.

IA-3-4 Peptide retention behavior during HILIC/CEX

Note that, in an analogous manner to the non-polar face of an amphipathic α -helix representing a preferred binding domain for RP-HPLC, the hydrophilic face of the α -helix would represent a preferred binding domain for a hydrophilic stationary phase such as the strong cation-exchange matrix employed for HILIC/CEX in the present study. Evidence for such hydrophilic preferred binding domains has been reported previously by our laboratory for both amphipathic α -helical peptides (Mant *et al.*, 1998b) and cyclic amphipathic β -sheet peptides (Mant *et al.*, 1998a). Peptides are usually eluted in order of increasing hydrophilicity and charge during HILIC/CEX. That is, peptides with the same net charge will be eluted mainly according to the extent of their hydrophilic interactions with the ion-exchange matrix, with the most hydrophobic peptide being eluted first (Hartmann *et al.*, 2003; Mant *et al.*, 1998a); in contrast, if the cation-exchange interactions were dominant in the mixed-mode separation process, peptides (*e.g.*, with different positive charges) should be eluted in order of the lowest to the highest positively-charged peptides (Zhu *et al.*, 1991; Zhu *et al.*, 1992). Moreover, in HILIC/CEX, if the hydrophilic interactions were the dominant effect, a peptide of higher net positive charge would be eluted earlier than a peptide of lower net positive charge if the overall hydrophobicity of the latter was greater than that of the former, which can be

dramatically changed for charged peptides depending on the concentration of organic solvent (Zhu *et al.*, 1992).

IA-3-5 Comparison of HILIC/CEX and RP-HPLC

To summarize HILIC/CEX: (1) the stationary phase used in HILIC/CEX is a strong cation-exchange packing, characterized by both hydrophilic and cation-exchange interactions with solutes; (2) the mobile phase in HILIC/CEX is generally composed of high constant concentration of organic solvent (usually acetonitrile) and increasing concentration of salts; (3) a high concentration of organic solvent promotes hydrophilic interaction between solutes and the column matrix; (4) increasing concentration of salts compete with column packing to elute peptides in order of charges and/or hydrophilicity; thus (5) the peptide with the least positive charge or the lowest hydrophilicity will generally be eluted first during HILIC/CEX, depending on mobile phase conditions.

The major difference between HILIC/CEX and RP-HPLC, by definition, is the mechanism of separating solutes. In addition to the separation mechanisms, there are other important variations between HILIC/CEX and RP-HPLC as shown in Table I-1. Interestingly, temperature also has opposite effects on peptide elution during HILIC/CEX and RP-HPLC. In the absence of any conformational effects, temperature increases generally result in a decrease in retention times of peptides during RP-HPLC, whereas an increase of retention times of peptides with increasing temperature has been observed in HILIC/CEX (Hartmann *et al.*, 2003; Hodges *et al.*, 2004). Figure I-6 exhibits the comparison of HILIC/CEX and RP-HPLC. In Figure I-6, it is clear that both HILIC/CEX and RP-HPLC showed significantly improved separation compared with CEC on the

peptide mixture. The elution order of peptides in the mixture was quite different between HILIC/CEX and RP-HPLC indicating that, as a powerful chromatographic tool, HILIC/CEX presents an excellent complement to RP-HPLC for peptide/protein separation/optimization protocols (Figure I-6).

Table I-1 Comparisons of HILIC/CEX and RP-HPLC

	HILIC/CEX	RP-HPLC
Stationary phase	Polar stationary phase, <i>i.e.</i> , cation-exchange matrix	Highly non-polar stationary phase
Mobile phase	Elution of solutes depends on increasing concentration of salts concomitant with constant concentration of organic solvent (or “modifier”) or decreasing concentration of an organic solvent in an aqueous mobile phase	Elution of solutes effected by increasing concentration of an organic solvent (or “modifier”) in an aqueous mobile phase
	High concentration of an organic modifier at the beginning of an elution; constant high concentration or lower concentration of the organic solvent at the end of the elution	No organic modifier or low concentration of organic modifier at the beginning of an elution; higher concentration of the organic solvent at the end of the elution
	No salt or low salt concentration at the beginning of an elution; higher concentration of salt at the end of the elution	No salt or constant salt concentration throughout elution
	Solutes are eluted in order of increasing hydrophilicity or increasing number of positive charges	Solutes are eluted in order of increasing hydrophobicity
Elution mechanism	Takes simultaneous advantage of both the ion-exchange and hydrophilic interactions between solutes and the column matrix	Takes advantage of hydrophobic interactions between solutes and the column matrix

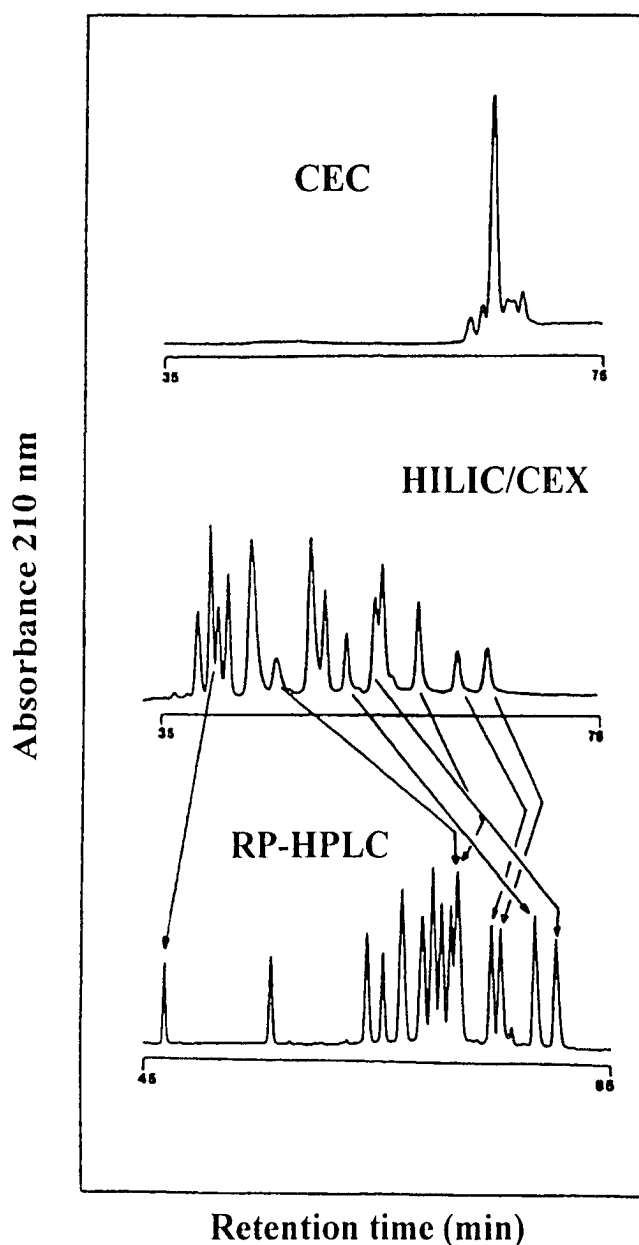


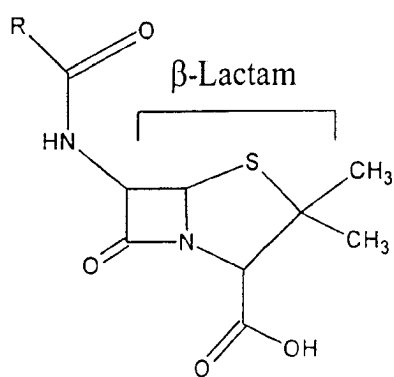
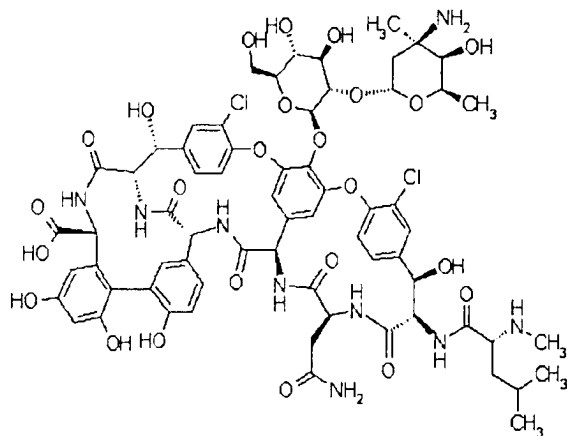
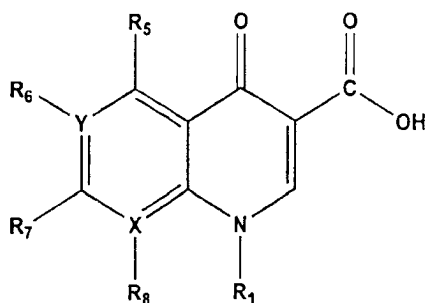
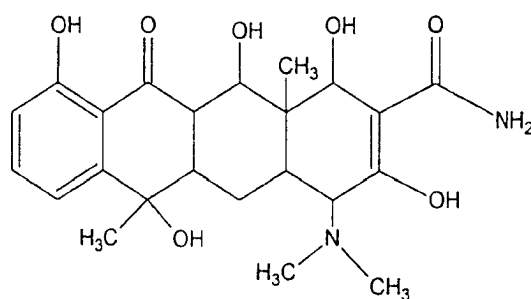
Figure I-6 Comparison of peptide separation by CEC (top), HILIC/CEX (middle), and RP-HPLC (bottom) (adapted from Mant, C. T. *et al.* 2002a). Columns: RP-HPLC, Zorbax SB300-C8 reversed-phase column (150×4.6 mm ID, 5 μm particle size, 300 Å pore size); CEC and HILIC/CEX, PolySulfoethyl A strong cation-exchange column (200×4.6 mm ID, 5 μm particle size, 300 Å pore size). Mobile phase for CEC and HILIC/CEX, linear AB gradient, where buffer A is 20 mM *aq.* TEAP, pH 3, and buffer B is buffer A plus 400 mM NaClO₄; acetonitrile is present in both buffers at a concentration (v/v) of 10% (CEC), or 90% in buffer A and 80% in buffer B (HILIC/CEX); gradient rate, 2.5 mM NaClO₄/min, following 5 min isocratic elution with buffer A; flow rate, 1 ml/min; temperature 30 °C. Mobile phase for RP-HPLC, linear AB gradient, where eluent A is 0.05% *aq.* TFA, pH 2, and eluent B is 0.05% TFA in acetonitrile; gradient rate 0.5% acetonitrile/min, flow rate 1 ml/min, temperature 70 °C. The arrows denote major selectivity differences between the HILIC/CEX and RP-HPLC modes.

B. Introduction to antimicrobial peptides

IB-1 Traditional antibiotics

The past 60 years have been marked as the “antibiotic era” in medical history in which natural, semisynthetic, or synthetic antibacterial chemicals have been used with great success against life-threatening infections. The first natural antibiotic, pyocyanase, was discovered in 1888 in bacteria *Pseudomonas aeruginosa*. However, the most successful antibiotic was penicillin, which made its clinical debut in 1942 (Travis, 1994). By killing the bacteria that cause many of humankind’s worst infectious diseases, such as tuberculosis and pneumonia, it saved countless lives. Because of the discovery and synthesis of the “miracle drug” penicillin, Florey, Chain and Fleming were awarded the Nobel Prizes in Medicine in 1945. More antibiotics were discovered over the following decades.

The antibiotic mechanisms of traditional antibiotics are quite different, which can be used to classify antimicrobial agents. Briefly, the major mechanisms include the inhibition of bacterial cell wall synthesis or damage to the cell wall (*e.g.*, penicillins, vancomycin), the inhibition of cytoplasmic membrane synthesis or the direct disruption of the membrane (*e.g.*, polyene antifungals), the inhibition of synthesis or metabolism of nucleic acids (*e.g.*, quinolones, nitroimidazoles), the prevention of protein biosynthesis (*e.g.*, tetracyclines, erythromycin) or the modification of energy metabolism (*e.g.*, sulfonamides, trimethoprim) (Neu, 1992). Examples of classical antibiotics are shown in Figure I-7. As so many antibiotics have been discovered, it appeared as though

**Penicillins****Vancomycins****Quinolones****Tetracyclines****Figure I-7** Examples of classical antibiotics.

humankind had an abundant supply of effective antimicrobial agents that could adequately control the spread of bacterial infections.

IB-2 The development of antibiotic resistance

Recently, the era of the antibiotic miracle may be coming to an end; at best antibiotics are progressively demonstrating decreased efficacy (Travis, 1994). In 1994, the World Health Organization's Scientific Working Group on Antibiotic Resistance and Surveillance stated that bacterial resistance to antibiotic agents was already a serious public health problem in both developed and developing countries. Levels of resistance have been increasing at an alarming rate and are expected to increase at even greater rate in the future as antibacterial agents lose their effectiveness (Hancock, 1997). Indeed, penicillin resistance showed up only a few years after its clinical debut in 1942 (Travis, 1994). Since antibiotics are effective through inhibiting bacterial cell wall synthesis, protein synthesis, and DNA replication, bacteria can then resist antibiotics as a result of chromosomal mutation or inductive expression of a latent chromosomal gene or by exchange of genetic material through transformation (the exchange of DNA), transduction (bacteriophage), or conjugation by plasmids (extrachromosomal DNA) (Finland, 1979; Milatovic *et al.*, 1987; Schaberg *et al.*, 1981). When one strain develops a new resistance strategy, it is able to share this strategy with others, an ability that has played a crucial role in the rapid spread of antibiotic resistance. For example, intergenus spread of resistance can occur between Gram-positive species such as staphylococci and enterococci and between Enterobacteriaceae and Pseudomonas or anaerobes such as Bacteroides (Arthur *et al.*, 1987; Brisson-Noel *et al.*, 1988; Morse *et al.*, 1986; Tally *et*

al., 1988). Gram-positive species can transfer resistance to Gram-negative species, but the reverse is uncommon (Neu, 1992). Some antibiotics can promote this transfer of resistance genes, *e.g.*, tetracycline can stimulate the transmission of a transposable element coding for tetracycline resistance by 5- to 100-fold (Torres *et al.*, 1991).

In addition to antibiotic resistance, no radically new structural class has been introduced into medical practice over the past 30 years (Hancock, 1997). Therefore, the development of a new class of antibiotics has become critical. Ideally, such antibiotics should possess both novel modes of action as well as different cellular targets compared with existing antibiotics to decrease the likelihood of development of resistance. Antimicrobial peptides can represent such a new class of antibiotics (Hancock, 1997; Neu, 1992; Travis, 1994).

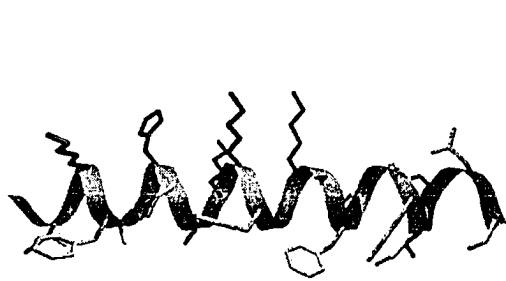
IB-3 Discovery of antimicrobial peptides

Although two groups of peptide antibiotics were discovered some time ago — namely, the gramicidins and the polymyxins, the major discovery of antimicrobial peptides was made in the late 1970s (Boman, 1991). At the beginning of the discovery, antimicrobial peptides were found in several different types of animals (frogs, moths, bees) as part of their innate immune systems (Boman, 1991); then, more and more antimicrobial peptides have been found from organisms throughout the phylogenetic tree for protection against microbes (Andreu *et al.*, 1998). It is clear that as relative latecomers to a world inhibited by prokaryotic microorganisms, only those animal and plant species able to prevent and overcome infections were likely to survive. Antimicrobial peptides were well involved in the host-defense mechanisms as

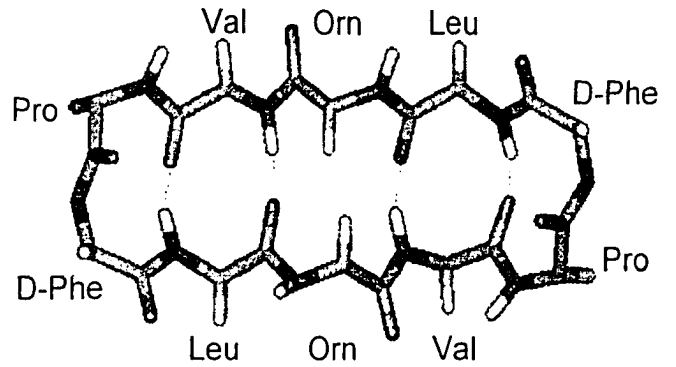
microorganism killers, exhibiting rapid killing effects (seconds to minutes *versus* hours for conventional antibiotics) across a broad spectrum of Gram-negative and Gram-positive microorganisms.

IB-4 Structural and physical characteristics of antimicrobial peptides

Antimicrobial peptides are generally small (11-50 amino acids) and positively charged (a net positive charge of +2 or more) due to the presence of excess basic residues (lysine or arginine) over acidic residues (Hancock *et al.*, 1995). Based on their secondary structure (as shown in Figure I-8), these peptides fit into four major classes: (i) α -helical peptides, including cecropins (Boman *et al.*, 1989; Christensen *et al.*, 1988; Piers *et al.*, 1994; Steiner *et al.*, 1981; Zhao *et al.*, 1997), magainins (Bechinger, 1997; Jacob *et al.*, 1994; Matsuzaki, 1999; Zasloff, 1987) and melittins (Andreu *et al.*, 1992; Shin *et al.*, 1997; Tosteson *et al.*, 1985); (ii) β -sheet structures stabilized either by two or three intramolecular disulfide bonds, *e.g.*, defensins (Ganz *et al.*, 1994), protegrins (Steinberg *et al.*, 1997), thionins (Stein *et al.*, 1999), tachyplesins (Iwanaga *et al.*, 1994), or by an N-terminal to C-terminal covalent bond forming a cyclic β -sheet peptide, *e.g.*, gramicidin S (Kondejewski *et al.*, 1996) and tyrocidines (Mootz *et al.*, 1997); (iii) extended helices with a predominance of one or more amino acids, *e.g.*, polyprohelicines (Falla *et al.*, 1996); and (iv) loop structures, *e.g.*, bactenecin and polymyxins (Wu *et al.*, 1999). Most well studied cationic antimicrobial peptides belong to the α -helical and β -sheet categories, the former generally existing as disordered structures in aqueous medium and becoming helical upon interaction with hydrophobic solvents or phospholipid vesicles (Blondelle *et al.*, 1999). In contrast, β -sheet peptides are far more constrained in this conformation,



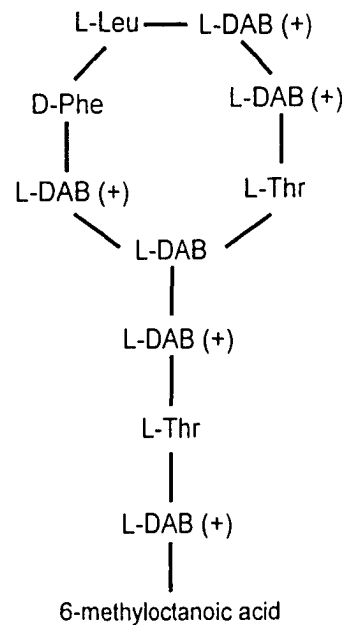
α -helical structure
(magainin)



cyclic structure
(gramicidin)



β -sheet structure
(protegrin)



loop structure
(polymyxin B)

Figure I-8 Antimicrobial peptides with different secondary structures

either by disulfide bonds or by cyclization of the backbone. Although they may be further stabilized in a non-polar environment, β -sheet peptides exist largely in a "preformed" β -sheet conformation in aqueous environments due to their structural constraints (Blondelle *et al.*, 1999).

IB-5 Proposed mechanisms of action

Many models have been proposed for the mechanism of action of antimicrobial peptides, including the barrel-stave mechanism, the carpet mechanism, the toroid pore or wormhole mechanism and the in-plane diffusion model. The mechanism by which these peptides induce permeability and traverse the microbial membranes is likely to differ for various antimicrobial peptides and the membrane environments in which they are studied. In brief, the barrel-stave mechanism describes the formation of transmembrane channels/pores by bundles of amphipathic α -helices, as their hydrophobic surfaces interact with the lipid core of the membrane and the hydrophilic surfaces point inward, producing an aqueous pore (Ehrenstein *et al.*, 1977); in contrast, the carpet model was proposed for the first time to describe the mechanism of action of dermaseptin S (Pouny *et al.*, 1992), describing the contact of antimicrobial peptides with the phospholipid head group throughout the entire process of membrane permeation which occurs only if there is a high local concentration of membrane-bound peptide. The major difference between the two mechanisms is, in the carpet model, peptides are not inserted into the hydrophobic core of the membrane, and neither do they assemble the aqueous pore with their hydrophilic faces, that is, the peptides lie parallel with the membrane surface. The toroid model is an adaptation of the barrel-stave model (Ludtke *et al.*, 1996; Matsuzaki,

1998). In the barrel-stave model, a large amount of positive charge is confined to a small space, facing the interior of pore/channel. In the toroid model, the negatively charged headgroups of lipids separate this charge, thus forming a transient supramolecular membrane-spanning complex with interior surface composed of polar and charged peptide side-chains and phospholipid head groups. For the in-plane diffusion model (Bechinger, 1997), membrane-associated peptides disturb the lipid packing over a large surface area. By diffusion of the antimicrobial peptides, these disturbances can overlap, resulting in the collapse of lipid packing and inducing temporary openings in the membrane.

Due to their diverse mode of action in biological environments, no general mechanism can be proposed for the biological activity of peptide antibiotics. Indeed, it is known that the extent of interaction between peptide and biomembrane is dependent on the composition of the lipid bilayer. Cell membranes composed predominantly of phosphatidylglycerol (PG), cardiolipin (CL) or phosphatidylserine (PS) tend to be highly negatively-charged; such compositions are found in many bacterial pathogens. In contrast, bilayers enriched in the zwitterionic phospholipids phosphatidylethanolamine (PE), phosphatidylcholine (PC) or sphingomyelin (SM), commonly found in mammalian cytoplasmic membranes, are generally neutral in net charge. Indeed, mammalian cytoplasmic membranes generally contain no or extremely low levels of the negatively-charged lipids PG and CL. Koppelman *et al.* (Koppelman *et al.*, 2001) have demonstrated that the cytoplasmic membrane of *E. coli* is substantially more enriched in CL than previously known. From these perspectives, composition likely provides an important determinant by which antimicrobial peptides target microbial versus host membranes. In

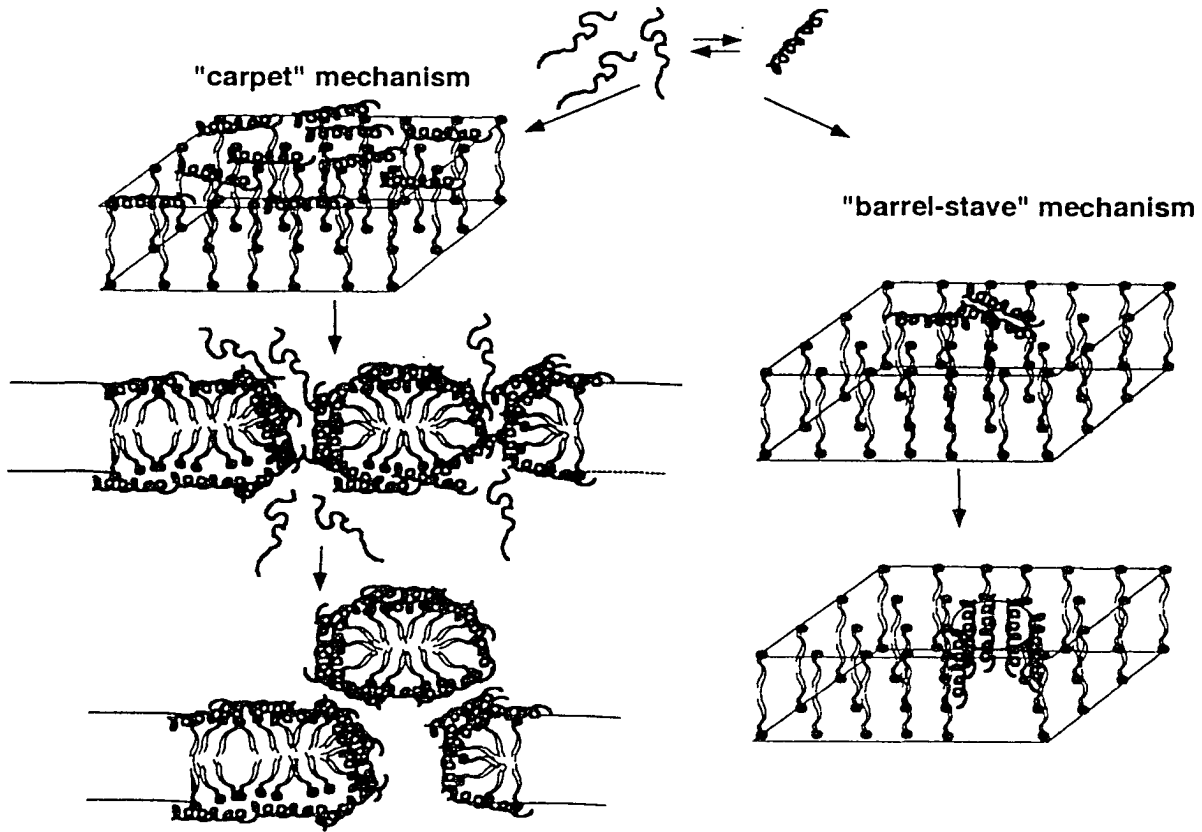


Figure I-9 Representation of the "barrel-stave" (right) and the "carpet" (left) models for membrane permeation (adapted from Shai, Y. 1999).

addition, recent evidence indicates that the distribution of phospholipids within cytoplasmic membranes of eukaryotic and prokaryotic cells is highly asymmetric (Florin-Christensen *et al.*, 2001); for example, only 2% of the total PE content in bovine erythrocytes is oriented toward the outer membrane leaflet. The differences of lipid composition and distribution between eukaryotic and prokaryotic cells may have great influence on the antimicrobial specificity of peptide antibiotics.

Although the cytoplasmic membrane is a major target of antimicrobial peptides, there is also evidence that antimicrobial peptides exert their activities through mechanisms other than membrane permeabilization. However, it is not easy to differentiate these other activities from secondary events arising from membrane permeabilization. For instance, some antimicrobial peptides have been proposed, to inhibit the synthesis of specific membrane proteins (Axen *et al.*, 1997; Engstrom *et al.*, 1984), to block the synthesis of DNA (Boman *et al.*, 1993), to break single-strand DNA (Bateman *et al.*, 1991) or to produce hydrogen peroxide (Leem *et al.*, 1996). Antimicrobial peptides have also been reported to trigger self-destructive mechanisms such as apoptosis in eukaryotic cells (Velasco *et al.*, 1997; Yoo *et al.*, 1997) or autolysis in bacterial targets (based on activation of amidases that degrade the peptidoglycan) (Sahl, 1994).

Traditional antibiotics kill bacteria in a highly specific fashion, by entering the cell interior and binding to a biomolecule both specific for the microorganism and necessary for cell survival, such as a cell wall component or an enzyme involved in transcription, translation, or metabolism. Although killing is not immediate, the interruption of bacterial metabolic processes eventually leads to cell death over the days

following the initial antibiotic treatment. Unfortunately, the high specificity of antibiotics provides a way for bacteria to become resistance to traditional antibiotics. In contrast, although the exact mode of action of antimicrobial peptides has not been established, it has been proposed that the cytoplasmic membrane is the main target of these peptides, where peptide accumulation in the membrane causes increased permeability and loss of barrier function (Duclohier *et al.*, 1989; Hancock *et al.*, 1998). For the antimicrobial peptides whose sole target is the cell membrane, the development of resistance to these membrane active peptides would not be expected because this would require substantial changes in the lipid composition of cell membranes. Since both their mode of action and cellular targets are different from those of traditional antibiotics, cationic antimicrobial peptides represent a truly new class of antibiotics. From numerous structure/activity studies on both natural and synthetic antimicrobial peptides, a number of factors believed to be important for antimicrobial activity have been identified: the presence of both hydrophobic and cationic residues, an inducible or preformed secondary structure (α -helical or β -sheet), and an amphipathic nature that segregates basic and hydrophobic residues to opposite sides of the molecule in lipid or lipid-mimicking environments (Blondelle *et al.*, 1999; Hancock, 1997; Hancock *et al.*, 1998). This amphipathic structural feature is believed to play a key role in the antimicrobial mechanism of action, with the hydrophilic (positively charged) domain of the peptide proposed to initiate peptide interaction with the negatively charged bacterial surface and the negatively charged headgroups of bilayer phospholipids. The hydrophobic domain of the amphipathic peptide would then permit the peptide to enter the membrane interior (Bechinger, 1997; Blondelle *et al.*, 1999; Epanand *et al.*, 1999).

IB-6 Drawbacks of antimicrobial peptides as therapeutics

Compared with traditional antibiotics, there are some fundamental drawbacks of antimicrobial peptides which have prevented their development as therapeutics. Since the specific molecules targeted by the traditional antibiotics are generally not present in human cells, the antibiotics have lower toxicity to the patient. In contrast, antimicrobial peptides interact with the general cytoplasmic membranes (the reason for the broad antibacterial spectrum) and, thus, are also toxic to eukaryotic cell membranes, normally expressed as hemolytic activity (toxicity to human red blood cells), which is the main reason preventing their applications as injectable therapeutics. In addition, due to enzymatic proteolysis *in vivo*, oral bioavailability of antimicrobial peptides may be low. Cationic charges on the majority of antimicrobial peptides, necessary to initialize peptide-lipid interaction during the mechanism of action, may also be screened by the presence of a high salt concentration, resulting in decreasing antimicrobial activity in high salt environments such as the mucus-covered lungs of cystic fibrosis patients (Goldman *et al.*, 1997).

IB-7 Peptide V₆₈₁

Zhang *et al* reported that by utilizing a semi-random mutagenesis technique, they obtained a series of active variants of an antimicrobial peptide CP2600 (Zhang *et al.*, 1998) (also named V26p (Zhang *et al.*, 1999)). V₆₈₁ is one of the variants of CP2600. As studied by Zhang and coworkers (Zhang *et al.*, 1999), in aqueous medium, V₆₈₁ is an unstructured peptide, whilst, in a non-polar environment, this 26-residue peptide is an amphipathic α -helical peptide. Upon addition to liposomes, fluorescence quenching

experiments indicate a relocation of the peptide into a more hydrophobic environment. Also, CD data demonstrate that V₆₈₁ exhibits an α -helical structure in liposomes with more than 90% α -helical content. V₆₈₁ exhibits a very high biological activity against all Gram-positive and Gram-negative bacteria with minimal inhibitory concentration (MIC) values ranging from 0.5 to 4 μ g/ml (Zhang *et al.*, 1999). However, the peptide is also highly hemolytic and lyses red blood cells at 8 μ g/ml. V₆₈₁ also showed an extremely high membrane permeabilization activity upon the NPN uptake assay. Therefore, this peptide is ideal for our antimicrobial peptide stability and biological activity study.

IB-8 *De novo* peptide design

We believe that a synthetic peptide approach to examining the effect of small incremental changes in hydrophobicity/hydrophilicity, amphipathicity and helicity of cationic antimicrobial peptides will enable rapid progress in rational design of peptide antibiotics. Our previous studies have successfully utilized such an approach to dissociate antimicrobial and hemolytic activities of *de novo* designed cyclic β -sheet gramicidin S analogs, by systematic alterations in amphipathicity through D-amino acid substitutions (Kondejewski *et al.*, 1999; Lee *et al.*, 2003a; Lee *et al.*, 2004). In recent work, we demonstrated that the helix-destabilizing properties of D-amino acids offer a systematic approach to the controlled alteration of the hydrophobicity, amphipathicity, and helicity of amphipathic α -helical model peptides (Chen *et al.*, 2002). By substituting different D-amino acids into the center of the hydrophobic face of an amphipathic α -helical model peptide, we demonstrated that different D-amino acids destabilized α -helical structure to different degrees, whilst the destabilized structure was still inducible to α -helix in

hydrophobic medium. The advantage of this method of single D- or L-amino acid substitutions at a specific site is to reduce the complexity of understanding the mechanism of action of these peptides.

In this thesis, peptide V₆₈₁ was used as the ideal framework for our antimicrobial peptide study of hydrophobicity/amphipathicity, stability and biological activity. By employing a rational approach to design V₆₈₁ analogs with varying hydrophobicity/amphipathicity and stability, we can obtain valuable information to explain the mechanism of action of α -helical antimicrobial peptides. In addition, since hemolytic activity is the main restriction of antimicrobial peptides being used clinically (Hancock, 1997; Hancock, 1998; Hancock *et al.*, 1995; Hancock *et al.*, 1998), the high hemolytic activity of V₆₈₁ also gives us a chance to study whether changing peptide hydrophobicity/amphipathicity and stability can help to dissociate hemolytic activity and antimicrobial activity in a similar fashion to that observed for cyclic β -sheet peptides (Kondejewski *et al.*, 1999).

CHAPTER II

Objectives, Hypotheses and Overview

Although this thesis describes studies on two major fields: HPLC methodology development and development of new antimicrobial peptides (as shown in Figure II-1), there are complementary aspects to these sections. *De novo* designed model peptides of different secondary structures were utilized in the development of HPLC methodology, in order to gain a better understanding of the retention behavior of peptides during RP-HPLC and HILIC/CEX. In the second major part of the thesis, the potent antimicrobial peptide V₆₈₁ was used as the structural framework in the development of α -helical antimicrobial peptides with improved biological activity and specificity. Both sections employ *de novo* approach of peptide design. More importantly, the methods and results of the HPLC methodology development strongly support the latter antimicrobial peptide studies.

Chapter IV presents the study of varying column packing, mobile phase conditions and temperature on the RP-HPLC retention behavior at pH 2.0 and pH 7.0 of peptides based on the amphipathic α -helical peptide sequence Ac-EAEKAAKEXEKAAKEAEK-amide, where position X is substituted by different L- and D-amino acids. The objective of this study was to understand the effects of varying RP-HPLC parameters on the retention behavior of peptides, necessary for the rational development of separation/optimization protocols.

In order to characterize the effect of temperature on the retention behavior and selectivity of separation of polypeptides and proteins in RP-HPLC, the chromatographic properties of four series of peptides, with two different peptide conformations (random

Thesis Research

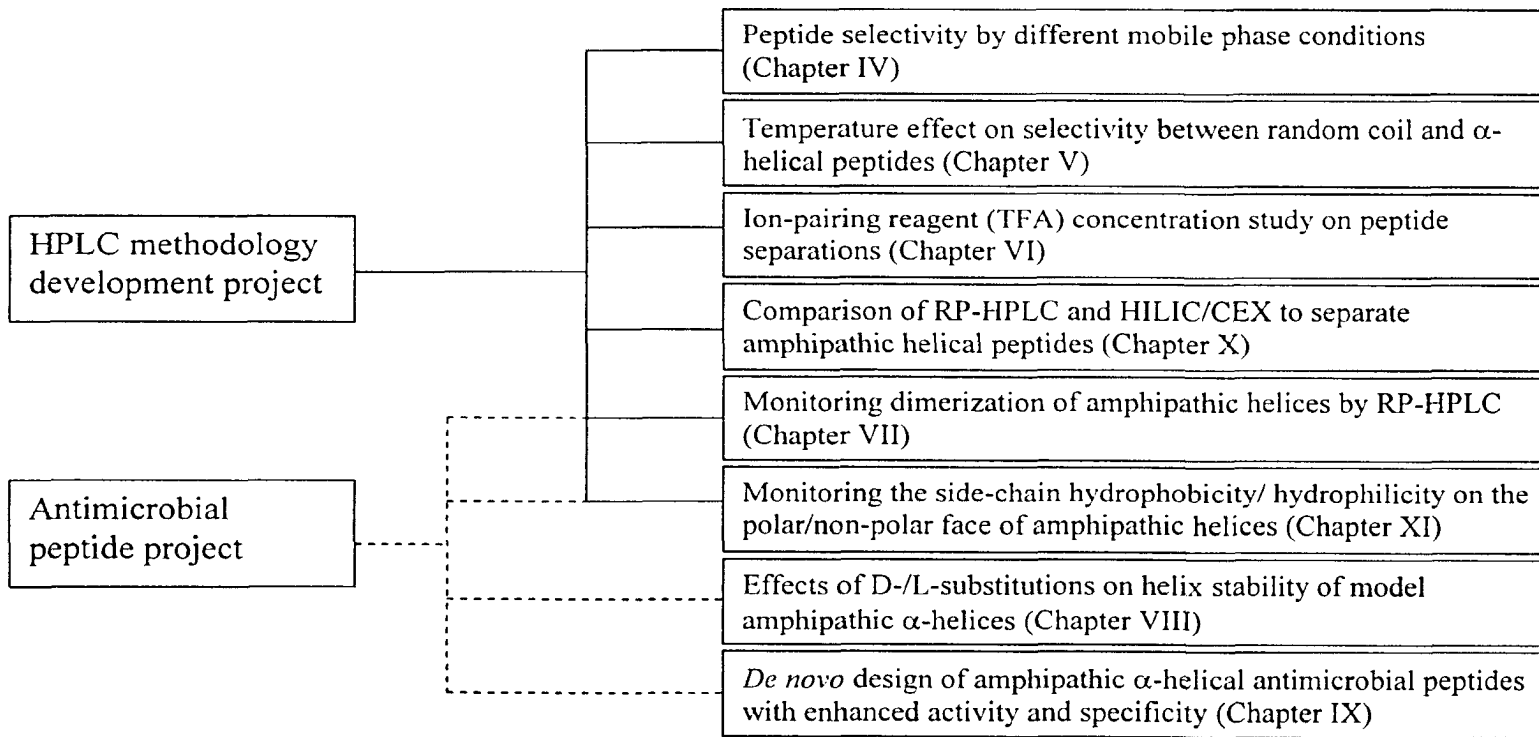


Figure II-1 Schematic diagram of the studies in this thesis

coil and α -helical structure), were studied as a function of temperature (5-80 °C), described in Chapter V. Our hypothesis was that, since α -helical peptides may unfold during increasing temperature, temperature would thus have greater effect on the selectivity of α -helical peptides compared with random coil peptides.

In Chapter VI, the objective of this study was to find out the optimum concentration of TFA for peptide separations. Routine use of higher TFA concentrations has generally been avoided, partially due to the concern of stationary phase degradation. However, with the advent of reversed-phase packings with superior stability towards both acidic mobile phases and high temperature, such concern has been overcome. Our hypothesis was that the traditional range of TFA concentrations employed for peptide studies (0.05%-0.1%) may not be optimum for many, perhaps the majority, of peptide separations.

One of the most interesting developments of liquid chromatography in recent years has been the emergence of RP-HPLC as a physicochemical probe of peptide and protein structure. The study in Chapter VII sets out to extend the utility of RP-HPLC to monitor dimerization and unfolding of *de novo* designed synthetic amphipathic α -helical peptides of varying hydrophobicity when run at temperatures ranging from 5 to 80 °C. Although peptides are eluted from a reversed-phase column mainly by an adsorption/desorption mechanism, peptides bound to a hydrophobic stationary phase will partition between the aqueous mobile phases in equilibrium with its bound state in a narrow range of acetonitrile concentrations during gradient elution. The rationale for monitoring peptide dimerization and unfolding by temperature profiling during RP-HPLC is based on several criteria described in detail in Chapter VII.

We believed that a step-by-step synthetic peptide approach to examining the effect of small incremental changes in hydrophobicity, amphipathicity and stability of cationic antimicrobial peptides would enable rapid progress in rational design of peptide antibiotics. With this in mind, we began by studying model α -helical peptides. In Chapter VIII, we describe a systematic study to determine the effect on secondary structure of D-/L-amino acid substitutions in the non-polar face of a *de novo* designed amphipathic α -helical model peptide. The objective of this study was to determine and quantify the inherent helix stability coefficients as well as helix stereochemistry stability coefficients due to the varying D-/L-amino acid substitutions. Our hypotheses were that, (1) by introducing different L-amino acids into the center of non-polar face of the helix, there would be varying changes of peptide apparent hydrophobicity and peptide conformation; and (2) although different D-amino acid substitutions will disrupt α -helical structure to different degrees in an aqueous medium, helical structure may still be induced in a hydrophobic environment of the membrane.

Based on the results from the study in Chapter VIII, we designed *de novo* a series of antimicrobial peptides with improved specificity in Chapter IX. The objective of this study was to improve the antimicrobial activity and specificity by altering the hydrophobicity/hydrophilicity, amphipathicity and stability of the α -helical structure. Our hypotheses were that: (1) disruption of α -helical structure in benign medium by D-amino acid substitutions, followed by helix induction in a hydrophobic environment, may increase biological activity and specificity; (2) single D-amino acid substitutions may dissociate the hemolytic and antimicrobial activities; and (3) altering the hydrophobicity/ hydrophilicity and amphipathicity of the peptides may improve the

antimicrobial activity and/or decrease the hemolytic activity, which improves specificity (therapeutic index).

The antimicrobial peptides with different hydrophobicity/hydrophilicity are also perfect models to compare the resolving power of HILIC/CEX and RP-HPLC for separation of mixtures of diastereomeric amphipathic α -helical peptide analogs. The objectives in Chapters X and XI were: (1) to monitor the hydrophobicity/hydrophilicity of amino acid side-chains in the non-polar and polar faces of amphipathic α -helices by RP-HPLC and HILIC/CEX; (2) to compare RP-HPLC and HILIC/CEX as complementary techniques in separating amphipathic α -helical peptides.

In general, in this thesis, we explored and optimized the separation methodology of RP-HPLC and HILIC/CEX, in order to improve the present methods of peptide/protein separation/optimization protocols, which are important to routine peptide/protein studies, and peptide/protein structure and function studies, as well as proteomic applications. In addition, since RP-HPLC has been well utilized as a sensitive physicochemical probe for peptide structures, RP-HPLC studies will also help to understand the hydrophobic interactions between peptides with different conformations and non-polar environments. Furthermore, we employed the results of peptide hydrophobicity/hydrophilicity and amphipathicity from model peptides during RP-HPLC to design α -helical antimicrobial peptides. The novel technique of temperature profiling during RP-HPLC was also demonstrated to be valuable in the determination of peptide association ability in solution, which proved important to the biological activities of antimicrobial peptides.

CHAPTER III

General Methods and Materials

III-1 Materials

All solutions were prepared in HPLC-grade water purchased from EMD Chemicals (Gibbstown, NJ) or prepared by an E-pure water purification system from Barnstead International (Dubuque, IA).

Table III-1 List of materials

Regent	Suppliers
acetic anhydride	Fisher Scientific (Fair Lawn, NJ)
acetonitrile (HPLC-grade)	EM Science (Gibbstown, NJ)
anisole	Aldrich (Oakville, ON, Canada)
<i>o</i> -benzotriazol-1-yl- <i>N,N,N',N'</i> -tetramethyluronium hexafluorophosphate (HBTU)	Advanced ChemTech (Louisville, KY)
<i>t</i> - <i>boc</i> -protected (tert-butylloxycarbonyl) amino acids	Advanced ChemTech (Louisville, KY)
diethyl ether	Fisher Scientific (Fair Lawn, NJ)
diisopropylethylamine (DIEA)	Caledon (Georgetown, ON, Canada)
dimethylformamide (DMF)	FisherBiotech (Fair Lawn, NJ)
1,2-ethanedithiol (EDT)	Aldrich (Oakville, ON, Canada)
hydrogen fluoride (HF)	Matheson Tri-Gas (Newark, CA)
<i>N</i> -hydroxybenzotriazole (HOBt)	Novabiochem (La Jolla, CA)
4-methylbenzhydrylamine resin hydrochloride salt (MBHA)	Advanced ChemTech (Louisville, KY)
orthophosphoric acid	Anachemia (Toronto, ON, Canada)
potassium phosphate, dibasic	Fisher Scientific (Fair Lawn, NJ)
potassium phosphate, monobasic	Fisher Scientific (Fair Lawn, NJ)
sodium perchlorate	FisherBiotech (Fair Lawn, NJ)
triethylamine (TEA)	Anachemia (Toronto, ON, Canada)
trifluoroacetic acid (TFA)	Halocarbon Products Corp. (River Edge, NJ)
2,2,2-trifluoroethanol (TFE)	Sigma (St. Louis, MO)

III-2 Solid-phase peptide synthesis (SPPS)

The major two methods of synthesis of peptides are solution-phase synthesis and solid-phase synthesis. SPPS now dominates synthetic peptide chemistry, and today the majority of peptides are made by this method. In this technique, a growing peptide chain is covalently linked to an insoluble polymeric support and amino acids are added sequentially to the N-terminus (Figure III-1). Thus, SPPS is carried out in the direction of C-terminus to N-terminus in contrast to the N-terminal to C-terminal order observed during ribosomal biosynthesis of proteins.

The peptides used in this thesis were synthesized either automated by an Applied Biosystems Model 430A peptide synthesizer (Foster City, CA) (Sereda *et al.*, 1994) or manually by the conventional *tert*-butyloxycarbonyl (*t*-Boc) amino acid solid-phase peptide synthesis methodology using methylbenzhydrylamine resin as described previously (Litowski *et al.*, 1999). There are four major steps involved in the solid-phase synthesis of peptides, including anchoring, deprotection, coupling and cleavage.

The anchoring step indicates the procedure of anchoring the first amino acid residue to the polymeric resin support through a preattached handle moiety. The types of handles determine the peptide C-terminal groups after the cleavage step. The C-terminal amide groups of all the peptides in this thesis required the handle with an active amino moiety which can couple with the carboxylate group of amino acids. Methylbenzhydrylamine resin used in this study is physically stable and is first allowed to swell in solvents such as dichloromethane (DCM) and dimethylformamide (DMF). The peptides were attached via an acid-labile amide bond which then can be cleaved with HF, yielding peptide amide products.

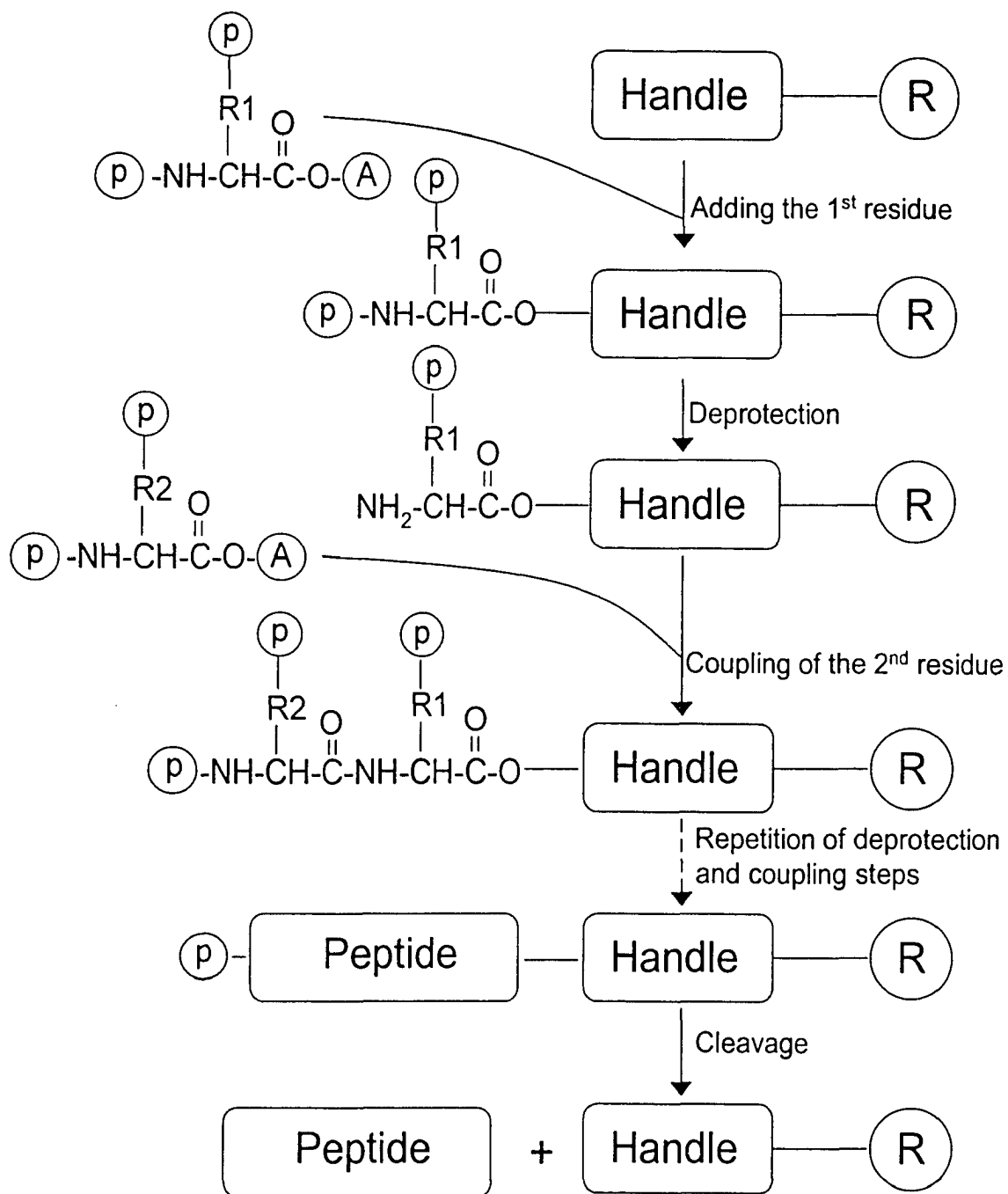


Figure III-1 Schematic diagram of solid-phase peptide synthesis. The polymeric resin support is labeled as **R**, the amino acid protecting groups (for side-chain protection and N-terminal protection) are labeled as **P**, the C-terminal activating groups are labeled as **A**.

In order to avoid unfavorable side reactions, the N-terminal α -amine was protected. After the attachment of the C-terminus to the resin, the N-terminal amine must be deprotected to allow the formation of a peptide bond with the subsequent amino acid residue. Generally, two types of N^α -protecting groups are used: *t*-Boc and 9-fluorenylmethoxycarbonyl (Fmoc) groups, which are acid and base labile, respectively. As previously mentioned, only *t*-Boc chemistry was used in this thesis. The Boc-group was removed with 50% (v/v) TFA/DCM to expose the active N-terminal amine group, and usually neutralized with diisopropylethylamine (DIEA), a tertiary amine (Figure III-2).

The coupling step involves a nucleophilic attack of a free N-terminal amine of the growing peptide chain upon an activated carboxyl group of the subsequent amino acid residue to be added. Due to the low reactivity, the carboxyl group has to be activated first by changing the hydroxyl group to an electron-withdrawing substituent to facilitate nucleophilic attack by the amine. A number of reagents are available for both *in situ* and preactivation of the amino acid (Albericio *et al.*, 1997; Novabiochem, 2004). Two commonly used examples are dicyclohexylcarbodiimide (DCC) and *o*-benzotriazol-1-yl-N,N,N',N'-tetramethyluronium hexafluorophosphate (HBTU). The coupling reagent used in this study is HBTU, which reacts with the α -carboxyl group to form the activated *o*-benzotriazolyl ester (Figure III-3). In the current study, an auxiliary nucleophile, N-hydroxybenzotriazole (HOBt) was added to the reaction to increase reaction rate and reduce side reactions. Activation and coupling were performed *in situ* by dissolving a 5-fold molar excess of amino acid (compared with resin) in DMF and activating with equal molar amounts of HBTU and HOBt and a 6-fold molar excess of DIEA (Figure III-3). D-

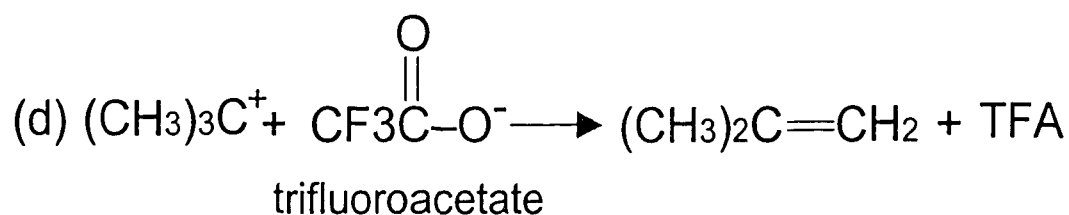
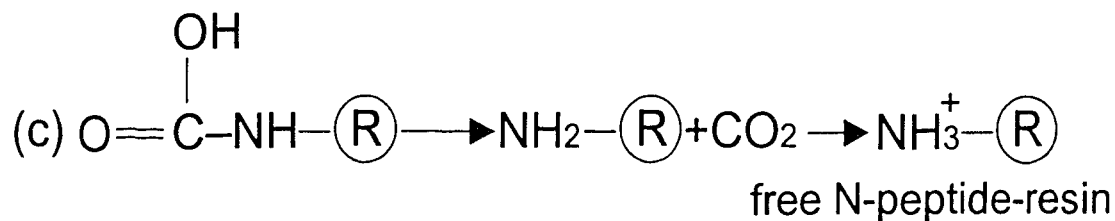
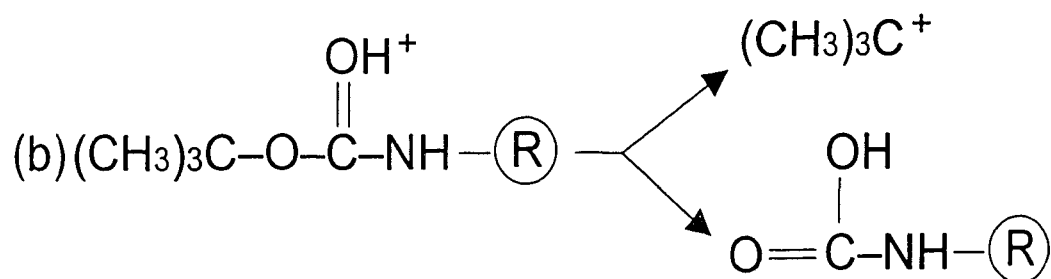
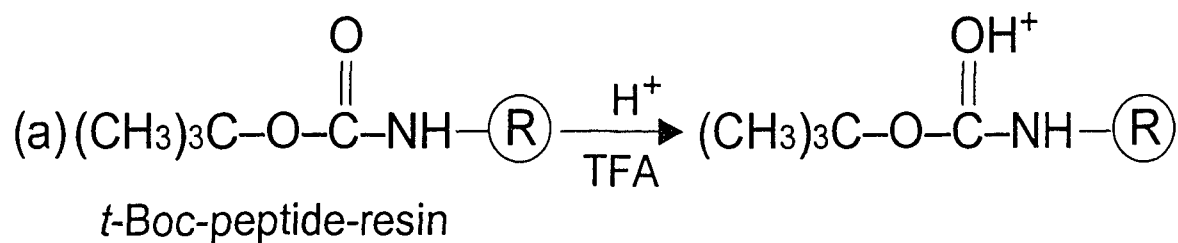


Figure III-2 TFA catalyzed removal of the *t*-Boc group. The polymeric resin support is labeled as **R**.

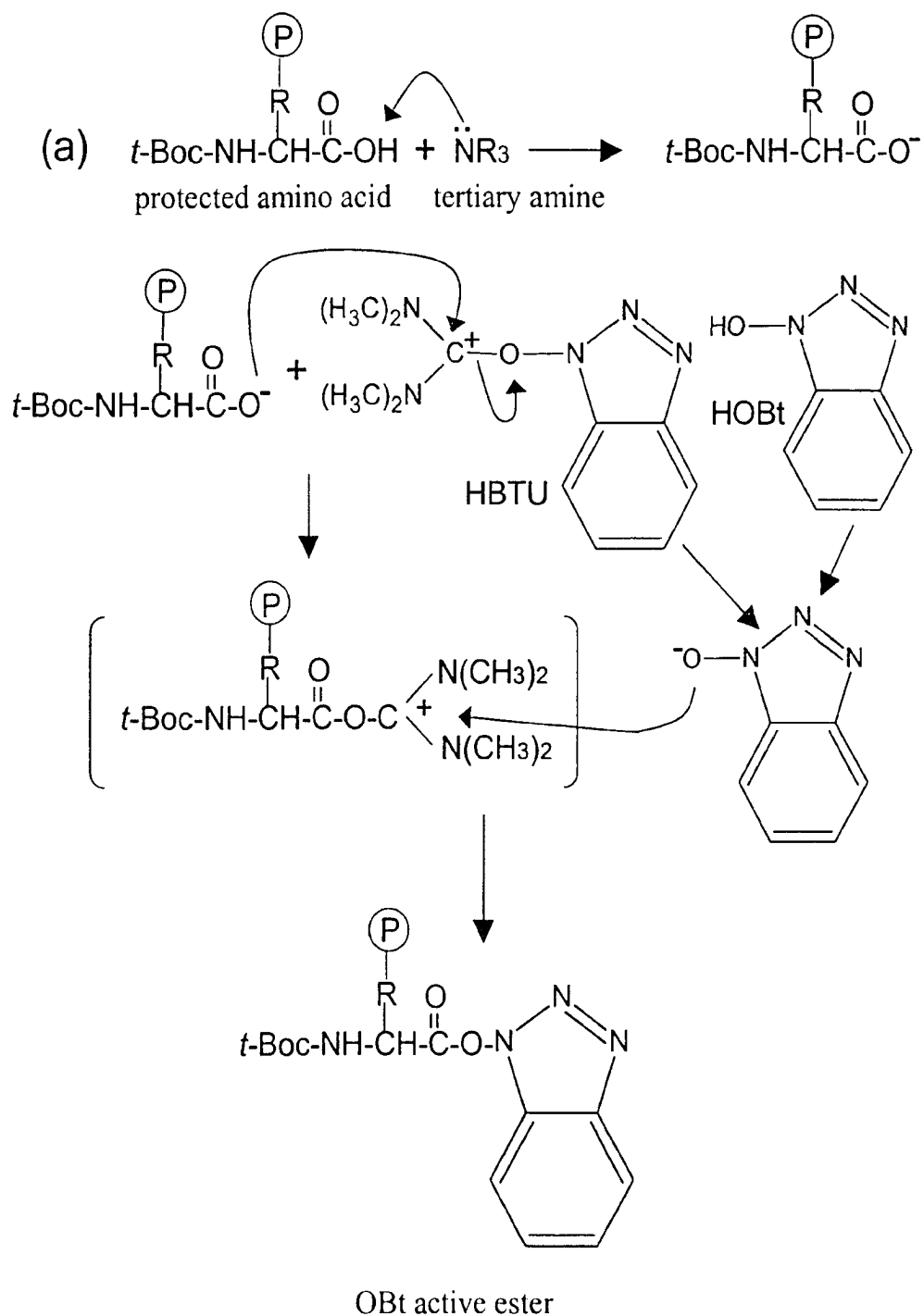


Figure III-3 (continued on the next page)

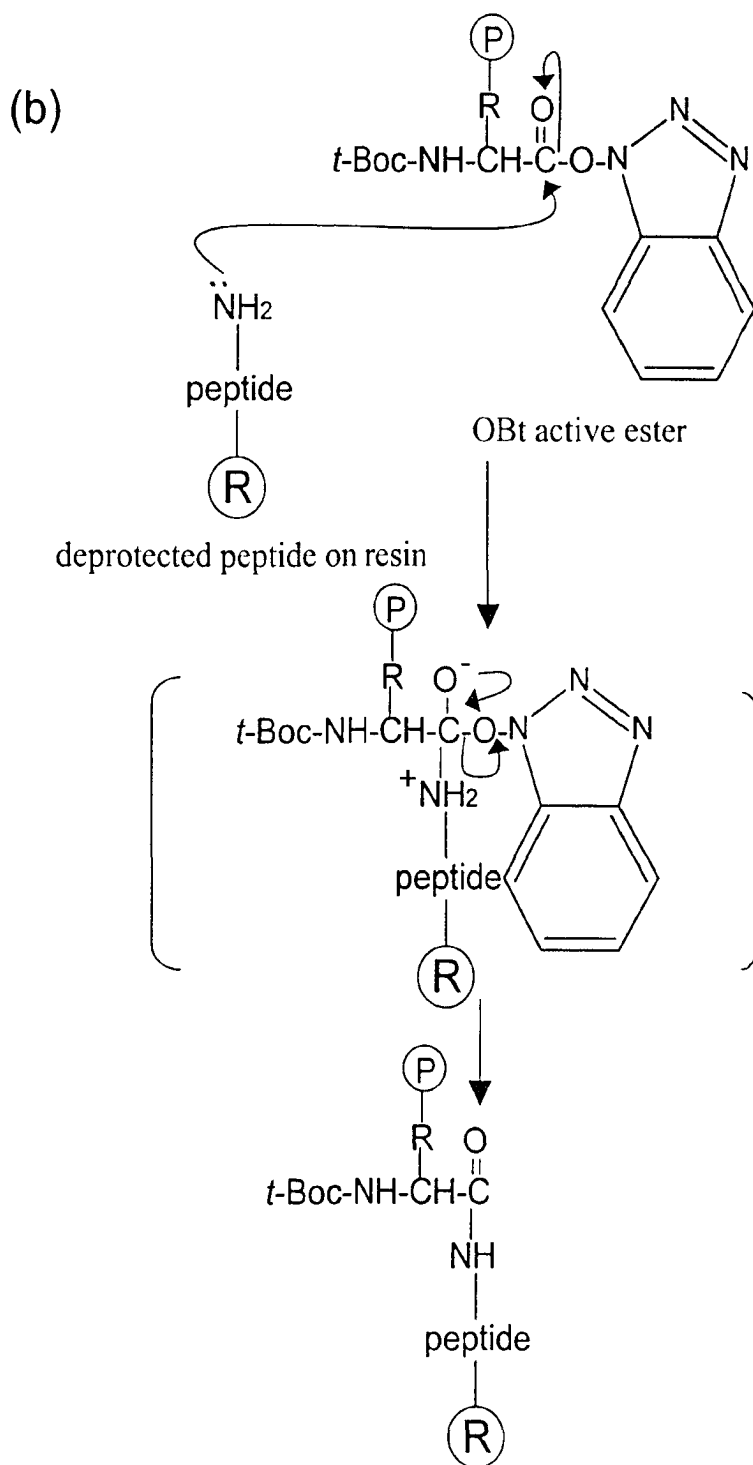


Figure III-3 (a) HBTU activation and (b) amino acid coupling during SPPS. Resin is labeled as **R**, the side-chain protecting group on the amino acid is labeled as **P**.

amino acid residues, in this thesis, were coupled in a significant longer time period to ensure the efficiency of coupling.

The ninhydrin test for reactive amines was performed at 120 °C. In brief, the primary free amines yield a blue/purple color due to the reaction with ninhydrin and hydrindantin; and the reaction with secondary amines (*e.g.*, proline) yields an orange color. The test is highly sensitive and can detect samples containing less than 0.5% of unreacted amine groups (Sarin *et al.*, 1981). In the event of a test with a positive result, the coupling reaction was repeated for a longer time and the ninhydrin test was repeated.

Repetitive deprotection and coupling steps ensure the stepwise elongation of the peptide chain. Once the peptide chain was complete, in this study, the N-terminal group was acetylated by reaction with 10% acetic anhydride in 20% DIEA/70% dichloromethane (*v/v/v*). The peptide was then cleaved from the resin with the strong acid, anhydrous HF (30ml/g resin), in a specially designed sealed Teflon apparatus at -5°C to 0°C for 1 hour. The side-chain protecting groups of amino acid residues were removed simultaneously with cleavage from the resin. Anisole was added as a scavenger to trap the released protecting groups, in order to prevent irreversible reattachment to the peptide. After cleavage, the resin and peptide mixture was washed with ethyl acetate to remove organic contaminants. The crude peptide was then extracted with acetonitrile from the resin and lyophilized.

III-3 Peptide purification by preparative RP-HPLC

The practical need for scalar extrapolation from analytical to semi-preparative and ultimately to the preparative separation of synthetic peptides has been well documented

(Rivier *et al.*, 1984; Sitrin *et al.*, 1986). Crude synthetic peptides are generally generated in large quantities and when obtained using a solid-phase peptide synthesis approach for example, can contain undesired impurities, yet these impurities are more likely to be very closely associated (in sequence) to the desired peptide. In fact, the crude peptidic preparations may contain the desired product as only a small fraction (1 to 70%) of the total (Mant *et al.*, 1991). Since the peptidic impurities cannot be tolerated for most physico-chemical and biological studies, we have spent considerable effort on the optimization of chromatographic methods directed at the purification of crude peptide mixtures.

The excellent resolving power and separation time of reversed-phase chromatography, coupled with the availability of volatile mobile phases, has made this mode of HPLC the favored method for preparative separation of peptides. Similar to analytical reversed-phase chromatography, preparative RP-HPLC can be optimized by alterations of varying HPLC parameters, such as column packings, mobile phase conditions including the solvents, gradient rate, flow rate and pH, *etc.*

Due to the large scale of peptide samples, most researchers would probably desire to increase the column volumes. Therefore, a column of preparative RP-HPLC is generally larger and longer than an analytical reversed-phase column. The column used in this thesis is a semi-preparative column with 250x9.4mm I.D., 6.5 μ m particle size, 300Å pore size (compared with an analytical column with 150x4.6 mm I.D.; 5 μ m particle size, 300Å pore size). Gradient rate is a practical parameter to improve the resolving power of HPLC. According to Burke *et al.*, a shallow gradient approach on a preparative column can be used to separate closely-related peptides (Burke *et al.*, 1991).

The gradient rate used in this thesis was generally 0.2% acetonitrile per minute (Figure III-4), although a shallower gradient (0.1% acetonitrile/min) was applied to crude peptide samples with closely-related deletions. In these studies, a flow rate of 2 ml per minute of mobile phase was used on the semi-preparative column.

In this thesis, after cleavage from the resin, the crude peptides were purified by preparative RP-HPLC on a Varian Vista Series 5000 Liquid Chromatograph (Varian, Walnut Creek, CA, USA) using a semi-prep Zorbax 300 SB-C₈ column (250x9.4mm I.D.; 6.5µm particle size, 300Å pore size; Agilent Technologies, Brockville, Ontario, Canada) with a linear AB gradient (0.2% acetonitrile/min) at a flow rate of 2 ml/min, where mobile phase A was 0.1% *aq.* trifluoroacetic acid in water and B was 0.1% TFA in acetonitrile. The peptides were further characterized by analytical RP-HPLC, electrospray mass spectrometry and amino acid analysis.

III-4 Analytical RP-HPLC

Analytical RP-HPLC in this thesis was carried out on an HP 1100 Liquid Chromatograph (Hewlett-Packard, Avondale, PA, USA), coupled with an HP 1100 series diode array detector and thermostatted column compartment, HP Vectra XA computer and HP LaserJet 5 printer. The background to analytical RP-HPLC has been discussed in depth in the introduction (Chapter I). The experimental details of using analytical RP-HPLC, including the column, mobile phases and running conditions, are described in each individual study as specific experimental methods.

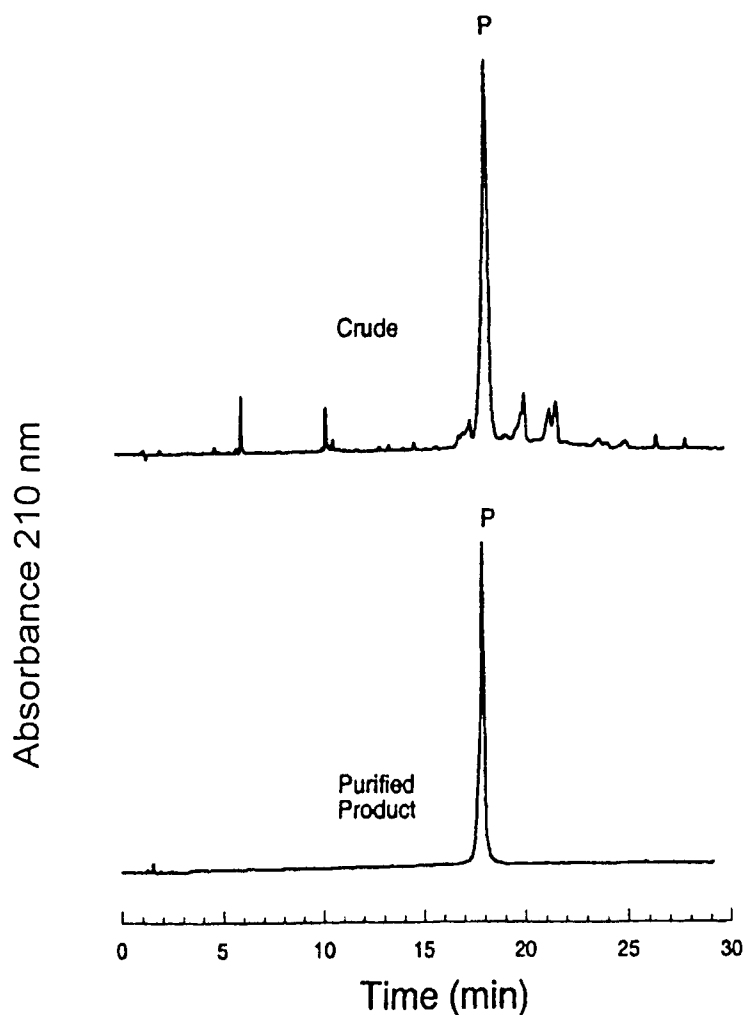


Figure III-4 RP-HPLC analysis comparison of the crude peptide and the peptide after purification. Column, instrumentation and run conditions are described in the Experimental section of Chapter VIII. The sequence of the peptide is acetyl-EAEKAAKESKAAKEAEK-amide, which was denoted as peptide S_L in Chapter VIII.

III-5 Amino acid analysis

Amino acid analysis was utilized to determine the concentration of peptides in solutions. The purified peptides were hydrolyzed in 6N HCl (including 0.1% phenol) at 160 °C for 1.5 hour in sealed evacuated tubes. Analysis was carried out on a Beckman System 6300 Amino Acid Analyzer (Beckman, San Ramon, CA). The mechanism of this amino acid analyzer is based on cation exchange chromatography and post column ninhydrin derivatization. Peptides are eluted based on net charge and hydrophobicity. Typical runs consist of a series of three buffers: 0.2 M sodium citrate, pH 3; 0.2 M sodium citrate, pH 4.3; and 0.35 M sodium citrate, 0.75 M NaCl, pH 7.9. Eluted samples are mixed with ninhydrin reagent and detected by spectrophotometry at 570 nm for primary amines and 440 nm for secondary amines.

III-6 Mass spectroscopy

The molecular masses of all the peptides were further confirmed by a VG Quattro electrospray/triple quadrupole mass spectrometer from VG BioTech (Altrincham, UK). 10 µl of samples were injected and delivered to the analyzer using 0.1 % formic acid in 50% aqueous CH₃CN at a flow rate of 50 µl/min. Samples were detected in positive ion mode and scanned 7-10 times from 500 to 1500 Da, and acquired data were subtracted, smoothed and centered.

III-7 Circular dichroism spectroscopy

The secondary structures of peptides were determined by circular dichroism (CD) spectroscopy, which plays a key role in the study of peptide/protein structure and folding

(Greenfield, 1996; Johnson, 1990; Kelly *et al.*, 1997; Woody, 1995). Circular dichroism is a phenomenon of circularly polarized light, in which the electric vector rotates about the direction of a light beam. This phenomenon results when chromophores in an asymmetrical environment interact with polarized light. In proteins the major optically active groups are the amide bonds of the peptide backbone at the range of far UV spectra (170-250 nm) and the aromatic side chains at the near UV region (250-300 nm). Polypeptides and proteins have regions where the peptide chromophores are in highly ordered arrays, such as α -helices or β -sheets. Depending on the orientation of the peptide bonds in the arrays, the optical transitions of the amide bond can be split into multiple transitions, the wavelengths of the transitions can be increased or decreased, and the intensity of the transitions can be enhanced or decreased. As a consequence, many common secondary structure motifs, such as the α -helix, β -pleated sheets, β -turns, and random coils, have very characteristic CD spectra (Figure III-5). α -Helices have intense spectra with a characteristic positive band at 190 nm and double minima at 208 and 222 nm. A β -sheet spectrum is characterized by a negative band at 215 nm and a positive band at 198 nm. Negligible secondary structure regions (random coils) generally show a large negative band below 200 nm and a small positive band at 220 nm.

CD spectra were recorded on a Jasco J-720 spectropolarimeter (Jasco, Easton, MD) running a J700 for Windows Standard Measurement Software Version 1.10.00, equipped with a Lauda model RMS circulating water bath (Lauda, Westbury, NY) to control the temperature of the cuvette holder. The spectropolarimeter was routinely calibrated with an aqueous solution of recrystallized D-10-(+)-camphorsulfonic acid at 290.5 nm. Cylindrical quartz cells were used, with path lengths of 0.02 cm. Exceptions

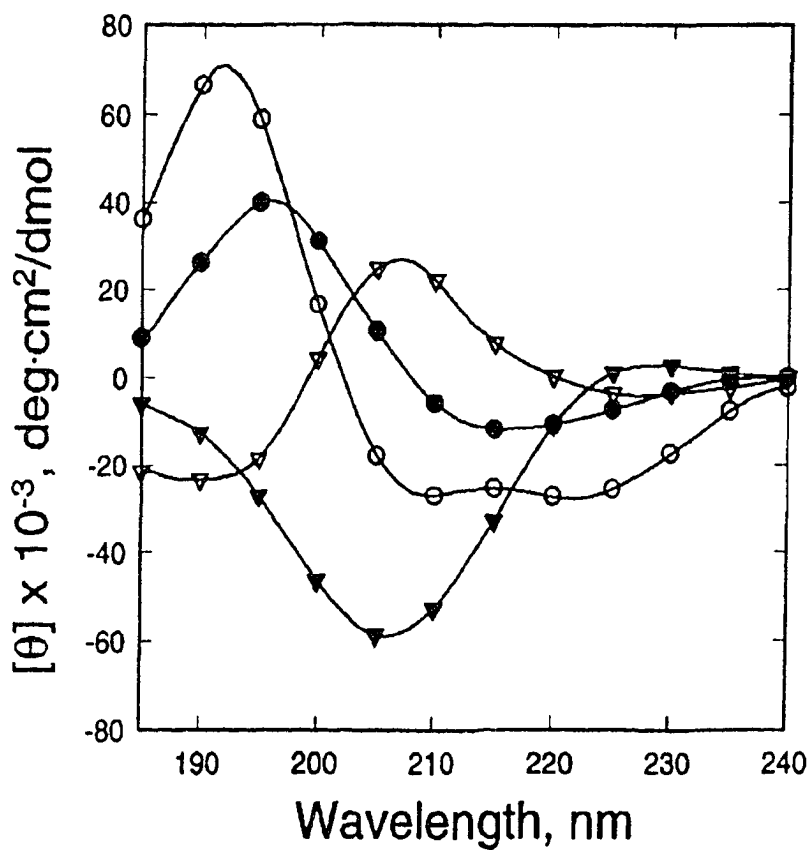


Figure III-5 CD spectra of peptides with representative varying secondary structures, (○) α -helix, (●) β -sheet, (▽) β -turn and (▼) random coil (adapted from Greenfield, 1996).

were occasionally adapted; for example, a 0.01 cm cell could be used for CD scans to achieve more spectral data at lower wavelength where solvent cutoff was a problem but the CD signal was also reduced in half. The results are expressed as mean residue molar ellipticity $[\theta]$ with units of $\text{deg}\cdot\text{cm}^2\cdot\text{dmol}^{-1}$ and calculated from the following equation:

$$[\theta]=([\theta]_{\text{obs}} \times \text{MRW})/(10lc)$$

where $[\theta]_{\text{obs}}$ is the observed ellipticity measured in millidegrees, MRW is the mean residue molecular weight (molecular weight of the peptide divided by the number of amino acid residues), l is the optical path length of the cell in cm, and c is the peptide concentration in mg/ml. For wavelength scans, data was collected from 190 to 255 nm at 0.05 nm intervals, and the average of 10 scans reported. Samples in this thesis were prepared by diluting an aqueous peptide stock solution of known concentration into buffer (50 mM PO_4 , 100 mM KCl, pH 7.0). For the scans in the presence of trifluoroethanol (TFE), the above buffer was diluted to 50% with TFE. For peptide secondary structure characterization, a 10-fold dilution of a ~ 500 μM stock solution of the peptide analogs was loaded into a 0.02 cm fused silica cell and its ellipticity scanned from 190 nm to 250 nm. The values of molar ellipticities of the peptide analogs at wavelength 222 nm were used to determine the relative α -helical propensity of each peptide in these studies.

III-8 Trifluoroethanol titration

A TFE titration study was carried out in order to find out the optimum concentration of TFE used in the CD temperature denaturation study of peptides. For a CD temperature denaturation study, peptides have to be fully folded at the beginning of

the experiment. TFE was used as the helix-inducing reagent to ensure the folded helical structure of peptides. However, the optimum concentration of TFE is critical to the accuracy of the results, since higher or lower concentrations of TFE than the optimum concentration can result in overly stable or unstable α -helical structure of peptides. In a TFE titration, peptide stock solutions were dissolved in benign buffer (15mM *aq.* PO₄/20mM KCl, pH 7.0) at a concentration of 1 mg/ml. Thirty microliters of stock peptide solution were mixed with a calculated volume of TFE and diluted with water to a final volume of 100ml. Each sample solution was then loaded into a 0.02cm fused silica cell and its ellipticity from 190nm to 250nm was measured at 5 °C using a Jasco J720 spectropolarimeter (Jasco, Easton, MD, USA) running a J700 for Windows Standard Measurement Software Version 1.10.00. Each spectrum is the average of four or eight scans collected every 0.05 or 0.1nm from 250nm to the far UV limit of the sample.

III-9 CD temperature denaturation

Temperature denaturation of peptides was performed in a Jasco J720 spectropolarimeter (Jasco, Easton, MD, USA); temperature was controlled with a Lauda model RMS circulating water bath (Lauda, Westbury, NY). Based on the TFE titration study, 40% TFE was the minimal concentration required to obtain maximal helical structure. Each peptide was dissolved in 50mM *aq.* PO₄ containing 100mM KCl and 40% TFE, pH 7.0, to give a peptide concentration of about 0.5mg/ml. Each solution was loaded into a 0.02 cm fused silica cell and its ellipticity at 222 nm was measured over a temperature range of 5-85 °C. The ratio of the molar ellipticity at a particular temperature (*t*) relative to that at 5 °C ($([\theta]_t - [\theta]_{10}) / ([\theta]_5 - [\theta]_{10})$) was calculated and plotted against

temperature in order to obtain the thermal melting profiles, where $[\theta]_f$ and $[\theta]_u$ represent the ellipticity values for the fully folded and fully unfolded species, respectively. The average molar ellipticity of all peptides at 222 nm in the presence of 50% TFE at 5 °C was taken to represent the 100% helical structure ($[\theta]_f = -28,500 \text{ deg}\cdot\text{cm}^2\cdot\text{dmol}^{-1}$) and that in the presence of 8M urea (average of $1500 \text{ deg}\cdot\text{cm}^2\cdot\text{dmol}^{-1}$) was taken to represent a totally random coil state ($[\theta]_u$). The melting temperature (T_m) was calculated as the temperature at which the α -helix was 50% denatured ($([\theta]_t - [\theta]_u) / ([\theta]_f - [\theta]_u) = 0.5$) and the values were taken as a measure of α -helix stability.

In Chapter VII, temperature denaturation was performed in 0.1% *aq.* TFA containing 40% TFE, pH 2.0. However, in Chapter IX, temperature denaturation of an antimicrobial peptide, V_{681} , was carried out in 0.05% *aq.* TFA, pH 2 to mimic the acidic environment frequently characteristic of RP-HPLC. 50% TFE was added in solution to ensure the fully α -helical structure of peptide V_{681} , due to its relatively negligible helical content in aqueous environment.

III-10 Calculation of resolution (R_s) during RP-HPLC

Peak resolution in chromatography is the ability of a column to separate chromatographic peaks. Resolution is a very important parameter to represent resolving power of HPLC. One attempts to achieve the best resolution possible. The value of resolution depends upon two factors: narrowness of the peak and the distance between peak maxima. One way of improving resolution is to increase column efficiency which decreases the width of the peak. Column efficiency is a function of such column parameters as mobile phase flow rate, particle size of the column packing and the solvent

viscosity. Column selectivity, a result of the interaction of the solute with the solvent and the column packing, is another way to improve resolution (Mant *et al.*, 1991). Figure III-6 illustrates how column efficiency and selectivity affect resolution. Resolution can be calculated in two ways:

$$(1) \quad R_s = 1/4(N)^{1/2}(\alpha-1)(1/1+k')$$

where N is the theoretical plate number, k' is the capacity factor and α is the peak selectivity.

$$(2) \quad R_s = (t_{r,2} - t_{r,1})/1/2(t_{w,2} + t_{w,1}) = 2 \Delta t / (t_{w,2} + t_{w,1})$$

where $t_{r,2}$ and $t_{r,1}$ are retention times of the retained components measured at the peak maximum and Δt is the difference between $t_{r,2}$ and $t_{r,1}$. The values of $t_{w,2}$ and $t_{w,1}$ are the peak widths in units of time measurement at the base. It is often more convenient to measure peak widths at high height, then equation (2) can also be described as:

$$(2) \quad R_s = 1.176\Delta t_R/(W_1+W_2)$$

where Δt_R is the difference in retention time between two peptide peaks (1 and 2) and W_1 and W_2 are their peak widths at half height. This equation is satisfied if the units of retention time and peak width are the same, such as minutes. In this thesis, resolution calculations were based on this modified equation.

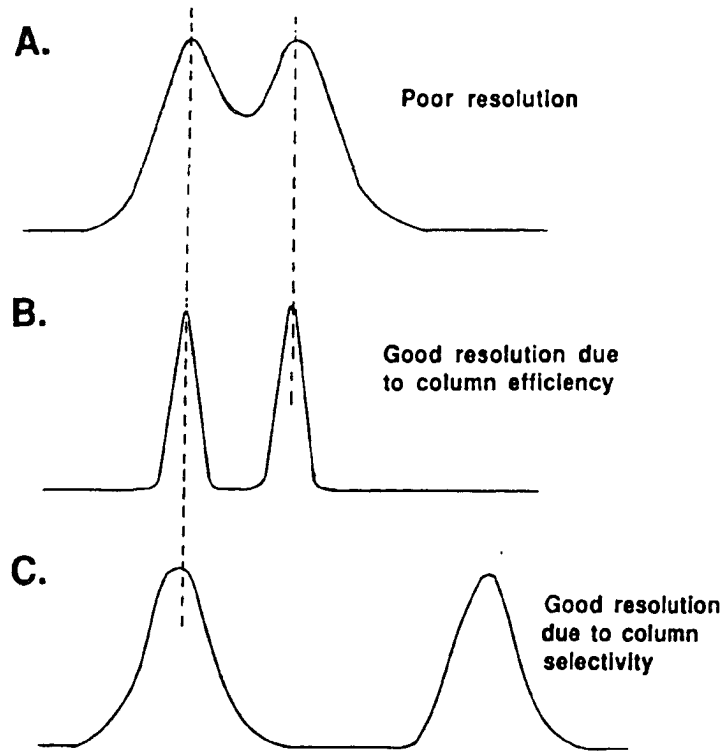


Figure III-6 Illustration of relationship among resolution, column efficiency and column selectivity (adapted from Mant *et al.*, 1991, pp 84)

CHAPTER IV

Selectivity Differences in the Separation of Amphipathic α -Helical Peptides during Reversed-Phase Chromatography at pH 2.0 and pH 7.0: Effects of Different Packings, Mobile Phase Conditions and Temperature

A version of this chapter has been published: Chen, Y., Mant, C. T. and Hodges, R. S. (2004) *J. Chromatogr. A* **1043**, 99-111. Only methods unique to this chapter are described in the **Experimental** section, the remaining general methods are described in Chapter III.

IV-1 Abstract

In an ongoing effort to understand the effect of varying reversed-phase high-performance liquid chromatography (RP-HPLC) parameters on the retention behaviour of peptides, necessary for the rational development of separation/optimization protocols, we believe it is important to delineate the contribution of α -helical structure to the selectivity of peptide separations. The present study reports the effects of varying column packing, mobile phase conditions and temperature on RP-HPLC retention behaviour at pH 2.0 and pH 7.0 of peptides based on the amphipathic peptide sequence Ac-EAEKAAKEXEKAAKEAEK-amide (with position X in the centre of the hydrophobic face of the α -helix), where position X is substituted by L- or D- amino acids. At pH 2.0, an increase in trifluoroacetic acid concentration or the addition of sodium perchlorate to a phosphoric acid-based mobile phase had the similar effect of improving peak shape as well as increasing peptide retention time due to ion-pairing effects with the positively-charged peptides; in contrast, at pH 7.0, the addition of salt had little effect save an improvement in peak shape. Temperature was shown to have a complex influence on peptide selectivity due to varying effects on peptide conformation. In addition, subtle

effects on peptide selectivity were also noted based on the column packings employed at pH 2.0 and pH 7.0.

IV-2 Introduction

The amphipathic α -helix is a very commonly encountered structural motif in peptides and proteins (Segrest *et al.*, 1990). Approximately 50% of all helices in soluble globular proteins are amphipathic (Cornette *et al.*, 1987; Segrest *et al.*, 1990), with soluble proteins, by definition, having come to terms with an aqueous environment requiring burial of hydrophobic residues in the protein interior. Peptides that exhibit this structural motif have been extensively used as model systems to understand peptide or protein folding, stability and function (Chen *et al.*, 2002; Hodges, 1996; Mant *et al.*, 1993). For example, amphipathic helical structures are now known to play an important role in the mechanism of action of antimicrobial peptides, since the hydrophilic (positively charged) domain of the antimicrobial peptide initiates peptide interaction with the negatively charged bacterial phospholipids and the hydrophobic domain of the peptide would then permit the peptide to enter the membrane interior (Bechinger, 1997; Blondelle *et al.*, 1999; Epanand *et al.*, 1999; Wu *et al.*, 1999).

Reversed-phase high-performance liquid chromatography (RP-HPLC) is one of the most widely used techniques for the separation and purification of peptides and proteins (Mant *et al.*, 1991; Mant *et al.*, 2002a). Moreover, RP-HPLC also turns out to be a useful physicochemical probe for investigation of amphipathic helices induced or stabilized in hydrophobic environments (Blondelle *et al.*, 1992a; Blondelle *et al.*, 1995; Chen *et al.*, 2002; Hodges *et al.*, 1994; Mant *et al.*, 1993; Purcell *et al.*, 1995c; Steer *et*

al., 1998; Zhou *et al.*, 1990). For example, the hydrophobic interactions between polypeptides and the nonpolar stationary phase (typically aliphatic alkyl chains attached to a silica support) upon which RP-HPLC depends may well reflect similar intraprotein interactions between the nonpolar residues that stabilize the folded or three-dimensional structure of the native protein molecule (Mant *et al.*, 1993). In addition, the interaction of amphipathic α -helices with a hydrophobic surface during RP-HPLC is likely to be a good model for peptide binding to biological membranes or receptors (Mant *et al.*, 2002b; Mant *et al.*, 2002c; Sereda *et al.*, 1994). In previous studies (Chen *et al.*, 2002; Chen *et al.*, 2003; Sereda *et al.*, 1995; Zhou *et al.*, 1990), we have stressed the importance of delineating the contribution of α -helical structure (both amphipathic and non-amphipathic) to the selectivity of peptide separations, particularly since peptide fragments from chemical or proteolytic digests of proteins typically contain peptides with α -helical potential. With RP-HPLC applied to the separation of such peptide mixtures, any peptides with α -helical potential will be induced into such secondary structure by the non-polar environment characteristic of this technique (hydrophobic matrix and non-polar eluting solvent (Blondelle *et al.*, 1995; Purcell *et al.*, 1995c; Steer *et al.*, 1998; Zhou *et al.*, 1990)).

In our aforementioned previous studies, we have (1) demonstrated the selectivity that may be obtained in a reversed-phase separation based on differences in peptide conformation (α -helical versus random coil) and highlighted by their retention time behaviour at varying gradients of organic modifier (Sereda *et al.*, 1995); (2) we have utilized RP-HPLC to monitor the quantitative changes of apparent peptide side-chain hydrophobicity/hydrophilicity and peptide amphipathicity caused by single L- or D-

amino acid substitutions in the centre of the hydrophobic face of a model amphipathic α -helical peptide (Chen *et al.*, 2002); and (3), we illustrated interesting temperature selectivity effects in RP-HPLC due to conformation differences between non-helical and L- or D-amino acid substituted α -helical peptides (Chen *et al.*, 2003). In an ongoing effort to understand the effect of varying RP-HPLC parameters on the retention behaviour of peptides, necessary for the rational development of separation/optimization protocols, we report here the effects of varying column packing, mobile phase conditions and temperature on RP-HPLC retention behaviour at pH 2.0 and pH 7.0 of peptides based on the amphipathic peptide sequence Ac-EAEKAAKEXEKAAKEAEK-amide (with position X in the centre of the hydrophobic face of the α -helix), where position X is substituted by L- or D-amino acids.

IV-3 Experimental

IV-3-1 Columns and HPLC conditions

Analytical RP-HPLC was carried out on a Zorbax 300 SB-C₈ column (150 x 2.1 mm I.D.; 5- μ m particle size; 300-Å pore size) and a Zorbax Eclipse XDB-C₈ column (150 x 2.1 mm I.D.; 5 μ m; 300Å) from Agilent Technologies, using a linear AB gradient (0.5% acetonitrile/min) at a flow-rate of 0.25 ml/min, at pH 2.0 and pH 7.0. Mobile phase systems used in this study were divided into two groups: at pH 7.0, eluent A was 20 mM aq. PO₄ containing 0 mM, 10 mM, 25 mM, 50 mM or 100 mM NaClO₄ and eluent B was eluent A also containing 50% (v/v) acetonitrile; at pH 2.0, eluent A was, 20 mM aq. H₃PO₄ or 20 mM aq. H₃PO₄ containing 100 mM NaClO₄ and eluent B was eluent A also containing 50% (v/v) acetonitrile. For an alternative pH 2.0 system, eluent A was

6 mM, 10 mM, 25 mM, 50 mM or 100 mM aq. TFA and eluent B was the corresponding concentration of TFA in acetonitrile.

IV-4 Results and discussion

IV-4-1 Amphipathic α -helical model peptides

IV-4-1-1 Design of model peptides

Our peptide models were designed based on the well-characterized sequence Ac-EAEKAAKEAEKAAKEAEK-amide, which exhibits a highly amphipathic α -helical structure (Figure IV-1) and is denoted as peptide AA9 in previous studies (Chen *et al.*, 2002; Mant *et al.*, 1993; Mant *et al.*, 2002b; Mant *et al.*, 2002c; Monera *et al.*, 1995; Sereida *et al.*, 1994; Zhou *et al.*, 1992; Zhou *et al.*, 1993; Zhou *et al.*, 1994a; Zhou *et al.*, 1994b). In the design of this model peptide, alanine was selected to form the hydrophobic face of the helix because it contains the minimum side-chain hydrophobicity needed to create an amphipathic α -helix and because of its high intrinsic helical propensity and stability contributions (Chou *et al.*, 1974; Monera *et al.*, 1995; Zhou *et al.*, 1994b). Lysine and glutamic acid were also selected to allow a potential for α -helix stabilizing electrostatic attractions at the $i \rightarrow i+3$ and $i \rightarrow i+4$ positions at neutral pH values (Scholtz *et al.*, 1993). In order to reduce the unfavourable dipole interactions of α -helical structure, all substituted model peptides were synthesized with N α -acetylated and C α -amidated termini (Shoemaker *et al.*, 1987). According to the study of Zhou *et al.* (Zhou *et al.*, 1994b), this amphipathic α -helical model exhibits the following important features: (a) the helix is single-stranded and non-interacting, enabling the determination of the effect of different amino acid substitutions in the non-polar face; (b) there is a uniform

X_D Ac-E-A-E-K-A-A-K-E- X_D -E-K-A-A-K-E-A-E-K-amide
 X_L Ac-E-A-E-K-A-A-K-E- X_L -E-K-A-A-K-E-A-E-K-amide
 C_3 Ac-K-L-K-K-G-G-L-K-G-E-L-G-G-E-E-L-E-E-amide

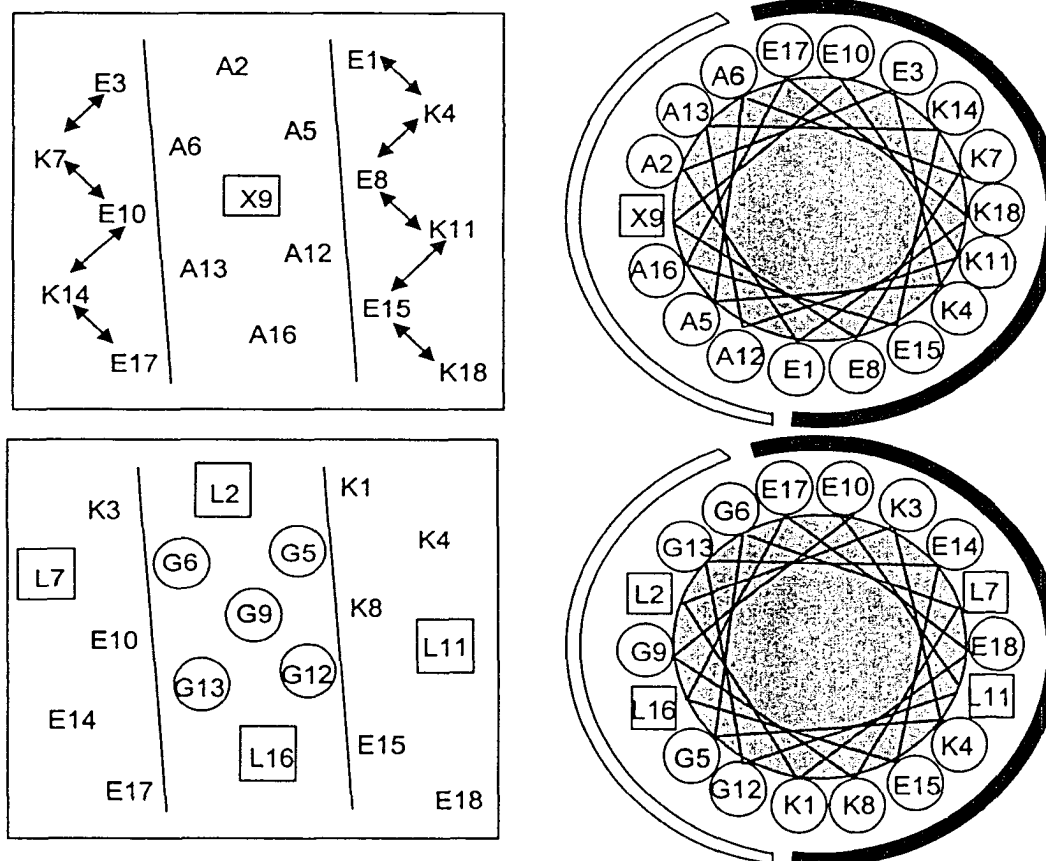


Figure IV-1 Sequences and representations of α -helical and random coil peptides, where X_D and X_L represent substituted D- and L-amino acids, respectively. (Bottom) Representations of the α -helical peptides as a helical net (A) and a helical wheel (B) and the random coil peptide, C_3 , as a helical net (C) and a helical wheel (D) if it were able to form α -helix. The non-polar face of the amphipathic peptide sequence is indicated between two parallel lines in A and as an open arc in B; the hydrophilic face is shown as a solid arc in B. The substitution "guest" site is at position 9 (boxed) of the non-polar face.

environment created by alanine residues surrounding the substitution site in the centre of the non-polar face (position 9 of this 18-mer model peptide); (c) the small size of the alanine side-chain methyl group ensures the minimal interactions with the “guest” amino acid residues; (d) the relatively small size of the peptide (18 residues) maximizes the effects of single amino acid substitutions.

The Ala residue in the centre of the non-polar face of the amphipathic α -helical sequence of AA9 was substituted for the present study with L- or D-proline, L- or D-serine and L- or D-glutamine, or by glycine. The side chains of proline, serine and glutamine are uncharged at pH 2.0 or pH 7.0, thus eliminating any chance of charge contributions of these substituted amino acids complicating interpretation of results. It should be noted that the intrinsic hydrophobicity of the non-polar face of the amphipathic α -helix is identical for each diastereomeric peptide pair. Since glycine does not exhibit optical activity, the Gly-substituted analogue represents a useful reference standard. Different α -helical peptide analogues were denoted by the one-letter code of the amino acid residue substituted at position 9 of the sequence (Figure IV-1). For example, peptide P_D represents the model peptide analogue with D-proline substituted at position 9 and peptide G denotes the glycine-substituted analogue, etc.

Peptide C3 represents a peptide designed to exhibit negligible secondary structure, *i.e.*, a random coil, although Figure IV-1C (helical net) and Figure IV-1D (helical wheel) present this peptide in the form it would take if it was able to become helical. This peptide was originally designed to be of the same length and similar composition to AA9, which may be viewed as the “native” peptide of the model amphipathic α -helical peptides. However, while AA9 contains seven Ala residues, C3

contains none (Figure IV-1). With seven Ala residues in the hydrophobic face of AA9 (hence, seven CH₃ groups) and five Gly and two Leu residues in a putative hydrophobic face for C3 (hence eight CH₂ and CH₃ groups, from the two Leu residues), overall hydrophobicity is essentially maintained. The two additional Leu residues in the putative hydrophilic face in C3, if it were α -helical, were designed to increase the retention time of the random coil peptide and to ensure that it could not form an amphipathic α -helix. From Figure IV-1D, it can be seen that, even if this peptide were able to be induced into α -helical structure, a non-amphipathic helix would result. However, the presence of five Gly residues, a well-known α -helix disrupter and, with the sole exception of proline, the amino acid with the lowest helical propensity (Monera *et al.*, 1995; Zhou *et al.*, 1994b), in place of five Ala residues was designed to make any secondary structure highly unlikely to occur. In addition, we have also shuffled the positions of positively-charged Lys and negatively-charged Glu residues to reduce further the possibility of intrachain electrostatic attractions, such as those able to stabilize the α -helical structure of AA9 (or other analogues) at pH 7.0 (compare Figure 1A for the amphipathic α -helical analogues with Fig. 1C for putative helical structure of C3).

IV-4-1-2 CD spectroscopy studies

In order to determine the effect of different substitutions on α -helical peptide conformation, CD spectra of the peptide analogues were measured under benign buffer conditions (50 mM PO₄, 100 mM KCl, pH 7.0) and also in the presence of the α -helix-inducing solvent TFE for all seven potentially α -helical analogues and for the reference standard C3.

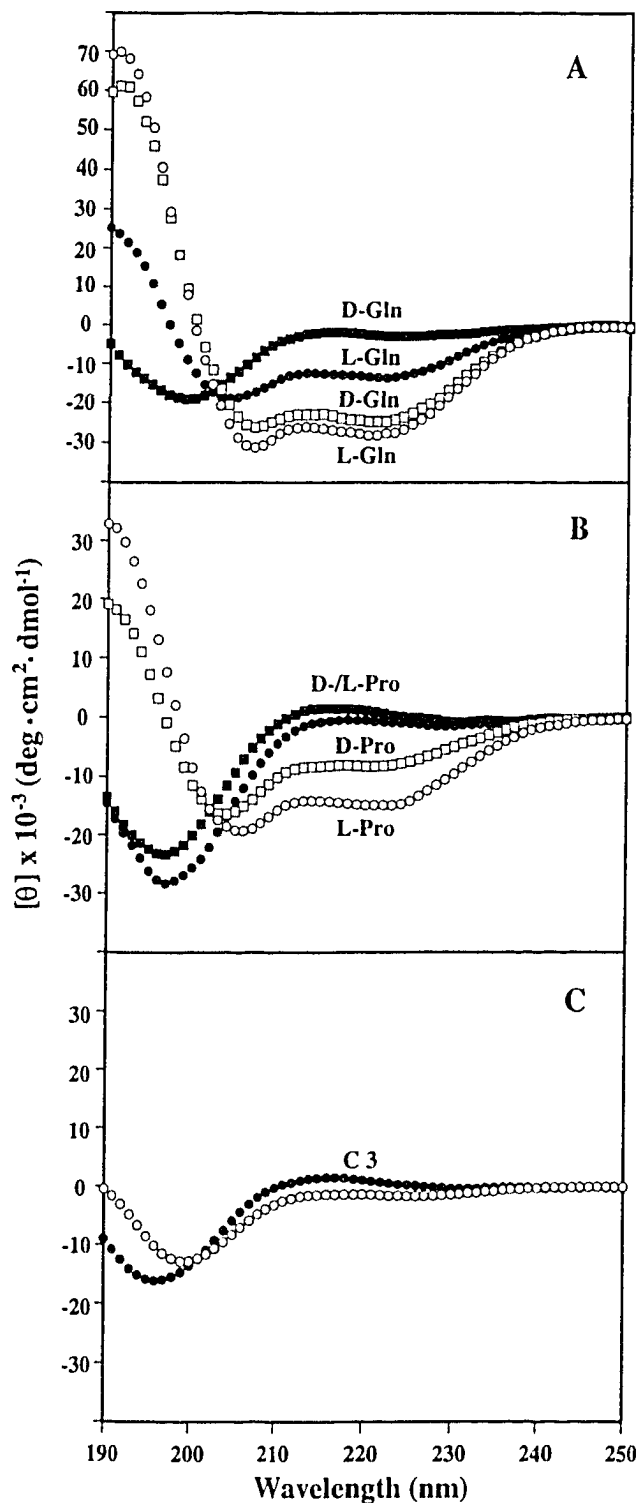


Figure IV-2 Circular dichroism spectra of synthetic model peptides. Solid symbols represent CD spectra of peptide analogs obtained under benign conditions (50 mM PO₄/100 mM KCl, pH 7.0); open symbols represent spectra obtained in the presence of 50% TFE. The sequences of the model peptides and the random coil peptide C3 are shown in Figure IV-1 with denotations described in the text.

From Figure IV-2A, it can be seen that although peptide Q_L ($[\theta]_{222} = -13450^\circ$) exhibited considerably more α -helical structure than its diastereomer, peptide Q_D ($[\theta]_{222} = -2560^\circ$) in benign buffer, the molar ellipticity values of this diastereomeric peptide pair were very similar ($[\theta]_{222} = -27650^\circ$ and -24450° for peptides Q_L and Q_D, respectively, in the presence of 50% TFE). The helix-disrupting characteristics in benign medium of D-amino acid residues in peptide sequences otherwise made up solely of L-amino acids is well documented (Aguilar *et al.*, 1993; Chen *et al.*, 2002; Krause *et al.*, 2000; Rothmund *et al.*, 1995; Rothmund *et al.*, 1996); in addition, the attainment of high helicity of even such D-substituted peptides in the presence of TFE has also been demonstrated. Thus, from a previous study in our laboratory (Chen *et al.*, 2002), all of the model peptide analogues, excluding the L-/D-proline substituted peptides, exhibited similar molar ellipticity values at 222 nm in the presence of 50% TFE, with > 90% helical content. Since TFE is recognized as a useful mimic of the hydrophobic environment characteristic of RP-HPLC (Zhou *et al.*, 1990), as well as being a strong α -helix inducer in potentially helical molecules (Cooper *et al.*, 1990; Nelson *et al.*, 1989; Sonnichsen *et al.*, 1992), elution of these peptide analogues as α -helices during RP-HPLC is ensured. In addition, the $[\theta]_{220}/[\theta]_{207}$ ratio values of Q_L and Q_D (and, indeed, S_L, S_D, and G) were less than 1.0 suggesting that, in the presence of 50% TFE, these peptides are single-stranded α -helices (Cooper *et al.*, 1990; Zhou *et al.*, 1993; Zhou *et al.*, 1994a). Hence, such observations also suggest that peptides Q_L, Q_D, S_L, S_D and G are eluted in a single-stranded α -helical conformation during RP-HPLC.

Both P_L and P_D exhibited molar ellipticities ($[\theta]_{222} = -700^\circ$ and 700° , respectively) characteristic of negligible secondary structure in benign medium (Figure IV-2B). Even

in the presence of 50% TFE, molar ellipticity values of just -14900° (P_L) and -8150° (P_D) were achieved, reflecting the strong helix-disrupting character of proline. Thus, with a Pro residue substituted into the centre of the non-polar face of the model helical peptide, $\sim 50\%$ (P_L) or 75% (P_D) of the sequence could not be induced into α -helical structure in the presence of TFE, suggesting that these peptides will be eluted only with partial α -helical structure during RP-HPLC.

Finally, from Figure IV-2C, peptide C3, designed as a random coil peptide standard, exhibited the expected negligible secondary structure in both benign buffer and in the presence of 50% TFE.

IV-4-1-3 RP-HPLC elution behavior of amphipathic α -helical peptides

It is well known that characteristic RP-HPLC conditions (hydrophobic stationary phase, non-polar eluting solvent) induce helical structure in potentially helical polypeptides (Blondelle *et al.*, 1995; Purcell *et al.*, 1995c; Steer *et al.*, 1998; Zhou *et al.*, 1990). Polypeptides, such as our model peptides (Figure IV-1), which are thus induced into an amphipathic α -helix on interaction with a hydrophobic RP-HPLC stationary phase will exhibit preferred binding of their non-polar face with the stationary phase. Zhou *et al.* (Zhou *et al.*, 1990) clearly demonstrated that, because of this preferred binding domain, amphipathic α -helical peptides are considerably more retentive than non-amphipathic peptides of the same amino acid composition. From Figure IV-1, as mentioned previously, the central substitution site of model peptide ensures intimate interaction of the substituting side-chain with the reversed-phase stationary phase; concomitantly, this is designed to maximize any observed effects on RP-HPLC retention behaviour of different amino acid substitutions at this site.

IV-4-2 HPLC run parameters investigated in this study**IV-4-2-1 Anionic ion-pairing reagents**

Peptides are charged molecules at most pH values and the presence of different counterions will influence their chromatographic behavior. The majority of researchers utilizing ion-pair RP-HPLC at low pH for the separation of peptide mixtures still take advantage of the excellent resolving power and selectivity of *aq.* TFA to TFA/acetonitrile gradients (Mant *et al.*, 1991; Mant *et al.*, 2002a), although *aq.* H₃PO₄/acetonitrile systems have also shown their worth for peptide applications (Gaertner *et al.*, 1985; Guo *et al.*, 1987; Mant *et al.*, 1991; Mant *et al.*, 2002a; Sereda *et al.*, 1993; Sereda *et al.*, 1995). Favoured models for the mechanism of ion-pair separations involve either formation of ion pairs with the sample solute in solution followed by retention of the solute molecules on a reversed-phase column (Horvath *et al.*, 1976; Horvath *et al.*, 1977), or a dynamic ion-exchange event in which the ion-pairing reagent is first retained by the reversed-phase column and then solute molecules exchange ions with the counterion associated with the sorbed ion-pair reagent (Horvath *et al.*, 1977; Kissinger, 1977; Kraak *et al.*, 1977; Van de Venne *et al.*, 1978). Whatever the mechanism, the resolving power of ion-pairing reagents is effected by interaction with the ionized groups of a peptide. Anionic counterions such as trifluoroacetate (TFA⁻) or phosphate (H₂PO₄⁻) will interact with the protonated basic residues of a peptide (Lys, Arg, His or a free α -amino group). A hydrophobic counterion such as TFA⁻ will, though interaction with the positive groups in the peptide, increase further the affinity of the peptides for the hydrophobic stationary phase; in contrast, a polar hydrophilic counterion such as H₂PO₄⁻, following ion-pair formation, will neutralize the positive charge on the peptides (thereby decreasing the

peptide hydrophilicity) but would be unlikely to interact with the non-polar sorbent (Guo *et al.*, 1987).

IV-4-2-2 Salt additives to mobile phase

Addition of salts to mobile phases over a pH range of approximately 4-7 is traditionally designed to suppress negatively charged silanol interactions with positively charged solutes (Gaertner *et al.*, 1985; Guo *et al.*, 1986a; Mant *et al.*, 1987b; Mant *et al.*, 1991; Mant *et al.*, 2002a; Meek, 1980; Sereda *et al.*, 1997; Snider *et al.*, 1988). However, the potentially beneficial effect of salt, specifically NaClO₄, on peptide separations at low pH has also been demonstrated (Sereda *et al.*, 1997). Indeed, the negatively charged perchlorate (ClO₄⁻) ions act as a hydrophilic anionic ion-pairing reagent and, thus, interact with positively charged groups in a similar manner to H₂PO₄⁻ and TFA⁻. NaClO₄ is also particularly useful as the salt additive to a RP-HPLC mobile phase since it is highly soluble in aqueous acetonitrile eluents, even at relatively high concentrations of this organic modifier (Zhu *et al.*, 1992).

IV-4-2-3 RP-HPLC stationary phases

Although optimization of peptide and protein separations during RP-HPLC has generally been achieved via manipulation of the mobile phase on a given reversed-phase column, the employment of different stationary phases, preferably with complementary selectivities, has also seen some success. Generally, for silica-based stationary phases, useful selectivity differences for peptides/proteins have been noted when the bonded-phase functionalities are significantly different, *e.g.*, n-alkyl bonded-phase versus cyanopropyl and/or phenyl bonded phases (Barry *et al.*, 1995; Burton *et al.*, 1988; Gurley *et al.*, 1983; Mant *et al.*, 1991; Marchylo *et al.*, 1992; Tarr *et al.*, 1983; Titani *et al.*, 1982;

Zhou *et al.*, 1991), or long chain n-alkyl bonded-phases (C₈, C₁₈) versus shorter n-alkyl functionalities (C₃, C₄) (Barry *et al.*, 1995).

In the present study, we wished to determine whether different columns containing identical bonded-phase functionality would offer useful selectivity differences for our model amphipathic α -helical peptides under varying mobile phase conditions. As noted by Barry *et al.* (Barry *et al.*, 1995), comparisons of bonded-phase mediated selectivity effects should be carried out using the same based silica support to minimize potential complications of varying silanol contributions to retention processes. Thus, the present study employed two C₈-bonded phases based on the same silica support and column dimensions (150 x 2.1 mm I.D.; 5- μ m particle size; 300-Å pore size) from the same manufacturer: (1) Zorbax SB-300C₈ ("SB" denoting "StableBond"), prepared from monofunctional *n*-octylsilane and based on protecting the siloxane bond between the silica and the C₈ group with bulky side groups, in this case two isopropyl groups (monochlorodiisopropyl *n*-octylsilane) (Barry *et al.*, 1995; Boyes *et al.*, 1993; Glajch *et al.*, 1990; Kirkland *et al.*, 1989); and (2) Zorbax XDB-C₈ ("XDB" denoting Extra Dense Bonding), prepared by bonding a dense monolayer of dimethyl-*n*-octylsilane to the silica support, followed by exhaustive double endcapping with dimethyl- and trimethylsilane groups (Kirkland *et al.*, 1997; Kirkland *et al.*, 1998). The SB packing was originally designed to protect the siloxane bond from acid hydrolysis at low pH, while the XDB packing was intended to shield the silica support from dissolution at pH values at neutrality and higher. In addition, both packings were also designed to exhibit thermal stability over a wide temperature range.

IV-4-2-4 Temperature

Generally, the variation of temperature for RP-HPLC applications has implied raising the temperature in order to attempt improvement of solute separations. Since reversed-phase stationary phases with excellent thermal stability have now been commercially available for several years (Barry *et al.*, 1995; Boyes *et al.*, 1993; Glajch *et al.*, 1990; Kirkland *et al.*, 1989; Kirkland *et al.*, 1997; Kirkland *et al.*, 1998), the potential of this separation approach is now being realized, not least for resolution of peptide mixtures (Chen *et al.*, 2003; Chloupek *et al.*, 1994; Hancock *et al.*, 1994; Mant *et al.*, 1997). For instance, an interesting recent example by our laboratory (Chen *et al.*, 2003) demonstrated that it is possible to manipulate polypeptide separations by subjecting mixtures of α -helical and random coil peptides to RP-HPLC at various temperatures (5°C – 80°C); depending on the stability of the individual components of secondary structure in the mixture, the molecules unfolded to different extents at different temperatures and, hence, interact with the stationary phase to differing extents, thus effecting a separation based on variations in peptide stability.

IV-4-3 Effect of run parameters on RP-HPLC of amphipathic α -helical peptides

IV-4-3-1 Effect of salt on RP-HPLC of model peptides at pH 2.0 and pH 7.0

Figure IV-3 shows the elution behaviour of the seven model peptides at pH 7.0 in the absence (Figure IV-3A) and presence (Figure IV-3B) of 100 mM NaClO₄ on the XDB-C₈ column. From Figure IV-3 and Table IV-1, in both the absence and presence of salt, L-amino acid substituted peptides are consistently retained longer than their D-amino acid substituted counterparts; in addition, peptide elution order remains the same in the absence and presence of salt. The lesser retentiveness of the D-analogues

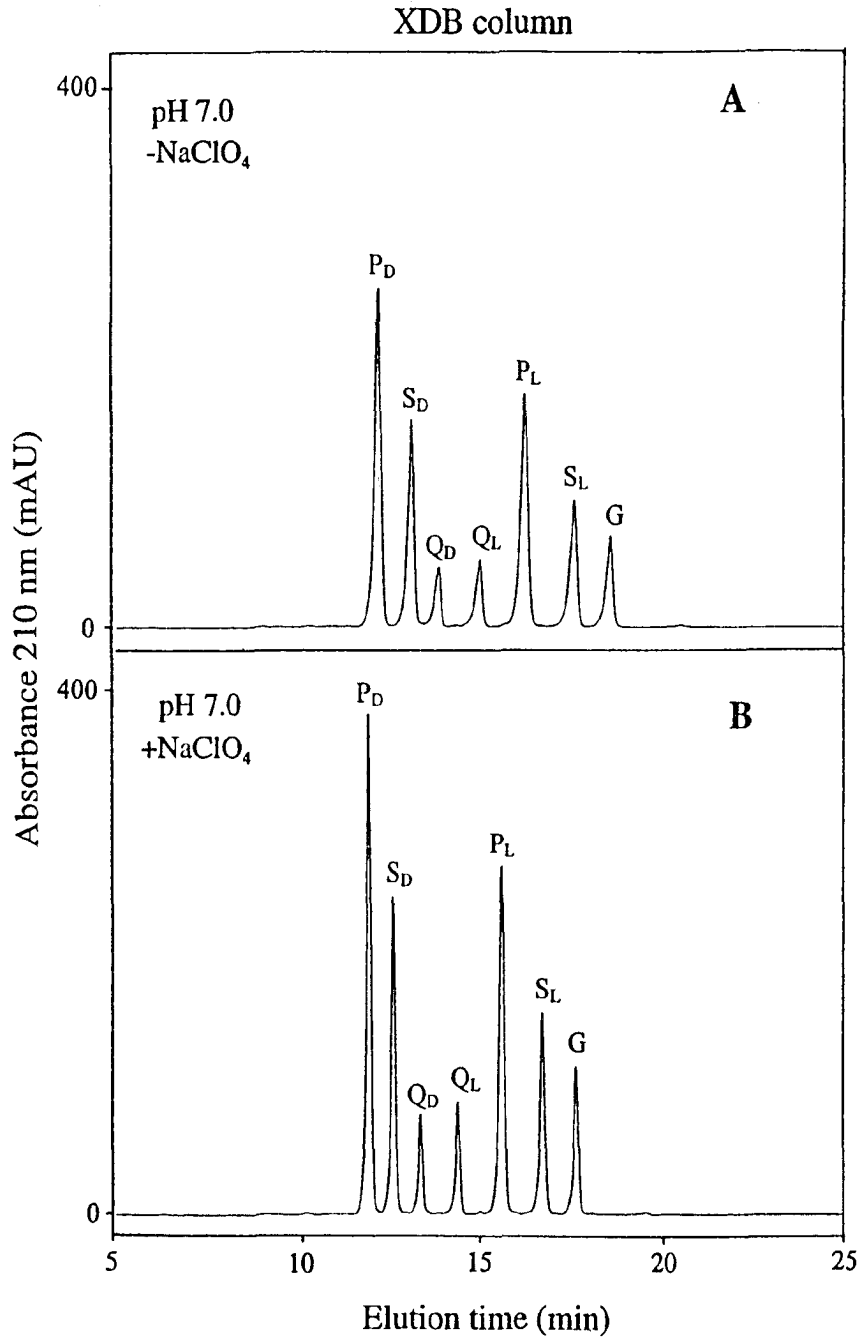


Figure IV-3 Effect of salt on RP-HPLC elution profile of model peptides at pH 7.0. Conditions: (A) linear AB gradient (0.5% CH₃CN/min) at a flow rate of 0.25ml/min, where eluent A is 20 mM *aq.* PO₄, pH 7.0, and eluent B is eluent A containing 50% CH₃CN; (B) same as (A) except for the addition of 100 mM NaClO₄ to both eluents; temperature, 65 °C.

compared to their L-enantiomers is likely due to disruption of the non-polar face of the amphipathic α -helix when introducing a D-amino acid into an α -helix otherwise made up of L-amino acids (Chen *et al.*, 2002; Krause *et al.*, 2000; Rothmund *et al.*, 1995; Rothmund *et al.*, 1996); the apparent hydrophobicity of this preferred binding domain will thus be diminished relative to the amphipathic α -helix made up entirely of L-amino acids, resulting in the observed lower retention times of the D-amino acid substituted peptides of the L-/D-peptide pairs. It is interesting to note that P_L is eluted prior to both S_L and G, considering that Pro is considered to be a more hydrophobic residue than Ser or Gly (Guo *et al.*, 1986a). However, since the presence of Pro severely disrupts the α -helix (Figure IV-2), with only ~50% of P_L able to be induced into an α -helical structure, its concomitant severe disruption of P_L amphipathicity (and, hence, non-polar face) would result in a lesser retention time compared to the fully folded S_L and G analogues, despite the relatively lesser hydrophobicity of these two residues compared to Pro. A similar, albeit even more dramatic, observation was made for P_D (only ~25% able to be induced into α -helical structure; Figure IV-2), which was eluted prior to all peptide analogues.

From Figure IV-3, there is a small reduction in retention time of all peptides in the presence of salt (Figure IV-3B) compared to its absence (Figure IV-3A), concomitant with decreasing peak widths ($W_{1/2}$) (Figure IV-3; Table IV-1), this decrease in $W_{1/2}$ values also resulting in an increase in resolution (R_s) between adjacent peptides (Figure IV-3; Table IV-2).

As noted above, the addition of salt above pH 4 is frequently necessary to block non-specific interactions between underivatized, negatively charged silanol groups on the silica support and positively charged residues, such interactions resulting in longer

Table IV-1 Effect of NaClO₄ on peptide retention time and peak width during RP-HPLC at pH 7.0^a

Peptides ^b	t_R (-NaClO ₄) ^c (min)	t_R (+NaClO ₄) ^c (min)	$W_{1/2}$ (-NaClO ₄) ^d (min)	$W_{1/2}$ (+NaClO ₄) ^d (min)
P _D	12.20	11.93	0.1744	0.1301
S _D	13.11	12.61	0.1749	0.1261
Q _D	13.86	13.36	0.1739	0.1202
Q _L	15.02	14.41	0.1822	0.1251
P _L	16.28	15.62	0.2049	0.1519
S _L	17.63	16.76	0.1935	0.1366
G	18.64	17.67	0.1935	0.1353

a. Conditions: RP-HPLC at pH 7.0 on XDB-C₈ column (see in Figure IV-3).

b. For peptide denotions, see Section IV-4-1-1.

c. Denotes the retention times of the peptides during RP-HPLC at pH 7.0, with (+) or without (-) 100mM NaClO₄.

d. Denotes the peak width at half height of the peptides (in time units) during RP-HPLC at pH 7.0, with (+) or without (-) 100mM NaClO₄.

Table IV-2 Effect of NaClO₄ on peptide resolution during RP-HPLC at pH 7.0^a

Peptide pair ^b	Δt_R (-NaClO ₄) ^c (min)	Δt_R (+NaClO ₄) ^c (min)	R_S (-NaClO ₄) ^d	R_S (+NaClO ₄) ^d
S _D - P _D	0.91	0.68	3.06	3.12
Q _D - S _D	0.75	0.75	2.53	3.58
Q _L - Q _D	1.16	1.05	3.83	5.03
P _L - Q _L	1.26	1.21	3.83	5.14
S _L - P _L	1.35	1.14	3.98	4.65
G - S _L	1.01	0.91	3.07	3.94

a. Conditions: RP-HPLC at pH 7.0 on XDB-C₈ column (see Figure IV-3).

b. Denotes the later eluted peptide minus the adjacent faster eluted peptide on the chromatogram in Figure IV-3. For peptide denotions, see Section IV-4-1-1.

c. Denotes the difference in retention time between two adjacent peptides in the same peptide pair during RP-HPLC at pH 7.0 with (+) or without (-) 100mM NaClO₄; $\Delta t_R = t_R$ of former peptide minus t_R of adjacent earlier eluted peptide.

d. Denotes the resolution of every two adjacent peaks during RP-HPLC at pH 7.0 with (+) or without (-) 100mM NaClO₄.

retention times and peak broadening. However, it is a testament to the dense bonded phase of this XDB, concomitant with the exhaustive endcapping during its production, that the peptide elution profiles in both the absence (Figure IV-3A) and presence (Figure IV-3B) of NaClO_4 were quite similar.

Figure IV-4 shows the elution behaviour of the seven model peptides at pH 2.0 under mobile phase conditions employing 20 mM H_3PO_4 in the absence (Figure IV-4A) or presence (Figure IV-4B) of 100 mM NaClO_4 , 6 mM TFA (Figure IV-4C) and 50 mM TFA (Figure IV-4D). In contrast to results obtained at pH 7.0 (Figure IV-3; Table IV-1), the retention times of all seven peptide analogues increased considerably in the presence of salt at pH 2.0 (Figure IV-4B) compared to its absence (Figure IV-4A). With the exception of the now coeluted $\text{Q}_{\text{D}}/\text{P}_{\text{L}}$, the resolution of adjacent peptide pairs improved in the presence of salt (Figure IV-4B; Table IV-3) due, in a similar manner to the effect of salt at pH 7.0 (Figure IV-3B; Tables IV-1 and IV-2), the decreasing $W_{1/2}$ values compared to its absence (Figure IV-4A). Interestingly, increasing the concentration of TFA from 6 mM (Figure IV-4C) to 50 mM (Figure IV-4D) had a similar effect to that of salt addition, *i.e.*, an increase in peptide retention times concomitant with an increase in resolution between adjacent peptides (Table IV-3), mainly due again to a decrease in $W_{1/2}$ at the higher TFA concentration. Note also that Q_{D} and P_{L} are again coeluted in the presence of 50 mM TFA (Figure IV-4D) in a similar manner to the presence of 100 mM NaClO_4 (Figure IV-4B). An increase in retention time of positively charged peptides with increasing TFA concentration has been previously demonstrated (Guo *et al.*, 1987).

The explanation for the increase in peptide retention times in the presence of salt (Figure IV-4B) compared to its absence (Figure IV-4A) is likely due to ion-pairing of the

five basic, positively charged lysine residues with the negatively charged ClO_4^- anion, neutralizing the hydrophilic, charged character of the lysine side-chains and concomitantly enhancing the hydrophobicity of the peptides. Support for this view, rather than an induction of hydrophobic interactions with the reversed-phase packing in the presence of 100 mM NaClO_4 , also lies in the similar effect of increasing the concentration of TFA from 6 mM (Figure IV-4C) to 50 mM (Figure IV-4D). Note that the selectivity of the peptide separations effected by the ClO_4^- or TFA^- anions was the same.

A point of significance from Figure IV-4 also lies in the relative effectiveness of the ClO_4^- and TFA^- anions in increasing peptide retention time with increasing anion concentration, *i.e.*, an increase in TFA^- concentration of just 44 mM (50 mM in Figure IV-4D minus 6 mM TFA in Figure IV-4C) has a similar effect as the addition of 100 mM ClO_4^- (Figure IV-4B) compared to its absence (Figure IV-4A). This result is likely due to the aforementioned relative hydrophilic/hydrophobic properties of these anions. Thus, the presence of the hydrophilic ClO_4^- counterion simply reduces the hydrophilicity of the peptides via ion-pairing with the positively charged residues, thus increasing peptide retention time; in contrast, the hydrophobic TFA^- counterion not only reduces the hydrophilicity of the peptides through such ion-pairing but also further increases peptide hydrophobicity due to the hydrophobic nature of the TFA^- anion. Hence, a lower concentration of TFA will have a similar effect on peptide retention time as a significantly higher (about double, in this instance) concentration of NaClO_4 .

At pH 2.0 (Figure IV-4), the glutamic acid residues are uncharged and the peptides have a net charge of +5. However, at pH 7.0 (Figure IV-3), both the lysine and

Table IV-3 Effect of eluent system on peptide resolution during RP-HPLC at pH 2.0 ^a

Peptide pair ^b	20mM H ₃ PO ₄ ^c		20mM H ₃ PO ₄ / 100mM NaClO ₄ ^c		6mM TFA ^c		50mM TFA ^c	
	Δt_R^d (min)	R_S^e	Δt_R^d (min)	R_S^e	Δt_R^d (min)	R_S^e	Δt_R^d (min)	R_S^e
S _D -P _D	2.97	5.09	2.69	7.59	2.21	3.75	2.50	7.28
P _L -S _D	1.18	2.06	1.29	4.20	0.70	1.26	0.95	2.52
Q _D -P _L	0.87	1.72	— ^f	— ^f	0.70	1.42	— ^f	— ^f
Q _L -Q _D	3.00	6.86	2.99	9.59	2.38	5.97	2.87	7.46
S _L -Q _L	0.96	1.90	1.43	4.63	0.76	1.58	1.14	3.48
G-S _L	1.94	3.65	0.89	2.77	1.17	2.35	1.01	3.22

a. Conditions: RP-HPLC at pH 2.0 on SB-C₈ column (see Figure IV-4).

b. Denotes the later eluted peptide minus the adjacent faster eluted peptide on the chromatogram in Figure IV-4. For peptide denotations, see Section IV-4-1-1.

c. Denotes the different eluent systems as shown in Figure IV-4.

d. Denotes the difference in retention time between two adjacent peptides (peptide pair) in the corresponding eluent systems during RP-HPLC at pH 2.0; $\Delta t_R = t_R$ of former peptide minus t_R of adjacent earlier eluted peptide.

e. Denotes the resolution of every two adjacent peaks (peptide pair) in the corresponding eluent systems during RP-HPLC at pH 2.0.

f. Dash denotes the co-eluted peptides.

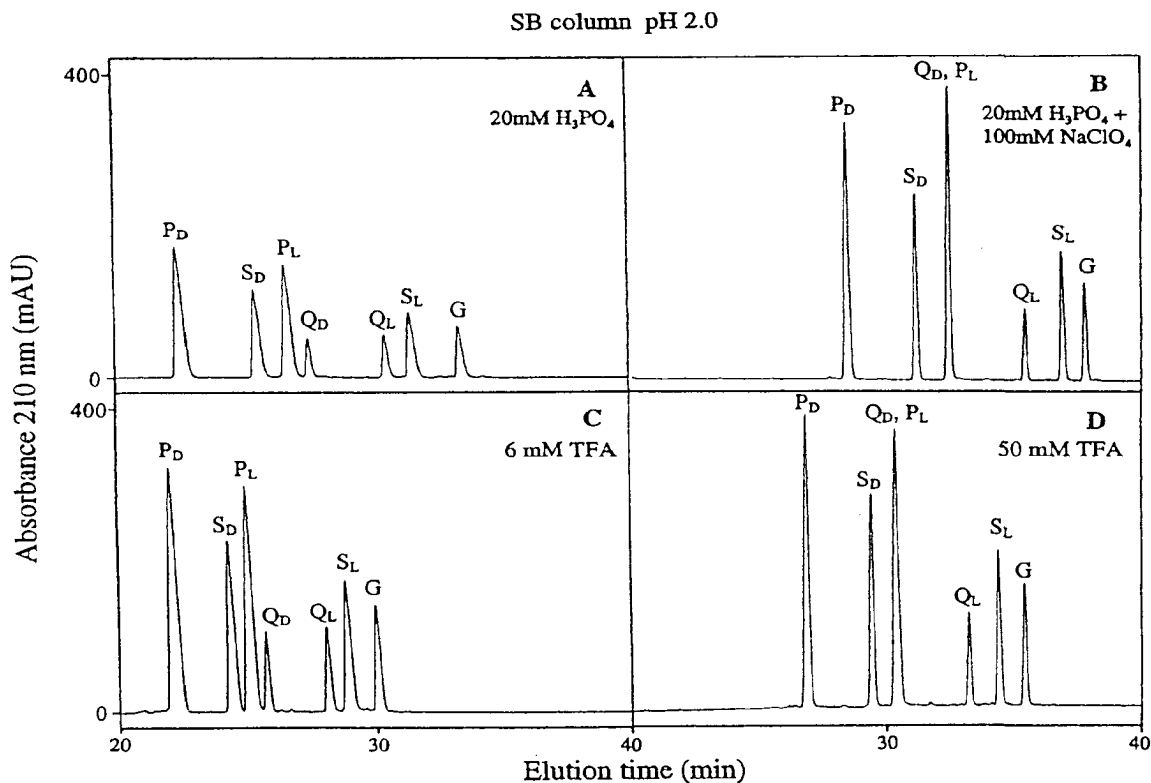


Figure IV-4 Effect of mobile phase conditions on RP-HPLC elution profile of model peptides at pH 2.0. Conditions: all runs carried out with a linear AB gradient (0.5% CH₃CN/min) at a flow rate of 0.25 ml/min; (A) eluent A is 20 mM *aq.* H₃PO₄, pH 2.0, and eluent B is eluent A containing 50% CH₃CN; (B) same as (A) except for the addition of 100 mM NaClO₄ to both eluents; (C) eluent A is 6 mM *aq.* TFA and eluent B is 6 mM TFA in CH₃CN; (D) eluent A is 50 mM *aq.* TFA and eluent B is 50 mM TFA in CH₃CN; temperature 65 °C.

glutamic acid residues are charged, producing an overall -1 charge on the peptides. Thus, the observation that the retention times of the peptides do not increase on the addition of salt at pH 7.0 (Figure IV-3) can be explained on the basis of overall net charge. In addition, these results at pH 7.0 (Figure IV-3), with no increase in peptide retention times in the presence of salt, also again suggests that induction of hydrophobic interactions with the column packing by the inclusion of 100 mM NaClO₄ is not a factor.

Figure IV-5 illustrates graphically the effect of concentration of anionic ion-pairing reagents on peptide retention time at both pH 2.0 (Figure IV-5A, TFA⁻ anion; Figure IV-5B, ClO₄⁻ anion) and pH 7.0 (Figure IV-5C, ClO₄⁻ anion). From Figure IV-5, the similar effect of TFA⁻ (5A) and ClO₄⁻ (5B) is quite clear, *i.e.*, an increase in retention time of the α -helical peptides with increasing anion concentration. In addition, an increase in salt concentration at pH 7.0 (Figure IV-5C) is again (see Figure IV-3) seen to have negligible effect on peptide retention time.

A significant result from Figure IV-5 is the similarity of the profile for the random coil peptide, C3, compared to those of the α -helical peptides. At pH 7.0, a fully folded α -helical peptide would allow intrachain electrostatic interactions between lysine and glutamic acid residues. Potentially, the negligible effect of ClO₄⁻ at pH 7.0 could be viewed as an inability to compete with the negatively charged glutamic acid residues for ion-pairing with the lysine side-chains, *i.e.*, a conformational aspect to the differences in peptide elution behaviour at pH 2.0 versus pH 7.0 rather than simply a matter of overall net charge (+5 and -1 , respectively). However, the random coil C3 is unable to exhibit such intrachain interactions; indeed, P_L and (particularly) P_D would also be limited in this respect. Thus, the observation that the random coil C3, the partially folded P_L and P_D and

the fully folded G, S_L, S_D, Q_L and Q_D all exhibited similar responses to increases in perchlorate concentration at both pH 2.0 and pH 7.0 indicates that counterion concentration effects are *conformation independent*.

IV-4-3-2 Effect of column packing on RP-HPLC of model peptides at pH 2.0 and pH 7.0

Figure IV-6 compares the retention behaviour of the α -helical peptides on the XDB (Figure IV-6A and 6B; pH 2.0 and pH 7.0, respectively) and SB (Figure IV-6C and 6D; pH 2.0 and pH 7.0, respectively) C₈ columns. From Figure IV-6B, selectivity differences between the two column packings are apparent both at pH 2.0 (panels A and C) and pH 7.0 (panels B and D). Thus, at pH 2.0, there is considerable movement of Q_D and Q_L relative to the other peptides between the two columns: Q_D/S_D and P_L/Q_L are coeluted peptide pairs on the XDB column (Figure IV-6A), while Q_D/P_L is a coeluted pair on the SB column (Figure IV-6C). At pH 7.0, Q_L is eluted prior to P_L on the XDB column (Figure IV-6B) and after P_L on the SB column (Figure IV-6D). Further, for this peptide mixture, pH 7.0 resulted in better resolution of all six peptides in both columns compared to pH 2.0.

All peptides are eluted considerably earlier on both columns at pH 7.0 compared to pH 2.0. As noted previously for Figure IV-4, the sodium perchlorate (specifically, the ClO₄⁻ anion) is able to act as an ion-pairing reagent at pH 2.0 since the peptides have an overall +5 net charge. In contrast, at pH 7.0, the overall net charge on the peptides is -1; thus, the salt is able to mask any unfavourable electrostatic interactions between the peptides and the hydrophobic stationary phase at this pH but does not act as an ion-pairing reagent, *i.e.*, the charged character of the peptides makes them more hydrophilic at pH 7.0 compared to pH 2.0 where ion-pairing can take place.

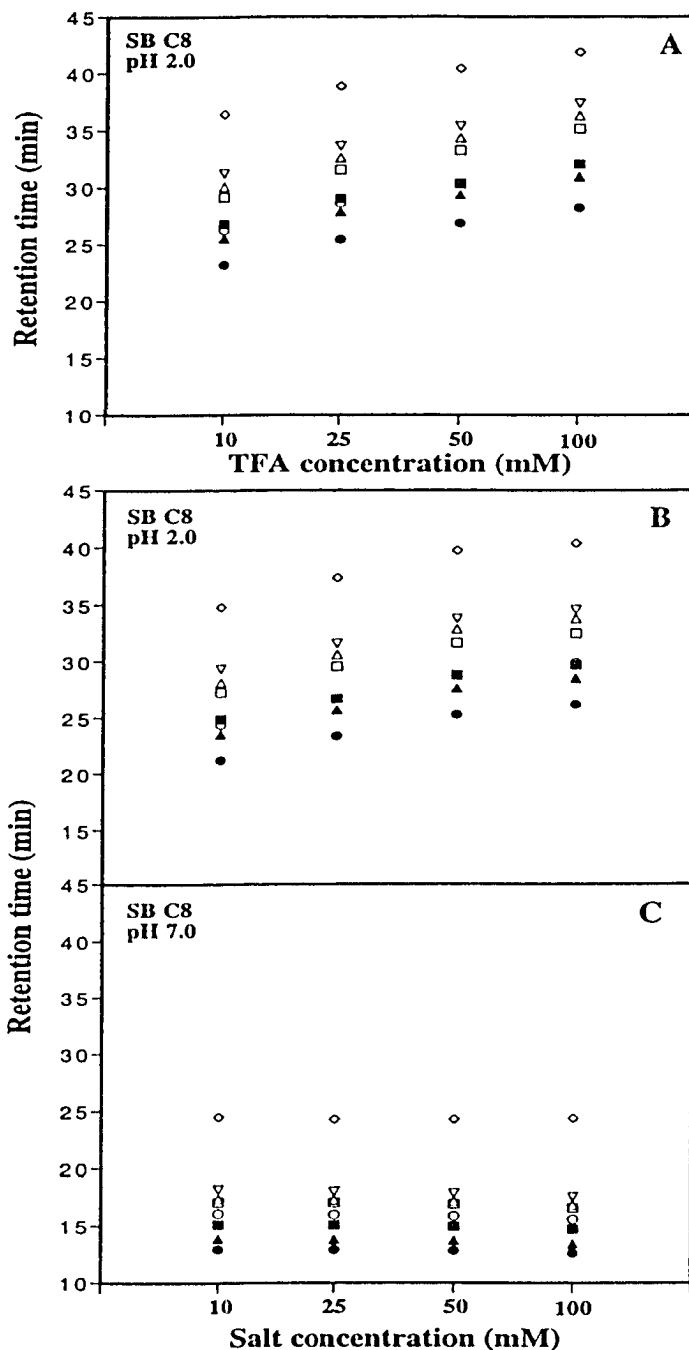


Figure IV-5 Effect of concentration of anionic ion-pairing reagents on the retention time of model peptides at pHs 2.0 and 7.0. Conditions: linear AB gradient (0.5% CH₃CN/min) at a flow-rate of 0.25 ml/min for all runs; (A) eluent A is 10, 25, 50 or 100 mM *aq.* TFA and eluent B is the corresponding TFA concentration in CH₃CN; (B) eluent A is 10, 25, 50 or 100 mM NaClO₄ in 20 mM *aq.* H₃PO₄, pH 2.0, and eluent B is the corresponding eluent A containing 50% CH₃CN; (C) eluent A is 10, 25, 50 or 100 mM NaClO₄ in 20 mM *aq.* PO₄, pH 7.0, and eluent B is the corresponding eluent A containing 50% CH₃CN; temperature, 65 °C. Symbols used are open diamonds for random coil peptide C3, open inverted triangles for G, open upright triangles for S_L, closed upright triangles for S_D, open squares for Q_L, closed squares for Q_D, open circles for P_L and closed circles for P_D.

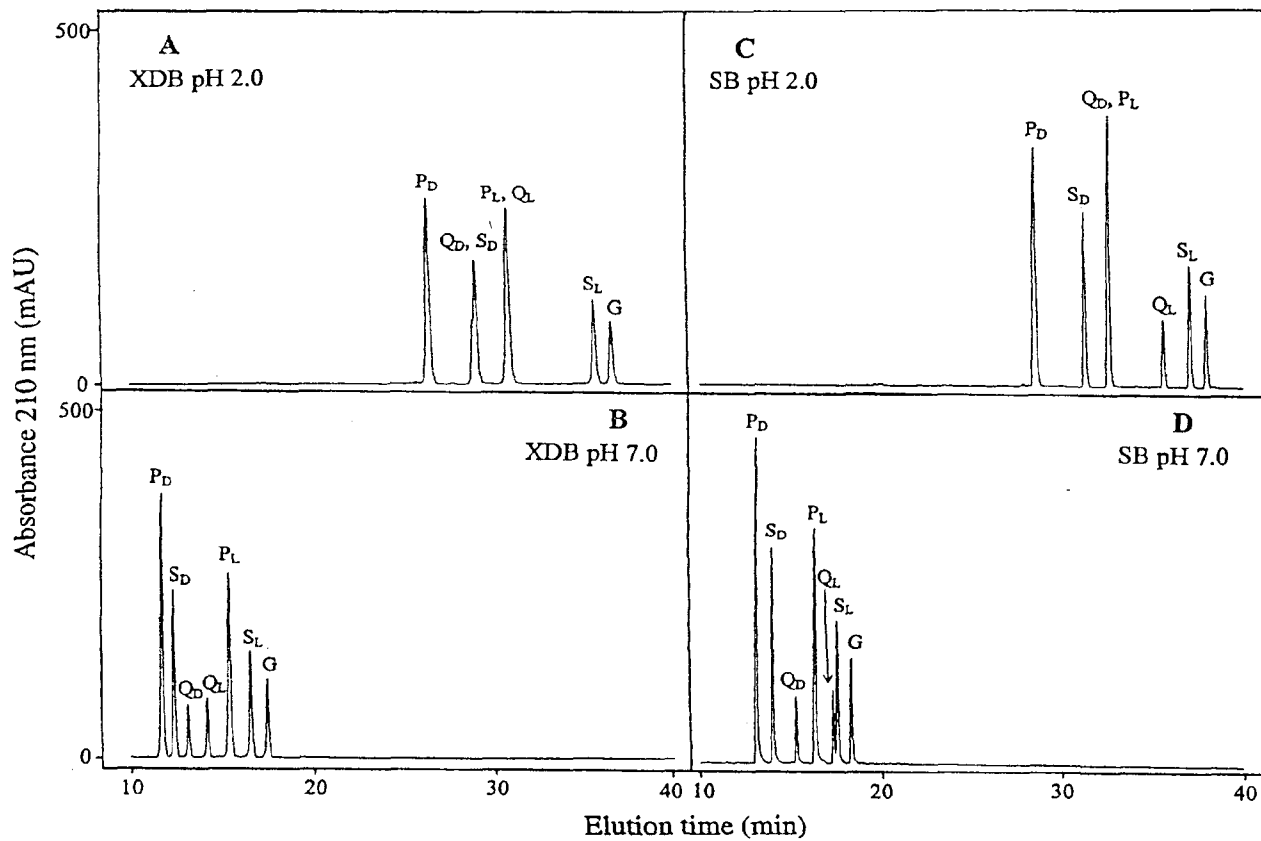


Figure IV-6 Comparison of RP-HPLC retention behavior on XDB and SB-C₈ columns at pH 2.0 and pH 7.0. Conditions: all runs were carried out by linear gradient elution (0.5% CH₃CN/min) at a flow rate of 0.25 ml/min; (A and C) eluent A is 20 mM *aq.* H₃PO₄, pH 2.0, and eluent B is eluent A containing 50% CH₃CN, both eluents containing 100 mM NaClO₄; (B and D) eluent A is 20 mM *aq.* PO₄, pH 7.0, and eluent B is eluent A containing 50% CH₃CN, both eluents containing 100 mM NaClO₄, temperature, 65 °C.

IV-4-3-3 Effect of temperature on RP-HPLC of model peptides at pH 2.0 and pH 7.0

Figure IV-7 illustrates the effect of temperature on elution behaviour of the α -helical peptides at pH 2.0 on the SB-C₈ column (designed, as noted previously, to exhibit excellent stability at acidic pH values (Boyes *et al.*, 1993; Glajch *et al.*, 1990; Kirkland *et al.*, 1989)). From Figure IV-7, increasing temperature both reduces peptide retention time and decreases peak widths, due to an enhancement of the mass-transfer rate of the peptide solutes between the mobile and stationary phases (a higher mass-transfer rate will reduce peak broadening and, hence, increase efficiency) (Antia *et al.*, 1988; Boyes *et al.*, 1993; Li *et al.*, 1997a; Li *et al.*, 1997b). For this peptide mixture, optimum resolution was obtained at 65°C (Figure IV-7B; Table IV-4), with Q_D and P_L being coeluted at 80°C (Figure IV-7C; Table IV-4).

The major selectivity changes with increasing temperature at pH 2.0 arise mainly from the behavior of P_D and P_L which decrease in retention time less with increasing temperature relative to the other peptides. This is likely due to the different conformation-dependent responses of the peptides with temperature (Mant *et al.*, 2003a; Mant *et al.*, 2003b), with unfolding of the amphipathic peptides (and, hence, disruption of the preferred binding domain, *i.e.*, the non-polar face) in solution as the temperature is raised, thus leading to a decrease in retention time (an average drop in t_R for the α -helical peptides of ~14 min between 15°C and 80°C). In contrast, P_D and P_L (an average drop in t_R for P_D and P_L of ~8 min and 10 min, respectively, between 15°C and 80°C) are already 75% (P_D) or 50% (P_L) in a random coil configuration, even at low temperature; hence, their response to a temperature increase would not be as marked as that of a fully folded peptide analogue (Mant *et al.*, 2003a).

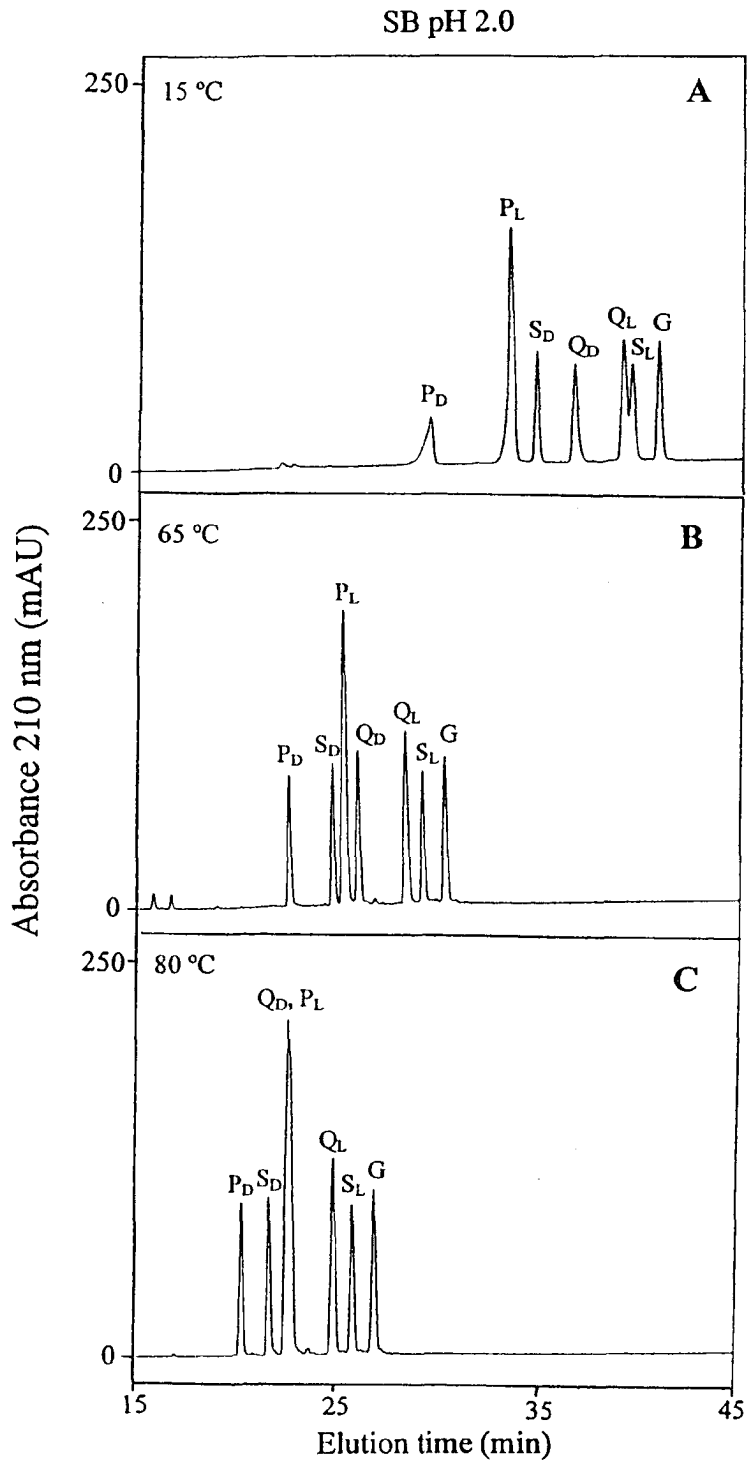


Figure IV-7 Effect of temperature on RP-HPLC elution profile of model peptides at pH 2.0. Conditions: linear AB gradient (0.5% CH₃CN/min) at a flow rate of 0.25 ml/min, where eluent A is 0.05% *aq.* TFA, pH 2.0, and eluent B is 0.05% *aq.* TFA in CH₃CN; temperature, 15 °C (A), 65 °C (B) and 80 °C (C).

Table IV-4 Effect of temperature on peptide resolution during RP-HPLC at pH 2.0 ^a

Peptide pair ^b	Temperature (°C) ^c					
	15 °C		65 °C		80 °C	
	Δt_R^d (min)	R_S^e	Δt_R^d (min)	R_S^e	Δt_R^d (min)	R_S^e
S _D -P _D	5.15	9.52	2.20	6.79	1.39	4.11
P _L -S _D	-1.24 ^f	2.87	0.52	1.35	0.87	1.68
Q _D -P _L	3.14	6.37	0.73	1.79	— ^g	— ^g
Q _L -Q _D	2.35	4.81	2.37	6.26	2.34	4.27
S _L -Q _L	0.42	0.88	0.89	2.33	0.99	2.51
G-S _L	1.31	3.00	1.10	2.94	1.09	2.81

a. Conditions: RP-HPLC at pH 2.0 on SB-C₈ column (see Figure IV-7).

b. Denotes the later eluted peptide minus the adjacent faster eluted peptide on the chromatogram in Figure IV-7; for peptide denotations, see Section IV-4-1-1.

c. Chromatograms at the different temperatures are shown in Figure IV-7.

d. Denotes the difference in retention time between two adjacent peptides (peptide pair) at the corresponding temperature during RP-HPLC at pH 2.0; $\Delta t_R = t_R$ of former peptide minus t_R of adjacent earlier eluted peptide.

e. Denotes the resolution of every two adjacent peaks (peptide pair) at the corresponding temperature during RP-HPLC at pH 2.0.

f. At 15 °C P_L elutes prior to S_D.

g. Dash denotes the co-eluted peptides.

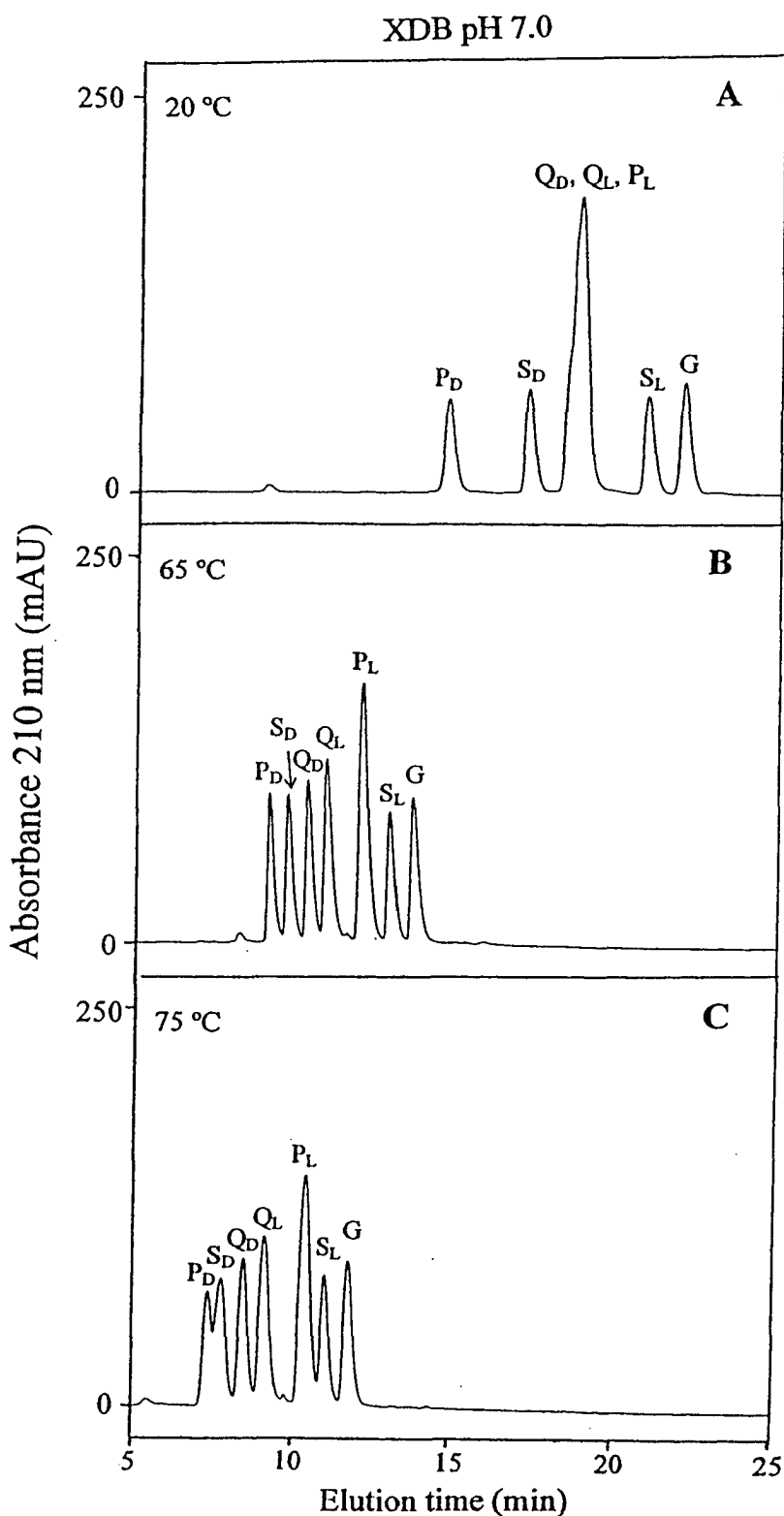


Figure IV-8 Effect of temperature on RP-HPLC elution profile of model peptides at pH 7.0. Conditions, linear AB gradient (0.5% CH₃CN/min) at a flow rate of 0.25 ml/min, where eluent A is 20 mM *aq.* PO₄, pH 7.0, and eluent B is eluent A containing 50% CH₃CN, both eluents containing 100 mM NaClO₄; temperature, 20 °C (A), 65 °C (B) and 75 °C (C).

Table IV-5 Effect of temperature on peptide resolution during RP-HPLC at pH 7.0 ^a

Peptide pair ^b	Temperature (°C) ^c					
	20 °C		65 °C		75 °C	
	Δt_R ^d (min)	R_S ^e	Δt_R ^d (min)	R_S ^e	Δt_R ^d (min)	R_S ^e
S _D -P _D	2.50	4.23	0.59	1.52	0.39	0.75
Q _D -S _D	1.60	2.15	0.63	1.54	0.68	1.22
Q _L -Q _D	— ^f	—	0.61	1.34	0.66	1.13
P _L -Q _L	—	—	1.10	2.15	1.29	1.99
S _L -P _L	2.12	2.83	0.86	1.80	0.65	1.10
G-S _L	1.10	1.90	0.74	1.63	0.73	1.38

a. Conditions: RP-HPLC at pH 7.0 on XDB-C₈ column (see Figure IV-8).

b. Denotes the later eluted peptide minus the adjacent faster eluted peptide on the chromatogram in Figure IV-8. For peptide denotions, see Section IV-4-1-1.

c. Chromatograms at the different temperatures are shown in Figure IV-8.

d. Denotes the difference in retention time between two adjacent peptides (peptide pair) at the corresponding temperature during RP-HPLC at pH 7.0, $\Delta t_R = t_R$ of former peptide minus t_R of adjacent earlier eluted peptide.

e. Denotes the resolution of every two adjacent peaks (peptide pair) at the corresponding temperature during RP-HPLC at pH 7.0.

f. Dash denotes the co-eluted peptides.

Figure IV-8 now illustrates the effect of temperature on elution behaviour of the α -helical peptides at pH 7.0 on the XDB-C₈ column (designed, as noted previously, to exhibit excellent stability at neutral and higher pH values (Kirkland *et al.*, 1997; Kirkland *et al.*, 1998)). From Figure IV-8, in a similar manner to pH 2.0 (Figure IV-7), increasing temperature decreases peptide retention time. Peak width also generally decreases with increasing temperature, with optimum resolution of the peptide mixture, in a similar manner to the pH 2.0 results (Figure IV-7; Table IV-4) being obtained at 65°C (Figure IV-8B; Table IV-5). Note that the broader peaks and reduced retention times of the peptides in Figure IV-8B compared to Figure IV-6B, where the same column and conditions were used, is likely due to column aging in the former. Between 20°C and 75°C (Figure IV-8A and IV-8C, respectively), the retention times of the α -helical analogues decreased by an average of ~10 min; in contrast, the retention time decrease for P_D and P_L was 7.5 min and 8 min, respectively. Such results, where P_D and P_L exhibit a different response to temperature variation relative to the other peptides, are similar to those observed at pH 2.0 (Figure IV-7).

IV-5 Conclusions

In the present study, we have demonstrated how variations in column packing, mobile phase conditions and temperature allow useful manipulation of elution profiles of amphipathic α -helical peptides at both pH 2.0 and pH 7.0. In particular, the perchlorate anion (ClO₄⁻) has proved to be an excellent hydrophilic ion-pairing reagent where there is a net positive charge on the peptide. In addition, it can be used as an ion-pairing reagent in the pH range of pH 2.0 – pH 7.0, unlike acidic anionic ion-pairing reagents such as

TFA. Coupled with the different selectivities observed for peptide separations achievable with different C₈ packings and/or temperature (the latter achievable *via* conformational differences between peptides), our observations are applicable to the rational development of separation/optimization protocols for peptide/proteomic applications.

CHAPTER V

Temperature Selectivity Effects in Reversed-Phase Chromatography Due to Conformation Differences between Helical and Non-Helical Peptides

A version of this chapter has been published: Chen, Y., Mant, C. T. and Hodges, R. S. (2003) *J. Chromatogr. A* **1010**, 45-61. Only methods unique to this chapter are described in the **Experimental** section, the remaining general methods are described in Chapter III.

V-1 Abstract

In order to characterize the effect of temperature on the retention behaviour and selectivity of separation of polypeptides and proteins in reversed-phase high-performance liquid chromatography (RP-HPLC), the chromatographic properties of four series of peptides, with different peptide conformations, have been studied as a function of temperature (5-80 °C). The secondary structure of model peptides was based on either the amphipathic α -helical peptide sequence Ac-EAEKAAKEX_{D/L}EKAAKEAEK-amide, (position X being in the centre of the hydrophobic face of the α -helix), or the random coil peptide sequence Ac-X_{D/L}LGAKGAGVG-amide, where position X is substituted by the 19 L- or D-amino acids and glycine. We have shown that the helical peptide analogues exhibited a greater effect of varying temperature on elution behaviour compared to the random coil peptide analogues, due to the unfolding of α -helical structure with the increase of temperature during RP-HPLC. In addition, temperature generally produced different effects on the separations of peptides with different L- or D-amino acid substitutions within the groups of helical or non-helical peptides. The results demonstrate that variations in temperature can be used to effect significant changes in selectivity

among the peptide analogues despite their very high degree of sequence homology. Our results also suggest that a temperature-based approach to RP-HPLC can be used to distinguish varying amino acid substitutions at the same site of the peptide sequence. We believe that the peptide mixtures presented here provide a good model for studying temperature effects on selectivity due to conformational differences of peptides, both for the rational development of peptide separation/optimization protocols and a probe to distinguish between peptide conformations.

V-2 Introduction

Over the past two decades, reversed-phase high-performance liquid chromatography (RP-HPLC) has emerged as the main method in the development of separation protocols for peptide and protein mixtures (Cunico *et al.*, 1998; Mant *et al.*, 1991; Mant *et al.*, 2002a). The resolving power of this technique is reflected by its frequent use in multidimensional separations of polypeptides, including proteomics applications (Barnidge *et al.*, 2003; Link *et al.*, 1999; Liu *et al.*, 2002b; Wagner *et al.*, 2000; Wagner *et al.*, 2002; Washburn *et al.*, 2001; Wehr, 2002). Indeed, the combined desalting/purification aspect of RP-HPLC makes it ideal as the final step of a multidimensional separation protocol, notably prior to mass spectrometry of purified solutes.

Clearly, considering the complexity of proteomics applications of liquid chromatography, where the separation of hundreds or even thousands of peptides may be required, *e.g.*, from simultaneous digest of a multi-protein mixture, optimization of the separation protocol is of prime importance. Concerning RP-HPLC, such optimization has

traditionally been achieved by mobile phase variations (*e.g.*, changes in organic modifier, ion-pairing reagent or pH) (Cunico *et al.*, 1998; Mant *et al.*, 1991; Mant *et al.*, 1992; Mant *et al.*, 2002a), variations in the organic modifier gradient rate (Mant *et al.*, 1991; Mant *et al.*, 1994; Sereda *et al.*, 1995), or even changes in column packing to take advantage of selectivity differences offered by different stationary phase ligands (Mant *et al.*, 1997; Zhou *et al.*, 1991). In addition, the introduction in recent years of stationary phases stable to high temperatures has added to the arsenal of RP-HPLC approaches for optimization of the resolution of polypeptide mixtures (Barry *et al.*, 1995; Boyes *et al.*, 1993; Chloupek *et al.*, 1994; Glajch *et al.*, 1990; Hancock *et al.*, 1994; Kirkland *et al.*, 1989; Kirkland *et al.*, 1993; Kirkland *et al.*, 1997; Lee *et al.*, 2003b; Mant *et al.*, 1997; Mant *et al.*, 2003a; Mant *et al.*, 2003b; McNeff *et al.*, 2000; Zhu *et al.*, 1996a; Zhu *et al.*, 1996b).

Many and varied influences will have an impact on the way a particular peptide interacts with a reversed-phase column, not least of which include characteristics of the peptide itself, *e.g.*, amino acid composition (Guo *et al.*, 1986a; Zhou *et al.*, 1990), residue sequence (Houghten *et al.*, 1987; Zhou *et al.*, 1990), peptide length (Mant *et al.*, 1988; Mant *et al.*, 1989), and the presence of any secondary structure (α -helix or β -sheet) (Blondelle *et al.*, 1992a; Heinitz *et al.*, 1988; Mant *et al.*, 1998a; Mant *et al.*, 1998b; Steer *et al.*, 1998; Steiner *et al.*, 1991; Zhou *et al.*, 1990); indeed, RP-HPLC of peptides and proteins at varying temperature has also allowed an insight into the role of conformation in the retention behaviour of peptides and proteins (Lee *et al.*, 2003b; Mant *et al.*, 1989; Mant *et al.*, 2003a; Mant *et al.*, 2003b; Purcell *et al.*, 1993; Purcell *et al.*, 1995a; Purcell *et al.*, 1995b; Purcell *et al.*, 1995c; Richards *et al.*, 1994). The importance of delineating

the contribution of α -helical structure (both amphipathic and non-amphipathic) to the selectivity of peptide separations cannot be underestimated, particularly when one considers that peptide fragments from chemical or proteolytic digests of proteins typically contain peptides with α -helical potential. During RP-HPLC, such peptides will be induced into α -helical structure by the non-polar environment characteristic of this technique (hydrophobic matrix and non-polar eluting solvent) (Blondelle *et al.*, 1995; Purcell *et al.*, 1995c; Steer *et al.*, 1998; Zhou *et al.*, 1990).

A previous study in our laboratory (Sereda *et al.*, 1995) illustrated the selectivity that may be obtained in a reversed-phase separation based on peptide conformational differences (α -helical *versus* random coil), highlighted by their retention time behaviour at varying gradients of organic modifier. Thus, the present study examines the effect of temperature on RP-HPLC retention behaviour at pH 2.0 of four series of peptides, based on either the amphipathic peptide sequence Ac-EAEKAAKEXEKAAKEAEK-amide (with position X in the centre of the hydrophobic face of the α -helix) or the random coil peptide sequence Ac-XLGAKGAGVG-amide, where position X is substituted by the 19 L- or D-amino acids. We believed that observation of the temperature effect on retention behaviour of such peptide models would have implications, not only for the rational development of separation/optimization protocol, but also for the understanding of the hydrophobic interactions between RP-HPLC stationary phases and peptides with conformational differences.

V-3 Experimental

V-3-1 Columns and HPLC conditions

Analytical RP-HPLC was carried out on a Zorbax 300 SB-C₈ narrowbore column (150 x 2.1 mm I.D.; 5- μ m particle size, 300-Å pore size) from Agilent Technologies with a linear AB gradient (0.5% acetonitrile/min) at a flow-rate of 0.25 ml/min, where eluent A was 0.05% *aq.* TFA, pH 2.0, and eluent B was 0.05% TFA in acetonitrile. This C₈ column (with SB denoting StableBond) was chosen for this study due to its excellent temperature stability at low pH (Barry *et al.*, 1995; Boyes *et al.*, 1993; Chloupek *et al.*, 1994; Glajch *et al.*, 1990; Hancock *et al.*, 1994; Kirkland *et al.*, 1989; Kirkland *et al.*, 1993; Kirkland *et al.*, 1997; Lee *et al.*, 2003b; Mant *et al.*, 1997; Mant *et al.*, 2003a; Mant *et al.*, 2003b; McNeff *et al.*, 2000; Zhu *et al.*, 1996a; Zhu *et al.*, 1996b).

V-4 Results

V-4-1 Peptide design and designation

The amphipathic α -helix is a very commonly encountered structural motif in peptides and proteins and approximately 50% of all helices in soluble globular proteins are amphipathic (Cornette *et al.*, 1987; Segrest *et al.*, 1990). In order to study the effect of temperature on selectivity of peptide separations, we believed that the best initial approach was to compare the retention behaviour of peptides with extremes of structure, *i.e.*, either with as close to 100% α -helical conformation as possible or with the complete absence of α -helix. In addition, in a previous study, we showed that α -helical peptides with D-amino acid substitutions exhibited considerably different retention behaviour during RP-HPLC compared with L-diastereomeric analogues (Chen *et al.*, 2002), due to

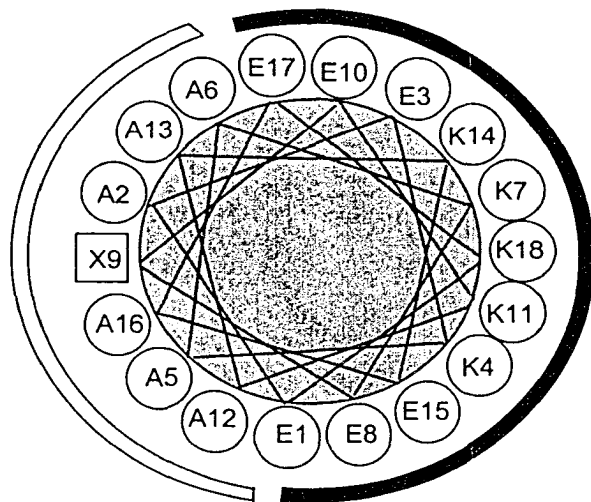
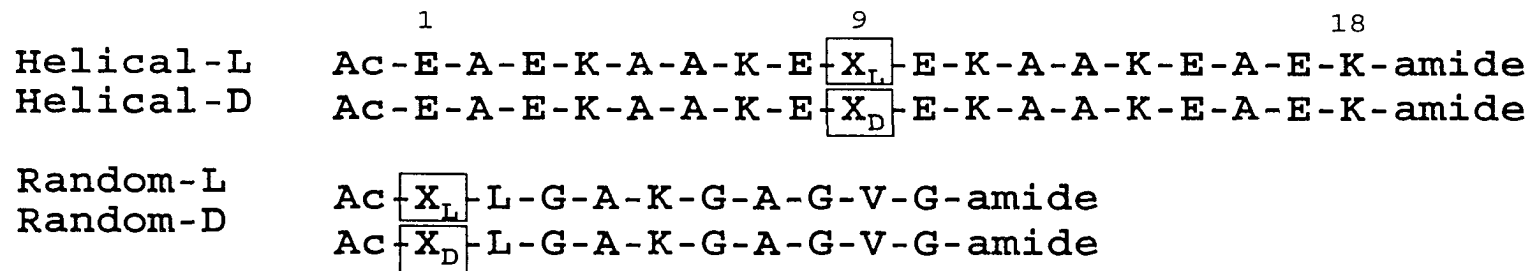


Figure V-1 Model synthetic peptides with conformational differences. Top: sequences of the model amphipathic helical and random coil peptides with L- or D-amino acid substitutions at position X (boxed), which represents the substitution site at position 9 in the helical peptides and position 1 in random coil peptides, respectively. Bottom: helical wheel representation of the model amphipathic α -helical peptide with the substitution site at position 9 (boxed) in the hydrophobic face. The closed arc denotes the hydrophilic face; the open arc denotes the hydrophobic face.

the helix-disrupting characteristics of D-amino acids when substituted into an α -helix made up solely of L-amino acid residues (Aguilar *et al.*, 1993; Chen *et al.*, 2002; Krause *et al.*, 2000; Rothmund *et al.*, 1995; Rothmund *et al.*, 1996). Hence, this study set out to explore whether temperature has a different effect on the separation of D- versus L-peptide diastereomers. Four series of peptides designed to exhibit markedly different conformational characteristics during RP-HPLC were synthesized, the sequences of which are shown in Figure V-1.

Two series of random coil decapeptide analogues, designed to exhibit negligible α -helical structure, were substituted with a single L- or D-amino acid at position 1 (Random-L and Random-D, Figure V-1). The sequence of Ac-X_{D/L}LGAKGAGVG-amide, containing 4 Gly residues, was chosen since it lacks any ability to form any specific secondary structure (Sereda *et al.*, 1993; Sereda *et al.*, 1995). A 10-residue length for the peptide analogues was chosen to avoid significant effect of chain length on the retention behaviour (Mant *et al.*, 1988) and to mimic the average sized fragment of a proteolytic digest of a protein. The presence of a lysine residue at position 5 of the peptide analogues ensures sufficient peptide solubility.

The two series of α -helical peptide analogues were synthesized (Helical-L and Helical-D, Figure V-1), based on the well-characterized sequence of Ac-EAEKAAKEAEKAAKEAEK-amide (also denoted as AA9) (Mant *et al.*, 1993; Mant *et al.*, 2002b; Mant *et al.*, 2002c; Monera *et al.*, 1995; Sereda *et al.*, 1994; Zhou *et al.*, 1992; Zhou *et al.*, 1993; Zhou *et al.*, 1994a; Zhou *et al.*, 1994b). L- and D-amino acids were used to substitute the Ala residue at position 9 in the centre of the non-polar face of this amphipathic α -helical sequence (helical wheel, Figure V-1). The use of such amphipathic

α -helices was also designed to reflect the common occurrence of such helices in nature, with, as noted above, approximately 50% of all helices in globular proteins being amphipathic (Cornette *et al.*, 1987; Segrest *et al.*, 1990). Since glycine does not exhibit optical activity, the Gly-substituted analogues in both helical and random coil categories represent useful reference standards during RP-HPLC.

In the present study, since we have a large number (78) peptide analogues (19 L- and D-amino acids substituted at position 1 of the random coil peptide or position 9 of the α -helical peptide, respectively (plus two glycine-substituted peptides), in order to avoid the complexity of designation of these analogues, the peptides are divided into two main categories as "Random" and "Helical" to represent random coil and amphipathic α -helical peptides, respectively; within each category, peptide analogues are named after the substituting amino acid residues at position 1 of Random peptides or position 9 of Helical peptides. For instance, within Helical, L_D or L_L represents the α -helical peptide with amino acid D-leucine or L-leucine substitution at position 9 in the centre of the non-polar face, respectively. However, when comparing temperature effects on L- or D-diastereomeric peptide analogues, we put all the peptides into two groups as "L-Peptides" and "D-Peptides"; within each category, peptides are named after both the substituting amino acid residue and the peptide structure, *e.g.*, L_R and L_H in D-Peptides represent the random coil peptide and the α -helical peptide with a D-leucine substitution at the corresponding position, respectively.

V-4-2 *Conformation of model peptides*

The secondary structures of model Random and Helical peptide categories as represented by L_L and L_D peptides in the presence of the α -helix-inducing solvent 50%

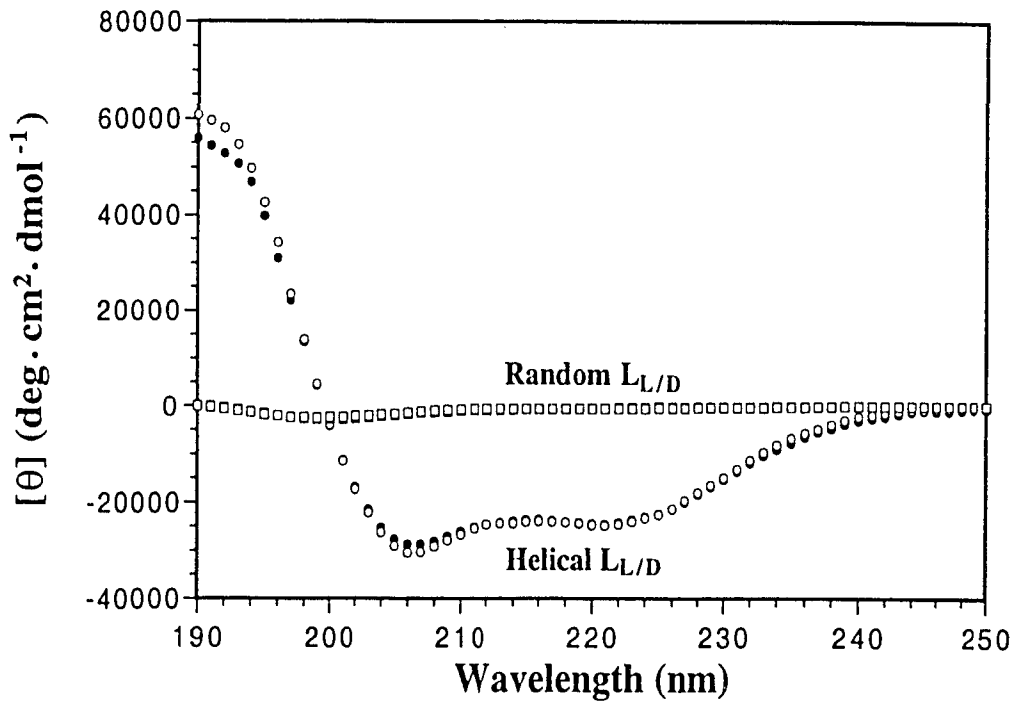


Figure V-2 Circular dichroism (CD) spectra of helical and random coil L_L and L_D peptides. The solution is buffered by 50 mM *aq.* PO_4 containing 100 mM KCl in the presence of 50% TFE at pH 7.0 and 25 °C. Solid symbols represent the CD spectra of L_D peptides, whereas open symbols represent the CD spectra of L_L peptides. The symbols used are circles for helical peptides and squares for random coil peptides.

TFE at pH 7.0 are shown in Figure V-2. The high helicity of the amphipathic peptide series in the presence of TFE has been previously well documented (Chen *et al.*, 2002; Monera *et al.*, 1995; Zhou *et al.*, 1994b). According to our previous study (Chen *et al.*, 2002) all of the amphipathic peptide analogues with L-/D-amino acid substitutions showed similar molar ellipticity values at 222 nm in the presence of 50% TFE with over 90% helical content, with the exception of the L-/D-proline substituted peptides. Since TFE is recognized as a useful mimic of the hydrophobic environment characteristic of RP-HPLC (Zhou *et al.*, 1990), as well as being a strong α -helix inducer for potentially helical molecules (Cooper *et al.*, 1990; Kentsis *et al.*, 1998; Lau *et al.*, 1984a; Nelson *et al.*, 1989; Sonnichsen *et al.*, 1992), elution of these peptide analogues as α -helices during RP-HPLC is ensured. In addition, the $[\theta]_{222}/[\theta]_{208}$ ratio values of Helical L_I and L_D are less than 1, suggesting that, in the presence of 50% TFE, these peptides are single-stranded α -helices (Cooper *et al.*, 1990; Zhou *et al.*, 1993; Zhou *et al.*, 1994a). Taken together, these observations suggest that the helical peptides in this study are bound and eluted in the single-stranded amphipathic α -helical conformation during RP-HPLC. In contrast, the peptides designed as model random coil peptides showed, as expected, no secondary structure, even in the presence of 50% TFE (Figure V-2).

V-4-3 *Temperature effect on RP-HPLC selectivity of amphipathic α -helical peptides*

The effect of temperature on the selectivity of amphipathic α -helical model peptides during RP-HPLC is shown in Figure V-3. As noted above, it is known that characteristic RP-HPLC conditions (hydrophobic stationary phase, non-polar eluting solvent) induce helical structure in potentially helical polypeptides (Blondelle *et al.*, 1995; Purcell *et al.*, 1995c; Steer *et al.*, 1998; Zhou *et al.*, 1990) in a manner similar to

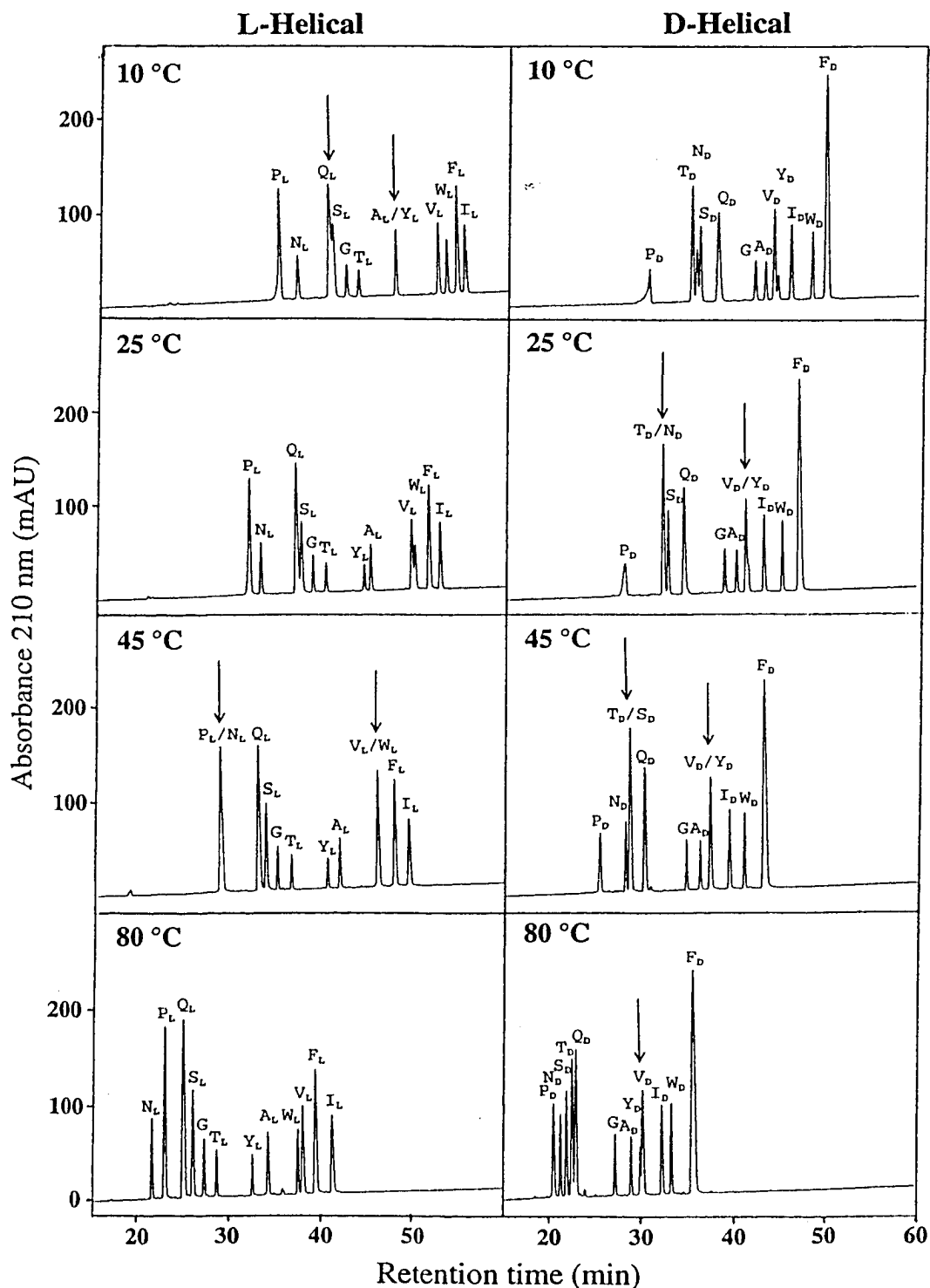


Figure V-3 Effect for temperature on RP-HPLC selectivity for model α -helical peptides with L- or D-amino acid substitutions. Column: SB-C8 300 column (150x2.1 mm I.D.; 5 μ m particle size, 300 \AA pore size). Conditions: linear AB gradient (0.5% acetonitrile/min) at a flow rate of 0.25 ml/min, where eluent A is 0.05% aq. TFA, pH 2.0, and eluent B is 0.05% TFA in acetonitrile. Arrows in chromatograms point out the co-eluted or poorly resolved peaks of different peptides. Helical peptides are denoted by the substituting L- or D-amino acid at position 9 in the hydrophobic face (Figure V-1).

that of the helix-inducing solvent TFE. Polypeptides, such as our model peptides (Figure V-1), which are thus induced into amphipathic α -helices on interaction with a hydrophobic RP-HPLC stationary phase will exhibit preferred binding of their non-polar face with the stationary phase, resulting in considerably more retentive behaviour than non-amphipathic peptides of the same amino acid composition (Zhou *et al.*, 1990). In Figure V-3, RP-HPLC chromatograms at low temperature (10 °C), intermediate temperatures (25 °C and 45 °C) and high temperature (80 °C) were chosen as examples to show the effect of temperature on the separation of Helical peptides with different L- or D-amino acid substitutions. It is clear that there is a wide range of retention times as would be expected given the differences in side-chain hydrophobicity of the substituted L- or D-amino acids, ranging as they do from the highly non-polar (*e.g.*, Ile, Leu, Phe, Trp) to the polar (*e.g.*, Ser, Thr, Asn, Gln) (Chen *et al.*, 2002; Monera *et al.*, 1995; Sereda *et al.*, 1994). As has previously been observed (Chen *et al.*, 2002), Helical P_L and P_D were eluted early, due both to the strong helix-disrupting nature of proline (which also disrupts the amphipathicity of P_L and P_D) and its comparatively low hydrophobicity compared to other non-polar peptide analogues.

From Figure V-3 (left panels), the most obvious phenomenon is that all L- and D-Helical peptide analogues became less retentive at higher temperature than those at lower temperature, as expected due to the general effects of increasing temperature resulting in increased solubility of the solute in the mobile phase as the temperature rises (Cohen *et al.*, 1984; Guo *et al.*, 1986b; Hancock *et al.*, 1986; Ingraham *et al.*, 1985) as well as causing a decrease in solvent viscosity and an increase in mass transfer between the mobile and stationary phases (Dolan, 2002). For L-Helical peptides (left column), the

profile at 10 °C shows that A_L and Y_L were co-eluted, with Q_L and S_L poorly resolved, as indicated by the arrows. However, with the increase of temperature, these peptide analogues were well resolved at 45 °C and resolution improved even more at higher temperatures (80 °C). In contrast, some peptide analogues (*e.g.*, P_L and N_L, V_L and W_L) were well resolved at 10 °C, but were then co-eluted at 45 °C; however, these peptides were again resolved at 80%, albeit with a reversal of their elution order compared to 10 °C.

Interestingly, similar phenomena are apparent in the profiles of the D-Helical peptides (Figure V-3, right panels). At 10 °C, Helical T_D was eluted faster than the adjacent peptide analogues N_D and S_D, but T_D and N_D were co-eluted at 25 °C. Furthermore, at 45 °C, N_D was eluted before T_D. In contrast, T_D was co-eluted with S_D, the latest eluted peptide among the three analogues at low temperature. Finally, an elution order change was observed at 80 °C, with N_D being eluted first and T_D eluted last, with all three peptides well resolved. A similar change in elution order can also be seen for Helical V_D and Y_D analogues from 10 °C to 80 °C, albeit to a lesser degree.

From the RP-HPLC elution profiles in Figure V-3, three effects of temperature on the retention behavior of Helical peptide analogues are apparent: (i) the retention times of Helical peptide analogues decreased with increasing temperature; (ii) temperature affected the retention behaviour of different Helical peptide analogues to differing extents; (iii) the overall trend of temperature effect on the Helical peptides with either L- or D-amino acid substitutions is without significant difference. Of particular note is the alteration of peak height of peptide analogues during the change of temperature in Figure

V-3, where an increase in temperature resulted in increased peak height and decreased peak width during RP-HPLC, which may be important to increase elution resolution.

V-4-4 Temperature effect on RP-HPLC selectivity for random coil peptides

Random coil peptides used in the present study are molecules without specific secondary structure in a non-polar environment (Figure V-2). Therefore, the separation of Random peptides with varying L-/D-amino acid substitutions are merely dependent on side-chain hydrophobicity of the substituting amino acid residue, as the peptides with the less hydrophobic substituting amino acid residues (*e.g.*, Gly, Glu, Pro) are eluted faster and the peptides with the more hydrophobic residues (*e.g.*, Trp, Phe, Leu) are eluted slower (Figure V-4; L-peptides). From Figure V-4, temperature has similar effects on the L-/D-amino acid substituted random coil peptide analogues as was observed for the Helical peptides and described above (Figure V-3), *i.e.*, (i) overall, increasing temperature decreased the retention times of the Random peptides; (ii) temperature affected the retention behavior of the Random peptides to different degrees; and (iii) the influence of temperature on the L- and D- Random peptides during RP-HPLC is similar. For instance, L-Val- and L-Tyr-substituted random coil peptides (denoted as V_R and Y_R in Figure V-4, left) were separated, co-eluted and separated once more over the temperature range of 25 °C to 75 °C, albeit with reversal of elution order at 75 °C compared to 25 °C.

V-4-5 Comparison of temperature effect on L- or D-Helical and Random model peptides

Figure V-4 shows RP-HPLC elution profiles of temperature effect on selectivity of both Helical and Random peptides with varying L-/D-amino acid substitutions. The temperatures chosen were designed to indicate the alteration of peptide elution profiles

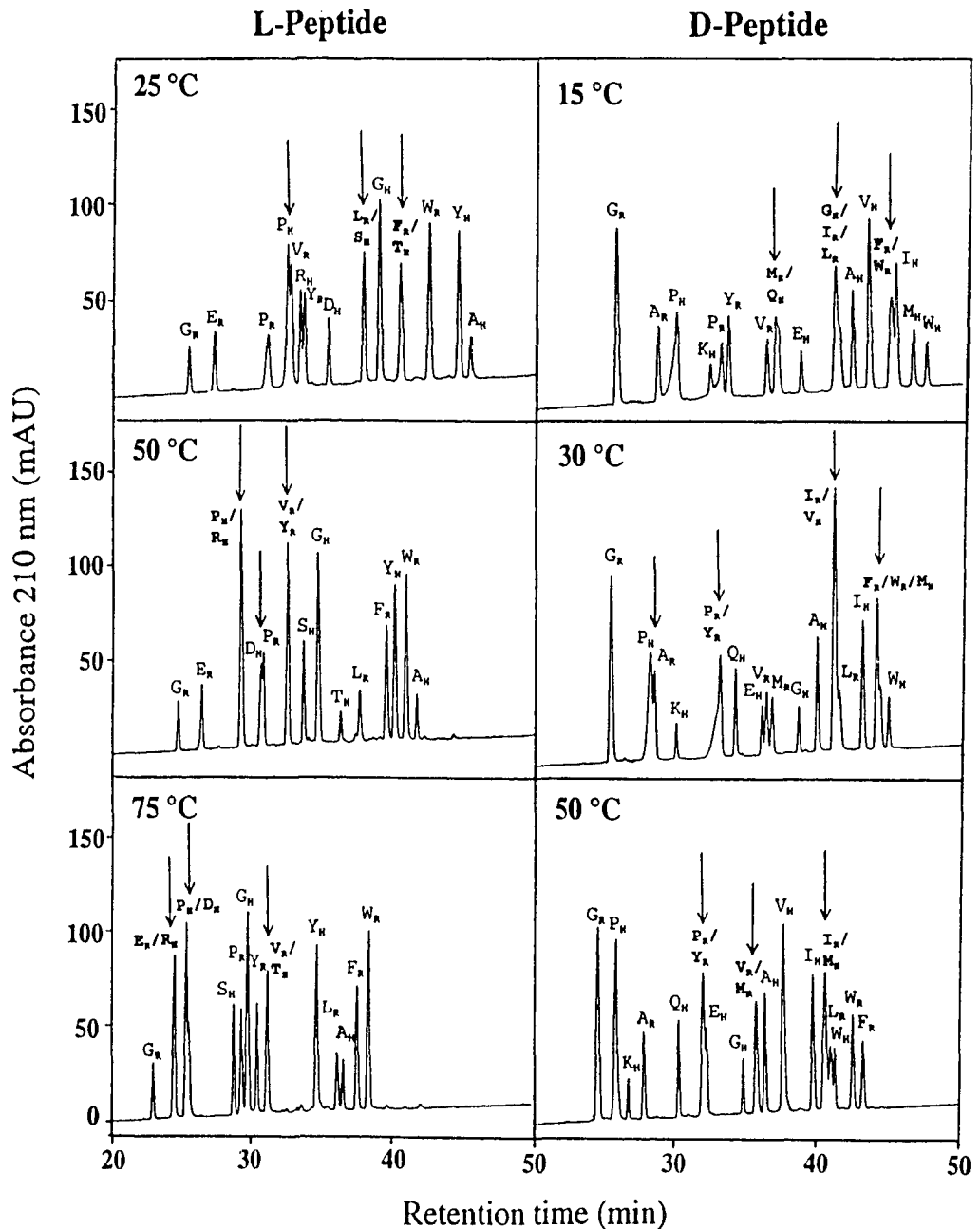


Figure V-4 Effect of temperature on RP-HPLC selectivity for random coil and α -helical peptides. Column and conditions same as for Figure V-3. Arrows in chromatograms point out the co-eluted or poorly resolved peaks of different peptides. Peptide designation is based on the substituting amino acid as described in the text. Subscripts of letter R and H denote random coil or helical peptide, respectively.

with different co-eluted peaks (highlighted in bold letters) at different temperatures. Although all peptide analogues (Helical and Random) again exhibit the trend of reducing retention time with increasing temperature, it is also apparent that temperature affects retention behavior of different peptides to different extents. Thus, co-eluted peaks are composed of different Helical and Random peptide analogues at different temperatures.

Figure V-5 plots the relationship of RP-HPLC retention time versus temperature of Helical and Random peptide analogues. Temperature has a much greater effect on retention time of the α -helical peptide analogues (both L-amino acid substituted helical peptide analogues in Panel A and D-amino acid substituted peptide analogues in Panel B) than the random coil peptides. Although not shown here, the slope values of the best fitting lines of peptide retention data within the temperature range 10-75 °C vary from -0.14 to -0.19 for L-Helical peptides and -0.02 to -0.07 for L-Random peptides (Figure V-5, Panel A). Similarly, the slopes vary from -0.11 to -0.18 and -0.02 and -0.08 for D-Helical and D-Random peptide analogues, respectively (Figure V-5, Panel B). The significant difference in magnitude of the slopes of the plots for the Helical and Random peptides highlights again that temperature has a greater effect on the L-/D-Helical peptide analogues compared to the L-/D-Random peptide analogues, which can be attributed to differences in peptide structural changes. In addition, the slope variations within Helical or Random peptides show the subtle differences that temperature can have on peptide analogues in the same structural category with different amino acid substitutions. It is interesting to see that the overall effect of temperature on L- or D-amino acid substituted peptides with the same secondary structure is extremely similar. It is important to note

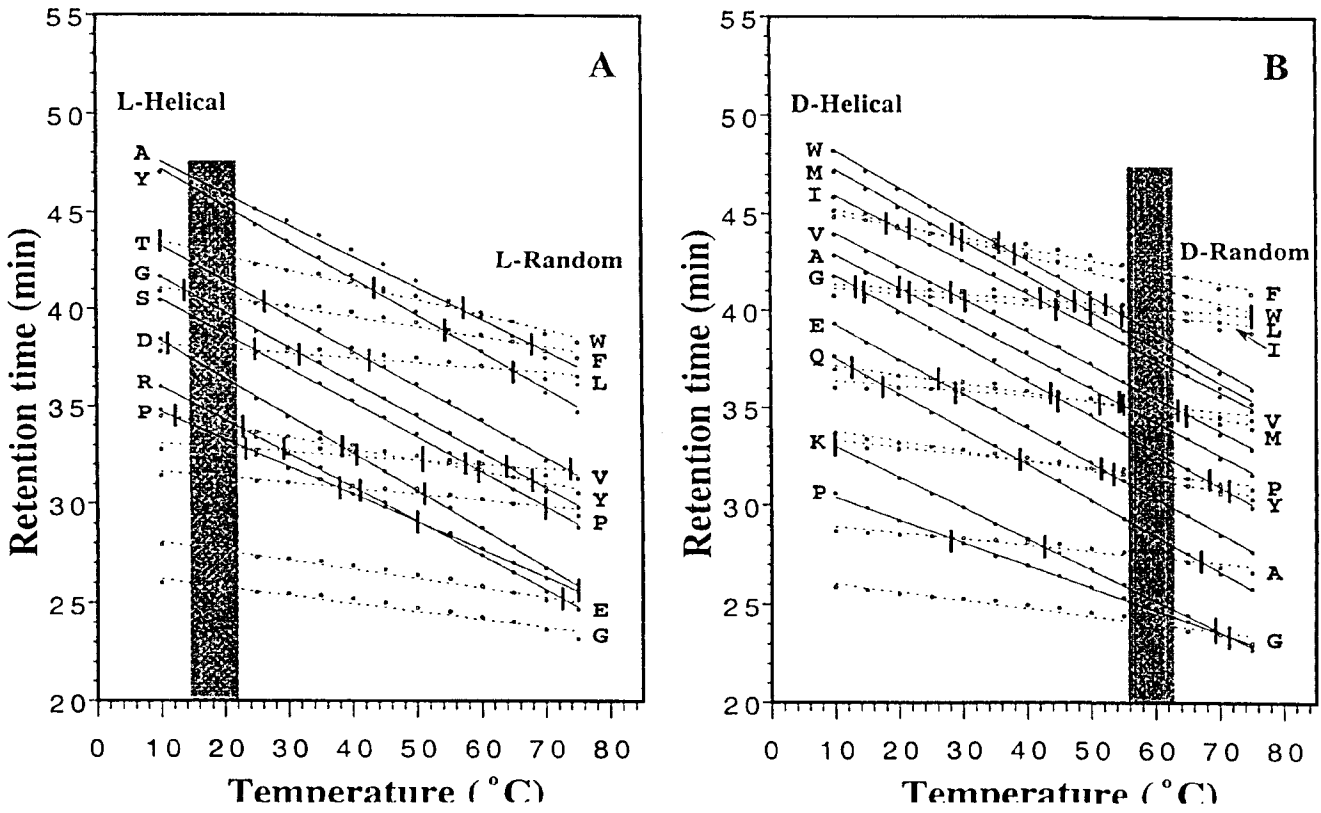


Figure V-5 Effect of temperature on RP-HPLC retention time of helical and random coil peptides. Column and conditions same as for Figure V-3. Panels A and B show the temperature effect on helical and random coil peptides with L-amino acid or D-amino acid substitutions, respectively. In both (A) and (B), solid lines with solid symbols represent helical peptides and dotted lines with open symbols denote random coil peptides. Co-elution or poor resolution of peptide peaks are marked with small black bars. The grey column in each panel shows the temperature zone in which the optimum separation of the peptide mixture can be obtained. See text for peptide designation.

that the linearity of the best fitting lines in Figure V-5 have correlation coefficients greater than 0.97 for most peptides, reflecting the generality of the conclusions.

V-4-6 *Optimum separation of peptide mixtures of α -helical and random coil peptides*

From Figure V-5, marked as short black vertical bars, the co-elution points of any two peptides illustrate the complexity of RP-HPLC elution in Helical and Random peptide mixtures within the temperature range used. The prospective optimum separation zones of L- or D-peptide mixtures are denoted as grey columns in Figure V-5, 0.5 °C away (on the X-axis) from the nearest co-elution point on both sides of these zones. Hence, in order to obtain the optimum separation of L- or D-peptide mixtures, RP-HPLC was carried out in 0.5 °C increments within the prospective optimum separation zones of the L-peptides (encompassing 16 L-amino acid substituted Helical and Random model peptides) and the D-peptides (encompassing 20 D-amino acid Helical and Random peptides). Figure V-6 shows the RP-HPLC elution profiles of the L- and D-peptide mixtures used in Figure V-4 and Figure V-5, with the optimum separation (middle panels) as well as the RP-HPLC profiles obtained at temperatures several degrees lower (upper panels) or higher (lower panels) than the corresponding optimum temperatures. Considering the number of α -helical and random coil peptide analogues in each mixture, excellent separations have been observed at 21 °C and 62.5 °C for L-peptides and D-peptides, respectively. In addition, the optimum temperatures of L- and D-peptides are both in the corresponding empirical prospective optimum zones (Figure V-5), indicating the validity of the temperature-based optimization protocol. In contrast to the optimum elution profiles, the chromatograms at higher or lower temperature represent the sensitivity of the varying temperature approach to influence the selectivity of peptides

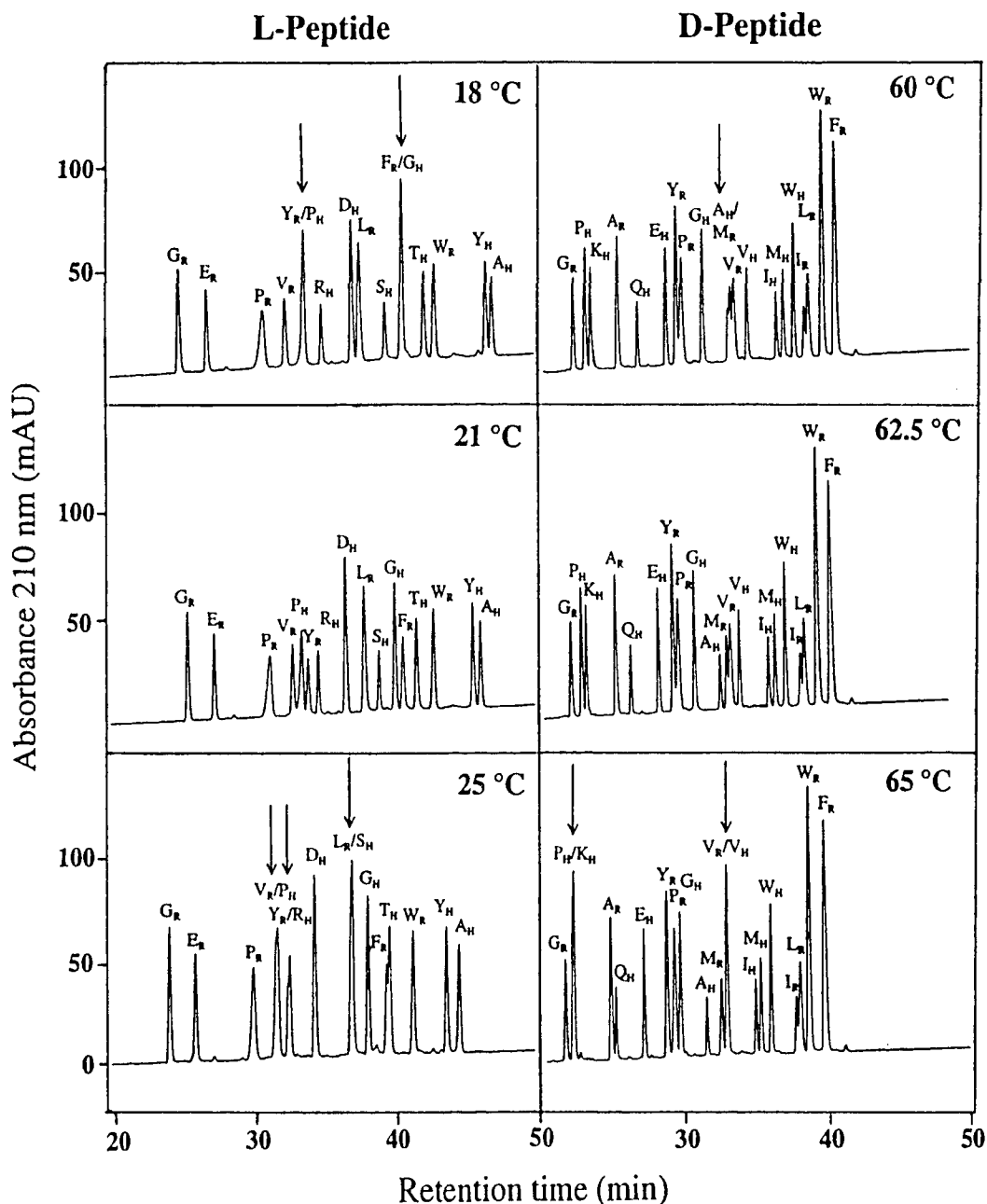


Figure V-6 RP-HPLC separation of random coil and helical L- or D-peptides around the optimum temperatures. Column and conditions same as for Figure V-3. Arrows in chromatograms point out the co-eluted or poorly resolved peaks of different peptides. Peptide designation is based on the substituting amino acid as described in the text. Subscripts of letter R and H denote random coil or helical peptide, respectively.

with conformational differences. It is important to note that, from shifts in temperature in the range of just 2.5 °C to 4° C from the optimum temperature, the RP-HPLC profiles clearly show considerably different retention behavior with different peptides co-eluted (indicated by the arrows), underlining the effectiveness of subtle temperature changes to alter the elution profiles of the peptide models in this RP-HPLC temperature selectivity study.

V-5 Discussion

Although the retention times of all the Helical and Random peptides decreased with increasing temperature, it is clear that the overall retention of the α -helical model peptides decreased to a greater extent than that of the Random peptide analogues. Since the Helical or Random model peptides have different conformations, *i.e.*, as single-stranded amphipathic α -helical peptides or random coil peptides, respectively, the varying results of temperature effect on peptide retention behaviour may be mainly attributed to structural differences (Figure V-4, Figure V-5) with the conformation of the α -helical peptides in solution during RP-HPLC strongly influenced by temperature. Indeed, in our previous study (Chen *et al.*, 2002), we showed that the helical conformation of the model peptides could be denatured to different degrees with a temperature increase in the presence of helix-inducing 40% trifluoroethanol (TFE). In fact, on binding to a reversed-phase column, the high hydrophobicity of the stationary phase stabilizes secondary (α -helical) structure, mimicking the effect of TFE when the peptide is in solution (Sereda *et al.*, 1994). Therefore, during RP-HPLC, a temperature increase may also induce peptide denaturation and, as a result, disrupt peptide

amphipathicity, thereby reducing the retention time of the model peptide. In contrast, the elution of random coil peptides was merely influenced by the general effects of temperature (as described above) with a concomitant lesser effect on retention behaviour compared to the α -helical peptide analogues.

From Figure V-5, the retention behaviour of all L- and D-Helical peptides with a change of temperature was similar except for that of L-/D-proline substituted Helical peptides. Due to the well-documented helix-disrupting characteristic of proline (Chen *et al.*, 2002; Monera *et al.*, 1995; Zhou *et al.*, 1994b), proline-substituted model peptides would not be fully helical even in a strong hydrophobic environment, *e.g.*, in the presence of 50% TFE or the hydrophobic conditions of RP-HPLC. As a result, the effect of temperature denaturation on Helical P_L and P_D would not be as dramatic as the effect on other α -helical model peptide analogues, since, for all intents and purposes, the Helical P_L and P_D analogues are already partially denatured. Interestingly, the slope values of the temperature profiles of the various peptide analogues appear to be related to their the molar ellipticity values, *i.e.*, slope values of Helical P_L and P_D during temperature variation are smaller than those of α -helical peptide analogues with other amino acid substitutions, and greater than those of random coil peptides; concomitantly, the molar ellipticity values of Helical P_L and P_D in the presence of 50% TFE are smaller than those of other α -helical analogues but greater than those of random coil peptides (Chen *et al.*, 2002) (Figure V-2). Thus, our results support again the premise that temperature can be used as a sensitive probe of peptide conformation during RP-HPLC (Lee *et al.*, 2003b; Mant *et al.*, 1989; Mant *et al.*, 2003a; Mant *et al.*, 2003b; Purcell *et al.*, 1993; Purcell *et al.*, 1995a; Purcell *et al.*, 1995b; Purcell *et al.*, 1995c; Richards *et al.*, 1994).

Figure V-7 shows the temperature effect on RP-HPLC retention behaviour of L-/D-amino acid substituted α -helical model peptides. Thus, the retention behaviour of hydrophobic (Val, Ile, Ala) and hydrophilic (Asn, Gln) L-/D-amino acid substituted Helical peptide analogues over a temperature range of 5 °C to 80 °C were examined by plotting peptide retention time at a specific temperature minus its retention time at 5 °C *versus* temperature in order to highlight differences in the elution behaviour of peptides as the temperature is raised. The Gly-substituted Helical peptide was also selected as a standard to evaluate the effect of temperature on L-/D-diastereomeric peptide analogues, due to the characteristic non-optical activity of glycine. From Figure V-7, it is clear that L-Helical peptides of different amphipathicity/hydrophobicity behave quite similarly during RP-HPLC at different temperatures (Panel A), as do the D-amino acid substituted α -helical diastereomers (Panel B). High correlations were obtained with $R=0.985$ for L-Helical peptides and $R=0.995$ for D-Helical peptides, respectively. In addition, in our previous study (Chen *et al.*, 2002), D-amino acid substituted peptides generally showed lower helicity in aqueous environment, due to the helix-disrupting characteristics of D-amino acid residues (Aguilar *et al.*, 1993; Chen *et al.*, 2002; Krause *et al.*, 2000; Rothmund *et al.*, 1995; Rothmund *et al.*, 1996); however, the peptides are induced to an highly helical conformation in an hydrophobic environment. In Figure V-7 Panel C, temperature has a similar effect on L-/D-Helical diastereomeric peptides and the Gly peptide ($R=0.989$), confirming once again that, not only do the hydrophobic conditions of RP-HPLC mimic the helix-inducing properties of TFE, thus inducing Helical peptides to fully helical conformation, but also that this temperature-based approach to RP-HPLC is useful for the identification of peptide secondary structures.

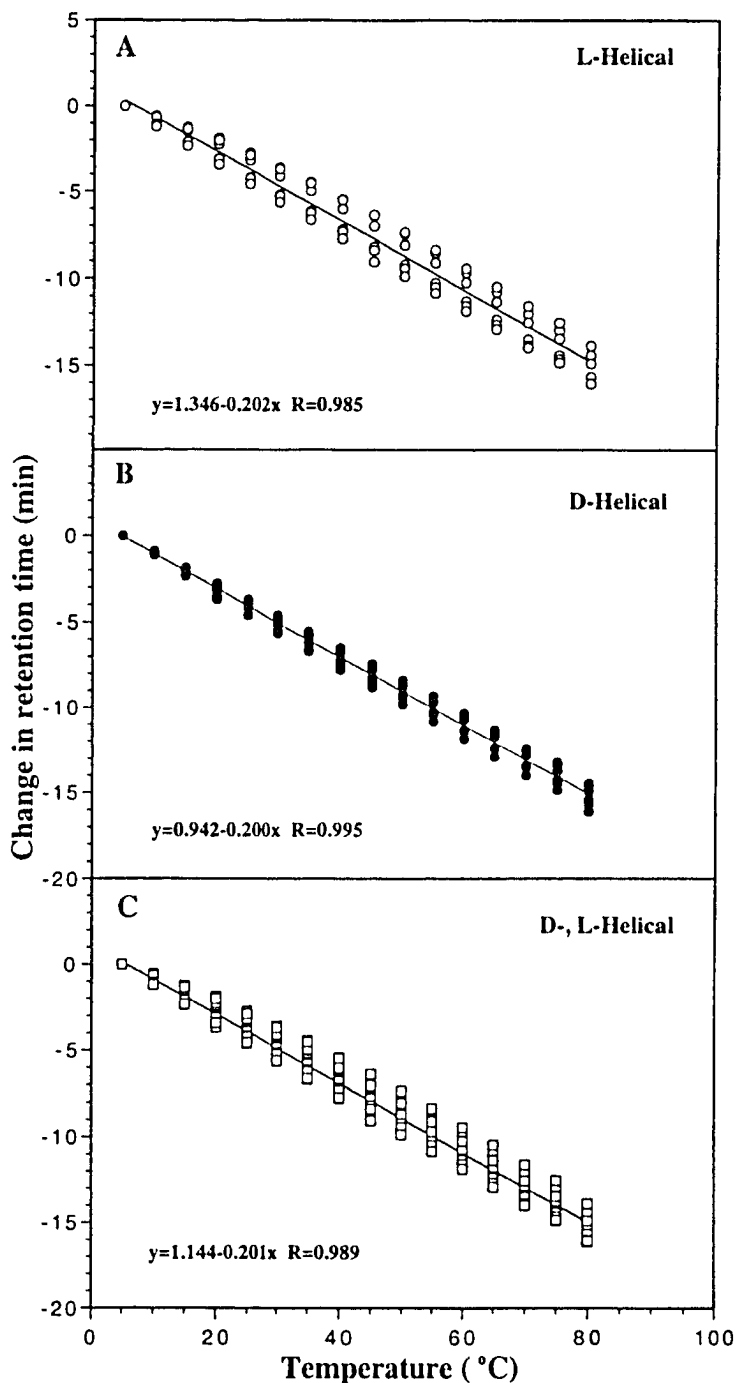


Figure V-7 Comparison of temperature effect on RP-HPLC of L- and D-helical peptides. Column and conditions same as for Figure V-3. (Panels A, B and C) Temperature plotted versus peptide retention time at a specific temperature minus its retention time at 5 °C (change in retention time) for L-helical peptides, D-helical peptides and L- and D-helical diastereomeric peptides, respectively. The symbols used are (O) for L-helical peptides, (●) for D-helical peptides and (□) for both L- and D-helical diastereomeric peptide analogs. Least square fit analysis resulted in the correlations shown in each panel. Only L- and D-peptides of Ile, Val, Ala, Gln, Asn and Gly substituted helical peptides were used in this figure.

Generally, as shown in Figure V-5, temperature is demonstrated to have a similar effect on the retention behaviour of random model peptide analogues with either L- or D-amino acid substitutions. However, subtle differences in the effect of temperature are apparent for different peptide analogues. Thus, Figure V-8 illustrates the surprising results of different temperature effects on aromatic and aliphatic L-/D-amino acid substituted Random peptides. Although there is no dramatic difference in temperature effects (represented by the slopes of the plots) on retention time of individual peptides (Figure V-8A, V-8B), a significant variation in retention behavior emerged between aromatic and aliphatic L-/D-amino acid substituted Random peptides as the temperature is raised incrementally from 10 °C to 75 °C (Figure V-8C, V-8D), when peptide retention data were presented as peptide retention time at a specific temperature minus its retention time at 10 °C *versus* temperature. Using the Gly-substituted Random peptide as an internal standard, Figure V-8C and V-8D indicate that aliphatic amino acid substituted Random peptides (Figure V-8D) are more stably bound to the stationary phase of the C₈ column (with plots shallower than that of the standard Gly peptide) than aromatic amino acid substituted analogues (with plots steeper than that of the standard Gly peptide) (Figure V-8C) as the temperature is raised; in other words, temperature is more effective in altering the bound status of aromatic Random peptides than that of aliphatic Random peptides during RP-HPLC. In addition, since aromatic Random F_L and F_D are more hydrophobic (*i.e.*, are eluted later) than aliphatic Random peptide analogues during RP-HPLC, while, in contrast, the aromatic Y_L and Y_D are less hydrophobic (*i.e.*, are eluted earlier) than aliphatic Random peptide analogues, this alteration of bound status of the model peptides during temperature is independent of peptide hydrophobicity. Calculated

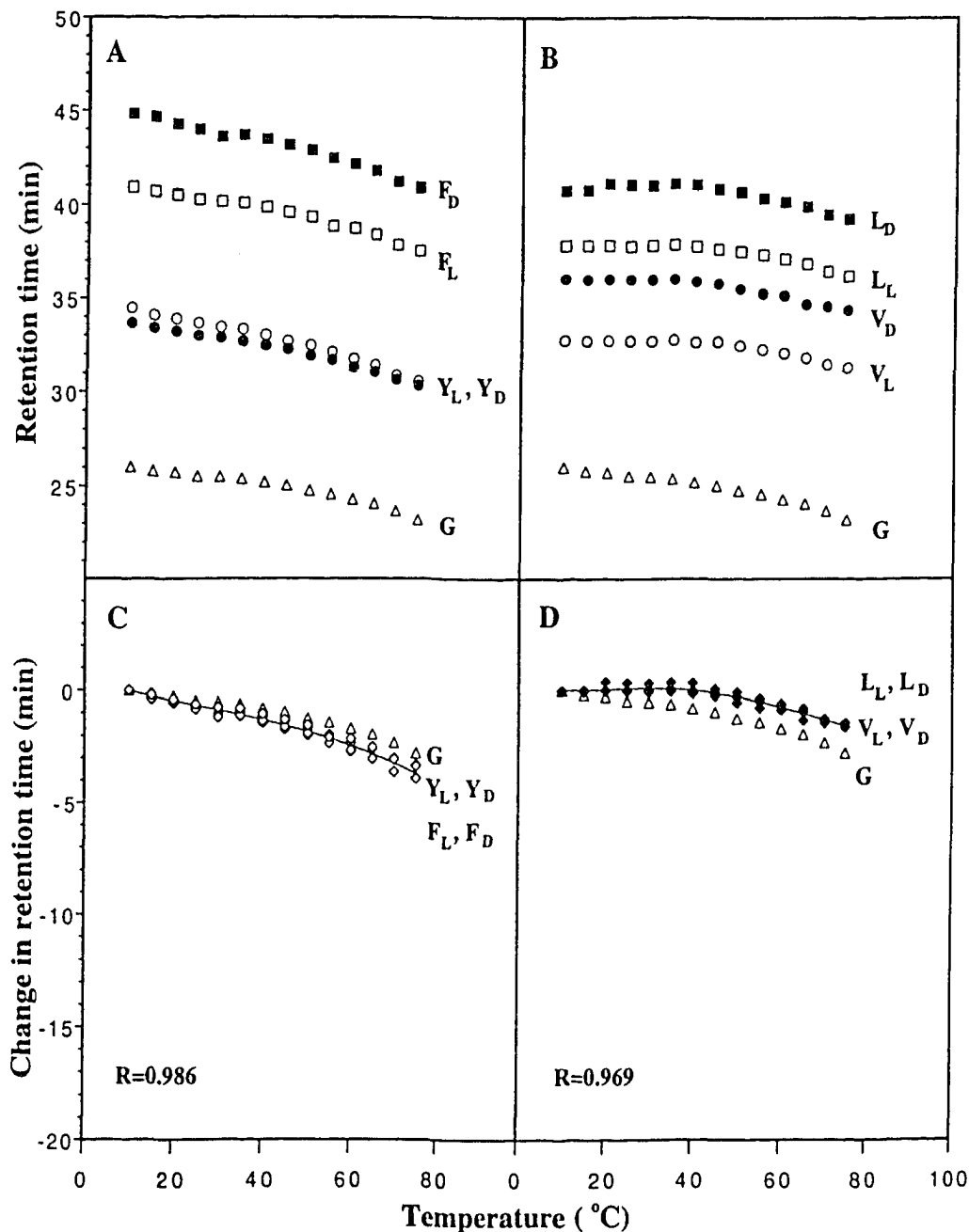


Figure V-8 Comparison of temperature effect on RP-HPLC of random coil peptides. Column and conditions same as for Figure V-3. (A and B) Effect of temperature on the retention time of different random coil peptides. (C and D) Temperature plotted versus peptide retention time at a specific temperature minus its retention time at 10 °C of random coil peptide analogs. In (A) and (B), closed circles and closed squares are used to represent D-random coil peptides; open circles and open squares represent L-random coil peptides; open triangles denote the Gly-substituted random coil peptides. In (C) and (D), open diamonds and closed diamonds represent the aromatic and aliphatic amino acid substituted random coil peptides, respectively; open triangles denote the Gly-substituted random coil peptide. Curvy-linear correlation is shown in (C) and (D). Peptide designation is based on the substituting amino acid as described in the text.

by polynomial curve fitting analysis, the excellent curvy-linear correlations shown in Figure V-8C and V-8D also demonstrate the sensitivity and the validity of this temperature approach to distinguish peptides with aliphatic and aromatic amino acid substitutions. Note that the large difference in retention times between Random L- and D-substituted peptide pairs (which possess the same inherent hydrophobicity and lack the potential for D-amino acid disruption of secondary structure) could be attributed to nearest-neighbor effects, since the substitution site at position 1 of the sequence is next to a L-Leu residue at position 2 (Figure V-1).

Although, as previously described (Chen *et al.*, 2002; Mant *et al.*, 2003a), the monomeric status of the α -helical peptide analogues used in this study is ensured, the possibility that Random peptide analogues may exhibit a degree of association/oligomerization was investigated by comparing the temperature profiles of these peptides with that of the random coil standard, G_R (Random Gly-substituted peptide). Thus, the data from Figure V-7C, Figure V-8C and V-8D were normalized relative to the temperature profile of the G_R , as presented in Figure V-9. Based on previous studies by our laboratory (Lee *et al.*, 2003b; Mant *et al.*, 2003a; Mant *et al.*, 2003b) which introduced the concept of detecting self-association of peptidic solutes by “temperature profiling” in RP-HPLC, the positive profiles of the aliphatic random coil peptides may indeed be indicative of some degree of association, albeit subtle, compared with aromatic random coil peptides, possibly offering an explanation of different temperature effects between these two kinds of Random peptide analogues. From Figure V-9, the negative slopes for the Helical peptides are considerably steeper than those of Random peptides. Since the data were normalized relative to the Random standard G_R ,

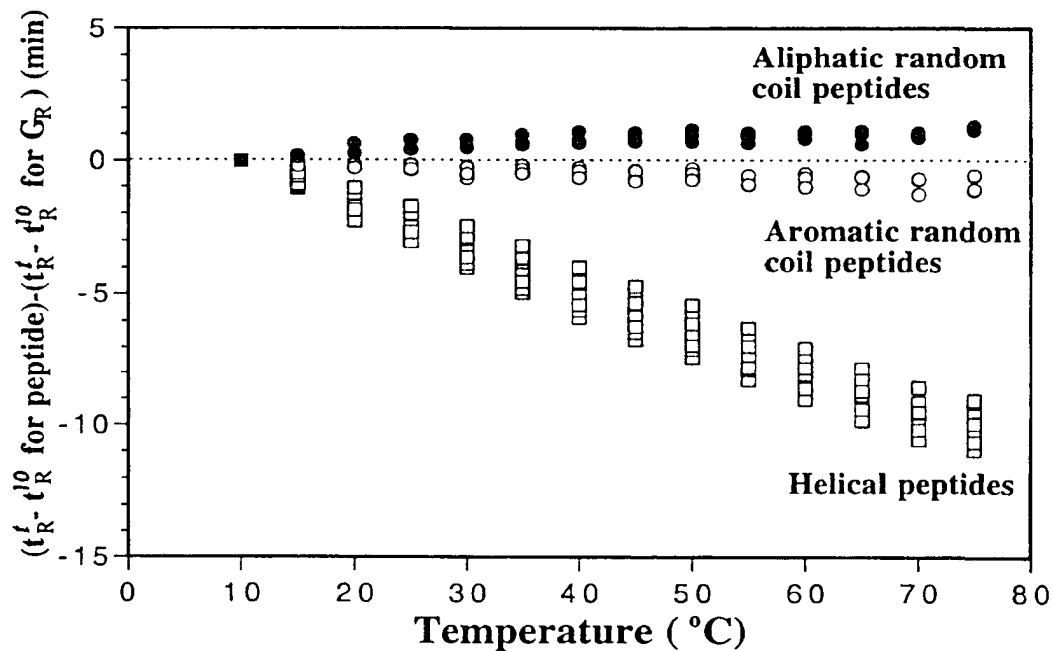


Figure V-9 Effect of temperature on RP-HPLC of helical and random coil peptides: normalization to retention behavior of the random coil Gly peptide. Column and conditions same as for Figure V-3. The retention behavior of the peptides was normalized to that of random coil Gly peptide through the expression $(t_R^t - t_R^{10}) / (t_R^t - t_R^{10} \text{ for Gly peptide})$, where t_R^t is the retention time at a specific temperature of a helical or random coil peptide and t_R^{10} is the retention time at 10 °C.

other factors which can influence peptide retention behavior (the aforementioned effects on mobile phase viscosity and mass transfer effects, for example) are already taken into account in the Helical plots shown in Figure V-9. Thus, as discussed in detail in our previous study (Mant *et al.*, 2003a), the steep negative profiles of the Helical peptides indicate considerable unfolding of the α -helices with increasing temperature. Briefly, at low temperature, the bound monomeric α -helices are in equilibrium with the same monomeric folded states free in solution, with their retention times dependent on the hydrophobicity of their non-polar faces. At high temperature, a considerable amount of the random, disrupted helical forms of these peptides are now present in solution, concomitant with a loss of amphipathicity (note that these peptides are assumed to always be bound to the stationary phase as α -helices (Mant *et al.*, 2003a)). The fast exchange between folded α -helical structure and unfolded form in solution now becomes a major determinant of the observed retention time, *i.e.*, the more random coil present in solution, the greater the decrease in retention time and, hence, the much steeper negative profiles illustrated in Figure V-9 compared to Random peptides which possess only negligible secondary structure throughout the entire temperature range.

V-6 Conclusions

In this study, we report the use of four series of synthetic model peptides (non-helical and amphipathic α -helical peptides with L-/D-amino acid substitutions) in order to demonstrate the selectivity, based on peptide conformational differences, that may be obtained in a reversed-phase separation during temperature alterations. Temperature variations resulted in dramatically different effects on the retention behaviour of α -helical

and random coil peptides. In contrast to random coil peptides, α -helical peptides underwent a temperature-induced unfolding process during RP-HPLC, resulting in considerable selectivity variations. The optimum resolution of mixtures of random coil and α -helical peptide analogues was obtained simply by varying the temperature of the RP-HPLC separation, taking advantage of the different responses to temperature of peptides with secondary structure potential compared to those with no such potential. In addition to aiding the rational development of peptide separation/optimization protocols, this study also confirms the value of employing RP-HPLC at varying temperatures as a sensitive and practical probe to distinguish peptide conformations, a role which should prove valuable for peptide/protein structure studies.

CHAPTER VI

Optimum Concentration of Trifluoroacetic Acid (TFA) for Reversed-Phase Chromatography of Peptides Revisited

A version of this chapter has been published: Chen, Y., Mehok, A. R., Mant, C. T. and Hodges, R. S. (2004) *J. Chromatogr. A* 1043, 9-18; and has also been selected in *Proteomics Select* issue 12, July 20, 2004 (www1.elsevier.com/vj/proteomics). Only methods unique to this chapter are described in the **Experimental** section, the remaining general methods are described in Chapter III.

VI-1 Abstract

Trifluoroacetic acid (TFA) remains the dominant mobile phase additive for reversed-phase high-performance liquid chromatography (RP-HPLC) of peptides after more than two decades since its introduction to this field. Generally, TFA has been employed in a concentration range of 0.05% - 0.1% (6.5 mM – 13 mM) for the majority of peptide separations. In order to revisit the question as to whether such a concentration range is optimum for separations of peptide mixtures containing peptides of varying net positive charge, the present study examined the effect of varying TFA concentration on RP-HPLC at 25°C and 70°C of three groups of synthetic 10-residue synthetic peptides containing either one (+1) or multiple (+3, +5) positively charged groups. The results show that the traditional range of TFA concentrations employed for peptide studies is not optimum for many, perhaps the majority, of peptide applications. For efficient resolution of peptide mixtures, particularly those containing peptides with multiple positive charges, our results show that 0.2% - 0.25% TFA in the mobile phase will achieve optimum resolution. In addition, the use of high temperature as a complement to such TFA concentration levels is also effective in maximizing peptide resolution.

VI-2 Introduction

Since its introduction over two decades ago as an anionic ion-pairing reagent for reversed-phase high-performance liquid chromatography (RP-HPLC), trifluoroacetic acid (TFA) has become the most extensively used mobile phase additive for RP-HPLC of peptides (Cunico *et al.*, 1998; Mant *et al.*, 1991; Mant *et al.*, 2002a). Its efficacy in this role lies in its volatility and UV transparency, coupled with the hydrophobic, negatively charged trifluoroacetate ion (TFA^-) which is able to interact with basic, positively charged amino acid side-chains (Arg, Lys, His), as well as free $\text{N}\alpha$ -amino groups (Cunico *et al.*, 1998; Guo *et al.*, 1987; Mant *et al.*, 1991; Mant *et al.*, 2002a). In addition, at low pH values (*e.g.*, pH 2.0), protonation of acidic residues enhances the interaction of peptides with the reversed-phase packing, concomitant with the suppression of free silanol ionization, thereby avoiding undesirable ionic interactions with positively charged peptide solutes (Mant *et al.*, 1987b; Mant *et al.*, 2002a; Regnier, 1983).

Favored models for the mechanism of such ion pair separations involve either formation of ion-pairs with the sample solute in solution followed by retention of the solute molecules on a reversed-phase packing (Horvath *et al.*, 1976; Horvath *et al.*, 1977) or a dynamic ion-exchange event whereby the ion-pairing reagent is first retained by the reversed-phase column and then solute molecules exchange ions with the counterion associated with the sorbed ion-pair reagent (Horvath *et al.*, 1977; Kissinger, 1977; Kraak *et al.*, 1977; Van de Venne *et al.*, 1978). Whatever the mechanism, the resolving power of negatively charged, anionic ion-pairing reagents such as TFA is effected through their interaction with the aforementioned positively charged groups in a peptide (Guo *et al.*, 1987; Mant *et al.*, 2002a). Indeed, hydrophobic anions such as TFA^- will not only

neutralize the positively charged groups, thereby decreasing peptide hydrophilicity, but will increase further the affinity of the peptides for the reversed-phase sorbent (Guo *et al.*, 1987).

In the past, concentrations of TFA in mobile phases (*aq.* TFA/acetonitrile mobile phase systems being the most commonly employed for peptides (Cunico *et al.*, 1998; Guo *et al.*, 1987; Mant *et al.*, 1991; Mant *et al.*, 2002a)) have mainly been limited to a range of 0.05% - 0.1% (v/v). However, an early study in our laboratory (Guo *et al.*, 1987) demonstrated the potential use of varying TFA concentrations (0.01% - 0.8%) on peptide selectivity, where increasing TFA concentration resulted in an increase in peptide retention time; further, the greater the number of positive charges on a peptide, the greater the increase in peptide retention, demonstrating potential manipulation of peptide elution profiles by varying anionic counterion concentration. Such an approach has also been reported for the preparative RP-HPLC separation of very hydrophilic, histidine-rich peptides, where 1% TFA was employed to ensure retention of the peptides by the RP-HPLC packing (Hong *et al.*, 1991). Considering the range of positively charged peptides which may be present in peptide mixtures – in proteomic applications, for instance, where protein digests may contain thousands of peptides with multiple charges – we believe the question of whether traditionally employed concentrations of TFA in mobile phase systems are indeed optimized for general peptide applications should be revisited.

Routine use of higher TFA concentrations has generally been avoided in the past, perhaps partly due to concerns of stationary phase degradation, *e.g.*, cleavage of alkyl chains from silica-based packings *via* acid hydrolysis of the siloxane bond linking the stationary phase functional group with surface silanols (Glajch *et al.*, 1987; Guo *et al.*,

1986b). However, with the advent of reversed-phase packings with excellent stability towards both acidic mobile phases and high temperature (Boyes *et al.*, 1993; Glajch *et al.*, 1990; Kirkland *et al.*, 1989), such concerns have been overcome. Thus, the present study determines the effect of varying TFA concentration and temperature on RP-HPLC of three groups of synthetic model peptides, these groups containing peptides of +1, +3 or +5 net charge. From the retention behavior of these peptides, conclusions could be drawn about optimum mobile phase conditions for sample mixtures containing peptides of varying net charge.

VI-3 Experimental

VI-3-1 Column and HPLC conditions

Analytical RP-HPLC runs were carried out on a Zorbax SB300-C₈ column (150 x 2.1 mm I.D.; 5- μ m particle size, 300-Å pore size) from Agilent Technologies (Little Falls, DE, USA), using a linear AB gradient (1% acetonitrile/min) at a flow-rate of 0.25 ml/min, where eluent A was 2 – 32 mM aq. TFA and eluent B was the corresponding concentration of TFA in acetonitrile; runs were carried out at 25°C and 70°C. Approximately 1 μ mol of each of the peptides in the 10-peptide mixtures was injected in a total sample volume of 10 μ l.

VI-4 Results and Discussion

VI-4-1 Design of synthetic model peptides

We have always believed that studies attempting to equate peptide elution behavior in HPLC generally, and RP-HPLC specifically, with varying run parameters is

Table VI-1 Sequence and name of the peptides in this study

Peptide group ^a	Peptide name	Peptide sequence ^b	Increase in the number of carbon atom ^c
+1	1a	Ac-GGGGGLGLGK-amide	0
	1b	Ac-GGAGGLGLGK-amide	1
	1c	Ac-GGAAGLGLGK-amide	2
	1d	Ac-GGVGGLGLGK-amide	3
	1e	Ac-GGVAGLGLGK-amide	4
	1f	Ac-GGIGGLGLGK-amide	4
	1g	Ac-GGIAGLGLGK-amide	5
	1h	Ac-GGVVGLGLGK-amide	6
	1i	Ac-GGIVGLGLGK-amide	7
	1j	Ac-GGIIGLGLGK-amide	8
+3	3a	Ac-GRGGKLGLGK-amide	0
	3b	Ac-GRAGKLGLGK-amide	1
	3c	Ac-GRAAKLGLGK-amide	2
	3d	Ac-GRVGKLGLGK-amide	3
	3e	Ac-GRVAKLGLGK-amide	4
	3f	Ac-GRIGKLGLGK-amide	4
	3g	Ac-GRIAKLGLGK-amide	5
	3h	Ac-GRVVKLGLGK-amide	6
	3i	Ac-GRIVKLGLGK-amide	7
	3j	Ac-GRIIKLGLGK-amide	8
+5	5a	NH ₃ ⁺ -RRGGKLGLGK-amide	0
	5b	NH ₃ ⁺ -RRAGKLGLGK-amide	1
	5c	NH ₃ ⁺ -RRAAKLGLGK-amide	2
	5d	NH ₃ ⁺ -RRVGKLGLGK-amide	3
	5e	NH ₃ ⁺ -RRVAKLGLGK-amide	4
	5f	NH ₃ ⁺ -RRIGKLGLGK-amide	4
	5g	NH ₃ ⁺ -RRIAKLGLGK-amide	5
	5h	NH ₃ ⁺ -RRVVKLGLGK-amide	6
	5i	NH ₃ ⁺ -RRIVKLGLGK-amide	7
	5j	NH ₃ ⁺ -RRIIKLGLGK-amide	8

a. The charge of the peptide is shown as at pH 2.0

b. The different amino acid substitutions are showed in bold letters.

c. The increase of the number of carbon atoms is assigned from the peptides 1a, 3a and 5a as zero.

best achieved by initial studies using defined model peptide systems, the results of which can then be extrapolated to peptides as a whole. Thus, we have designed and synthesized three groups of model peptides exhibiting variations in hydrophobicity and net positive charge (Table VI-1). From Table VI-1, each group of peptides contains 10 peptides with the same net positive charge, arising from the presence of a single lysine residue (+1 group), two lysine residues and an arginine residue (+3 group) or two lysine residues, two arginine residues and a free N-terminal α -amino group (+5 group). Within each peptide group, hydrophobicity varies only subtly between adjacent peptides, *i.e.*, peptide hydrophobicity varying by just one methyl or methylene group (equivalent to an increase of one carbon atom) from one peptide to the next. The presence of several glycine residues ensured negligible secondary structure for these peptides (Monera *et al.*, 1995; Zhou *et al.*, 1994b) (*i.e.*, they have a “random coil” configuration), to avoid complications in interpretation of data due to selectivity differences in peptide RP-HPLC retention behavior arising from conformational variations (Chen *et al.*, 2003; Sereda *et al.*, 1995). The 10-residue length of the peptides was chosen to mimic the size of an average peptide fragment arising from proteolytic digests of proteins. Peptides are denoted by charge and relative hydrophobicity order, *e.g.*, the peptide with one positive charge and the lowest hydrophobicity within this +1 group (a –GG– substitution; Table 1) is denoted 1a; the peptide with three positive charges and the highest hydrophobicity within this +3 group (a –II– substitution; Table VI-1) is denoted 3j, *etc.*

VI-4-2 *RP-HPLC stationary phase*

The Zorbax SB-300C₈ (“SB” denoting “Stable Bond”) is prepared from monofunctional n-octylsilane based on protecting the siloxane bond between the silica

and the C₈ group with bulky side groups, in this case two isopropyl groups (Boyes *et al.*, 1993; Glajch *et al.*, 1990; Kirkland *et al.*, 1989). This packing was originally designed to protect the siloxane bond from acid hydrolysis at low pH (Boyes *et al.*, 1993; Glajch *et al.*, 1990; Kirkland *et al.*, 1989) and has shown excellent thermal stability at pH 2 (Chen *et al.*, 2003; Hancock *et al.*, 1994; Mant *et al.*, 1997; Mant *et al.*, 2003a; Mant *et al.*, 2003b).

VI-4-3 Effect of TFA concentration on elution behavior of model peptide mixtures

The effect of TFA concentration on the RP-HPLC retention behavior of mixtures of positively charged peptides was determined by running the three 10-peptide groups (+1, +3 and +5; Table VI-1) in *aq.* TFA/acetonitrile mobile phases containing 2 mM, 4 mM, 8 mM, 16 mM and 32 mM TFA (equivalent to a range of ~ 0.016% - 0.25% TFA, *i.e.*, encompassing the 0.05% - 0.1% TFA range traditionally used for such separations) at 25°C and 70 °C. It should be noted that we chose to express TFA concentrations in mM *versus* % in order to be able to make a direct comparison of the effectiveness of TFA with alternative ion-pairing reagents, the subject of a separate study. The pH value of the *aq.* TFA (eluent A) ranged from pH 2.8 (2 mM TFA) to pH 1.7 (32 mM), which we refer to generally as pH 2. Note that even the highest pH value (pH 2.8 for 2 mM *aq.* TFA) is far enough below the pK_a values of the positively charged groups in the peptides so as not to affect the full positive charge on the peptides; in addition, if any underivatized silanol groups (pK_a ~ 4.0) remained on the Stable Bond packing, they also would remain protonated (*i.e.*, neutral) under the RP-HPLC conditions used in the present study, thus preventing any potential undesirable electrostatic interactions between the positively

charged peptides and the hydrophobic stationary phase. Elution time data for all peptides at 25 °C and 70 °C are presented in Table VI-2.

Figure VI-1 compares the results obtained at 70 °C when running the three groups of peptides in the 2 mM TFA, 8 mM TFA and 32 mM TFA mobile phase systems. From Figure VI-1, increasing TFA concentration generally results in increasing peptide retention time and improved peak shape. In addition, this effect of increasing TFA concentration is more marked the greater the positive charge on the peptides, *i.e.*, +1 group < +3 group < +5 group. This effect is especially dramatic for the +5 group, where early eluted peptides, in particular, showed severe tailing and poor peak shape at low (2 mM) TFA concentration.

An interesting observation from Figure VI-1 is the effect of TFA concentration on the elution time range of the peptides, *i.e.*, Δt_R (j analogue – a analogue) for each peptide group. At 32 mM TFA, the values were 11.8 min (+1 group), 9.8 min (+3 group) and 7.2 min (+5 group), *i.e.*, the larger the number of positive charges, the smaller the elution range. These Δt_R values for the +1 and +3 groups remained essentially constant over the entire range of TFA concentrations examined (2 mM – 32 mM); for the +5 groups, these values remained essentially constant over the 8 mM – 32 mM TFA range. Also from Figure VI-1, an increase in TFA concentration dramatically improved resolution for specific peptide pairs. Thus, for the +5 group, peptides 5f and 5g are almost completely separated to baseline at 32 mM TFA but poorly resolved at lower TFA concentrations. Similarly, for the +3 group, peptides 3g and 3h are almost completely separated to baseline at 32 mM TFA. Further, for the +1 group, 1g and 1h are coeluted for the entire TFA concentration range even though there has been an increase in overall resolution of

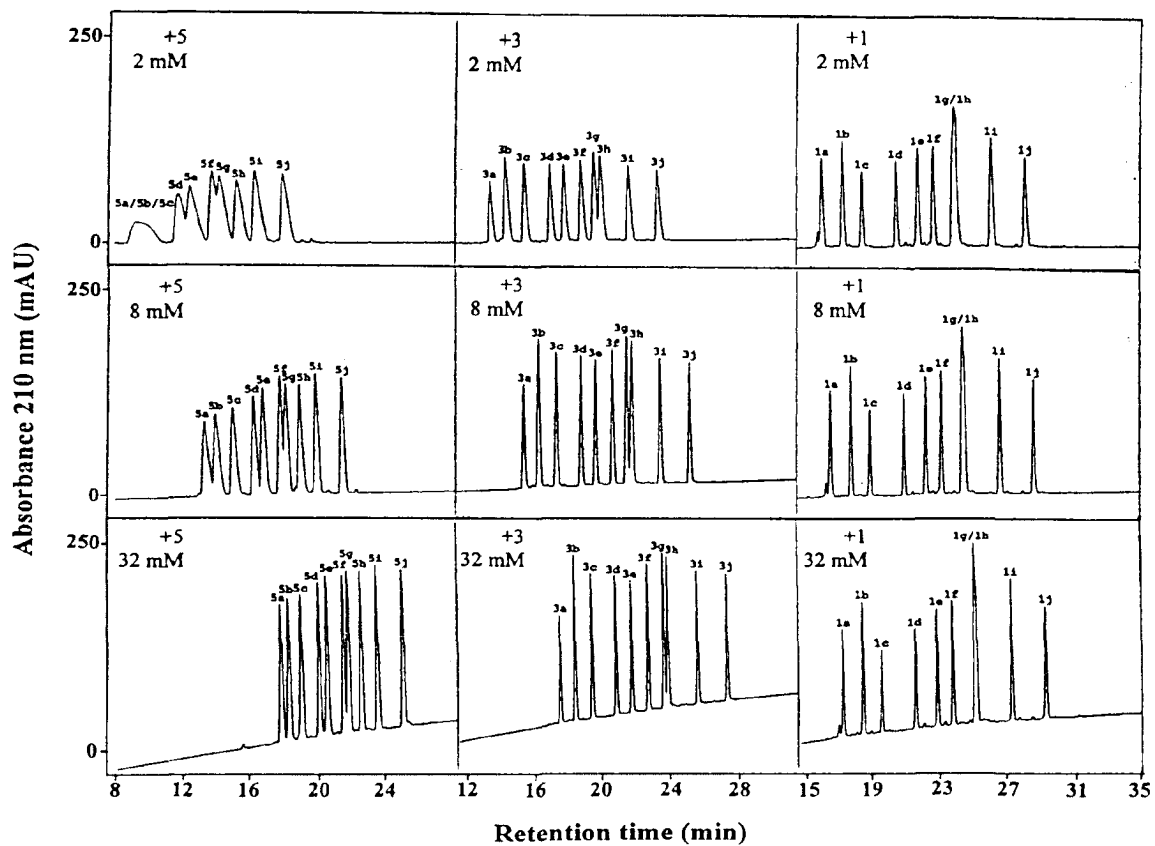


Figure VI-1 Effect of TFA concentration on RP-HPLC retention behavior of positively charged model peptide mixtures. Conditions: linear AB gradient (1% acetonitrile/min) at a flow rate of 0.25 ml/min, where eluent A is 2, 8 or 32 mM *aq.* TFA and eluent B is the corresponding TFA concentration in acetonitrile; temperature, 70 °C. The structures and denotations of the peptides are shown in Table VI-1; +5, +3 and +1 refer to the net charge of all peptides in the peptide mixtures.

Table VI-2 Retention times of +1, +3 and +5 peptides in different TFA concentrations

Peptide group	TFA (mM)	Temperature (°C)	Retention time (min)										
			a ^a	b	c	d	e	f	g	h	i	j	
+1	2	25	17.89	19.04	20.09	22.00	23.16	24.16	25.43	24.87	27.04	28.96	
		70	16.40	17.63	18.78	20.77	22.03	22.93	24.11	24.11	26.32	28.29	
	4	25	18.20	19.34	20.37	22.28	23.44	24.44	25.71	25.17	27.34	29.25	
		70	16.71	17.93	19.06	21.06	22.33	23.23	24.44	24.44	26.62	28.59	
	8	25	18.48	19.59	20.60	22.50	23.65	24.66	25.92	25.37	27.53	29.44	
		70	16.95	18.15	19.27	21.27	22.53	23.44	24.66	24.66	26.84	28.81	
	16	25	18.78	19.88	20.87	22.77	23.93	24.94	26.20	25.68	27.83	29.75	
		70	17.28	18.47	19.57	21.56	22.83	23.74	24.99	24.99	27.15	29.11	
	32	25	19.08	20.16	21.14	23.03	24.19	25.21	26.47	25.98	28.13	30.06	
		70	17.56	18.73	19.82	21.81	23.08	23.99	25.26	25.26	27.42	29.40	
	+3	2	25	15.77	16.67	17.71	19.17	19.88	21.03	21.62	21.62	23.42	25.11
			70	13.96	14.87	15.99	17.51	18.34	19.35	20.11	20.48	22.13	23.82
		4	25	17.02	17.85	18.82	20.22	20.94	22.07	22.69	22.69	24.45	26.13
			70	15.12	16.01	17.09	18.57	19.41	20.42	21.20	21.53	23.18	24.89
8		25	17.92	18.72	19.65	21.00	21.72	22.84	23.49	23.49	25.22	26.90	
		70	15.94	16.82	17.87	19.33	20.19	21.19	22.00	22.30	23.97	25.69	
16		25	19.06	19.84	20.74	22.05	22.80	23.89	24.60	24.60	26.32	28.01	
		70	17.12	17.99	19.02	20.45	21.32	22.30	23.16	23.42	25.13	26.85	
32		25	19.97	20.74	21.62	22.89	23.68	24.75	25.47	25.58	27.24	28.95	
		70	18.01	18.87	19.90	21.30	22.21	23.16	24.09	24.33	26.07	27.81	
+5		2	25	10.33	11.40	12.82	14.61	14.98	16.34	16.34	17.38	18.35	19.96
			70	9.35	9.35	9.35	11.73	12.42	13.71	14.14	15.15	16.20	17.84
		4	25	13.94	14.46	15.33	16.70	17.03	18.23	18.23	19.14	20.05	21.57
			70	10.25	11.32	12.69	14.17	14.73	15.84	16.19	17.08	18.07	19.61
	8	25	16.35	16.75	17.40	18.59	18.90	20.02	20.02	20.84	21.71	23.18	
		70	13.25	13.90	14.90	16.10	16.63	17.63	17.97	18.79	19.73	21.25	
	16	25	18.70	19.03	19.56	20.65	20.94	22.02	22.02	22.75	23.61	25.06	
		70	15.91	16.41	17.21	18.27	18.75	19.71	20.02	20.80	21.73	23.22	
	32	25	20.21	20.53	20.99	22.08	22.34	23.43	23.43	24.13	25.01	26.48	
		70	17.57	18.02	18.76	19.80	20.27	21.22	21.52	22.27	23.22	24.73	

a. For peptide names, see Table VI-1; RP-HPLC conditions, see section VI-3-1.

the peptide mixture at 32 mM TFA. There are also subtle selectivity differences between peptides with the same hydrophobicity difference within the three groups of peptides, *e.g.*, compare the g and h analogues, which are not resolved in the +1 group (1g/1h) but are resolved in the +3 (3g/3h) and +5 (5g/5h) groups.

Finally, a critical conclusion from the results presented in Figure VI-1 is that, for the efficient resolution of all three groups of peptides (at 70 °C), a TFA concentration of 32 mM (~ 0.25%) is required. Similar results were also obtained at 25 °C (data not shown).

VI-4-4 Effect of temperature on elution behavior of model peptide mixtures

Figure VI-2 illustrates the effect of temperature on elution behavior of the three groups of peptides in the presence of 32 mM TFA. This concentration of TFA was maintained due to its producing the best overall resolution for all three groups of peptides in Figure VI-1. From Figure VI-2, an increase in temperature reduces peptide retention time, due to an enhancement of the mass-transfer rate of the peptide solutes between the stationary and mobile phases (Antia *et al.*, 1988; Boyes *et al.*, 1993; Li *et al.*, 1997a; Li *et al.*, 1997b). Advantages of varying temperature may be seen in selectivity changes at 25 °C and 70 °C. Thus, peptide pairs 5f/5g (+5 group) and 3g/3h (+3 group) are coeluted at 25 °C but are resolved at 70 °C; conversely, peptides 1h and 1g (+1 group) are resolved to baseline at 25 °C but are completely coeluted at 70 °C. In addition, the peptide pair 5a/5b and 5d/5e (+5 group) is better resolved at 70 °C compared to 25 °C.

Interestingly, the elution range of the peptides, *i.e.*, Δt_R (j analogue – a analogue) appears to be affected by a temperature change. Thus, at 25 °C, Δt_R values are 6.3 min, 9.0 min and 11.0 min for the +5, +3 and +1 groups, respectively; in contrast, these values

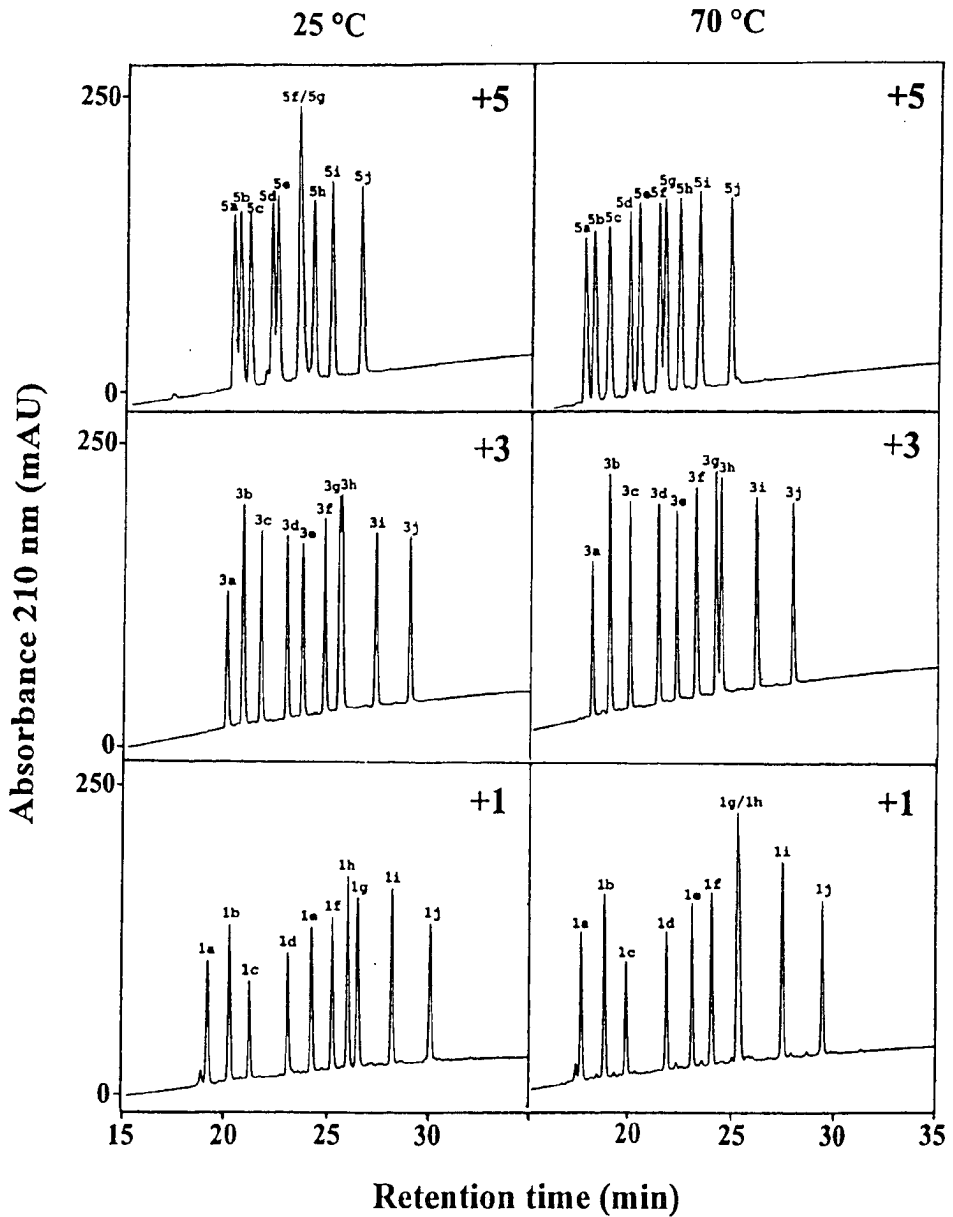


Figure VI-2 Effect of temperature on RP-HPLC retention behavior of positively charged model peptide mixtures. Conditions: linear AB gradient (1% acetonitrile/min) at a flow rate of 0.25 ml/min, where eluent A is 32 mM *aq.* TFA and eluent B is 32 mM TFA in acetonitrile. The structures and denotations of the peptides are shown in Table VI-1; +5, +3 and +1 refer to the net charge of all peptides in the peptide mixtures.

have increased to 7.2 min, 9.9 min and 11.8 min, respectively, at 70 °C, *i.e.*, an average increase for all these peptide groups of ~ 0.9 min.

Finally, it should be noted that the option to be able to use a relatively high TFA concentration (32 mM) combined with high temperatures for manipulation of elution profiles of peptide mixtures highlights well the advantages of chemically and thermally resistant silica-based RP-HPLC packings.

VI-4-5 *Effect of nearest-neighbor effects on elution behavior of model peptide mixtures*

Deviations from expected elution behavior for small peptides are generally explained in terms of sequence-specific effects, which can be divided into two categories – nearest-neighbor and conformation effects (Zhou *et al.*, 1990). The former implies that such effects are amino acid sequence-dependent, but independent of differences in secondary structure; in comparison, amino acid sequence-dependent conformational effects would be an apparent reduction or enhancement of the overall hydrophobicity of the peptide as a result of the peptide adopting an unique conformation on interacting with the stationary phase, compared to the hydrophobicity of the peptide if it existed as a random coil, *i.e.*, lacking an unique conformation (Zhou *et al.*, 1990). The random coil nature of the model peptides in the present study, assured by the presence of multiple glycine residues, suggests that subtle selectivity differences during RP-HPLC are likely due to nearest-neighbor effects within specific peptides and/or the environment within which residue substitutions are made. Thus, even through the peptide analogues in all three groups of peptides have the same series of residue substitutions (Table VI-1), the environment surrounding these substitutions varies substantially. For instance, for the +5 group, the substitutions are made within the sequence $^+H_3N-RR-X-X-K-$ (where X-X

denotes substituted residues), *i.e.*, within a highly charged environment, in addition to three adjacent positive charges at its N-terminus; for the +3 group, substitutions are made within the sequence Ac-GR-X-X-K-, *i.e.*, within a much lesser charged environment than the +5 group; finally, for the +1 group, substitutions are made within the sequence Ac-GG-X-X-G-, *i.e.*, with no ionizable groups close to the substitution positions.

From Figure VI-1, peptide analogues g and h, which differ by a full carbon atom (partial sequence of –GIAG– for g and –GVVG– for h; Table VI-1), were not resolved in the +1 group (1g/1h) at any TFA concentration (2 mM – 32 mM TFA) at 70°C; however, they were baseline resolved at 25°C (Figure VI-2). Interestingly, the same sequence variations for the +3 group (–RIAK– for 3g and –RVVG– for 3h) could not be resolved at 25 °C but could be resolved at 70 °C (Figure VI-2). For the +5 group (–RIAK– for 5g and –RVVG– for 5h), the two peptides are readily resolved at 25 °C and 70 °C (Figure VI-2), where the only difference between the +3 and +5 groups is the replacement of the N-terminal glycine residue in the +3 groups with an arginine residue with a free α -amino group in the +5 group. Such a result illustrates the sensitivity of RP-HPLC to subtle changes in sequence not immediately adjacent to the dipeptide sequence where the hydrophobicity changes. Further, what is even more interesting is the separation of peptides 1g and 1h at 25°C (Figure VI-2). Peptide 1h has a greater intrinsic hydrophobicity than 1g by 1 carbon atom out of the 10-residue sequence (Table VI-1), yet peptide 1h is eluted prior to 1g at 25 °C while the two peptides are coeluted at 70 °C (Figure VI-2). This result suggests that nearest-neighbor effects are greater at 25 °C and such effects are being diminished at high temperature.

Another interesting example of a nearest-neighbor effect lies in the behavior of the e and f analogues of the three peptide groups. Thus, e analogues contain the sequence –VA–, whilst f analogues contain the sequence –IG–, *i.e.*, they were designed to contain the same number of carbon atoms (four) in the substitution positions and, thus, the same apparent intrinsic hydrophobicity, where there is an increase of one methyl group in going from valine to isoleucine and a decrease of one methyl group in going from alanine to glycine (Table VI-1). Regardless of the surrounding residues (–GVAG– and –GIGG– in the +1 group; –RVAK– and –RIGK– in the +3 group and +5 group; Table VI-1), the peptides are readily separated at both 25°C and 70°C (Figure VI-2). It is perhaps significant that the e analogues (with the –VA– substitution) are consistently eluted prior to the f analogues (with the –IG– substitution). Thus, the inherent hydrophobicity of the isoleucine side-chain (f analogues), adjacent as it is to glycine with no appreciable side-chain, is likely to be fully expressed on interaction with the hydrophobic stationary phase. In contrast, instead of being additive, it is likely that the combined hydrophobicity of the valine and alanine side-chains (e analogues) is not being fully expressed, *i.e.*, the apparent hydrophobicity of this dipeptide is being diminished relative to –IG– of the f analogues, perhaps due to “shielding” of the hydrophobicity of one residue by the other via conformational constraints between these adjacent residues.

VI-4-6 *Effect of TFA concentration and temperature on elution characteristics of model peptides*

Figure VI-3 summarizes graphically the effect of increasing TFA concentration (expressed as $\text{Log}_{10} [\text{TFA}]$) on Δt_R (32 mM – 8 mM) (*i.e.*, the difference in peptide retention time between that obtained at a concentration of 32 mM TFA compared to 8

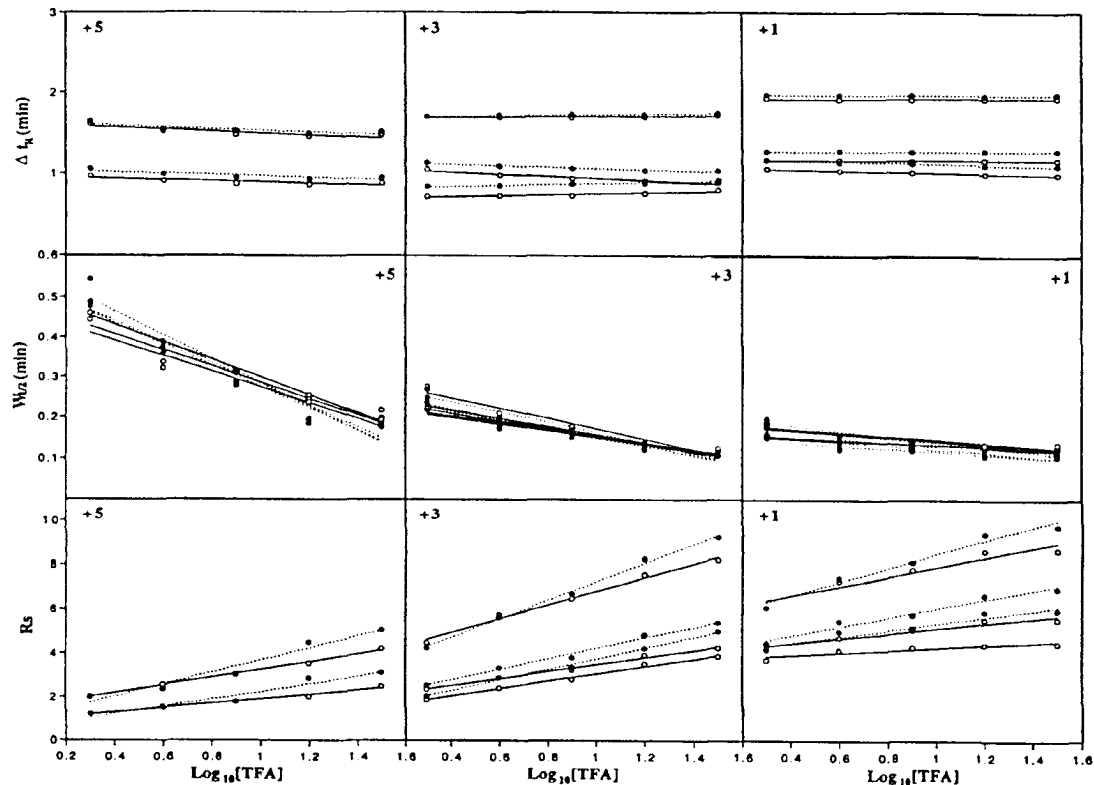


Figure VI-3 Effect of TFA concentration on retention characteristics of model positively charge peptides at 25 and 70 °C. Δt_R denotes difference in retention time between adjacent peptides; $W_{1/2}$ denotes peak width at half height of peptides; R_s denotes resolution of adjacent peptides. Open symbols with solid lines represent results obtained at 25 °C; closed symbols with dotted lines represent results obtained at 70 °C. The +5 group peptides are represented by peptide pairs 5h/5i and 5i/5j; the +3 group peptides are represented by peptide pairs 3b/3c, 3d/3e and 3i/3j; the +1 group peptides are represented by peptide pairs 1b/1c, 1d/1e and 1i/1j. Sequences of all peptides are shown in Table VI-1.

mM TFA), peptide peak width at half height ($W_{1/2}$) and peptide resolution. To simplify interpretation of data, only profiles obtained from selected peptide data are shown: thus, only values obtained for 5h/5i and 5i/5j (+5 group); 3b/3c, 3d/3e and 3i/3j (+3 group); and 1b/1c, 1d/1e and 1i/1j (+1 group) are presented. However, the data presented in Figure VI-3 represents the observed elution behavior for all peptide analogues and can be viewed as summarizing general rules for effect of TFA concentration on peptides of varying net charge.

From Figure VI-3, Δt_R (32 mM – 8 mM values) are essentially independent of TFA concentration for all three peptide groups at both 25 °C and 70 °C. Table VI-3 shows the change in peptide retention times between the 8 mM and 32 mM TFA systems at both 25 °C and 70 °C. Due to the comparatively poor retention of the +5 group peptides at concentrations of 2 mM TFA (Figure VI-1) and 4 mM TFA (data not shown), 8 mM was chosen as the lower TFA concentration limit to ensure accuracy of data. Note that the average Δt_R /positive charge values are essentially constant at both 25 °C and 70 °C for all three groups, albeit there is an increase in the values as the net charge increases, *i.e.*, +1 < +3 < +5. This increase reflects the earlier observation (Figure VI-1) that the elution range of the peptides (t_R j analogue – a analogue) increases with increasing net positive charge.

Clearly, peptide peak width is decreasing with increasing TFA concentration (as well as increasing temperature), this effect being more marked the higher the net positive charge on the peptides. Indeed, the effect on peak width by an increase in both TFA concentration and temperature is most dramatic for the +5 group, as had been noted from the elution profiles shown in Figure VI-1. The overall general trend of decreasing peak

Table VI-3 Difference of retention times of +1, +3 and +5 peptides between 8 and 32 mM of TFA

Peptide group	Temperature (°C)	$\Delta t_{R(32-8\text{ mM})}$ (min) ^a										Average ^b	Average/charge ^c
		a ^d	b	c	d	e	f	g	h	i	j		
+1	25	0.60	0.57	0.54	0.53	0.54	0.55	0.55	0.61	0.60	0.62	0.57	0.57
	70	0.61	0.58	0.55	0.54	0.55	0.55	0.60	0.60	0.58	0.59	0.58	0.58
+3	25	2.05	2.02	1.97	1.89	1.96	1.91	1.98	2.09	2.02	2.05	1.99	0.66
	70	2.07	2.05	2.03	1.97	2.02	1.97	2.09	2.03	2.10	2.12	2.05	0.68
+5	25	3.86	3.78	3.59	3.49	3.44	3.41	3.41	3.29	3.30	3.30	3.49	0.70
	70	4.32	4.12	3.86	3.70	3.64	3.59	3.55	3.48	3.49	3.48	3.72	0.74

a. Denotes the difference of peptide retention times between 8 mM and 32 mM of TFA.

b. Average denotes the average values of the $\Delta t_{R(32-8\text{ mM})}$ of 10 peptides analogs in the same group.

c. Average/charge denotes the average values of the $\Delta t_{R(32-8\text{ mM})}$ of 10 peptides analogs in the same group divided by the number of charges on the peptides.

d. For peptide names, see Table VI-1; RP-HPLC conditions, see section VI-3-1.

width with an increase in TFA concentration and temperature is also illustrated in Table VI-4 which reports the difference in $W_{1/2}$ values obtained between 8 mM TFA and 32 mM TFA (*i.e.*, $W_{1/2}$ at 32 mM minus $W_{1/2}$ at 8 mM). The average $W_{1/2}$ value/net positive charge is presented simply to highlight the effect of temperature. Thus, over this entire TFA concentration range, the average $W_{1/2}$ /charge is always lower (*i.e.*, this value is more negative) at 70°C compared to 25°C.

Finally from Figure VI-3, for all three peptide groups, increasing TFA concentration clearly increases resolution of adjacent peptide pairs. In addition, as reflected by the steeper slopes of the 70 °C data, increasing the temperature from 25 °C also increases peptide resolution over the entire TFA concentration range. The effects of these two run parameters is underlined in Table VI-5, which reports the relative increase in peptide resolution at 70°C *versus* 25°C on increasing the TFA concentration from 2 mM TFA to 32 mM TFA. Thus, for instance, for the +1 group, resolution increases 1.21-fold at 32 mM TFA compared to 2 mM TFA at 25 °C for the 1b/1c peptide pair compared to 1.44-fold at 70 °C; these values are 1.32-fold (25 °C) and 1.57-fold (70 °C) for the 1d/1e peptide pair; and 1.42-fold (25 °C) and 1.60-fold (70 °C) for the 1i/1j peptide pair. The same trend is also observed for the +3 and +5 group peptides. Also from Table VI-5, it is clear that, the higher the net positive charge on the peptides, the greater the improvement in resolution on raising the TFA concentration from 2 mM TFA to 32 mM TFA. Thus, taking the i/j analogues as an example, the resolution of 1i/1j, 3i/3j and 5i/5j peptide pairs improves by 1.42-fold, 1.83-fold and 2.07-fold, respectively, at 25°C; at 70 °C, the resolution of these peptide pairs improves 1.60-fold, 2.18-fold and 2.54-fold, respectively. Finally, Table VI-5 again highlights interesting selectivity

Table VI-4 Difference of peak width at half height of +1, +3 and +5 peptides between 8 and 32 mM of TFA

Peptide group	Temperature (°C)	$\Delta W_{1/2} (32-8 \text{ mM}) (\text{min})^a$										Average ^b	Average/charge ^c
		a ^f	b	c	d	e	f	g	h	i	j		
+1	25	-0.0185	-0.0119	-0.0057	-0.0074	-0.0112	-0.0141	-0.0168	-0.0171	-0.0202	-0.0055	-0.0128	-0.0128
	70	-0.0217	-0.0252	-0.0144	-0.0172	-0.0258	-0.0293	- ^d	-	-0.0272	-0.0187	-0.0224	-0.0224
+3	25	-0.0451	-0.0513	-0.0440	-0.0344	-0.0307	-0.0366	-	-	-0.0323	-0.0294	-0.0380	-0.0127
	70	-0.0415	-0.0523	-0.0474	-0.0466	-0.0402	-0.0476	-0.0446	-0.0424	-0.0425	-0.0380	-0.0443	-0.0148
+5	25	-	-	-	-	-	-	-	-0.0852	-0.0710	-0.0862	-0.0808	-0.0162
	70	- ^e	-0.1865	-0.1732	-0.1774	-0.0928	-	-	-0.1319	-0.1325	-0.1078	-0.1432	-0.0286

a. Denotes the difference of peptide peak width at half height between 8 and 32 mM of TFA.

b. Average denotes the average values of the $\Delta W_{1/2} (32 \text{ mM} - 8 \text{ mM})$ of the corresponding peptides analogs in the same group.

c. Average/charge denotes the average values of the $\Delta W_{1/2} (32 \text{ mM} - 8 \text{ mM})$ of the corresponding peptides analogs in the same group divided by the number of charges on the peptides.

d. Dashes denote the co-eluting peaks or the poorly resolved peaks, for which the peak width at half height can not be determined.

e. Peptide 5a is not retentive enough in 8 mM TFA at 70 °C, therefore, is not included in this table.

f. For peptide denotations, see Table VI-1; RP-HPLC conditions, see section VI-3-1.

Table VI-5 Relative increase in peptide resolution (R_s) between 2 and 32 mM of TFA^a

Peptide group	Temperature (°C)	Relative increase in R_s values ^b								
		a-b ^c	b-c	c-d	d-e	e-f	f-g	g-h	h-i	i-j
+1	25	1.31	1.21	1.24	1.32	1.13	1.54	1.27	1.51	1.42
	70	1.47	1.44	1.46	1.57	1.63	^d	-	-	1.60
+3	25	1.84	1.81	1.74	2.07	1.77	-	-	-	1.83
	70	2.06	2.12	2.13	2.45	2.00	2.69	1.44	2.26	2.18
+5	25	-	-	-	-	-	-	-	2.06	2.07
	70	-	-	-	-	-	-	-	2.58	2.54

a. RP-HPLC conditions, linear AB gradient (1% acetonitrile/min) at a flow-rate of 0.25 ml/min, where eluent A is 2 or 32 mM aq. TFA and eluent B is the corresponding TFA concentration in acetonitrile.

b. Calculated by the expression (R_s of peptide pair at 2 mM TFA)/(R_s of peptide pair at 32 mM TFA)

c. Denotes adjacent peptide pair from which R_s values were derived; sequences shown in Table VI-1.

d. Denotes situations where poorly resolved or coeluted peaks prevented measurement of R_s .

differences with increasing TFA concentration. Such selectivity differences vary from peptide pair to peptide pair and, thus, the improvement in resolution between peptide pairs is not identical in all cases. A clear example of this from Table VI-5 is that the relative increase in resolution at 70 °C for 3g/3h is significantly lower (1.44) than the general range of the peptides (2.00-2.45), whereas the 3f/3g pair is somewhat higher (2.69), *i.e.*, the elution behavior is causing these anomalies. Thus, for the 3g/3h peptide pair, the difference in retention times between the peptides has actually decreased on raising the TFA concentration from 2 mM to 32 mM, although the concomitant decreases in peak widths still lead to an overall relative increase in resolution (1.44), albeit significantly less than might be expected. In contrast, the difference in retention time between 3f and 3g has increased with increasing TFA concentration; thus, with the concomitant decrease in peak widths, the relative increase in resolution (2.69) is somewhat greater than the remaining adjacent peptide pairs. Such results again confirm the advantage of being able to employ high TFA concentration and/or high temperature to improve resolution of peptide mixtures.

Raising the TFA concentration further to 64 mM and 128 mM was found to be impractical due to considerable loss of peak detection sensitivity at high TFA concentrations. Thus, at 64 mM TFA, peptide peak areas were already somewhat smaller than those observed at 32 mM TFA; at 128 mM TFA > 80% of peak area compared to 32 mM TFA had been lost. Such results likely arise from the strong UV-absorbing characteristics of TFA at high concentration interfering with peptide bond detection at 210 nm. However, considering the excellent results achieved with 32 mM TFA concomitant with only incremental further improvements in peptide resolution at higher

TFA concentrations, this loss of detection sensitivity at TFA concentrations > 32 mM TFA is of no practical concern.

From the results of this study, it is apparent that the concentrations of TFA generally employed for RP-HPLC of peptides (0.05% - 0.1%, *i.e.*, ~ 6.5 mM – 13 mM) are somewhat at the low end of a favorable concentration range for such purposes, particularly for peptides containing multiple charges (*e.g.*, +5 group in Fig. 1). Indeed, we suggest that the concentration of TFA employed for general peptide applications should be altered to the 0.2% - 0.25% range (~ 26 mM – 32 mM) to ensure optimum peptide resolution, particularly considering the now ready availability of stable, silica-based RP-HPLC packings.

VI-5 Conclusions

The present study has investigated the effect of varying TFA concentration and temperature on RP-HPLC of three groups of synthetic model peptides containing either one (+1) or multiple (+3, +5) positively charged groups. The results clearly show that the traditional range of TFA concentrations employed for peptide studies (0.05% - 0.1%) is not optimum for many, perhaps most, peptide applications. For efficient resolution of peptide mixtures, particularly those containing peptides with multiple positive charges, our results suggest that 0.2% - 0.25% TFA in the mobile phase will achieve the desired goal of optimum peak resolution and detection sensitivity. In addition, the use of high temperature as a complement to such levels of TFA concentration has also proved effective in maximizing peptide resolution.

CHAPTER VII

Temperature Profiling of Polypeptides in Reversed-Phase Chromatography: I. Monitoring of Dimerization and Unfolding of Amphipathic α -Helical Peptides

A version of this chapter has been published: Mant, C. T., Chen, Y. and Hodges, R. S. (2003) *J. Chromatogr. A* 1009, 29-43. Only methods unique to this chapter are described in the **Experimental** section, the remaining general methods are described in Chapter III.

VII-1 Abstract

The present study sets out to extend the utility of reversed-phase chromatography (RP-HPLC) by demonstrating its ability to monitor dimerization and unfolding of *de novo* designed synthetic amphipathic α -helical peptides on stationary phases of varying hydrophobicity. Thus, we have compared the effect of temperature (5 °C to 80 °C) on the RP-HPLC (C_8 or cyano columns) elution behavior of mixtures of peptides encompassing amphipathic α -helical structure, amphipathic α -helical structure with L- or D-substitutions or non-amphipathic α -helical structure. By comparing the retention behavior of the helical peptides to a peptide of negligible secondary structure (a random coil), we rationalize that “temperature profiling” by RP-HPLC can monitor association of peptide molecules, either through oligomerization or aggregation, or monitor unfolding of α -helical peptides with increasing temperature. We believe that the conformation-dependent response of peptides to RP-HPLC under changing temperature has implications both for general analysis and purification of peptides but also for the *de novo* design of peptides and proteins.

VII-2 Introduction

One of the most interesting developments of liquid chromatography in recent years has been the emergence of reversed-phase chromatography (RP-HPLC) as a physicochemical probe of peptide and protein structure. Such studies are based on the premise that the hydrophobic interactions between polypeptides and the non-polar stationary phase characteristic of RP-HPLC (Mant *et al.*, 1991; Mant *et al.*, 1996; Mant *et al.*, 2002a) mimic the hydrophobicity and interactions between non-polar residues which are the major driving forces for protein folding and stability. Thus, RP-HPLC has demonstrated its potential for correlating the retention behavior of peptides (Aguilar *et al.*, 1993; Blondelle *et al.*, 1996; Heinitz *et al.*, 1988; Henderson *et al.*, 1990; Lazoura *et al.*, 1997; Lee *et al.*, 1997; Lork *et al.*, 1989; Purcell *et al.*, 1989; Purcell *et al.*, 1995a; Purcell *et al.*, 1995b; Purcell *et al.*, 1995c; Steer *et al.*, 1998; Steiner *et al.*, 1991; Zhou *et al.*, 1990) and proteins with their conformational stability, for monitoring hydrophobicity and amphipathicity of α -helices and β -sheet molecules (Benedek, 1993; Chen *et al.*, 2002; Hodges *et al.*, 1994; Kondejewski *et al.*, 1999; Mant *et al.*, 1989; Mant *et al.*, 1998a; Mant *et al.*, 1998b; Mant *et al.*, 2002a; Richards *et al.*, 1994; Rosenfeld *et al.*, 1993; Tripet *et al.*, 2000; Yu *et al.*, 2000) and for assessing how the pKa values of potentially ionizable side-chains, frequently important as enzyme catalytic groups, are influenced by their microenvironment (Sereda *et al.*, 1993). In addition, we have previously described the design and development of a single model ligand-receptor system based on observing the retention behaviour of *de novo* designed single-stranded amphipathic α -helical peptide ligands binding to a complementary receptor (RP-HPLC stationary phase) (Mant *et al.*, 2002b; Mant *et al.*, 2002c; Sereda *et al.*, 1994) since

hydrophobic interactions play a key role in the binding of ligands to receptors in biological systems.

Much of the efficacy of RP-HPLC as a probe of stability, folding and conformation of peptides and proteins lies in the wealth of stationary phases and/or mobile phase conditions available to the researcher when gauging the potential of relating peptide elution behavior with structural features (*e.g.*, the amphipathicity of α -helices or cyclic β -sheet peptides; destabilization of conformation) and/or biological activity (*e.g.*, antimicrobial potency, receptor binding). Temperature has also added another dimension to such applications, with physicochemical studies of RP-HPLC of polypeptide solutes under conditions of varying temperature allowing even more insight into conformational stability of peptides and proteins as well as the way such peptidic solutes interact with hydrophobic stationary phases (Mant *et al.*, 2003b; Purcell *et al.*, 1989; Purcell *et al.*, 1995c).

The present study sets out to extend the utility of RP-HPLC as an effective physicochemical probe of polypeptide structure by demonstrating its ability to monitor dimerization and unfolding of *de novo* designed synthetic amphipathic α -helical peptides on stationary phases of varying hydrophobicity when run at temperatures ranging from 5°C to 80 °C. Significantly, interactions between non-polar residues, specifically between the non-polar faces of amphipathic α -helical sequences in a protein (50% of α -helices found in proteins are amphipathic) (Cornette *et al.*, 1987; Segrest *et al.*, 1990) are the major driving force for protein folding and stability. In addition, dimerization is a critical factor in explaining biological activity, folding and stability of biological molecules. Thus, we believe that the conformation-dependent response of peptides to RP-HPLC

under changing temperature (temperature profiling) has implications, not only for the approach to general analysis and purification of peptides, but also for the *de novo* design of peptides and proteins, since the contribution of different amino acid side-chains to stability of α -helical structure and oligomerization may be rapidly ascertained through this RP-HPLC approach.

VII-3 Experimental

VII-3-1 Columns

Analytical RP-HPLC runs were carried out on Zorbax SB300-C₈ and SB300-CN columns (150 x 4.6 mm I.D., 5- μ m particle size, 300-Å pore size) from Agilent Technologies (Little Falls, DE, USA).

VII-4 Results

VII-4-1 *Synthetic model peptides used in this study*

Table VII-1 shows the sequence of the synthetic model peptides employed for the present study, these peptides divided generally into three groups: (1) amphipathic α -helical peptides; (2) non-amphipathic α -helical peptides; and (3) a peptide internal standard (C1) with negligible secondary structure (random coil). Figure VII-1 shows representations of selected peptides from Table VII-1 as α -helical nets.

From Figure VII-1, peptides LL9 and AA9 represent “native” model amphipathic α -helical peptides based on the sequence Ac-EnEKnnKEXEKnnKENEK-amide, where *n* denotes Ala (AX9 peptides) or Leu (LX9 peptides) and X denotes the residue substituted at position 9 of the sequence. Thus, the LL9 “native” analogue has Leu substituted at

Table VII-1 Synthetic peptides used in this study

Peptide Sequence ^a	Denotation
<i>Amphipathic α-helical peptides^b</i>	
Ac-ELEKLLKELEKLLKELEK-amide	LL9
Ac-ELEKLLKEKEKLLKELEK-amide	LK9
Ac-EAEKAAKEAEKAAKEAEK-amide	AA9
Ac-EAEKAAKEKEKAAKEAEK-amide	AK9
<i>Amphipathic α-helical peptides with stereoisomeric substitutions^c</i>	
Ac-EAEKAAKEAEKAAKEAEK-amide	A _L
Ac-EAEKAAKELEKAAKEAEK-amide	L _L , L _D
Ac-EAEKAAKEIEKAAKEAEK-amide	I _L , I _D
Ac-EAEKAAKETEKAAKEAEK-amide	T _L , T _D
Ac-EAEKAAKEPEKAAKEAEK-amide	P _L , P _D
Ac-EAEKAAKEGEKAAKEAEK-amide	G
<i>Non-amphipathic α-helical peptides^d</i>	
Ac-EELKLLKLELELKLKLEEK-amide	naL
Ac-EEAKAKAEAEAKAKAEK-amide	naA
<i>Random coil peptide^e</i>	
Ac-ELEKGGLEGEKGGKELEK-amide	C1

a. Peptide sequences are shown using the one-letter code for amino acid residues; Ac- denotes N^α-acetyl and -amide denotes C-terminal amide.

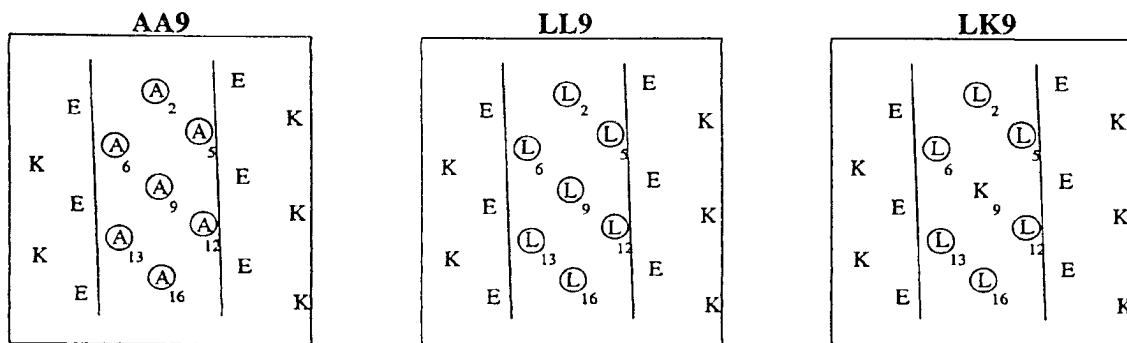
b. The amphipathic α -helical peptide LL9 has 7 Leu residues in the non-polar face (Figure VII-1), while AA9 has 7 Ala residues in the non-polar face. Bold residues denote differences between peptide sequences, e.g., LL9 and LK9 have a Leu or a Lys residue, respectively, at position 9 of the otherwise identical sequence, while AA9 and AK9 have an Ala or a Lys residue, respectively, at position 9 of the otherwise identical sequence.

c. Subscript letter denotes L- or D-amino acid substitution at position 9 of the 18-residue sequence of AA9 (Figure VII-1), e.g., L_L denotes substitution of L-Leu at position 9, L_D denotes substitution of D-Leu at position 9, etc. Bold residues denote different L- or D-amino acids substituted at position 9 of the otherwise identical sequence.

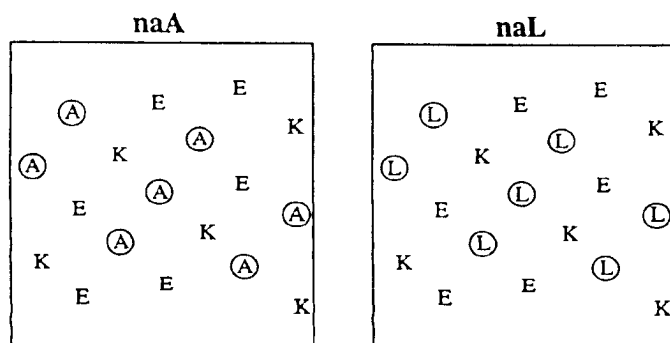
d. naL and naA represent non-amphipathic α -helical analogues of LL9 and AA9, respectively, i.e., same amino acid composition but different sequence; hence, "na" denotes non-amphipathic.

e. C1 denotes random coil control peptide 1.

Amphipathic α -Helices



Non-amphipathic α -Helices



Random Coil Peptide

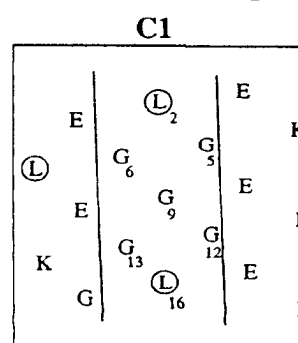


Figure VII-1 Representation of synthetic α -helical peptides as α -helical nets. For the “native” amphipathic α -helical peptides, LL9 and AA9, the area between the solid lines on the top of the two nets represents the hydrophobic face [made up of Leu (LL9) or Ala (AA9) residues]. The substitution site for peptide analogs (position 9) is the center of the non-polar face of these “native” peptides, e.g., the analogs with Lys at position 9 is denoted LK9. For the non-amphipathic α -helical peptides, naA and naL, which represent SCDS (same composition, different sequence analogs) of AA9 and LL9, respectively, the distribution of the Ala (naA) or Leu (naL) residues results in non-amphipathic structures. A random coil standard, C1, is also presented as an α -helical net, in order to illustrate the unlikelihood of such secondary structure.

position 9; similarly, the AA9 “native” analogue has Ala substituted at position 9. The result of this well-characterized sequence (Mant *et al.*, 1993; Mant *et al.*, 2002b; Mant *et al.*, 2002c; Monera *et al.*, 1995; Sereda *et al.*, 1994; Zhou *et al.*, 1992; Zhou *et al.*, 1994b), which has a high potential to form α -helical structure, is an amphipathic helix with a wide hydrophobic face (between the solid lines in the helical net representations of LL9 and AA9; Figure VII-1) made up of non-polar residues at positions 2, 5, 6, 9, 12, 13 and 16; the hydrophilic face is made up of Lys and Glu residues. In addition, the LL9 and AA9 peptides are amphipathic α -helical peptides with non-polar faces representing hydrophobic domains of very different hydrophobicities, *i.e.*, a very hydrophobic environment represented by the Leu residues of LL9 and a much less hydrophobic environment created by the Ala residues of AA9. From Figure VII-1 and Table VII-1, LK9, with Lys substituted at position 9 of the LX9 peptides, represents an amphipathic α -helical peptide analogue with a highly hydrophilic, positively charged residue situated in the centre of a very hydrophobic environment; similarly, AK9, with Lys substituted at position 9 of the AX9 peptides, represents an amphipathic α -helical peptide with this positively charged residue situated in the centre of only a moderately hydrophobic environment.

From Table VII-1, the peptides denoted with subscript L or D refer to the L- or D-amino acid substitutions in the centre of the non-polar face of the AX9 peptide sequence. Thus, A_L denotes the analogue with L-Ala substituted at position 9 of the sequence (identical to AA9), L_D denotes the analogue with D-Leu substituted at position 9 of AX9, *etc.*

From Table VII-1 and Figure VII-1, the peptides denoted naL and naA represent SCDS (same composition, different sequence) analogues of LL9 and AA9, respectively. As shown in the helical net representations (Figure VII-1), the distribution of the Leu (naL) or Ala (naA) residues results in non-amphipathic structures (hence, “na”, which denotes non-amphipathic).

Finally, peptide C1 represents a peptide designed to exhibit negligible secondary structure, *i.e.*, a random coil. This peptide was designed to be of similar length and composition to AA9, as well as retention time of similar magnitude to that of AA9. While AA9 contains seven Ala residues, C1 contains none. Instead, five Gly residues and two Leu residues are present in the C1 preferred binding domain if it were α -helical. Thus, with seven Ala residues in AA9 (hence seven CH₃ groups) and five Gly and three Leu residues in C1 (hence twelve CH₂ and CH₃ groups, from the three Leu residues), overall hydrophobicity is essentially maintained. The additional Leu is required to increase the retention time of the random coil peptide to a value similar to that of AA9 with the preferred binding domain. The positioning of the three Leu residues was designed to ensure that they could not form an amphipathic α -helix and, hence, override the destabilizing effect of the Gly residues. From Figure VII-1, it can be seen that, even if this peptide was able to be induced into α -helical structure, a non-amphipathic helix would result. However, the presence of five Gly residues (Gly is a known α -helix disrupter and the amino acid with the lowest helical property (Monera *et al.*, 1995; Zhou *et al.*, 1994b)) in place of five Ala residues (Ala being the amino acid with highest helical propensity (Monera *et al.*, 1995; Zhou *et al.*, 1994b)) was designed to make any secondary structure highly unlikely to occur.

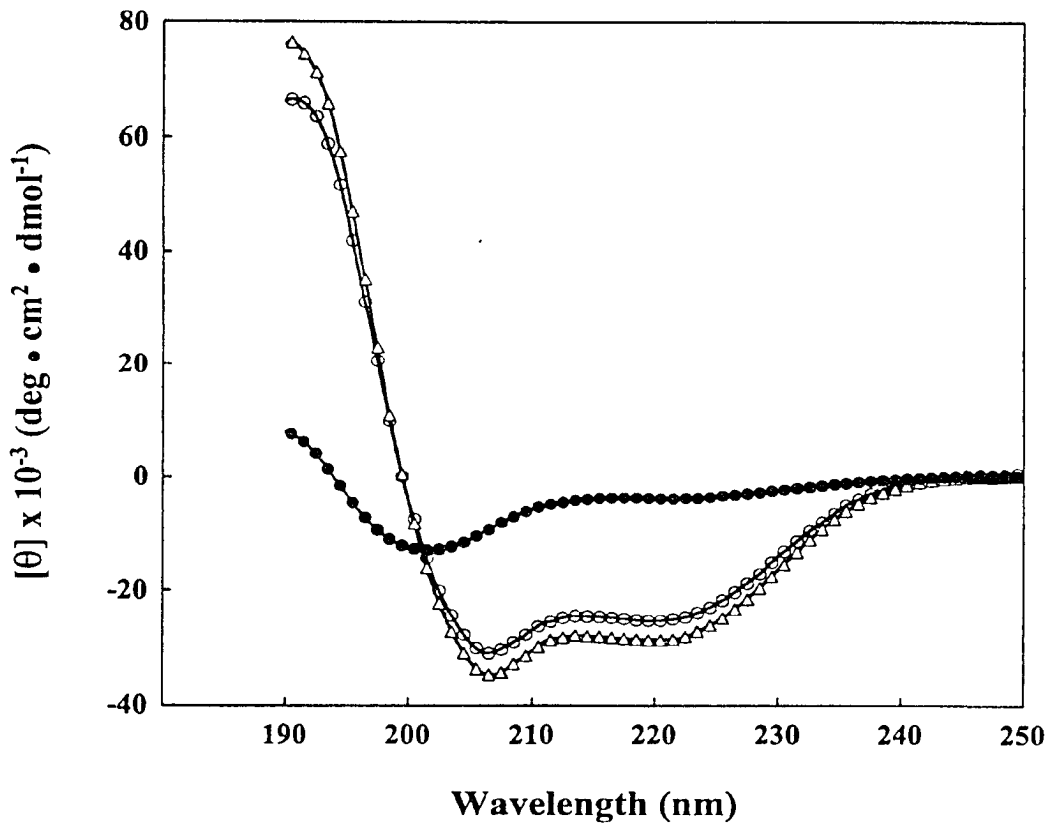


Figure VII-2 Circular dichroism spectra of synthetic peptide analogs. The spectra were measured in 40% TFE in 0.1% *aq.* TFA, pH 2.0. The sequences and nomenclature of the peptides are defined in Table VII-1. Symbols used are C1 (●), LL9 (○) and LK9 (△).

Illustration of the strong α -helicity of LK9 ($[\theta]_{222} = -28,450^\circ$) and LL9 ($[\theta]_{222} = -24,900^\circ$) in the presence of the α -helix-inducing solvent TFE (Cooper *et al.*, 1990; Lau *et al.*, 1984a; Nelson *et al.*, 1989; Sonnichsen *et al.*, 1992) at pH 2.0 (50% TFE in 0.1% *aq.* TFA) is shown in Figure VII-2. The high helicity of the amphipathic peptide series in the presence of TFE, of which AA9 is the “native” analogue, has been well documented (Monera *et al.*, 1995; Zhou *et al.*, 1992; Zhou *et al.*, 1994b). In addition, the non-amphipathic analogue of AA9, *i.e.*, naA, has also been shown previously to exhibit strong helicity in the presence of 50% TFE (Guo *et al.*, 1986a), as does the LL9 non-amphipathic analogue, naL, in the present study (data not shown). Since TFE is recognized as a useful mimic of the non-polar environment characteristic of RP-HPLC (Zhou *et al.*, 1990), as well as being a strong α -helix inducer in potentially helical molecules (Cooper *et al.*, 1990; Lau *et al.*, 1984a; Nelson *et al.*, 1989; Sonnichsen *et al.*, 1992), elution of these peptide analogues as α -helices during RP-HPLC is ensured. In contrast, from Figure VII-2, the peptide designed as a random coil standard, C1, clearly exhibits negligible secondary structure, even in the presence of 50% TFE and at the low temperature of 5°C ($[\theta]_{222} = -3,950^\circ$). Finally, it has also been previously demonstrated that the L- and D-peptide analogues (with the exception of P_L and P_D) all exhibit high α -helical content in the presence of 50% TFE (Chen *et al.*, 2002).

VII-4-2 Retention behavior of model peptides during RP-HPLC

It is well known that the chromatography conditions of RP-HPLC (hydrophobic stationary phase, non-polar eluting solvent) induce and stabilize helical structure in potentially helical polypeptides (Purcell *et al.*, 1995c; Steer *et al.*, 1998; Zhou *et al.*, 1990) in a manner similar to that of the helix-inducing solvent TFE. Polypeptides which

are thus induced into an amphipathic α -helix on interaction with a hydrophobic RP-HPLC stationary phase will exhibit preferred binding of their non-polar face with the stationary phase (Zhou *et al.*, 1990). Figure VII-3 shows the RP-HPLC elution profile of α -helical peptides on the C₈ column. From Figure VII-3, for peptide pairs AA9/naA and LL9/naL, the amphipathic analogues (AA9 and LL9) were eluted later than their non-amphipathic analogues (naA and naL, respectively), due to the preferred binding domains (*i.e.*, the non-polar faces) of AA9 and LL9. In addition, the retention times of naL and LL9 are greater compared to naA and AA9, respectively, due to the considerably greater hydrophobicity of Leu compared to Ala (Guo *et al.*, 1986a; Guo *et al.*, 1986b). Also from Figure VII-3, it is clear that substitution of a positively charged Lys residue into the centre of the non-polar face of an amphipathic α -helical peptide (AK9, LK9) decreases significantly the hydrophobicity of the non-polar face, as evidenced by the reduction in RP-HPLC elution times of AK9 and LK9 compared to AA9 and LL9, respectively. It should be noted that the illustrated RP-HPLC run was carried out at 40 °C due to the relatively poor peak shape of naL at lower temperatures.

Figure VII-4B shows the RP-HPLC elution profile of L- and D- peptide pairs on the C₈ column. From Figure VII-4B, the D-substituted analogues were eluted faster than their corresponding diastereomers. This decrease in retention times of the D-analogues compared to the L-analogues can be rationalized as being due to disruption of the hydrophobic face of the amphipathic α -helix due to the introduction of a D-amino acid (Aguilar *et al.*, 1993; Krause *et al.*, 2000; Rothmund *et al.*, 1995; Rothmund *et al.*, 1996). The overall effect would thus be a decrease in the apparent hydrophobicity of the non-polar face of the amphipathic α -helix when substituted with a D-amino acid relative

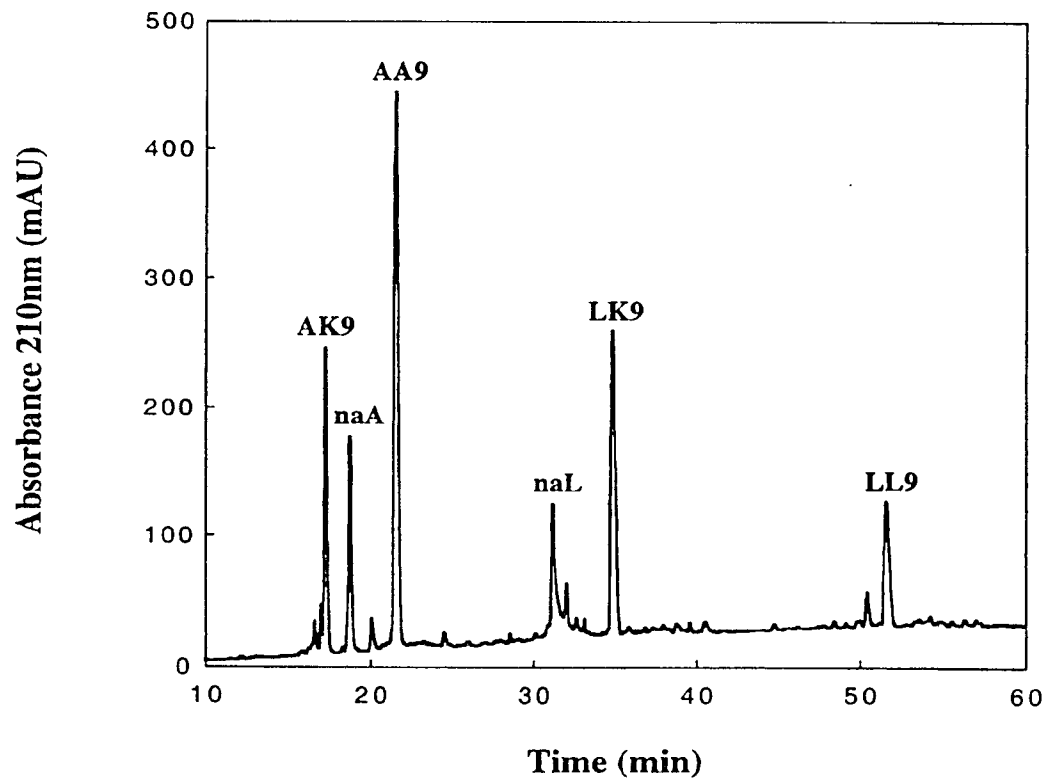


Figure VII-3 RP-HPLC of synthetic amphipathic and non-amphipathic α -helical peptides. Columns: Zorbax SB300-C₈ (150x4.6 mm I.D., 5 μ m particle size, 300 Å pore size). Conditions: linear AB gradient (1%B/min) at a flow rate of 0.25 ml/min, where eluent A is 0.05% *aq.* TFA and eluent B is 0.05% TFA in acetonitrile; temperature, 40 °C. The structures of the amphipathic (AA9, AK9, LL9, LK9) and non-amphipathic (naA, naL) α -helical peptides are shown and defined in Table VII-1, with helical net representations of AA9, LL9, LK9, naA and naL also shown in Figure VII-1.

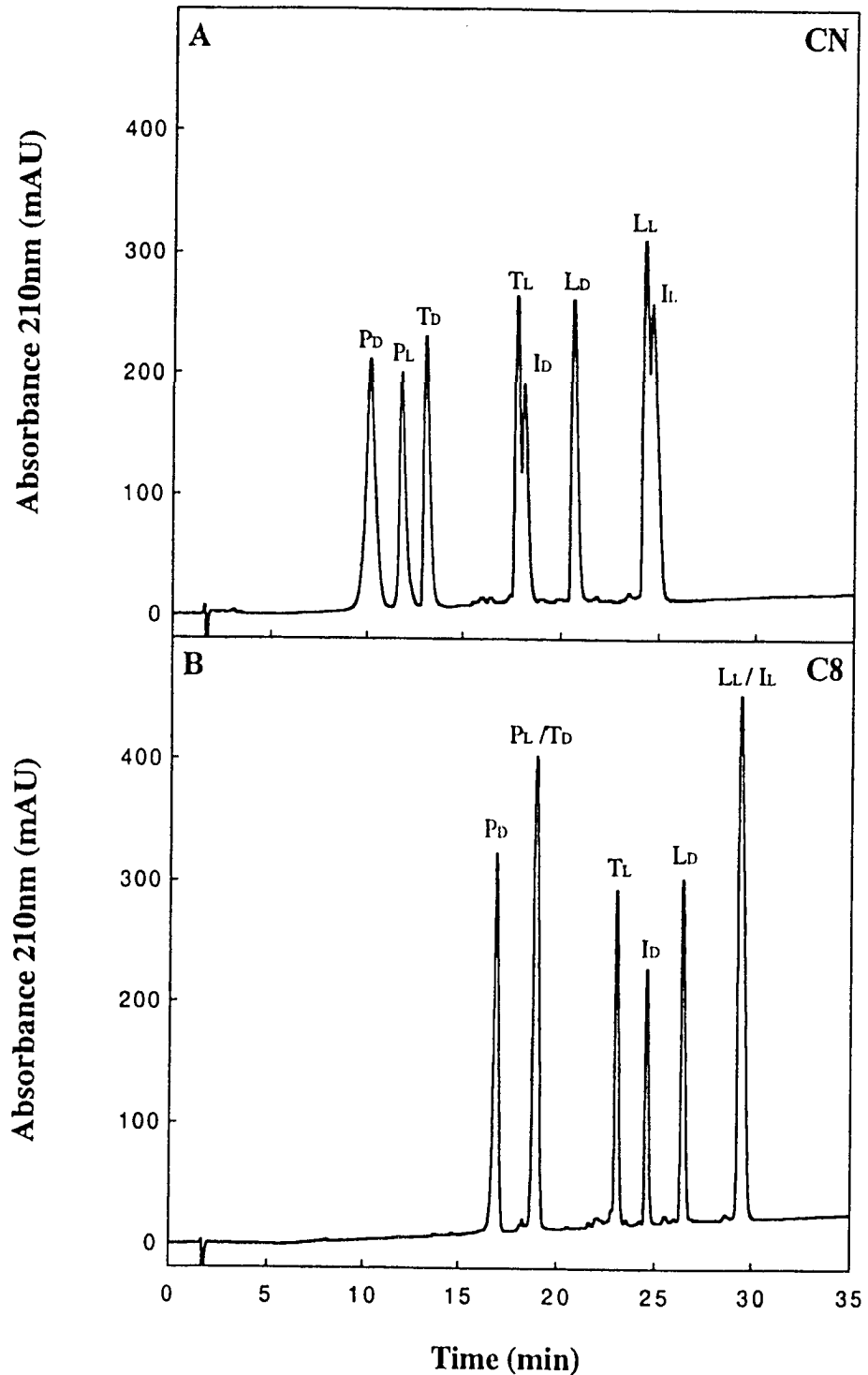


Figure VII-4 RP-HPLC of diastereomeric peptide pairs. Columns: Zorbax SB300-C₈ (B) and Zorbax SB300-CN (A) (150x4.6 mm I.D., 5 μ m particle size, 300 \AA pore size). Conditions: linear AB gradient (1%B/min) at a flow rate of 0.25 ml/min, where eluent A is 0.05% *aq.* TFA and eluent B is 0.05% TFA in acetonitrile; temperature, 25 $^{\circ}$ C. The structures and descriptions of the peptides are shown in Table VII-1.

to its L-diastereomer and, hence, a decrease in retention time of the former compared to the latter. Figure VII-4A shows the RP-HPLC elution profile of the same peptide mixture on a CN column under the same conditions. Interestingly, peptides co-eluted on the C₈ column (Figure VII-4B) are now completely or partially resolved on the CN column (P_L, T_D and L_L, I_L). Also the retention times of all the peptides are reduced on the CN column (Figure VII-4A) relative to the C₈ column, underlining the lesser hydrophobicity of the cyano-substituted stationary phase compared to the C₈ column matrix.

It is important to note that the SB300-C₈ and SB300-CN columns (with SB denoting StableBond) were chosen for this study due to their excellent temperature stability at low pH values (Barry *et al.*, 1995; Kirkland *et al.*, 1997; McNeff *et al.*, 2000).

VII-4-3 Effect of temperature on RP-HPLC of α -helical peptides

Figure VII-5 illustrates the effect of temperature on the retention behavior of peptides at varying conformation, amphipathicity and stability by presenting the elution profile of a 6-peptide mixture at 5 °C (top), 45 °C (middle) and 80 °C (bottom). The profile at 5 °C again shows the effect of amphipathic (AA9) versus non-amphipathic (naA) helical peptide retention behavior (*i.e.*, AA9 is eluted later than its non-amphipathic homologue, naA) as well as the effect of substituting a positively charged residue (Lys) in the centre of a non-polar face of an amphipathic peptide (*i.e.*, LL9 and AA9 are eluted later than their Lys-substituted counterparts LK9 and AK9, respectively). Of particular note is the elution position of the random coil C1 peptide, whose overall hydrophobicity is clearly similar to that of the apparent hydrophobicities of the AX9 peptides (“apparent” due to the preferred binding of the non-polar face of such peptides to the RP-HPLC stationary phase), an important consideration when subsequently

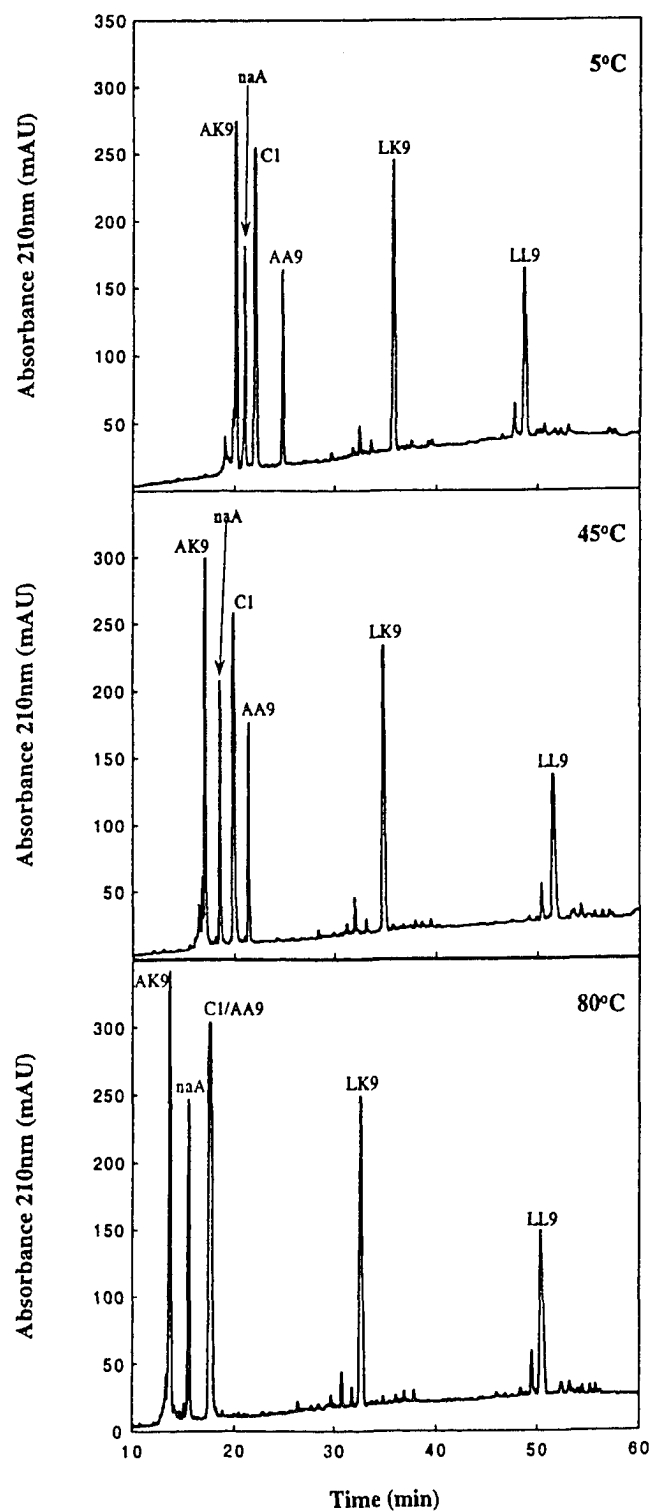


Figure VII-5 RP-HPLC of α -helical peptides at 5 °C, 45 °C and 80 °C. Column: Zorbax SB300-C₈ (150x4.6 mm I.D., 5 μ m particle size, 300 Å pore size). Conditions: linear AB gradient (1%B/min) at a flow rate of 0.25 ml/min, where eluent A is 0.05% *aq.* TFA and eluent B is 0.05% TFA in acetonitrile. The structures and descriptions of the peptides are shown in Table VII-1.

attempting to distinguish between the RP-HPLC elution behavior of amphipathic α -helical peptides versus random coil peptides as the temperature is increased.

At 45 °C (Figure VII-5, middle), all peptides, with the exception of LL9, have decreased in retention relative to 5 °C (Figure VII-5, top) albeit to differing extents and, thus, leading to a selectivity change in the elution profile which is particularly evident in the separation of the first four eluted peptides (AK9, naA, C1, AA9). In contrast to the other five peptides, the retention time of LL9 has increased at 45 °C compared to 5 °C. Finally, at 80 °C (Figure VII-5, bottom), the retention times of all six peptides have decreased relative to 45 °C (Figure VII-5, middle). In addition, selectivity changes effected by this high temperature relative to 45 °C (Figure VII-5, middle) and 5 °C (Figure VII-5, top) are again clearly apparent for the first four peptides eluted, particularly evident by the co-elution of the amphipathic α -helical AA9 and the random coil C1.

Figure VII-6 illustrates the overall effect of temperature on the RP-HPLC elution behavior of α -helical peptides on the C₈ column. The data are reported as peptide retention time at a particular temperature (t_R) minus its retention time at 5 °C ($t_{R5\text{ °C}}$; panel A) or 80 °C ($t_{R80\text{ °C}}$; panel B) *versus* temperature in order to highlight differences in the elution behavior of peptides as the temperature is raised. From Figure VII-6, it is clear that peptides of different amphipathicity/hydrophobicity and conformation behave quite differently during RP-HPLC at different temperatures, although all (with the sole exception of LL9) decrease in retention time relative to the value at 5 °C with increasing temperature (panel A), or (again with the exception of LL9) increase in retention time relative to the value at 80 °C with decreasing temperature (panel B).

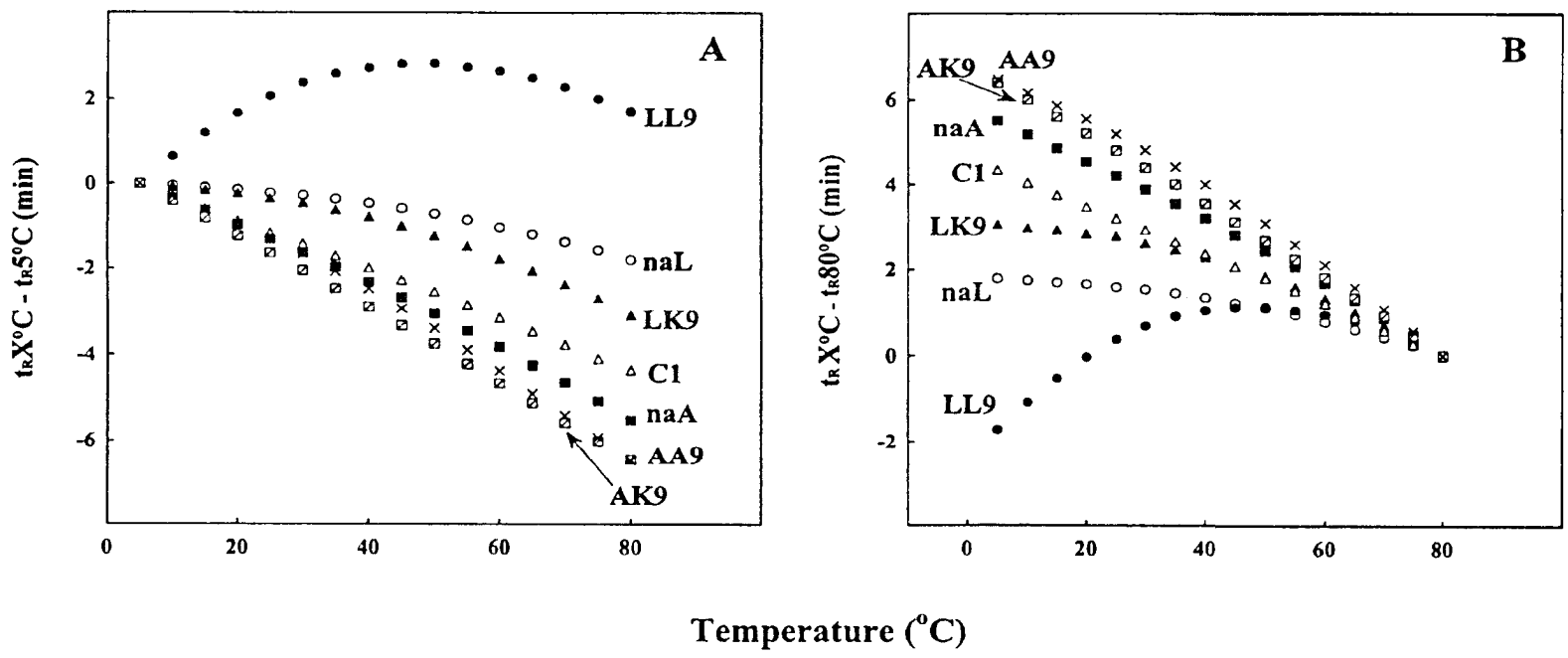


Figure VII-6 Effect of temperature on RP-HPLC of α -helical peptides. Column: Zorbax SB300- C_8 (150x4.6 mm I.D., 5 μm particle size, 300 \AA pore size). Conditions: linear AB gradient (1%B/min) at a flow rate of 0.25 ml/min, where eluent A is 0.05% *aq.* TFA and eluent B is 0.05% TFA in acetonitrile; temperature, 5-80 $^{\circ}\text{C}$ in 5 $^{\circ}\text{C}$ increments. (A) Temperature against peptide retention time at a specific temperature minus its retention time at 5 $^{\circ}\text{C}$ ($t_{R,X}^{\circ}\text{C} - t_{R,5}^{\circ}\text{C}$). (B) Temperature against peptide retention time at a specific temperature minus its retention time at 80 $^{\circ}\text{C}$ ($t_{R,X}^{\circ}\text{C} - t_{R,80}^{\circ}\text{C}$). The structures and descriptions of the peptides are shown in Table VII-1.

The random coil peptide (C1) was included in peptide mixtures to correct for effects of temperature on peptide solubility, mobile phase viscosity and mass transfer, *etc.*, hence assuring that only effects on secondary and tertiary/quaternary structure were being observed. Thus, conclusions concerning the effect on peptide conformation of raising the temperature may be made based on comparing the temperature profiles of the α -helical peptides to that of the random coil peptide standard. From Figure VII-6A, the rate of decrease of retention time of naL and LK9 as the temperature is raised incrementally from 5 °C to 80 °C is less rapid than for the random coil C1. In contrast, the rate of change for naA, AA9 and AK9 is more rapid than that of C1. Finally, the retention behaviour of LL9 is unique in this peptide mixture in that its retention time increases with increasing temperature (up to ~50 °C) and then decreases once more with a further temperature increase. From Figure VII-6B, the rate of increase of retention time of naL and LK9 as the temperature is lowered incrementally from 80 °C to 5 °C is less rapid than for the random coil C1. However, the rate of change for naA, AA9 and AK9 is more rapid than that of C1. Finally, the retention time of LL9 increases up to ~50 °C with decreasing temperature and then decreases once more with a further temperature decrease.

Figure VII-7 illustrates the effect of temperature on the RP-HPLC elution behavior of monomeric α -helical diastereomeric peptide pairs on the cyano column. The column was chosen over the considerably more hydrophobic C₈ column (Zhou *et al.*, 1991) since it was hoped that the lesser hydrophobicity, although of a great enough magnitude to induce and/or stabilize α -helical structure when the peptide is bound to the stationary phase, would help not only to allow maximum detection of unfolding of α -

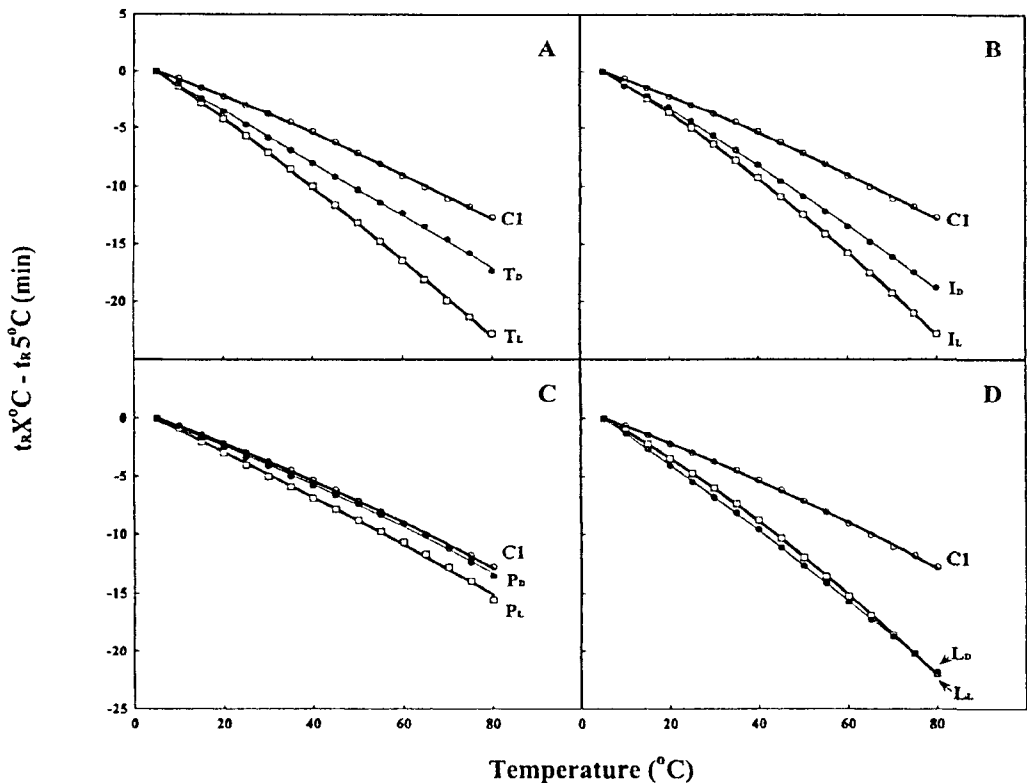


Figure VII-7 Effect of temperature on RP-HPLC of L- and D-diastereomeric α -helical peptides. Column: Zorbax SB300-CN (150x4.6 mm I.D., 5 μ m particle size, 300 \AA pore size). Conditions: linear AB gradient (0.5%B/min) at a flow rate of 0.25 ml/min, where eluent A is 0.05% *aq.* TFA and eluent B is 0.05% TFA in acetonitrile; temperature, 5-80 $^{\circ}\text{C}$ in 5 $^{\circ}\text{C}$ increments. (A-D) Peptide retention time at a specific temperature minus its retention time at 5 $^{\circ}\text{C}$ ($t_{R} - t_{R} 5^{\circ}\text{C}$) for diastereomeric peptide pairs of Thr-, Ile-, Pro- and Leu-substituted analogs, respectively. The random coil peptide C1 was also included in all runs. Peptide structures and descriptions are shown in Table VII-1.

helical peptides in solution but also highlight any differences in profiling behavior between L- and D-peptide pairs. From Figure VII-7A-7D, in a similar manner to AK9 and AA9 on the C8 column (Figure VII-6), the rate of change in retention behavior from 5 °C to 80 °C is faster for all L- and D-peptide pairs compared to the random coil C1. Finally, from Figure VII-8, it is interesting to note that a comparison of the effect of temperature on RP-HPLC of several monomeric amphipathic α -helices, all with L-amino acid substitutions at the centre of the non-polar face (L_L , I_L , A_L and G) revealed similar RP-HPLC temperature profiles for all the peptides.

VII-5 Discussion

VII-5-1 Hypothesis for monitoring dimerization and unfolding of α -helical peptides by temperature profiling in RP-HPLC

Although peptides are eluted from a reversed-phase column mainly by an adsorption/desorption mechanism (Mant *et al.*, 1991; Mant *et al.*, 2002a), even a peptide strongly bound to a hydrophobic stationary phase will partition between the aqueous mobile phase in equilibrium with its bound state in a narrow range of acetonitrile concentrations during gradient elution.

From Figure VII-9 (top) our hypothesis for monitoring peptide dimerization by temperature profiling during RP-HPLC within the small partitioning “window” characteristic of peptides (Mant *et al.*, 1987a) is based on four criteria: (1) at low temperature, an amphipathic α -helical peptide able to dimerize in aqueous solution (i.e., associate through its hydrophobic, non-polar face) will dimerize in solution during partitioning, i.e., the concentration of monomer in solution is low and dimer

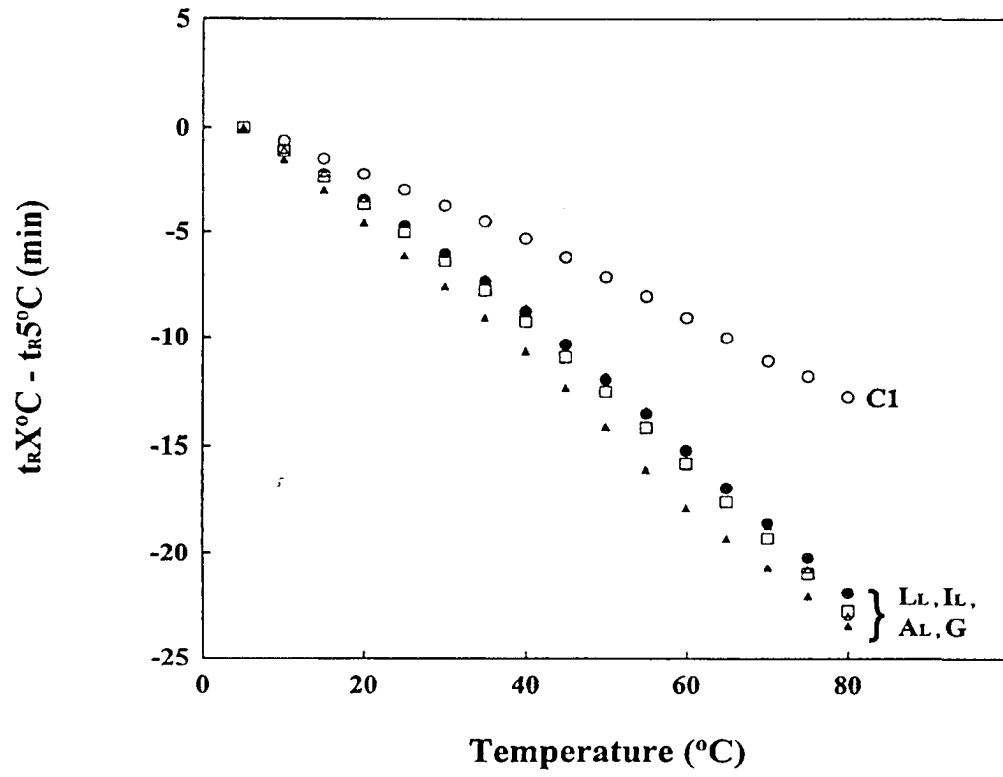


Figure VII-8 Effect of temperature on RP-HPLC of monomeric α -helical peptides. Column and conditions: see Figure VII-7. The effect of temperature on peptide retention behavior is plotted as peptide retention time at a specific temperature minus its retention time at 5 °C. Peptide structures and descriptions of the L-substituted Leu-, Ile- and Ala-substituted analogs (●, □, △) as well as those of the Gly-substituted analog (▲) and the random coil peptide C1 (○) are shown in Table VII-1.

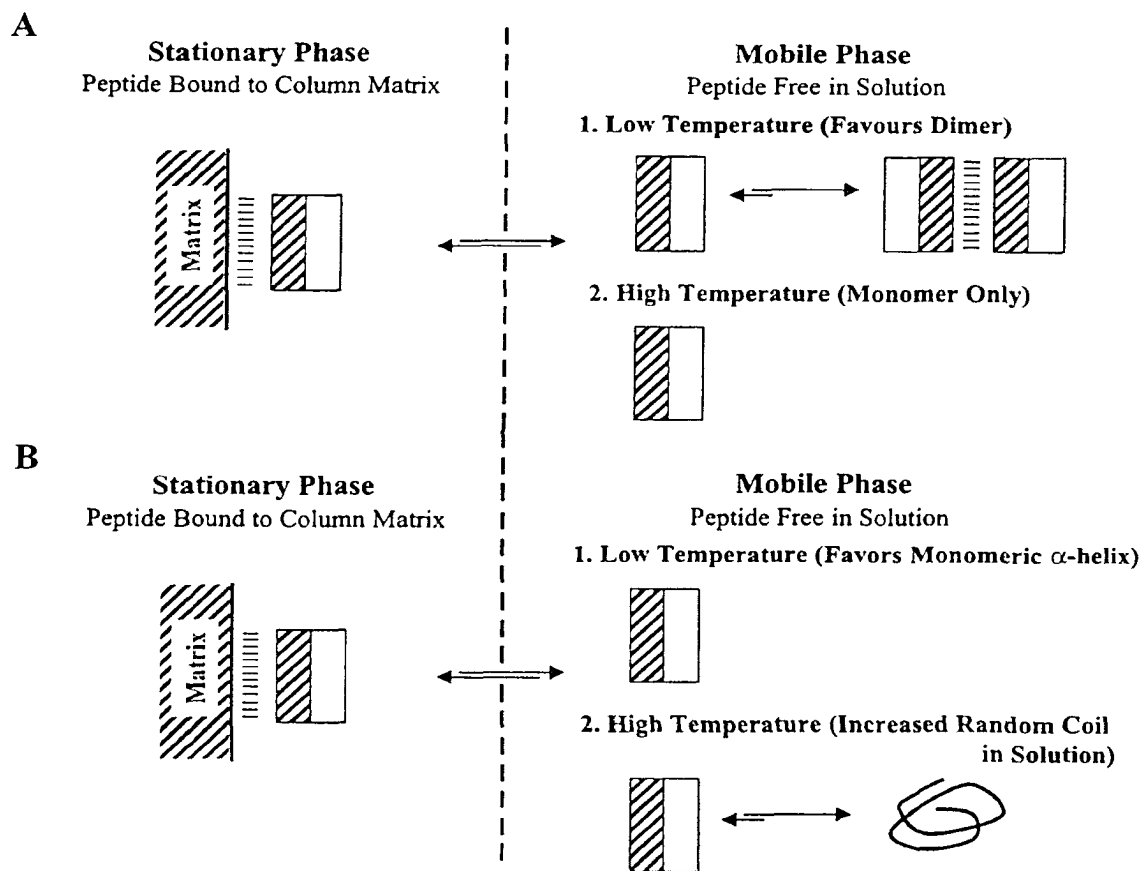


Figure VII-9 Hypothesis for monitoring peptide dimerization (top) and unfolding of monomeric α -helices (bottom) by temperature profiling in RP-HPLC.

concentration is high; (2) at higher temperatures, the monomer-dimer equilibrium favors the monomer as the dimer is disrupted, thus increasing the concentration of monomer and decreasing the concentration of dimer in solution; (3) at high temperatures, only monomer is present in solution; and (4) whether in the monomeric or dimeric form in solution, the peptide is always bound in its monomeric helical form to the hydrophobic stationary phase. Disruption of the dimer is required for rebinding of the non-polar face of the amphipathic peptide. Thus, the rate of rebinding is faster at lower dimer concentration.

From Figure VII-9 (bottom), our hypothesis for monitoring peptide unfolding during RP-HPLC by temperature profiling is based on three criteria: (1) at low temperature, an α -helical peptide is fully folded in solution; (2) as the temperature increases, there is a gradual shift in equilibrium from α -helix to random coil as the peptide unfolds; and (3) at high temperature, whether the peptide is in its monomeric α -helical form or in an unstructured, random coil form in solution, the peptide is always bound to the hydrophobic stationary phase in its monomeric α -helical form.

VII-5-2 *Monitoring dimerization and unfolding of α -helical peptides during RP-HPLC*

The retention behavior of LL9, containing a highly hydrophobic non-polar face, suggests dimerization at low temperature with concomitant shielding of the non-polar face of the peptide. As the temperature is raised, there is disruption of dimerization, exposing more of the hydrophobic face of the peptide and, thus, switching the dimer \leftrightarrow monomer equilibrium to more monomeric α -helix at higher temperatures. In addition, the temperature at the maximum Δt_R ($t_R - t_{R5^\circ C}$) value for LL9 may represent the stability of the dimer under the conditions of chromatography. Interestingly, the helicity of LL9 in

the presence of 40% TFE decreased to a small extent ($[\theta]_{222} = -24,900^\circ$) compared to its helicity in its absence ($-27,300^\circ\text{C}$), the only analogue to exhibit this result. TFE disrupts tertiary and quaternary structure whilst promoting/maximizing helical structure. Thus, it is possible that, in the absence of TFE, there was interaction between the hydrophobic faces of two LL9 molecules (*i.e.*, dimerization) which also helped to stabilize LL9 helical structure in the absence of a helix-inducing environment. Such helix-helix interaction would subsequently be disrupted in the presence of TFE (as well as by the combined effect of a rise in temperature and the hydrophobic environment of RP-HPLC) even while α -helicity was maintained.

Although LL9 represents the analogue exhibiting the most dramatic effects on retention time of temperature variation, which we speculate as being due to dimerization at lower temperatures, the possibility that other analogues may exhibit a degree of oligomerization was investigated by comparing the temperature profiles of these peptides with that of the random coil standard, C1. Thus, the data from Figure VII-6A were now normalized relative to the temperature profile of the random coil standard, the results of which are presented in Figure VII-10. From Figure VII-10, the positive profile of LL9 suggests little or no unfolding of this very stable peptide ($T_m = 67.6^\circ\text{C}$), even at higher temperatures. Interestingly, the positive profiles of naL and LK9 (Figure VII-10) also indicate some association of these molecules at lower temperatures. Significantly, naL exhibited poor peak shape during RP-HPLC at low temperatures, as well as poor solubility in 100% aqueous solution, indicating a tendency to aggregate at low temperature and in the absence of organic modifier. Thus, the positive profile for naL shown in Figure VII-10A may indeed be indicative of association (in this case,

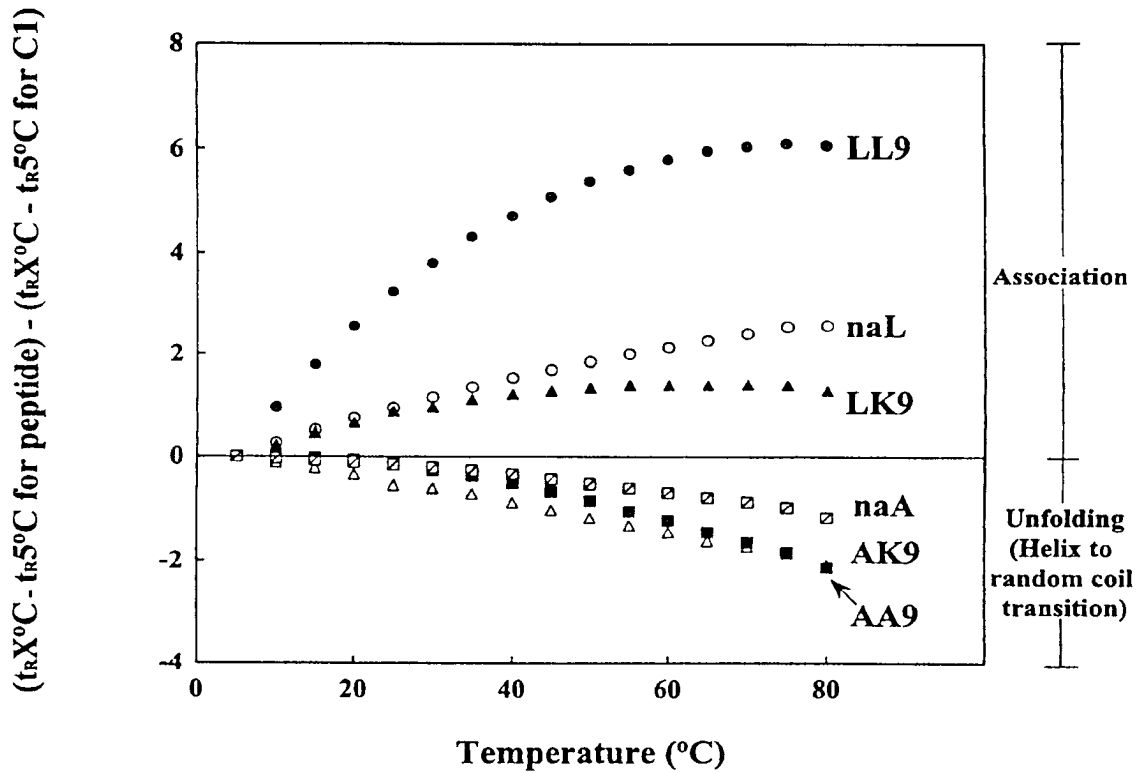


Figure VII-10 Effect of temperature on RP-HPLC of α -helical peptides: normalization to retention behavior of random coil peptide. Column and conditions: see Figure VII-5. The retention behavior of the peptides was normalized to that of random coil peptide C1 through the expression $(t_R - t_{R\ 5\ ^\circ\text{C}})$ minus $(t_{R\ \text{C1}} - t_{R\ \text{C1}\ 5\ ^\circ\text{C}})$, where t_R and $t_{R\ \text{C1}}$ are the retention times at a specific temperature of a helical peptide and the random coil peptide, respectively, and $t_{R\ 5\ ^\circ\text{C}}$ and $t_{R\ \text{C1}\ 5\ ^\circ\text{C}}$ are the retention times at 5 $^\circ\text{C}$. Peptide structures and descriptions are shown in Table VII-1.

aggregation) of naL molecules. Concerning LK9, despite its lesser amphipathicity compared to LL9 (due to the presence of the positively charged Lys residue in the center of the non-polar face of the helix), a combination of the high hydrophobicity of the remainder of the wide non-polar face, still containing six Leu residues (Figure VII-1), and the good stability of LK9 ($T_m = 30.7^\circ\text{C}$) may well result in some dimerization at low temperatures. Indeed, it is perhaps a testament to the sensitivity of this profiling approach that such lesser levels of dimerization may be detected. Finally, the negative profiles of the least stable AA9 and AK9 analogues (T_m values of just 17.0°C and 17.2°C , respectively) in Figure VII-10B (derived from the temperature profiles shown in Figure VII-6A), arising from the faster rates of change relative to C1 in Figure VII-6, suggest considerable unfolding of the α -helices with increasing temperature. Thus, at low temperature, the bound monomeric α -helical AA9 and AK9 are in equilibrium with the same monomeric folded states free in solution. Their retention times, at a given temperature, then depend strictly on the hydrophobicity of the moderately non-polar faces of the helices. At high temperature, a considerable amount of the random, unfolded forms of these peptides is now present in solution and the peptides have lost amphipathicity, *i.e.*, no preferred binding domain of AA9 or the lesser amphipathic AK9 is now present. The fast exchange between folded α -helix and random coil affects the retention time, *i.e.*, the more random coil, the greater the decrease in retention time.

To summarize the results presented in Figure VII-10, positive profiles relative to the random coil C1 represent an indication of association of peptide molecules, either through oligomerization (*e.g.*, dimerization of LL9 and LK9) or aggregation (*e.g.*, naL); conversely, negative profiles relative to C1 indicate unfolding of the peptides as the

temperature is increased, *i.e.*, a helix to random coil transition for naA, AK9 and AA9. In addition, the profiles shown in Figure VII-10 (and, indeed, Figure VII-6A from which the Figure VII-10 profiles are derived) are representative of the effect of increasing temperature on the fully folded state of the peptides, relative as they are to their retention times at 5 °C. In contrast, the data shown in Figure VII-6B are representative of the effect of decreasing temperature on the dissociated state of the peptides, relative as they are to their retention times at 80 °C.

Factors which influence the rate of unfolding of monomeric α -helical peptides were further clarified through comparison of the temperature profiles of the L- and D-peptide analogue pairs (Figure VII-7). For instance, as described above, the rate of change in peptide retention behavior as the temperature is increased from 5 to 80 °C is faster (that is, the temperature profiles are steeper) for all L- and D-peptide pairs compared to the random coil peptide standard, C1, suggesting a helix \rightarrow random coil unfolding is occurring in solution during RP-HPLC. The rate of unfolding is apparently slower for D-substituted peptides compared to the corresponding L-diastereomer, likely due to the greater folding of the L-peptides compared to the D-peptides at 5 °C as a result of the α -helix disrupting properties of D-amino acids in an α -helix made up of L-amino acids (Krause *et al.*, 2000; Rothmund *et al.*, 1995; Rothmund *et al.*, 1996). Thus, in the presence of 50% TFE, the maximum molar ellipticities of L-analogues (excluding P_L) were essentially the same (average $[\theta]_{222} = -27,150$), suggesting a fully α -helical structure for each peptide analogue (Chen *et al.*, 2002). For example T_L (Figure VII-7) is more folded at 5 °C ($[\theta]_{222} = -27,200$) than T_D ($[\theta]_{222} = -16,150$); thus, more α -helix has to unfold during the helix \rightarrow random coil transition. In contrast, for T_D, there is less helix to

unfold and, therefore, the temperature profile more closely resembles the random coil (C1) profile than the folded T_L .

There are distinct temperature profile differences between the diastereomeric peptide pairs, this difference appearing to depend on the maximum α -helicity of the individual peptides in the helix-inducing 50% trifluoroethanol (TFE). As noted previously, TFE is a useful mimic of hydrophobic stationary phases (Zhou *et al.*, 1990); thus, the helicity measured in 50% TFE is likely a good measure of the helicity of the peptides when bound to the stationary phase. From Figure VII-7A, there is a substantial temperature profile difference between T_L and T_D , reflecting significant molar ellipticity (in 50% TFE) differences of 27,200° and 16,150°, respectively. From Figure VII-7B, there is also a substantial (though lesser, relative to the T_L/T_D pair) profile difference between I_L and I_D , reflecting molar ellipticity differences of 26,900 and 22,150, respectively. Figure VII-7C illustrates a yet smaller profile difference between P_L and P_D , reflecting molar ellipticity differences of 14,900 and 8,150, respectively. Significantly, such values indicate that just half of the P_L peptide and only ~one-third of the P_D peptide were induced into α -helix in the presence of 50% TFE, reflecting the helix-disrupting properties of Pro. Thus, large proportions of these peptides are already unstructured prior to raising the temperature, which likely explains the temperature profiles, particularly that of P_D , being closer to that of the random coil C1. Finally, from Figure VII-7D, the temperature profiles of L_L and L_D are very similar, reflecting essentially identical molar ellipticity values of 26,800 and 26,900, respectively, *i.e.*, when there is no difference in helical content, there is no difference in the temperature profile. It should be noted that the β -branch of the D-Ile amino acid is more disruptive to the α -helix than D-Leu (molar

ellipticity values for I_D and L_D of 22,150 and 26,900, respectively) and temperature profiling is able to detect this disruption. Temperature profiling is sensitive to conformational change; thus, if there is no change in conformation over the temperature range 5-80 °C, a random-coil peptide and helical peptide will behave similarly.

Figure VII-8 compared the effect of temperature on RP-HPLC of several monomeric amphipathic α -helical peptides, all with L-amino acid substitutions at the centre of the non-polar face (Figure VII-1). For peptides L_L , I_L , A_L and G, T_m values (*i.e.*, the temperature required to unfold 50% of the α -helix) have been measured as 82 °C, 77.5 °C, 62.5 °C and 51.5 °C, respectively, *i.e.*, they show a range of stabilities in solution. However, this stability difference is not reflected in their RP-HPLC temperature profiles (Figure VII-8), which are all very similar, *i.e.*, the rate of unfolding of the four peptides is similar. This observation may be rationalized by assuming that, in the bound state, all four peptides are fully induced and stabilized in an α -helical conformation, no matter what their stability in solution.

VII-6 Conclusions

We have compared the effect of temperature on the RP-HPLC elution behavior of mixtures of peptides encompassing amphipathic α -helical structure, amphipathic α -helical structure with L- versus D-amino acid substitutions in the centre of the non-polar face, non-amphipathic α -helical structure, or negligible secondary structure. From the observation of the retention behavior of these model peptides over a wide temperature range, we have been able to make initial conclusions concerning the potential efficacy of “temperature profiling” by RP-HPLC to monitor dimerization and/or unfolding of α -

helical peptides. It appears that temperature profiling is most appropriate for measuring the ability of molecules to oligomerize and dimerization is related to the stability of the oligomer in solution. The logical extension to the present study was to examine the feasibility of this profiling approach to examine the conformation and stability of polypeptides exhibiting higher levels of protein structure (*i.e.*, tertiary and quaternary structure) and this is the subject of a companion paper (Mant *et al.*, 2003b).

CHAPTER VIII

Determination of Stereochemistry Stability Coefficients of Amino Acid Side-Chains in an Amphipathic α -Helix

A version of this chapter has been published: Chen, Y., Mant, C. T. and Hodges, R. S. (2002) *J. Peptide Res.* **59**, 18-33. Only methods unique to this chapter are described in the **Experimental** section, the remaining general methods are described in Chapter III.

VIII-1 Abstract

We describe here a systematic study to determine the effect on secondary structure of D-amino acid substitutions in the non-polar face of an amphipathic α -helical peptide. The helix-destabilizing ability of 19 D-amino acid residues in an amphipathic α -helical model peptide was evaluated by reversed-phase HPLC and CD spectroscopy. L-amino acid and D-amino acid residues show a wide range of helix-destabilizing effects relative to Gly, as evidenced in melting temperatures (ΔT_m) ranging from -8.5 °C to 30.5 °C for the L-amino acids and -9.5 °C to 9.0 °C for the D-amino acids. Helix stereochemistry stability coefficients defined as the difference in T_m values for the L- and D- amino acid substitutions ($\Delta T_m' = T_{mL}$ and T_{mD}) ranging from 1 °C to 34.5 °C. HPLC retention times ($\Delta t_R(X_L-X_D)$) also had values ranging from -0.52 to 7.31 min at pH 7.0. The helix-destabilizing ability of a specific D-amino acid is highly dependent on its side-chain, with no clear relationship to the helical propensity of its corresponding L-enantiomers. In both CD and reversed-phase HPLC studies, D-amino acids with β -branched side chains destabilize α -helical structure to the greatest extent. A series of helix stability coefficients was subsequently determined, which should prove valuable

both for protein structure-activity studies and *de novo* design of novel biologically active peptides.

VIII-2 Introduction

From numerous structure/activity studies on both natural and synthetic α -helical and β -sheet cationic antimicrobial peptides (so-called by virtue of their possession of a net positive charge due to the presence of excess arginine and/or lysine residues), factors believed to be important for antimicrobial activity include the presence of both hydrophobic and basic residues, as well as an amphipathic nature that segregates these two classes of residues to opposite sides of the molecule in lipid or lipid-mimicking environments (Blondelle *et al.*, 1999; Hancock, 1997; Hancock *et al.*, 1998; Houston *et al.*, 1998; Kondejewski *et al.*, 1996; Kondejewski *et al.*, 1999; Oh *et al.*, 1999; Pathak *et al.*, 1995). This amphipathic structural feature is believed to play a key role in the antimicrobial mechanism of action, with the hydrophilic (positively charged) domain of the peptide proposed to initiate peptide interaction with the negatively charged bacterial surface and the negatively charged headgroups of bilayer phospholipids. The hydrophobic domain of the amphipathic peptide would then permit the peptide to enter the membrane interior (Bechinger, 1997; Blondelle *et al.*, 1999; Epanand *et al.*, 1999; Wu *et al.*, 1999); bilayer disruption or concomitant channel formation in, for example, the bacterial cytoplasmic membrane may subsequently lead to the leakage of cell contents and cell death (Bechinger, 1997; Epanand *et al.*, 1999; Sitaram *et al.*, 1999; Wu *et al.*, 1999). Indeed, antimicrobial α -helical peptides are excellent examples of biologically

active peptides for which disruption of α -helical structure in benign medium and induction of structure in hydrophobic medium may play an important role in activity.

We believe that a step-by-step synthetic peptide approach to examining the effect of small incremental changes in hydrophobicity, amphipathicity and stability of cationic antimicrobial peptides will enable rapid progress in rational design of peptide antibiotics. Such an approach has already been successfully utilized in our laboratory to dissociate antimicrobial and hemolytic activities in cyclic peptide diastereomers, designed on the basis of gramicidin S, by systematic alterations in amphipathicity (Kondejewski *et al.*, 1999). We now wished to extend this approach to the design of membrane active α -helical cationic antimicrobial peptides with improved efficacy. Our hypothesis is that by optimizing the disruption of α -helical structure in aqueous medium, yet producing an optimized inducible α -helical structure as the peptide enters the hydrophobic environment of the biological membrane, this will maximize biological activity. Specifically, we believe that the helix-destabilizing properties of D-amino acids (Aguilar *et al.*, 1993; Krause *et al.*, 2000; Rothmund *et al.*, 1995; Rothmund *et al.*, 1996) offer a systematic approach to the required controlled destabilization of α -helical structure in benign, aqueous medium, whilst retaining the ability to refold into a fully helical structure in a more hydrophobic environment.

The present study examines the feasibility of such a *de novo* design approach by substituting each of the D-amino acids into the center of the non-polar face of an amphipathic 18-residue α -helical synthetic model peptide. Through characterization by reversed-phase high performance liquid chromatography (RP-HPLC) and circular dichroism (CD) techniques, we investigated the effects of D-amino acid substitutions on

the formation and stability of α -helical structure. The well designed model peptide approach allows the determination of inherent helix stability coefficients in the absence of intrachain side-chain-side-chain interactions (hydrophobic, hydrogen bonding and electrostatic) characteristic of native sequences which complicate interpretation of results. Series of helix stability coefficients were determined for L- and D-amino acid side-chains as well as a set of helix stereochemistry stability coefficients which promise to prove valuable both for protein structure-function studies as well as for *de novo* design of novel antimicrobial peptides.

VIII-3 Experimental

VIII-3-1 Reversed-phase chromatography (RP-HPLC) of peptides

Analytical RP-HPLC was carried out on a Zorbax 300 SB-C₈ column (150x2.1mm I.D.; 5 μ m particle size, 300Å pore size) or a Zorbax Eclipse XDB-C₈ narrow bore column (150x2.1mm I.D.; 5 μ m particle size, 300Å pore size) from Agilent Technologies (Brockville, Ontario, Canada) at pH 2.0 and pH 7.0, respectively, on a Hewlett-Packard Model 1090 liquid chromatograph. For pH 2.0, mobile phase A was 0.1% *aq.* TFA and B was 0.1% TFA in acetonitrile; the linear AB gradient was 0.5% acetonitrile/min at a flow rate of 0.35ml/min. For pH 7.0 runs, buffer A was 50mM *aq.* PO₄, in water and buffer B was 50mM PO₄, in 50% *aq.* acetonitrile, both buffers containing 100mM NaClO₄; the gradient and flow rate conditions were the same as for pH 2.0. The retention time of each peptide analog was determined at 25 °C. The difference in retention times between each analog and that of the Gly analog ($\Delta t_{\text{R}}(\text{X-Gly})$) was taken as a measurement of side-chain hydrophobicity.

VIII-4 Results and Discussion

VIII-4-1 Design of model peptides

The 18-residue model peptide used in this study was based on the well-characterized sequence acetyl-EAEKAAKEAEKAAKEAEK-amide, which exhibits a highly amphipathic α -helical structure (Figure VIII-1) (Zhou *et al.*, 1994b). In the design of this model peptide, alanine was selected to form the hydrophobic face of the helix because it contains the minimum side-chain hydrophobicity needed to create an amphipathic α -helix and because of its high intrinsic helical propensity and stability contributions (Chou *et al.*, 1974; Monera *et al.*, 1995; Zhou *et al.*, 1994b). Lysine and glutamic acid were also selected to allow a potential for α -helix stabilizing intrachain electrostatic attractions at the $i \rightarrow i+3$ and $i \rightarrow i+4$ positions (Scholtz *et al.*, 1993). In order to reduce the unfavorable dipole interactions of α -helical structure, all substituted model peptides were synthesized with N-acetylated and C-amidated termini (Shoemaker *et al.*, 1987). According to the study of Zhou *et al.* (Zhou *et al.*, 1994b), this amphipathic α -helical model exhibits the following important features: (a) the helix is single-stranded and non-interacting, enabling the determination of the effect of different amino acid substitutions in the non-polar face; (b) there is a uniform environment created by alanine residues surrounding the substitution site in the center of the non-polar face (position 9 of this 18-mer model peptide); (c) the small size of the alanine side-chain methyl group ensures minimal interactions with the “guest” amino acid residues; (d) the small size of the peptide maximizes the effects of single amino acid substitutions.

Based on the model peptide sequence shown in Figure VIII-1, we synthesized two series of peptide analogs, where position 9 in the center of the non-polar face was

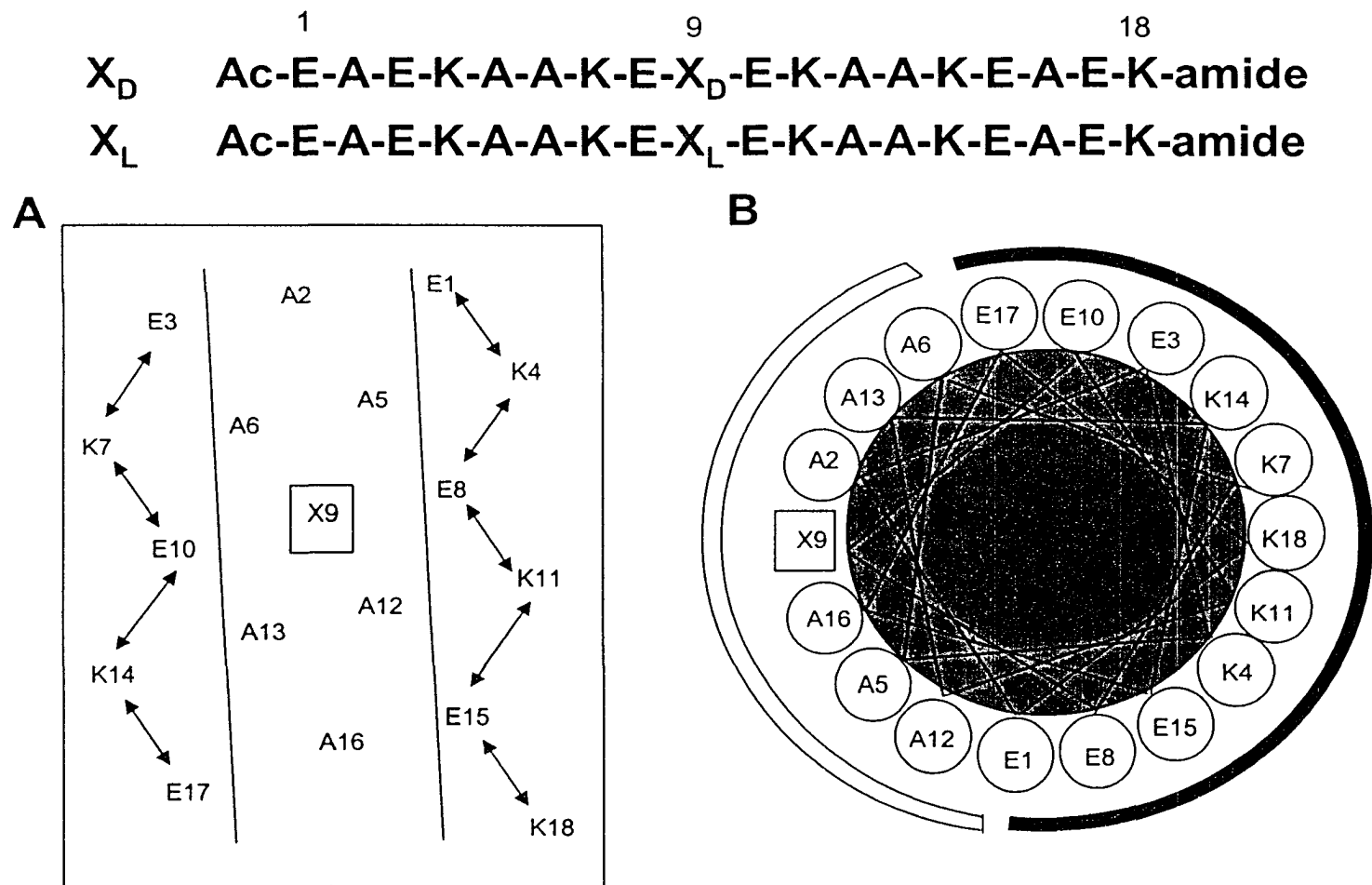


Figure VIII-1 (A) Helical net and (B) helical wheel of the “host” peptide used in this study. The hydrophobic face is indicated between two parallel lines in (A) and as an open arc in (B). The hydrophilic face is shown as a solid arc in (B). The substitution (“guest”) site is at position 9 (boxed) of the hydrophobic face. In the peptide sequences, X_D and X_L represent substituted D- and L-amino acid residues, respectively.

substituted either by each of the 19 L-amino acids (X_L series) or by the 19 D-amino acids (X_D series); since glycine does not exhibit optical activity, the Gly-substituted analog represents a useful reference standard for both series of peptides. It should be noted that the intrinsic hydrophobicity of the non-polar face of the amphipathic helix is identical for each enantiomeric peptide pair.

VIII-4-2 *Effect of D-amino acid substitutions on RP-HPLC retention behavior of peptides*

Elution times during RP-HPLC have frequently been utilized as a measure of relative hydrophobicity of peptide analogs (Guo *et al.*, 1986a; Monera *et al.*, 1995; Sereda *et al.*, 1994) and, in the present study, RP-HPLC of peptides was carried out at both pH 2.0 and pH 7.0 (representative elution profiles shown in Figure VIII-2). It was felt that a more complete evaluation of the feasibility of this RP-HPLC approach to gauging the effects of D-amino acid substitution on amphipathic α -helical structure required these two very different sets of chromatography conditions; thus, while the pH 7.0 runs reflect similar pH conditions to those used for CD measurements in the present study (see Experimental Procedures), the pH 2.0 mobile phase conditions are most commonly employed for RP-HPLC of peptides (Mant *et al.*, 1991).

It is well known that the chromatography conditions characteristic of RP-HPLC (hydrophobic stationary phase, non-polar eluting solvent) induce helical structure in potentially helical polypeptides (Blondelle *et al.*, 1995; Purcell *et al.*, 1995c; Steer *et al.*, 1998; Zhou *et al.*, 1990) in a manner similar to that of the helix-inducing solvent trifluoroethanol (TFE). Polypeptides which are thus induced into an amphipathic α -helix, such as our model peptide (Figure VIII-1), on interaction with a hydrophobic RP-HPLC stationary phase will exhibit preferred binding of their non-polar face with the stationary

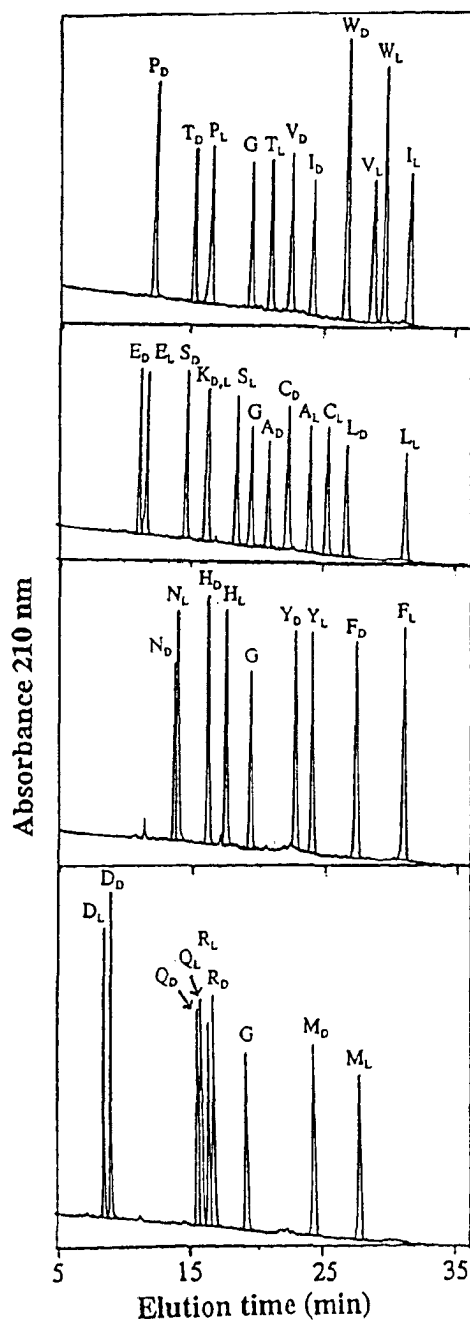


Figure VIII-2 Reversed-phase HPLC of D- and L-amino acid substituted peptides at pH 7.0. The Gly peptide was used as an internal standard for all runs. Peptide analogs are denoted by the L- and D-amino acid substitution at position 9 (see Figure VIII-1), for example, A_D and A_L represent the D-Ala and L-Ala substituted peptides, respectively. Column, instrumentation and run conditions are described in the Experimental section and the retention data are shown in Table VIII-1.

phase. Indeed, Zhou *et al* (Zhou *et al.*, 1990) clearly demonstrated that, due to this preferred binding domain, amphipathic α -helical peptides are considerably more retentive than non-amphipathic peptides of the same amino acid composition. From Figure VIII-1, it can be seen that the substitution site at position 9, in the center of the non-polar face of the helix, ensures intimate interaction of the substituting side-chain with the reversed-phase stationary phase; concomitantly, this is designed to maximize any observed effects on RP-HPLC retention behavior when substituting different residues at this site.

Table VIII-1 and Table VIII-2 summarize the RP-HPLC retention behavior of the L-substituted and D-substituted analogs at pH 7.0 and pH 2.0, respectively. The order of the analogs in both tables is based on decreasing retention time of the L-analogs (with the exception of the Gly and Pro analogs). Clearly, there is a wide range of retention times at both pH 7.0 (Table VIII-1; Figure VIII-2) and pH 2.0 (Table VIII-2), as would be expected given the differences in side-chain hydrophobicity of the substituted amino acids, ranging as they do from the highly non-polar (*e.g.*, Ile, Leu, Phe, Trp) to the polar (*e.g.*, Ser, Asn, Gln) (Guo *et al.*, 1986a; Monera *et al.*, 1995; Sereda *et al.*, 1994). Also clear from both Tables VIII-1 and VIII-2 is that the D-substituted analogs were almost all eluted faster than their corresponding diastereomers at both pH 7.0 and pH 2.0, respectively. The only exceptions were the Arg, Asp and Lys analogs at pH 7.0 (Table VIII-1; Figure VIII-2) and the His analog at pH 2.0 (Table VIII-2). It should also be noted from Tables VIII-1 and VIII-2 that the retention times of all L- and D-substituted analogs were significantly longer at pH 2.0 (Table VIII-2) compared to pH 7.0 (Table VIII-1). This is a result of protonation at pH 2.0 of the carboxyl groups of the Glu side-

Table VIII-1 RP-HPLC retention data of model peptide analogs at pH 7.0

Peptide	t_R^b (min)		$\Delta t_R(X\text{-Gly})^c$ (min)		$\Delta t_R(X_L\text{-}X_D)^d$ (min)	
	X^a	X_L	X_D	X_L	X_D	
Ile		31.35	24.04	12.05	4.74	7.31 ^c
Leu		31.26	26.82	11.96	7.52	4.44
Phe		31.00	27.35	11.70	8.05	3.65
Trp		29.50	26.66	10.20	7.36	2.84
Val		28.64	22.32	9.34	3.02	6.32
Met		27.85	24.34	8.55	5.04	3.51
Cys		25.27	22.17	5.97	2.87	3.10
Tyr		23.96	22.66	4.66	3.36	1.30
Ala		23.93	20.68	4.63	1.38	3.25
Thr		20.78	15.12	1.48	-4.18	5.66
Ser		18.33	14.60	-0.97	-4.70	3.73
His		17.40	16.03	-1.90	-3.27	1.37
Arg		16.45	16.84	-2.46	-2.85	-0.39
Lys		16.14	16.14	-3.16	-3.16	0
Gln		15.89	15.63	-3.41	-3.67	0.26
Asn		13.84	13.61	-5.46	-5.69	0.23
Glu		11.68	11.12	-7.62	-8.18	0.56
Asp		8.65	9.17	-10.65	-10.13	-0.52
Pro		16.37	12.18	-2.93	-7.12	4.19
Gly		19.30	19.30	0	0	0

a. Amino acid substitution at position X of sequence shown in Figure VIII-1.

b. RP-HPLC retention time of L- and D-amino acid substituted peptides at pH 7.0.

c. Difference in RP-HPLC retention time between L- or D-substituted analogs and the glycine substituted peptide.

d. Difference in RP-HPLC retention time between L- and D-substituted peptide analogs.

e. The boxed values are those of β -branched side-chains.

Table VIII-2 RP-HPLC retention data of model peptide analogs at pH 2.0

Peptide	t_R^b (min)		$\Delta t_R(X-Gly)^c$ (min)		$\Delta t_R(X_L-X_D)^d$ (min)	
	X ^a	X _L	X _D	X _L	X _D	
Ile		51.83	42.07	14.13	4.37	9.76 ^e
Leu		51.75	45.83	14.05	8.13	5.92
Phe		50.51	45.96	12.81	8.26	4.55
Trp		48.82	43.92	11.12	6.22	4.90
Val		48.62	40.10	10.92	2.40	8.52
Met		47.80	43.03	10.10	5.33	4.77
Cys		44.60	40.95	6.90	3.25	3.65
Ala		43.87	38.99	6.17	1.29	4.88
Tyr		43.16	40.04	5.46	2.34	3.12
Thr		39.07	31.15	1.37	-6.55	7.92
Glu		37.63	35.03	-0.07	-2.66	2.60
Ser		36.41	31.56	-1.29	-6.14	4.85
Gln		35.60	33.00	-2.10	-4.70	2.60
Asp		33.99	33.26	-3.71	-4.44	0.73
Arg		32.27	30.91	-5.43	-6.79	1.36
Asn		31.84	30.98	-5.86	-6.72	0.88
Lys		30.49	29.21	-7.21	-8.49	1.28
His		30.14	30.47	-7.56	-7.23	-0.33
Pro		30.89	26.82	-6.81	-10.88	4.07
Gly		37.70	37.70	0	0	0

f. Amino acid substitution at position X of sequence shown in Figure VIII-1.

g. RP-HPLC retention time of L- and D-amino acid substituted peptides at pH 2.0.

h. Difference in RP-HPLC retention time between L- or D-substituted analogs and the glycine substituted peptide.

i. Difference in RP-HPLC retention time between L- and D-substituted peptide analogs.

j. The boxed values are those of β -branched side-chains.

chains surrounding the non-polar face (made up of Ala residues and the substituted residue in the center of this face; Figure VIII-1), effectively increasing the size of this non-polar face and, hence, the overall hydrophobicity of the peptide.

The overall decrease in retention times of the D-analogs compared to the L-analogs summarized in Tables VIII-1 and VIII-2 can be generally rationalized as being due to disruption of the hydrophobic face of the amphipathic α -helix due to the introduction of a D-amino acid. The overall effect would thus be a decrease in the apparent hydrophobicity of the non-polar face of the amphipathic α -helix when substituted with a D-amino acid relative to its L-diastereomer and, hence, a decrease in retention time of the former compared to the latter. From Table VIII-1, when the retention time of the glycine analog (19.30 min) has been subtracted from the retention times of the other 19 L- and D-analogs ($\Delta t_R(X\text{-Gly})$), the resulting numbers represent a series of coefficients expressing side-chain hydrophobicity (or apparent side-chain hydrophobicity in the case of the D-amino acids) (values >0) or side-chain hydrophilicity (or apparent side-chain hydrophilicity in the case of the D-amino acids) (values <0) relative to glycine at pH 7.0. Similar coefficients may be generated for pH 2.0 from the retention data shown in Table VIII-2. Subtraction of these apparent side-chain hydrophilicity/hydrophobicity values ($\Delta t_R(X_D\text{-Gly})$) from the fully expressed side-chain hydrophilicity/hydrophobicity values ($\Delta t_R(X_L\text{-Gly})$) now produces an expression which represents the effect of a D- to L-amino acid substitution in the center of the non-polar face of the amphipathic α -helix ($\Delta t_R(X_L - X_D)$) in Tables VIII-1 and VIII-2). At both pH 7.0 (Table VIII-1) and pH 2.0 (Table VIII-2), the magnitude of the effect of a L- to D-amino acid substitution generally increased with increasing hydrophobicity of the side-

chain (as expressed by $\Delta t_R(X_L\text{-Gly})$ values). A major exception to this trend is Pro which has been shown to express similar hydrophobicity to Ala in model random coil peptides (Guo *et al.*, 1986a); however, in the present study, both the L- and D-Pro peptides were being eluted at similar times to peptides substituted with hydrophilic residues at pH 7.0 (Table VIII-1; 16.37 min and 12.18 min for L- and D-analogs, respectively) and pH 2.0 (Table VIII-2; 30.89 min and 26.82 min for L- and D-analogs, respectively). Proline is known to be highly helix-disruptive (the molar ellipticities ($\text{deg}\cdot\text{cm}^2\cdot\text{dmol}^{-1}$) of the L- and D-Pro peptides are -700 and 700 , respectively, in benign buffer and only $-14,900$ and $-8,150$, respectively, in the presence of 50% TFE; Table VIII-4); thus, it is not surprising that the RP-HPLC retention behavior of the two Pro analogs is anomalous. It is worth noting that the D-Pro peptide was eluted faster than the L-Pro peptide, possibly reflecting the even greater helix-disrupting capability of D-Pro compared to L-Pro. Due to these particular characteristics of the Pro analogs relative to the other peptides, these analogs are not included in any further discussion.

An interesting observation from both Tables VIII-1 and VIII-2 is that the three amino acids with β -branched side-chains (Ile, Val, Thr) show the greatest reduction in apparent side-chain hydrophobicity due to D-amino acid substitutions. Thus, at pH 7.0 (Table VIII-1) $\Delta t_R(X_L\text{-}X_D)$ values (boxed in Table) are 7.31 min, 6.32 min and 5.66 min for Ile, Val and Thr, respectively; at pH 2.0 (Table VIII-2), these values are 9.76 min, 8.52 min and 7.92 min for Ile, Val and Thr, respectively. A possible reason for this apparently disproportionate effect on apparent side-chain hydrophobicity of the L- to D-substitutions of β -branched side-chains is that the steric clash of β -branched side-chains

and the preceding turn of the α -helix increases destabilization of the helix (Krause *et al.*, 2000).

From Figure VIII-3, there is a good correlation ($R=0.93$) of the $\Delta t_R(X_L-X_D)$ values between the pH 2.0 and pH 7.0 RP-HPLC systems. This suggests that, though the magnitude of the effect of the L- to D-substitution may be different between the two mobile phases (the $\Delta t_R(X_L-X_D)$ values are higher for each peptide pair in the pH 2.0 mobile phase (Table VIII-2)), the directional effect on all L- to D-substitutions is similar when changing the pH of the RP-HPLC conditions. Thus, it is the diastereomeric variation between specific pairs of L- and D-amino acids at the mutation site of the amphipathic α -helical peptide that is the determining factor in determining the contribution of the mutation to the RP-HPLC retention behavior of the peptide.

VIII-4-3 Relative hydrophobicity of L- and D-amino acid side-chains

In order to visualize more easily the variation in hydrophobicity of the amino acid side-chains between the L- and D-isomers when substituted into the center of the non-polar face of the model amphipathic α -helical peptide, the $\Delta t_R(X-Gly)$ values reported in Table VIII-1 (pH 7.0) and Table VIII-2 (pH 2.0) were normalized relative to the value for maximum side-chain hydrophobicity (denoted 1.00), this value being $\Delta t_R(Ile-Gly) = 12.05$ min at pH 7.0 (Table VIII-1) and $\Delta t_R(Ile-Gly) = 14.3$ min at pH 2.0 (Table VIII-2). Table VIII-3 compares the relative hydrophobicity of the side-chains between the L- and D-isomers at both pH 7.0 and pH 2.0. The order of amino acid side-chains in Table VIII-3 is based on decreasing relative hydrophobicity of the L-isomers at pH 7.0, *i.e.*, from the most hydrophobic (L-Ile; relative hydrophobicity value of 1.00) to the most hydrophilic (L-Asp; relative hydrophobicity value of -0.88). The positioning of Gly (relative

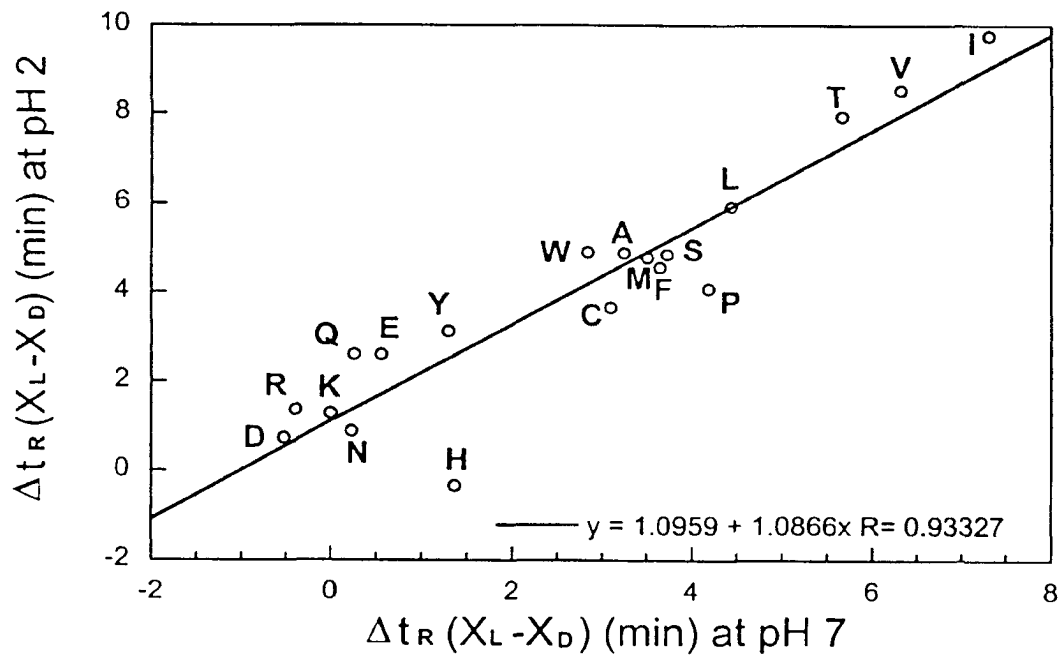


Figure VIII-3 Plot of the difference in reversed-phase HPLC retention times between D- and L-diastereomeric peptide pairs ($\Delta t_R(X_L - X_D)$) at pH 7.0 versus pH 2.0. Least squares fit analysis showed a correlation of $R=0.93$. Standard one-letter designations are used for the peptides with the corresponding substituted amino acid at position 9 of the peptide sequence. For RP-HPLC conditions, see Experimental section.

Table VIII-3 Relative hydrophobicity of amino acid side-chains
Relative hydrophobicity^a

Amino acid side-chains	pH 7.0		pH 2.0	
	X _L	X _D	X _L	X _D
Ile	1.00	0.39	1.00	0.31
Leu	0.99	0.62	0.99	0.58
Phe	0.97	0.67	0.91	0.58
Trp	0.85	0.61	0.79	
Val	0.78	0.25	0.77	0.17
Met	0.71	0.42	0.71	0.38
Cys	0.50	0.24	0.49	0.23
Tyr	0.39	0.28	0.39	0.17
Ala	0.38	0.11	0.44	0.09
Gly	0.00		0.00	
Thr	0.12	-0.35	0.10	-0.46
Ser	-0.08	-0.39	-0.09	-0.43
His	-0.16	-0.27	-0.54	-0.51
Arg	-0.20	-0.24	-0.38	-0.48
Lys	-0.26	-0.26	-0.51	-0.60
Gln	-0.28	-0.30	-0.15	-0.33
Asn	-0.45	-0.47	-0.41	-0.48
Glu	-0.63	-0.68	-0.01	-0.19
Asp	-0.88	-0.84	-0.26	-0.31

a. Relative hydrophobicity is defined as the ratio of $\Delta t_R(X\text{-Gly})$ values for the amino acid side-chains and the maximum hydrophobicity value obtained from RP-HPLC retention time ($\Delta t_R(X\text{-Gly})$ for L-Ile =12.05 min at pH 7.0, Table VIII-1; $\Delta t_R(X\text{-Gly})$ for Ile =14.13 min at pH 2.0, Table VIII-2), e.g., for L-Leu at pH 7.0 (Table VIII-1), relative hydrophobicity = $\Delta t_R(\text{Leu-Gly})/12.05 = 11.96/12.05 = 0.99$.

hydrophobicity value of 0.00) in the middle of the table reflects the general classification of aliphatic (*e.g.*, Ile, Met, Ala) and aromatic (Phe, Trp, Tyr) side-chains as non-polar/hydrophobic (*i.e.*, contributing substantially to increasing peptide retention time in RP-HPLC) and the remainder of the side-chains as polar/hydrophilic (*i.e.*, contributing little to increasing peptide retention time, *e.g.*, Thr, or contributing to decreasing retention time, *e.g.*, Ser, Arg, Gln, etc.). The data from Table VIII-3 are also presented in histogram format in Figure VIII-4.

Although not shown here, plots of relative hydrophobicity of the D-analogs *versus* the L-analogs at pH 7.0 and pH 2.0 showed good, and similar, correlations of 0.96 and 0.95, respectively. This result indicates that, although the magnitude of the relative hydrophobicity/hydrophilicity values for the side-chains are different for the L- and D-isomers, the directional effect on all side-chains is similar at either pH value. However, a closer scrutiny of the data presented in Table VIII-3 and Figure VIII-4 also indicates interesting trends for specific groups of side-chains which, although also apparent from Tables VIII-1 and VIII-2, now stand out more clearly. Thus, at both pH values (i), the relative hydrophobicity values of the non-polar D-isomer side-chains are generally considerably lower than those of their L-isomer counterparts; (ii) the relative hydrophobicity values of the polar D-isomer side-chains are generally quite similar to those of their L-isomer counterparts; and (iii) the β -branched side-chains (Ile, Val, Thr) show the greatest difference in relative hydrophobicity between their L- and D-isomers. Such results can be rationalized by considering the effect various L- to D-substitutions may have on the overall hydrophobicity of the non-polar preferred binding domain of the amphipathic α -helix. Thus, since the non-polar/hydrophobic side-chains contribute most

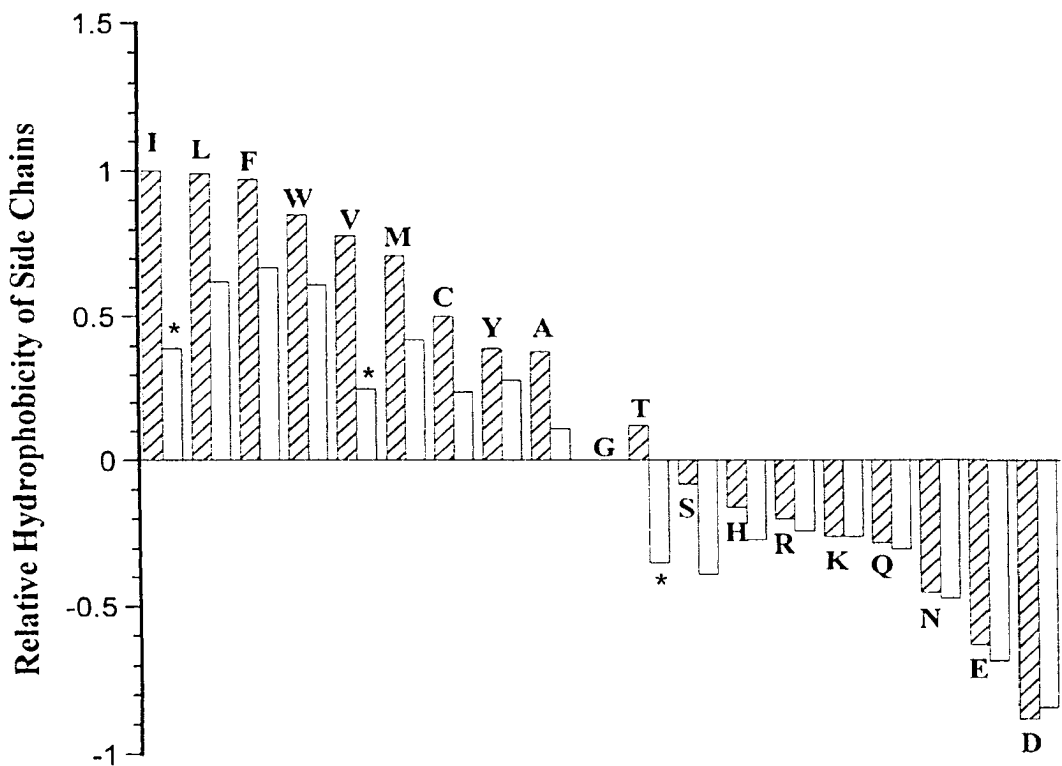


Figure VIII-4 Histogram illustrating relative hydrophobicity of L- (hatched) and D-diastereomeric (nonhatched) peptides at pH 7.0. Standard one-letter designations are used for the peptides with the corresponding substituted amino acid at position 9 of the peptide sequence. The stars denote β -branched D-amino acid side-chains.

to RP-HPLC peptide retention times, it is not surprising that an L- to D-side-chain substitution would disrupt the preferred binding domain substantially enough to reduce its hydrophobicity and, hence the retention time of the peptide. It should be noted that this disruption of the non-polar face of the amphipathic α -helix does not necessarily imply significant disruption of this α -helical structure since, as will be discussed later (Table VIII-4), both the L- and D-series peptides generally exhibit high helicity in the presence of the helix-inducing solvent trifluoroethanol (TFE; (Cooper *et al.*, 1990; Kentsis *et al.*, 1998; Sonnichsen *et al.*, 1992)), a good mimic for the non-polar conditions characteristic of RP-HPLC (Sereda *et al.*, 1994). In contrast to the hydrophobic side-chains, even L-isomer polar/hydrophilic side-chains can be viewed as disrupting the preferred binding domain of the helix simply by eliminating the monolithic character of the non-polar face, through the presence of such side-chains at the center of this face. Hence, a hydrophilic L- to D-isomer substitution at this position would not have as profound an effect on the apparent hydrophobicity of the preferred binding domain as was observed for the hydrophobic side-chains. Concerning the relatively disproportionate effect of the L- to D-isomer substitution of β -branched side-chains (Ile, Val, Thr), Krause *et al.* (Krause *et al.*, 2000) noted a similar effect during RP-HPLC of their amphipathic α -helical peptide models containing double D-amino substitutions. These authors suggested that a potential steric clash between the side-chain and the preceding turn of the helix might cause increased destabilization of the α -helix and, presumably, structural distortion of the non-polar face of the amphipathic α -helix. It is thus possible in the present study that some structural distortion of the preferred binding domain of the Ile, Val and Thr D-substituted analogs is enhancing the overall disruption of the

hydrophobicity of the non-polar face of the helix. Such an observation is supported by comparing the particularly disproportionate effect of the L- to D-Thr substitution (Figure VIII-4) (relative to the majority of the polar/hydrophilic residues) and the effect of such a substitution on the reduction in ellipticity ($[\theta]_{222}$) in 50% TFE (L-Thr = -27,200 degrees and D-Thr = -16,150 degrees, *i.e.*, a decrease in ellipticity of 11,500 degrees; Table VIII-4).

From Figure VIII-5, excellent correlations were obtained when comparing the relative hydrophobicity at pH 2.0 and pH 7.0 of the D-amino acids ($R = 0.993$) and L-amino acids ($R = 0.997$) when potentially ionizable groups (Asp, Glu, His, Lys, Arg) were excluded from the correlation plot, indicating that the relative hydrophobicities of both the non-ionizable (at physiological pH values) D-isomers (panel A) and L-isomers (panel B) are essentially unaffected by a change in pH from 2.0 to 7.0. From Figure VIII-5, the acidic amino acids, Glu and Asp, deviate from the correlation plot due to their being less hydrophilic at pH 2.0 (where the side-chain carboxyl group is protonated, *i.e.*, neutral) than at pH 7.0 (where the carboxyl group is deprotonated, *i.e.*, negatively charged). In contrast, the basic amino acid side-chains (His, Lys, Arg) are less hydrophilic at pH 7.0 compared to pH 2.0. Lys and Arg are positively charged at both pH 2.0 and pH 7.0; however, their apparent decrease in hydrophilicity at the higher pH value can be rationalized by considering the ionic strength of the anionic (negatively charged) counterions at pH 2.0 *versus* pH 7.0. Thus, at pH 2.0, a concentration of 0.1% TFA in the mobile phase is equivalent to a concentration of ~10 mM trifluoroacetate ions available to interact with positively charged groups in the peptides. In contrast, at pH 7.0, a buffer concentration of 100 mM NaClO₄ means that 100 mM perchlorate ions are available to

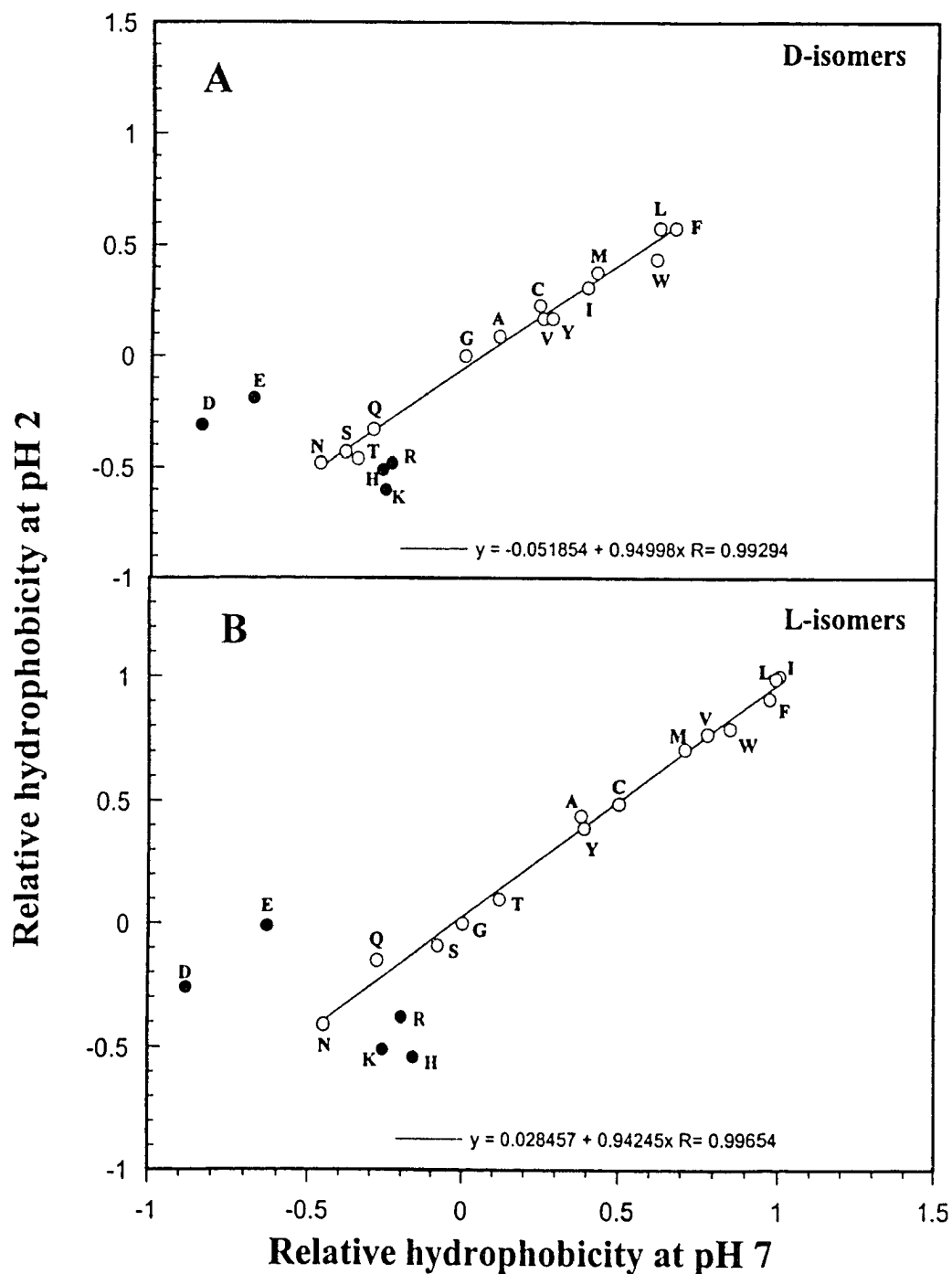


Figure VIII-5 Plot of relative hydrophobicity of D-peptides or L-peptides at pH 2.0 versus pH 7.0. Least squares fit analysis showed correlations of $R=0.993$ for D-isomers and $R=0.997$ for L-isomers. In both (A) and (B), open symbols represent the peptides used for correlations; solid symbols represent the potentially charged amino acid substituted peptides which were excluded from the comparison. Standard one-letter designations are used for the peptides with the corresponding substituted amino acid at position 9 of the peptide sequence.

Table VIII-4 CD data of model peptide analogs

Peptide	$[\theta]_{222}^a$ in benign buffer		$\Delta[\theta]_{222}^b$ $X_L - X_D$	$[\theta]_{222}^c$ in 50% TFE		$\Delta[\theta]_{222}^d$ (50% TFE-benign)	
	X_L	X_D		X_L	X_D	X_L	X_D
Arg	-18100	-3450	-14650	-27500	-27250	-9400	-23800
Ala	-18000	-2450	-15550	-27900	-24150	-9900	-21700
Leu	-15800	-1500	-14300	-26850	-26900	-11050	-25400
Lys	-15800	-1950	-13850	-27800	-23100	-12000	-21150
Met	-13900	-2450	-11450	-27600	-25850	-13700	-23400
Gln	-13450	-2650	-10800	-27650	-24450	-14200	-21800
Phe	-13100	-2300	-10800	-31050	-27400	-17950	-25100
Ile	-12500	-600	-11900	-26900	-22150	-14400	-21550
Ser	-11500	-1650	-9850	-29100	-23050	-17600	-21400
Trp	-11050	-3200	-7850	-25650	-22650	-14600	-19450
Tyr	-10800	-2750	-8050	-26550	-20300	-15750	-17550
His	-10600	-3450	-7150	-27300	-26300	-16700	-22850
Cys	-10500	-1750	-8750	-27600	-25950	-17100	-24200
Val	-10250	-450	-9800	-25650	-20750	-15400	-20300
Glu	-9250	-1050	-8200	-26550	-19800	-17300	-18750
Asn	-9150	-3350	-5800	-27450	-24050	-18300	-20700
Thr	-8900	-1600	-7300	-27200	-16150	-18300	-14550
Asp	-6650	-2550	-4100	-24200	-16900	-17550	-14350
Pro	-700	700	-1400	-14900	-8150	-14200	-8850
Gly	-5350	-5350	0	-25250	-25250	-19900	-19900

a. The mean residue molar ellipticities ($\text{deg}\cdot\text{cm}^2\cdot\text{dmol}^{-1}$) at wavelength 222nm were measured at 5 °C in benign buffer (100mM KCl, 50mM PO_4 pH 7.0).

b. Difference in molar ellipticity values of D- and L-peptide analogs in benign buffer.

c. The mean residue molar ellipticities ($\text{deg}\cdot\text{cm}^2\cdot\text{dmol}^{-1}$) at wavelength 222nm were measured at 5 °C in the above buffer diluted 1:1 (v/v) with TFE.

d. Difference in molar ellipticity values of D- and L-peptide analogs between the two buffer systems, e.g., $\Delta[\theta]_{222}$ for L-Leu = $[\theta]_{222}$ in 50% TFE - $[\theta]_{222}$ in benign = $-26850 - (-15800) = -11050$.

interact with positively charged groups. It is well known that there is a counterion concentration effect on peptide retention behavior during RP-HPLC (Guo *et al.*, 1987; Mant *et al.*, 1991), *i.e.*, the higher the concentration of anionic counterion, the longer the elution time of peptides containing positively charged side-chains and, hence, the lower the apparent hydrophilicity (or greater the apparent hydrophobicity) of side-chains such as Lys and Arg. His is positively charged at pH 2.0 and it is possible that it remains positively charged at pH 7.0, implying that an explanation for its apparent decrease in hydrophilicity at pH 7.0 compared to pH 2.0 is the same as that described above for Lys and Arg. However, the relatively low pKa value for the imidazole side-chain of His (~6.0-6.5 in peptides), coupled with the clear demonstration by Sereda *et al.* (Sereda *et al.*, 1993) that the hydrophobic conditions characteristic of RP-HPLC may lower the pKa of His even further, suggests that the decrease in hydrophilicity seen at pH 7.0 is, in fact, a result of deprotonation (*i.e.*, loss of positive charge) of the His side-chain.

VIII-4-4 CD Spectroscopy Studies

In order to determine the effect of L- to D-amino acid substitutions on α -helical peptide stability, the CD spectrum of the peptide analogues was measured under physiologically relevant, benign buffer conditions (100 mM KCl, 50 mM PO₄, pH 7.0) and also in 50% TFE for all analogs (Table VIII-4).

From Table VIII-4, the peptide analogs are ordered by increasing molar ellipticity values for the L-substituted analogs, with the exception of the Gly-substituted peptide which was considered as a control for the comparison of the effect of L- and D-amino acid substitutions. The L-analogs (the Pro-substituted peptide excluded) show about a three-fold range in molar ellipticities under benign conditions, from -6,650 to -18,100 deg cm²

dmol⁻¹ for Asp and Arg, respectively, indicating that each single L-amino acid substitution has a profound effect on the α -helical structure of these model peptides under benign conditions (Zhou *et al.*, 1994b). In contrast, in the presence of the α -helix inducing solvent TFE, the maximum negative molar ellipticities of the L-analogs were essentially the same (average $[\theta]_{222} = -27,150$, excluding the Pro-analog but including the Gly-analog), suggesting a fully α -helical structure for each peptide analog. In contrast, all of the D-substituted peptides exhibited molar ellipticities characteristic of negligible secondary structure under benign conditions, underlining the helix-disrupting properties of single D-amino acids. However, in the presence of 50% TFE, these D-analogs (except for Pro) all exhibited considerable increases in molar ellipticity, generally of the same or similar magnitude to their L-counterparts. Even in instances where a fully α -helical structure has not been induced (*e.g.*, D-Thr, D-Asp; $[\theta]_{222} = -16,150$ and $-16,900$, respectively), the increase in molar ellipticity over that obtained in benign medium ($-1,600$ and $-2,550$, respectively) is clear.

Figure VIII-6 illustrates two examples of the effect of L- and D-amino acids on α -helical content of the model peptides. These examples represent the extremes in molar ellipticity of L-analogs under benign conditions, ranging from $[\theta]_{222}$ values of $-18,100$ for Arg (Figure VIII-6A) and -700 for Pro (Figure VIII-6B) (Table VIII-1). From Figure VIII-6A, the considerable α -helical nature of the L-Arg analog compared to its D-substituted counterpart is clear, coupled with the essentially identical, fully α -helical structure of both analogs ($[\theta]_{222} = -27,500$ and $-27,250$, respectively) in the presence of 50% TFE. In contrast, both the L- and D-Pro analogs exhibited molar ellipticities ($[\theta]_{222} = -700$ and 700 , respectively) characteristic of negligible secondary structure in benign

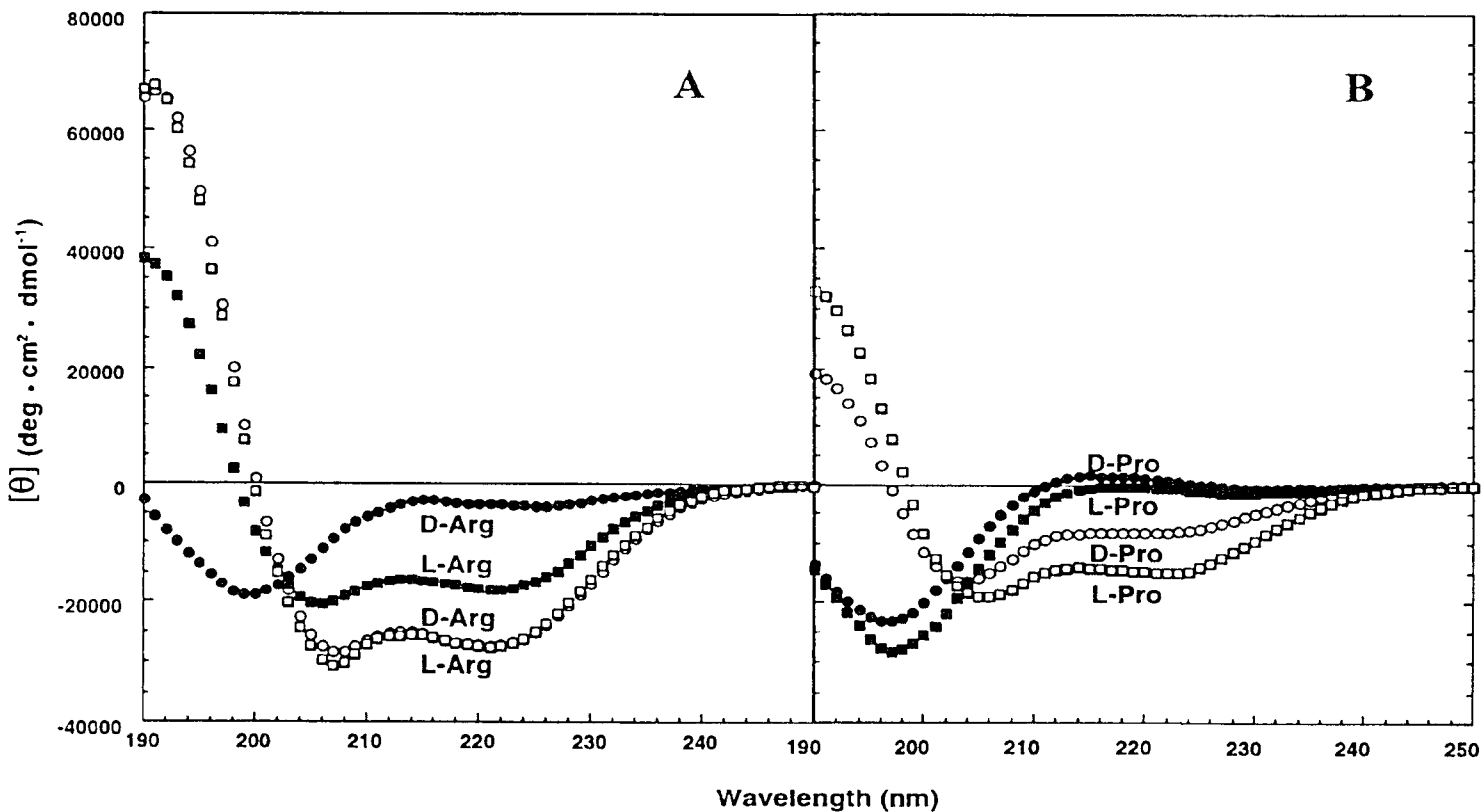


Figure VIII-6 Circular dichroism (CD) spectra of Arg (A) and Pro (B) peptides at pH 7.0 and 5 °C. The solution is buffered by 50 mM *aq.* PO₄ containing 100 mM KCl. Solid symbols represent the CD spectra of peptide analogs in benign buffer without TFE, whereas open symbols represent CD spectra obtained in the presence of 50% TFE. The symbols used are (O) for D-peptide analogs (G) for L-peptide analogs.

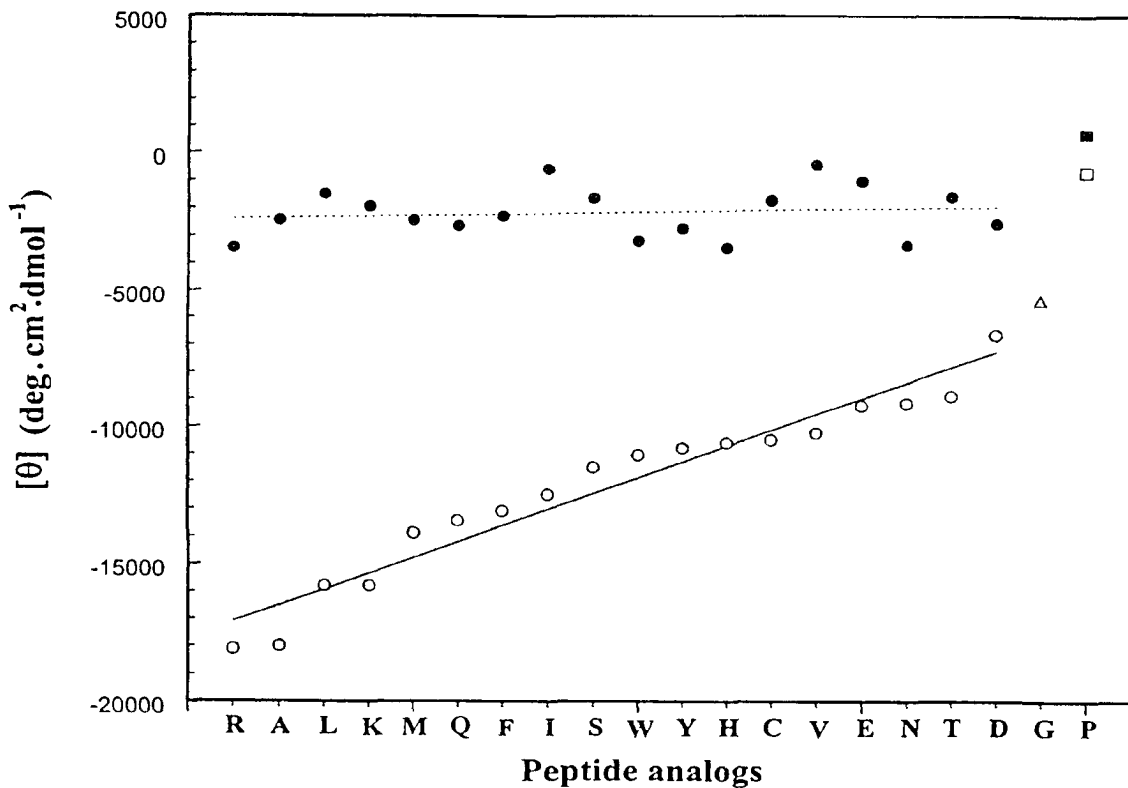


Figure VIII-7 Comparison of molar ellipticity of D- and L-peptide analogs in benign buffer (50 mM aqueous $\text{PO}_4/100$ mM KCl) at 5 °C, pH 7.0. The peptide analogs are arranged in order of decreasing α -helicity for the L-analogs (i.e. the L-Arg analog is the most helical and L-Asp is the least helical). The solid and dashed lines represent subsequent best fit lines for the L- and D-substituted peptides, respectively). The D-Pro, L-Pro and Gly peptides were excluded from this comparison. The symbols used are (O) for L-peptides, (●) for D-peptides, (□) for L-Pro, (■) for D-Pro and (Δ) for Gly. Standard one-letter designations are used for the peptides with the corresponding substituted amino acid at position 9 of the peptide sequence.

medium. Even in the presence of 50% TFE, molar ellipticity values of just $-14,900$ (L-Pro) and $-8,150$ (D-Pro) were achieved, *i.e.*, with Pro substituted in the center of the model peptide, 50% (L-Pro) or 75% (D-Pro) of the sequence could not be induced into α -helical structure in the presence of TFE. For this reason, the Pro analogs were excluded from further consideration.

From Figure VIII-7, the L-analogs have been arranged in order of decreasing molar ellipticity values in benign medium (Table VIII-4), from the highest (Arg; $[\theta]_{222} = -18,100$) to the lowest (Asp; $[\theta]_{222} = -6,650$), producing a linear plot of gradually decreasing α -helical content. In contrast, the molar ellipticity values of the D-analogs were randomly distributed about a horizontal line, *i.e.*, the values for all D-amino acid substituted peptides were in the range of $[\theta]_{222} = -1950 \pm 1500$, regardless of the value for their respective L-amino acid counterparts. The plots presented in Figure VIII-7 clearly indicate that the helix-destabilizing ability of each D-amino acid is unrelated to the α -helix propensity (as expressed by molar ellipticity in benign medium) of its corresponding L-enantiomer.

VIII-4-5 Temperature denaturation studies

In order to assess the stability of the L- and D-series peptide analogs, the ideal method would be to conduct temperature denaturation under benign conditions (Monera *et al.*, 1995). However, under such conditions, the starting α -helical contents were very different for each peptide and, in most cases, the initial structures were $<50\%$ α -helical for the L-series peptides and $<10\%$ α -helical for the D-series peptides (Table VIII-4, Figure VIII-7) compared with maximal α -helical structure induced by 50% TFE (Table VIII-4). This made it impossible to obtain temperature denaturation curves for all analogs

that were comparable to each other and, hence, alternative conditions had to be explored. Figure VIII-8 shows TFE titration curves for representative pairs of L- and D-peptide analogs: a bulky, hydrophobic side-chain (Leu); a small hydrophobic side-chain (Ala); and basic (Arg) and acidic (Asp) side-chains. The Gly analog was also included as an internal standard. An additional criterion was the range of molar ellipticities in benign medium which the L-analogs represented, from the highest (Arg, Ala, Leu; $[\theta]_{222} = -18,100, -18,000, -15,800$, respectively) to the lowest (Asp; $[\theta]_{222} = -6,650$) (Table VIII-4). Figure VIII-8 demonstrates that, for all representative peptides, 40% TFE was the minimal concentration required to obtain maximal helical structure. Therefore, temperature denaturation studies were conducted in the presence of 40% TFE.

Temperature denaturation profiles of selected L- and D-analog pairs are shown in Figure VIII-9, representing one of the most stable L-analogs (Ile; $T_m = 77.5^\circ\text{C}$) and the least stable L-analog (Asp; $T_m = 43.0^\circ\text{C}$) in 40% TFE (Table VIII-5). In addition, the peptides represent diastereomeric peptide pairs with the most difference in stability ($\Delta T_m'$, Ile_L – Ile_D = 34.5°C) and the least difference in stability ($\Delta T_m'$, Asp_L – Asp_D = 1.0°C) (Table VIII-6). The profiles clearly indicate a gradual unfolding of the α -helical structure for all four analogs and was also observed for the remainder of the L- and D-series analogs as well as the Gly peptide. As shown in Table VIII-5, there were wide variations in the melting temperatures of both series of analogs, ranging from a 39.0°C difference in T_m values between the most stable (Leu) and the least stable (Asp) L-analog, and a somewhat lesser difference of 18.5°C between the most stable (Phe) and the least stable (Asp) D-analog. The variations and well-dispersed distribution of T_m values for

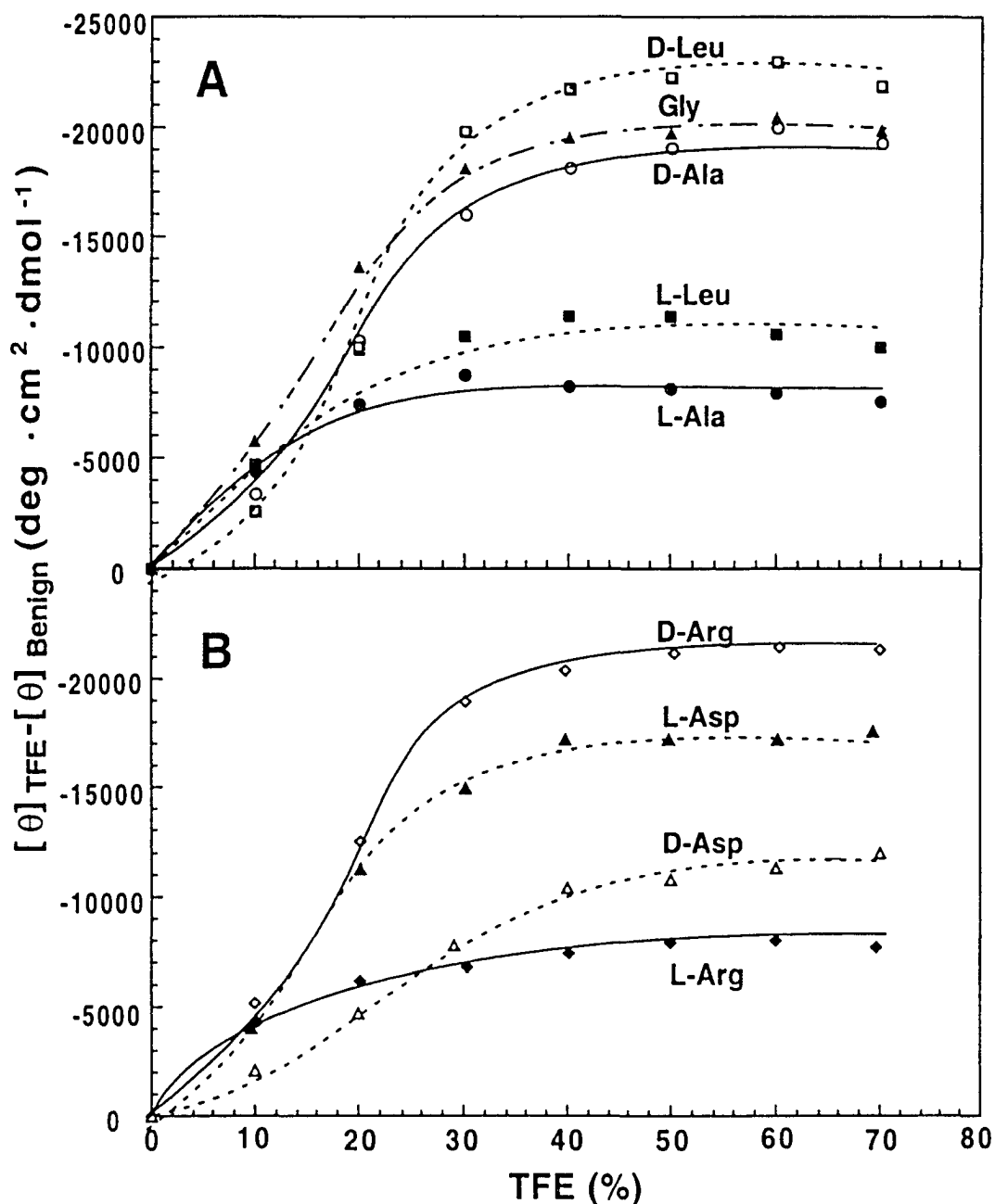


Figure VIII-8 TFE titration of representative peptide analogs at 5 °C, pH 7.0. The X-axis exhibits the percentage of TFE added to benign buffer, whereas the Y-axis shows the difference in molar ellipticity obtained for each peptide in the presence of varying levels of TFE ($[\theta]_{\text{TFE}}$) compared with its absence ($[\theta]_{\text{benign}}$). Solid symbols are used for L-peptide analogs and open symbols for D-peptide analogs. Ala peptides are denoted as (O), Leu peptides as (\square), and the Gly peptide as (\blacktriangle) in (A); Arg peptides are denoted as (\diamond) and Asp peptides as (\triangle) in (B).

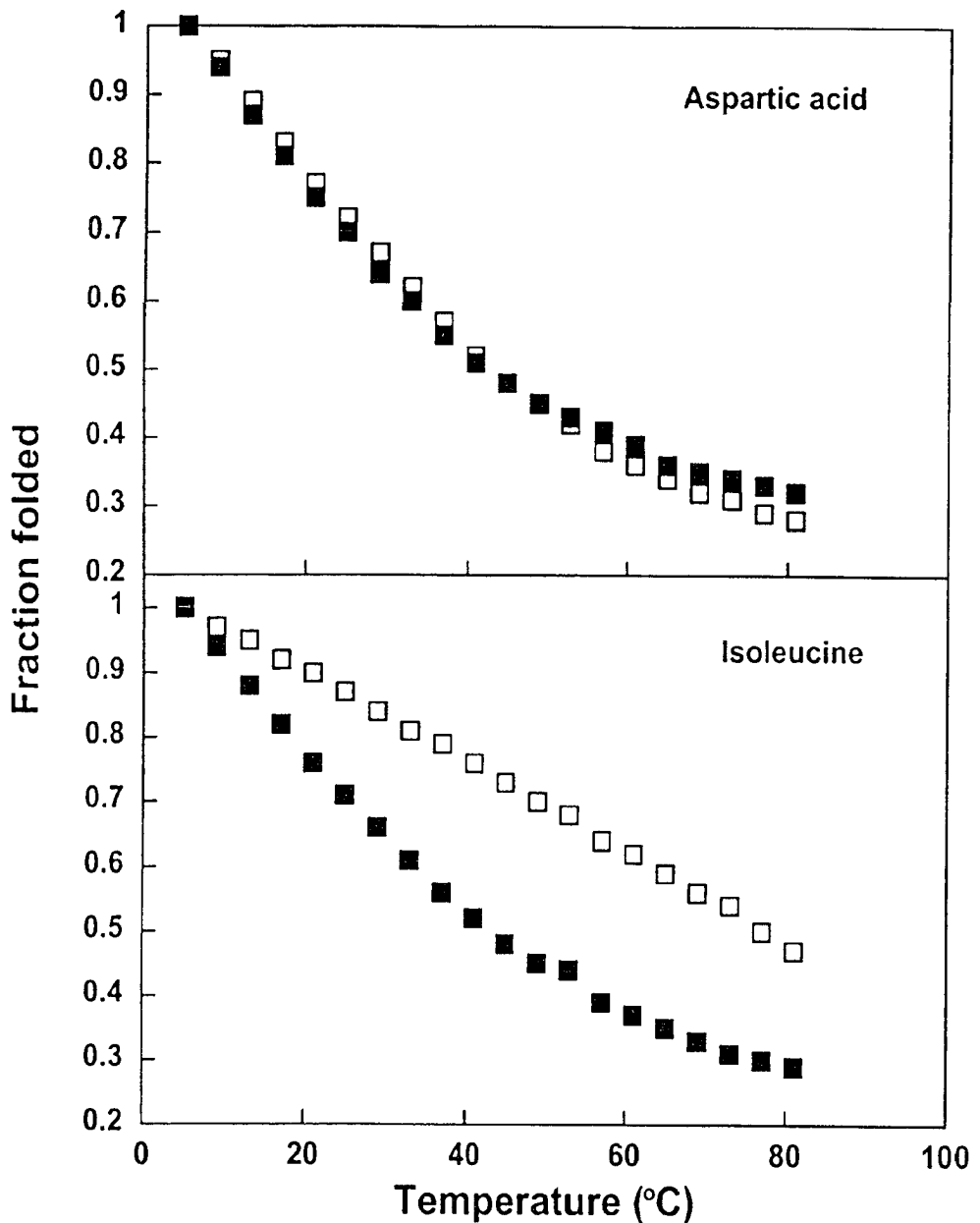


Figure VIII-9 Temperature denaturation profiles of representative peptide analogs. (A) Analogs with smallest difference in T_m value between a D- and L-peptide pair (Asp), (B) analogs with the greatest difference in T_m between a D- and L-peptide pair (Ile). Open symbols are used for the L-peptides and solid symbols for the D-peptides. The ratio of the molar ellipticity at a particular temperature relative to that at 5 °C was calculated and plotted against temperature in order to obtain the profiles (see Chapter III for details).

both sets of peptide analogs, each differing in sequence by only one amino acid residue, underlines the excellent suitability of our peptide model for helix stability studies.

From Table VIII-5, it is clear that, for the L-series analogs, α -helical stability generally decreased with decreasing hydrophobicity of the substituted side-chain (Sereda *et al.*, 1994), with bulky, non-polar side-chains (*e.g.*, Leu, Ile) contributing most to helix stability and polar (*e.g.*, Ser, Asn) and negatively charged (Glu, Asp) side-chains contributing the least. This variation in contribution to α -helical stability is particularly well illustrated in Figure VIII-10, which compares side-chain stability relative to the Gly-substituted peptide. Interestingly, L-Arg and L-Lys, both positively charged residues at pH 7.0, contributed quite significantly to α -helical stability (Table VIII-5, Figure VIII-10), in addition to being strong α -helix inducers (Table VIII-4) (Chakrabarty *et al.*, 1994; Monera *et al.*, 1995; Zhou *et al.*, 1994b). It is possible that the relative bulkiness of the Arg and Lys side-chains, coupled with their pairings with a relatively bulky phosphate ion from the pH 7.0 buffer, results in these significant contributions to helix propensity and stability. From both Table VIII-5 and Figure VIII-10, the helix-destabilizing effect of D-amino acid substitutions is clear. However, there was no clear pattern to the helix-destabilizing tendencies of the D-enantiomers (Table VIII-5, Figure VIII-10), although the hydrophobic β -branched side-chains of Ile and Val exhibited a disproportionate effect on helix destabilization, with (ΔT_m , $X_L - X_D$ values of 34.5 °C and 30.0 °C, respectively, the largest difference for all of the side-chain enantiomeric pairs (Table VIII-6). Such results for these β -branched amino acids were reflected previously for the disproportionate effect on side-chain hydrophobicity when substituting D-Ile and D-Val for their respective L-isomers (Table VIII-1, Table VIII-2, Figure VIII-4).

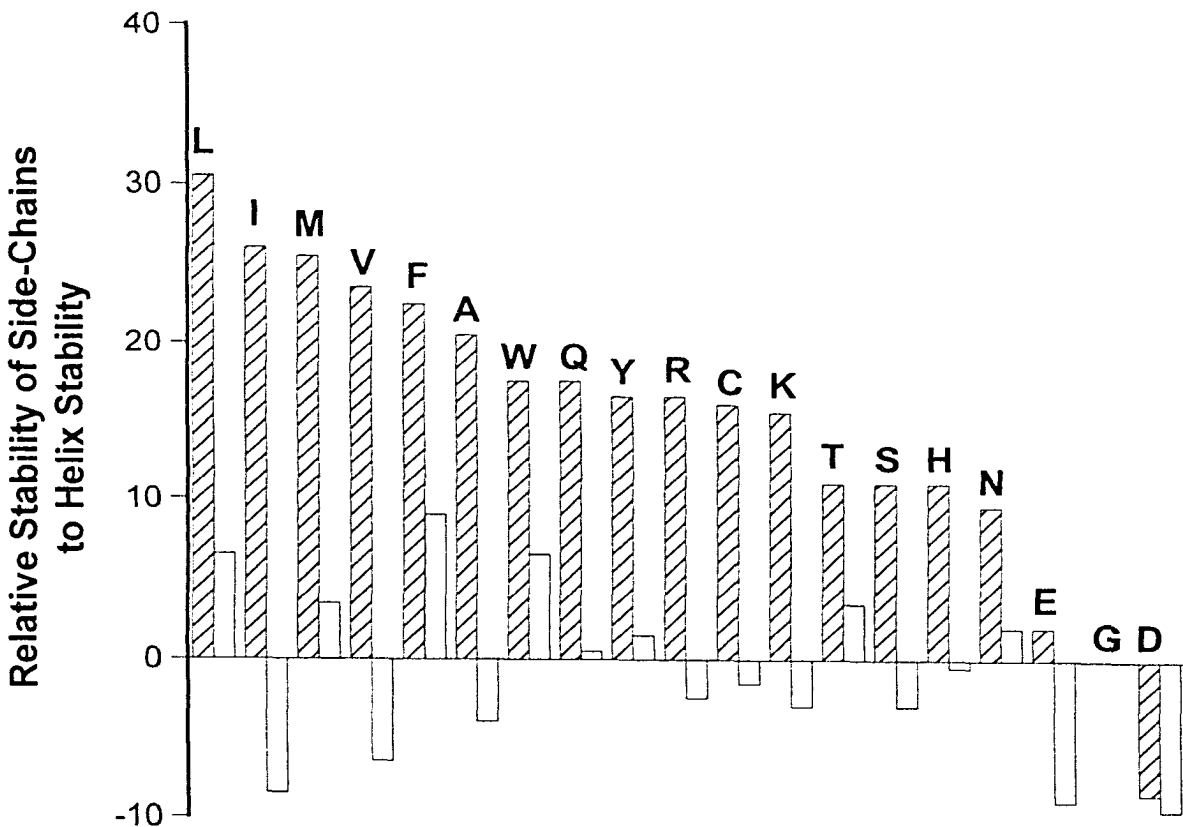


Figure VIII-10 Histograms illustrating relative contribution of L- (hatched) and D-amino acid (nonhatched) side-chains to helix stability at pH 7.0. Standard one-letter designations are used for the peptides with the corresponding substituted amino acid at position 9 of the peptide sequence. Relative contributions to stability (denoted amino acid helix stability coefficients in Table VIII-5) of the side-chains, ΔT_m , are defined as the difference T_m values between peptide analogs and the Gly-peptide.

Table VIII-5 Amino acid helix stability coefficients

Peptide	T_m (°C) ^a	ΔT_m (°C) ^b	Peptide	T_m (°C) ^a	ΔT_m (°C) ^b
	X_L	X_L		X_D	X_D
Leu	82.0	30.5	Phe	60.5	9.0
Ile	77.5	26.0	Trp	58.0	6.5
Met	77.0	25.5	Leu	58.0	6.5
Val	75.0	23.5	Met	55.0	3.5
Phe	74.0	22.5	Thr	55.0	3.5
Ala	72.0	20.5	Asn	53.5	2.0
Trp	69.0	17.5	Tyr	53.0	1.5
Gln	69.0	17.5	Gln	52.0	0.5
Tyr	68.0	16.5	Gly	51.5	0
Arg	68.0	16.5	His	51.0	-0.5
Cys	67.5	16.0	Cys	50.0	-1.5
Lys	67.0	15.5	Arg	49.0	-2.5
Thr	62.5	11.0	Lys	48.5	-3.0
Ser	62.5	11.0	Ser	48.5	-3.0
His	62.5	11.0	Ala	47.5	-4.0
Asn	61.0	9.5	Val	45.0	-6.5
Glu	53.5	2.0	Ile	43.0	-8.5
Gly	51.5	0	Glu	42.5	-9.0
Asp	43.0	-8.5	Asp	42.0	-9.5

a. T_m is defined as the temperature when 50% of α -helical structure is denatured compared with the fully folded conformation of the peptide in 40% TFE at 5°C.

b. D-amino acid helix stability coefficients are defined as the difference in T_m values between D-peptide analogs and the Gly peptide, *i.e.* ΔT_m

Table VIII-6 Helix stereochemistry stability coefficients

Peptide	T_m (°C) ^a		$\Delta T_m'$ (°C) ^b
	X_L	X_D	$X_L - X_D$
Ile	77.5	43.0	34.5
Val	75.0	45.0	30.0
Ala	72.0	47.5	24.5
Leu	82.0	58.0	24.0
Met	77.0	55.0	22.0
Arg	68.0	49.0	19.0
Lys	67.0	48.5	18.5
Cys	67.5	50.0	17.5
Gln	69.0	52.0	17.0
Tyr	68.0	53.0	15.0
Ser	62.5	48.5	14.0
Phe	74.0	60.5	13.5
His	62.5	51.0	11.5
Trp	69.0	58.0	11.0
Glu	53.5	42.5	11.0
Thr	62.5	55.0	7.50
Asn	61.0	53.5	7.50
Asp	43.0	42.0	1.00
Gly	51.5	51.5	0

a. T_m is defined as the temperature when 50% of α -helical structure is denatured compared with the fully folded conformation of the peptide in 40% TFE at 5°C.

b. Helix stereochemistry stability coefficients are defined as the difference in T_m values between L- and D- diastereomeric peptide pairs, *i.e.* $\Delta T_m'$

VIII-4-6 Amino acid helix stability and stereochemistry coefficients

Table VIII-5 reports the relative contributions of the L- and D-amino acids expressed relative to the T_m value for Gly, *i.e.*, $\Delta T_m = T_m$ for amino acid minus T_m for Gly. These ΔT_m values, or amino acid helix stability coefficients, quantify the ability of a specific L- or D-amino acid to stabilize or destabilize α -helical structure relative to Gly. Thus, a positive value represents a stabilizing influence on α -helical structure relative to Gly, whilst a negative coefficient represents a destabilizing conformation. These coefficients highlight well the overall positive contribution to helix stability effected by almost all L-amino acids (Asp being the only exception), coupled with this positive contribution generally decreasing with increasing side-chain polarity. In contrast, most of the D-amino acids destabilize α -helical structure (ranging from -0.5 for His to -9.5 for Asp), with the remainder offering relatively negligible positive contributions to stability (ranging from 0.5 for Gln to 9.0 for Phe). It is also interesting to note that the L- and D-Asp side-chains both destabilize the α -helix to a similar extent. From Table VIII-6, the peptides have been ordered by decreasing difference in T_m values between each pair of L- and D-amino acid substitutions. These values, $\Delta T_m'$ represent helix stereochemistry coefficients, *i.e.*, the destabilizing effects of L- to D-enantiomeric substitutions on helix stability.

The amino acid helix stability and helix stereochemistry coefficients listed in Tables VIII-5 and VIII-6, respectively, should prove valuable in both structure-activity studies of peptide and proteins as well as the *de novo* design of antimicrobial peptides with specifically required structural and stability features. Taking one example, through utilization of the helix stereochemistry stability coefficients, one can destabilize a pre-

existing α -helical structure to different extents by exchanging one L-amino acid with its D-enantiomer. Thus, one can disrupt the original helical structure to the greatest extent by substituting L-Ile with D-Ile (Table VIII-6; Figure VIII-9 and VIII-10); alternatively, helical stability is little affected by a L-Asp to D-Asp substitution (Table VIII-6; Figure VIII-9 and VIII-10). Such coefficients also complement the observed effect of D-amino acid substitutions on maximum helicity achievable in benign *versus* non-polar medium. For instance, substitution by D-Arg produced a peptide with negligible helicity under benign conditions but which exhibited 100% helicity in 50% TFE (Table VIII-4; Figure VIII-6), the very requirement we hypothesize to be necessary for optimizing biological activity of α -helical antimicrobial peptides, *i.e.*, disruption of α -helical structure in benign, aqueous medium followed by optimized inducible α -helical structure as the peptide enters the hydrophobic environment characteristic of biological membranes.

We believe the observed effects of L- and D-amino acid substitutions on apparent peptide amphipathicity and hydrophobicity (Table VIII-2) described in the present study, as well as the stability coefficients reported in Tables VIII-5 and VIII-6, will be of universal value in the field of peptide and protein chemistry, derived as they are from two criteria deemed absolutely necessary for accurate determination of the effect of individual amino acid substitutions on helix structure and stability: (i) a well-defined peptide model; and (ii) recognition that overall helix stability is dependent both on side-chain hydrophobicity and α -helical propensity. Thus, from (1), and as noted previously (see Design of model peptides), the Ala residues provide a uniform non-polar microenvironment surrounding the substitution site and can be expected to have minimal interactions with the “guest” L- or D-amino acid residue, such as, for example,

electrostatic interactions from charged side-chains and hydrophobic interactions from non-polar groups. This is in contrast to the 18-residue amphipathic α -helical model of Krause et al. (Krause *et al.*, 2000) where identical double substitutions of D-amino acids were made at adjacent positions in the non-polar face of the peptide. The double substitutions were made in order to enhance the destabilizing effects of D-amino acids on α -helical structure. However, it should be noted that, whereas two L-amino acid substitutions into a fully L-amino acid helix is likely genuinely additive, the chances of the same being true of two D-amino acid substitutions into a fully L-amino acid helix are not high. In addition to this questionable linear additivity rather than synergy of double D-amino acid substitutions, helical net analysis of this model peptide also revealed a non-uniform microenvironment surrounding the two substitution sites as well as the potential for significant non-polar and/or electrostatic $i \rightarrow i+3$ and $i \rightarrow i+4$ interactions with neighboring side-chains. These deviations from the requirements of an ideal peptide model likely explain the significant differences in apparent side-chain hydrophobicities of L- and D-amino acids, as determined by RP-HPLC peptide retention behavior, observed between the two model peptide systems. Also, it should be noted that just single amino acid substitutions in our peptide model produced a good range of both RP-HPLC retention times as well as peptide helicity, *i.e.*, no need for potentially misleading effects of double substitutions. Concerning point (ii) above, since the coefficients reported in Tables VIII-5 and VIII-6 are generated from temperature denaturation data, the combined contribution of side-chain hydrophobicity and α -helical propensity to helix stability is intrinsic to these values.

VIII-5 Conclusions

We have designed and synthesized a series of amphipathic α -helical peptides, where the position in the center of the hydrophobic face is substituted by L- or D- amino acids. From circular dichroism studies in benign medium and in the presence of 50% TFE, we have clearly shown the feasibility of controlled disruption of α -helical peptides by D-amino acid substitution in benign medium, whilst still allowing full folding in a more hydrophobic environment. In addition, comparison of the RP-HPLC retention behavior of the D-analogs with their L-enantiomers suggests that the employment of such D-analogs also allows modulation of the hydrophobicity/amphipathicity of the non-polar faces once the helix has been induced. From such data, we have also generated a series of helix stability coefficients which should prove valuable both for structure-activity studies as well as *de novo* design of novel antimicrobial peptides.

CHAPTER IX

Rational Design of α -Helical Antimicrobial Peptides with Enhanced Activities and Specificity/Therapeutic Index

A version of this chapter has been in press in *J. Biol. Chem.* 2005. Only methods unique to this chapter are described in the **Experimental** section, the remaining general methods are described in Chapter III.

IX-1 Abstract

In the present study, the 26-residue peptide sequence Ac-KWKSFLKTFKS-AVKTVLHTALKAISS-amide (V_{681}) was utilized as the framework to study the effects of peptide hydrophobicity/hydrophilicity, amphipathicity and helicity (induced by single amino acid substitutions in the center of the polar and nonpolar faces of the amphipathic helix) on biological activities. The peptide analogs were also studied by temperature profiling in RP-HPLC, from 5 °C to 80 °C, to evaluate the self-associating ability of the molecules in solution, another important parameter in understanding peptide antimicrobial and hemolytic activities. A higher ability to self-associate in solution was correlated with weaker antimicrobial activity and stronger hemolytic activity of the peptides. Biological studies showed that strong hemolytic activity of the peptides generally correlated with high hydrophobicity, high amphipathicity and high helicity. In most cases, the D-amino acid substituted peptides possessed an enhanced average antimicrobial activity compared with L-diastereomers. The therapeutic index of V_{681} was improved 90-fold and 23-fold against Gram-negative and Gram-positive bacteria, respectively. By simply replacing the central hydrophobic or hydrophilic amino acid residue on the nonpolar or the polar face of these amphipathic molecules with a series of

selected D-/L-amino acids, we demonstrated that this method can be used for the rational design of antimicrobial peptides with enhanced activities.

IX-2 Introduction

The extensive clinical use of classical antibiotics has led to the growing emergence of many medically relevant resistant strains of bacteria (Neu, 1992; Travis, 1994). Moreover, only three new structural classes of antibiotics (the oxazolidinone, linezolid, the streptogramins and the lipopeptid, edaptomycin (Calza *et al.*, 2004; Jacqueline *et al.*, 2004; Wagenlehner *et al.*, 2004)) have been introduced into medical practice in the past 40 years. Therefore, the development of a new class of antibiotics has become critical. The cationic antimicrobial peptides could represent such a new class of antibiotics (Andreu *et al.*, 1998; Hancock, 1997; Sitaram *et al.*, 2002). Although the exact mode of action of antimicrobial peptides has not been established, all cationic amphipathic peptides interact with membranes and it has been proposed that the cytoplasmic membrane is the main target of some peptides, whereby peptide accumulation in the membrane causes increased permeability and loss of barrier function (Duclohier *et al.*, 1989; Hancock *et al.*, 1998). The development of resistance to membrane active peptides whose sole target is the cytoplasmic membrane is not expected because this would require substantial changes in the lipid composition of cell membranes of microorganisms.

Two major classes of the cationic antimicrobial peptides are the α -helical and the β -sheet peptides (Andreu *et al.*, 1998; Devine *et al.*, 2002; Hancock, 1997; van 't Hof *et al.*, 2001). The β -sheet class consists of cyclic peptides constrained in this conformation

either by intramolecular disulfide bonds, *e.g.*, defensins (Ganz *et al.*, 1994) and protegrins (Steinberg *et al.*, 1997), or by an N-terminal to C-terminal covalent bond, *e.g.*, gramicidin S (Khaled *et al.*, 1978) and tyrocidines (Mootz *et al.*, 1997). Unlike the β -sheet peptides, α -helical peptides are linear molecules that mainly exist as disordered structures in aqueous media and become amphipathic helices upon interaction with the hydrophobic membranes, *e.g.*, cecropins (Christensen *et al.*, 1988), magainins (Zasloff, 1987) and melittins (Andreu *et al.*, 1992). From numerous structure/activity studies on both natural and synthetic antimicrobial peptides, a number of factors believed to be important for antimicrobial activity have been identified, including the presence of both hydrophobic and basic residues, an amphipathic nature that segregates basic and hydrophobic residues, and an inducible or preformed secondary structure (α -helical or β -sheet).

The major barrier to the use of antimicrobial peptides as antibiotics is their toxicity or ability to lyse eukaryotic cells. This is perhaps not a surprising result if the target is indeed the cell membrane (Andreu *et al.*, 1998; Hancock, 1997; Hancock *et al.*, 1998; Sitaram *et al.*, 2002). To be useful as a broad-spectrum antibiotic, it would be necessary to dissociate anti-eukaryotic activity from antimicrobial activity, *i.e.*, increasing the antimicrobial activity and reducing toxicity to normal cells. Recent studies on a number of α -helical and β -sheet peptides have attempted to delineate features responsible for these activities and found that high amphipathicity (Blondelle *et al.*, 1992b; Dathe *et al.*, 1997; Kondejewski *et al.*, 1999; Lee *et al.*, 2003a), high hydrophobicity (Dathe *et al.*, 1997; Kondejewski *et al.*, 1999; Kondejewski *et al.*, 2002; Oren *et al.*, 1997a), as well as high helicity or β -sheet structure (Kondejewski *et al.*, 1999; Oren *et al.*, 1997b; Shai *et al.*, 1996) were correlated with increased toxicity as

measured by hemolytic activity. In contrast, antimicrobial activity was found to be less dependent on these factors, compared with hemolytic activity (Blondelle *et al.*, 1992b; Dathe *et al.*, 1997; Kondejewski *et al.*, 1999; Lee *et al.*, 2003a; Lee *et al.*, 2004; Oren *et al.*, 1997a; Oren *et al.*, 1997b; Shai *et al.*, 1996). Therefore, specificity (or therapeutic index which is defined as the ratio of hemolytic activity and antimicrobial activity) for bacteria over erythrocytes could be increased in one of three ways: increasing antimicrobial activity, decreasing hemolytic activity while maintaining antimicrobial activity, or a combination of both.

We believe that a synthetic peptide approach to examining the effect of small incremental changes in hydrophobicity/hydrophilicity, amphipathicity and helicity of cationic antimicrobial peptides will enable rapid progress in rational design of peptide antibiotics. Our previous studies have successfully utilized such an approach to dissociate antimicrobial and hemolytic activities of *de novo* designed cyclic β -sheet gramicidin S analogs, by systematic alterations in amphipathicity/hydrophobicity through D-amino acid substitutions (Kondejewski *et al.*, 1999; Lee *et al.*, 2003a; Lee *et al.*, 2004). In recent work, we demonstrated that the helix-destabilizing properties of D-amino acids offer a systematic approach to the controlled alteration of the hydrophobicity, amphipathicity, and helicity of amphipathic α -helical model peptides (Chen *et al.*, 2002). By single substitutions of different D-amino acids into the center of the hydrophobic face of an amphipathic α -helical model peptide, we demonstrated that different D-amino acids disrupted α -helical structure to different degrees, whilst the destabilized structure could still be induced to fold into an α -helix in hydrophobic medium. The advantage of this method of single D- or L-amino acid substitutions at a specific site is that it enables a

greater understanding of the mechanism of action of these peptides. In this study, we have utilized the structural framework of an amphipathic α -helical antimicrobial peptide V₆₈₁ (Zhang *et al.*, 1998; Zhang *et al.*, 1999), to systematically change peptide amphipathicity, hydrophobicity and helicity by single D- or L-amino acid substitutions in the center of either the polar or nonpolar faces of the amphipathic helix. Peptide V₆₈₁ with excellent antimicrobial activity and strong hemolytic activity (Zhang *et al.*, 1998; Zhang *et al.*, 1999), was selected as an ideal candidate for our study. By introducing different D- or L-amino acid substitutions, we report here that hydrophobicity/amphipathicity and helicity have dramatic effects on the biophysical and biological activities and, utilizing this method, a significant improvement in antimicrobial activity and specificity can be achieved. In addition, it is plausible that high peptide hydrophobicity and amphipathicity also results in greater peptide self-association in solution. Since we have developed a novel method to measure self-association of small amphipathic molecules, namely temperature profiling in reversed-phase chromatography (Lee *et al.*, 2003b; Mant *et al.*, 2003a), we have applied this technique for the first time to investigate the influence of peptide dimerization ability on biological activities of α -helical antimicrobial peptides.

Thus, our objectives in this study were three-fold: first, to demonstrate the importance of the peptide self-association parameter in the *de novo* design of amphipathic α -helical antimicrobial peptides; second, to test the hypothesis that disruption of α -helical structure in benign conditions by D-amino acid substitutions or substitutions of hydrophilic/charged L-amino acids on the non-polar face can dramatically alter specificity in a similar manner to our previous work on cyclic β -sheet antimicrobial peptides (Kondejewski *et al.*, 1999; Lee *et al.*, 2004); and third, to observe if these

substitutions will enhance antimicrobial activity, decrease toxicity and improve antimicrobial specificity while maintaining broad spectrum activity for Gram-negative and Gram-positive bacteria.

IX-3 Experimental

IX-3-1 Analytical RP-HPLC of peptides

Peptides were analyzed on an Agilent 1100 series liquid chromatograph (Little Falls, DE). Runs were performed on a Zorbax 300 SB-C₈ column (150x2.1mm I.D.; 5µm particle size, 300Å pore size) from Agilent Technologies using linear AB gradient (1% acetonitrile/min) and a flow rate of 0.25 ml/min, where solvent A was 0.05% aqueous TFA, pH 2 and solvent B was 0.05% TFA in acetonitrile. Temperature profiling analyses were performed in 3 °C increments, from 5 °C to 80 °C.

IX-3-2 CD temperature denaturation study of peptide V₆₈₁

The native peptide V₆₈₁ was dissolved in 0.05% aqueous TFA containing 50% TFE, pH 2, loaded into a 0.02 cm fused silica cell and peptide ellipticity scanned from 190 to 250 nm at temperatures of 5, 15, 25, 35, 45, 55, 65 and 80 °C. The spectra at different temperatures were used to mimic the alteration of peptide conformation during temperature profiling analysis in RP-HPLC. The ratio of the molar ellipticity at a particular temperature (*t*) relative to that at 5 °C ($([\theta]_t - [\theta]_u) / ([\theta]_5 - [\theta]_u)$) was calculated and plotted against temperature in order to obtain the thermal melting profiles, where $[\theta]_5$ and $[\theta]_u$ represent the molar ellipticity values for the fully folded and fully unfolded species, respectively. $[\theta]_u$ was determined in the presence of 8M urea with a value of 1500 deg·cm²·dmol⁻¹ to represent a totally random coil state (Monera *et al.*, 1995). The melting

temperature (T_m) was calculated as the temperature at which the α -helix was 50% denatured ($([\theta]_t - [\theta]_u) / ([\theta]_5 - [\theta]_u) = 0.5$) and the values were taken as a measure of α -helix stability.

IX-3-3 Determination of peptide amphipathicity

Amphipathicity of peptide analogs was determined by the calculation of hydrophobic moment (Eisenberg *et al.*, 1982) using the software package JemBoss version 1.2.1 (Carver *et al.*, 2003), modified to include a hydrophobicity scale determined in our laboratory. The hydrophobicity scale used in this study is listed as follows: Trp, 32.31; Phe, 29.11; Leu, 23.42; Ile 21.31; Met, 16.13; Tyr, 15.37; Val, 13.81; Pro, 9.38; Cys, 8.14; Ala, 3.60; Glu, 3.60; Thr, 2.82; Asp, 2.22; Gln, 0.54; Ser, 0.00; Asn, 0.00; Gly, 0.00; Arg, -5.01; His, -7.03; Lys, -7.03 (Hodges, *et al.* unpublished data). These hydrophobicity coefficients were determined from reversed-phase chromatography at pH 2 of a model random coil peptide with single substitution of all 20 naturally occurring amino acids. In this case, the amphipathicity is valid for neutral and acidic pH since V_{681} and analogs do not have Asp and Glu residues in their sequences. We propose that this HPLC-derived scale reflects the relative differences in hydrophilicity/hydrophobicity of the 20 amino acid side-chains more accurately than previously determined scales.

IX-3-4 Measurement of antibacterial activity

Minimal inhibitory concentrations (MICs) were determined using a standard microtiter dilution method in LB (Luria-Bertani) no-salt medium (10 g of tryptone and 5 g of yeast extract per liter). Briefly, cells were grown overnight at 37 °C in LB and diluted in the same medium. Serial dilutions of the peptides were added to the microtiter plates in a volume of 100 μ l followed by 10 μ l of bacteria to give a final inoculum of

5×10^5 colony-forming units/ml. Plates were incubated at 37 °C for 24 hours and MICs determined as the lowest peptide concentration that inhibited growth.

IX-3-5 Measurement of hemolytic activity

Peptide samples were added to 1% human erythrocytes in phosphate buffered saline (0.08M NaCl; 0.043M Na₂PO₄; 0.011M KH₂PO₄) and reactions were incubated at 37°C for 12 hours in microtiter plates. Peptide samples were diluted 2 fold in order to determine the concentration that produced no hemolysis. This determination was made by withdrawing aliquots from the hemolysis assays, removing unlysed erythrocytes by centrifugation (800g) and determining which concentration of peptide failed to cause the release of hemoglobin. Hemoglobin release was determined spectrophotometrically at 562nm. The hemolytic titer was the highest 2-fold dilution of the peptide that still caused release of hemoglobin from erythrocytes. The control for no release of hemoglobin was a sample of 1% erythrocytes without any peptide added.

IX-4 Results and Discussion

IX-4-1 Peptide design

Peptide V₆₈₁, a 26-residue amphipathic antimicrobial peptide with a polar and non-polar face (Zhang *et al.*, 1999), was selected as the native parent peptide in this study (Figure IX-1). Its polar face consists of 14 residues: six lysine residues, one histidine, four serines and three threonines. In contrast, the non-polar face consists of 12 residues: three alanines, two valines, three leucines, two phenylalanines, one isoleucine and one tryptophan residue. In this study, we chose D-/L-amino acid substitution sites at the center of the hydrophobic face (position 13) and at the center of the hydrophilic face

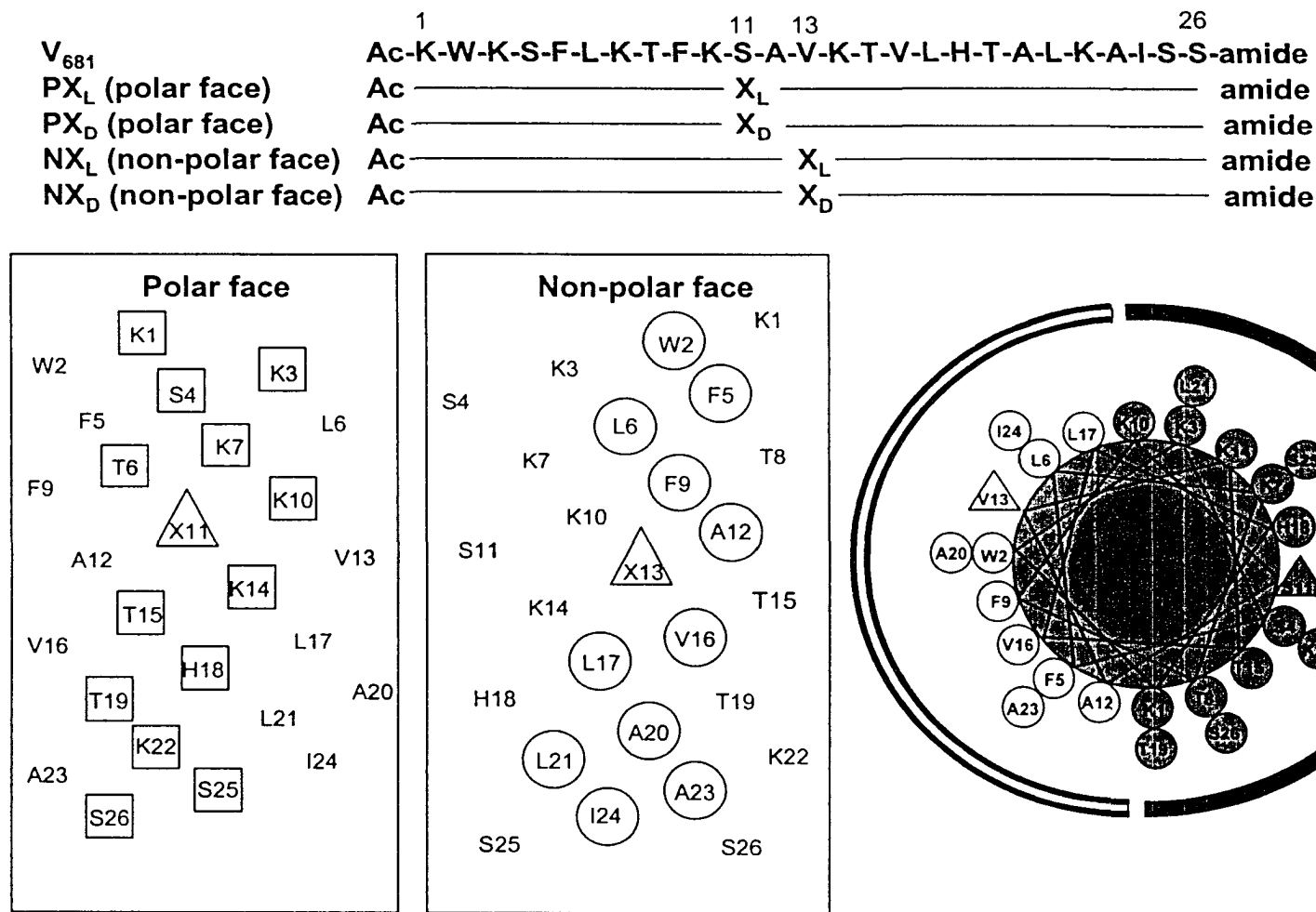


Figure IX-1 Representation of the "host" peptide V681 as helical nets showing the polar/hydrophilic face (boxed residues) and non-polar/hydrophobic face (circled residues) and helical wheel and the sequences of the synthetic peptide analogs used in this work. The hydrophobic face is indicated as an open arc, whilst the hydrophilic face is shown as a solid arc in the helical wheel. The substitution sites at positions 11 and 13 are triangled on the polar face and the non-polar face. In the peptide sequences, X_L and X_D denote the L- or D-substituting amino acids. P denotes the polar face and N denotes the non-polar face. Ac denotes N^α-acetyl and amide denotes C^α-amide. One-letter codes are used for the amino acid residues.

(position 11) of the helix, such that these substitution sites were also located in the center of the overall peptide sequence. This was based on our previous model peptide studies (Chen *et al.*, 2002; Monera *et al.*, 1995; Zhou *et al.*, 1994b) that demonstrated that these central location substitutions had the greatest effect on peptide secondary structure. To study the effects of varying hydrophobicity/hydrophilicity on peptide biological activities, in the design of V₆₈₁ analogs, five L-amino acids (Leu, Val, Ala, Ser, Lys) and Gly were selected out of the 20 natural amino acids as the substituting residues, representing a wide range of hydrophobicity. The hydrophobicity of these six amino acid residues decreases in the order Leu>Val>Ala>Gly>Ser>Lys (Chen *et al.*, 2002). Based on the relative hydrophobicity of amino acid side-chains (Chen *et al.*, 2002), leucine was used to replace the native valine on the non-polar face to increase peptide hydrophobicity and amphipathicity; alanine was selected to reduce peptide hydrophobicity/amphipathicity while maintaining high helicity; a hydrophilic amino acid, serine, was selected to decrease the hydrophobicity/amphipathicity of V₆₈₁ in the non-polar face; positively-charged lysine was used to decrease further peptide hydrophobicity and amphipathicity. In contrast, the same amino acid substitutions on the polar face would have different effects on the alteration of hydrophobicity/hydrophilicity and amphipathicity, since the native amino acid residue is serine on the polar face of V₆₈₁. As a result, on the polar face, leucine, valine and alanine were used to increase peptide hydrophobicity as well as decrease the amphipathicity of V₆₈₁, while lysine was selected to increase peptide hydrophilicity and amphipathicity. In previous studies, Kondejewski *et al.* (Kondejewski *et al.*, 1999; McInnes *et al.*, 2000) and Lee *et al.* (Lee *et al.*, 2004) successfully utilized D-amino acid substitutions to dissociate the antimicrobial activity

and hemolytic activity of gramicidin S analogs. In the present study, D-enantiomers of the five L-amino acid residues were also incorporated at the same positions on the non-polar/polar face of V₆₈₁ to change not only peptide hydrophobicity/hydrophilicity and amphipathicity but, more importantly, disrupt peptide helical structure. Since glycine does not exhibit optical activity and has no side-chain, the Gly-substituted analog was used as a reference for diastereomeric peptide pairs.

Since all peptide analogs were made based on a single amino acid substitution in either the polar or nonpolar faces of V₆₈₁, peptides were divided into two categories, N-peptides (nonpolar face substitutions) and P-peptides (polar face substitutions). Each peptide was named after the substituting amino acid residue, *e.g.*, the peptide analog with L-leucine substitution on the nonpolar face of V₆₈₁ is called NL_L. It is important to note that since the L-valine of the non-polar face and L-serine of the polar face are the original amino acid residues in the V₆₈₁ sequence (Figure IX-1), peptide analogs NV_L and PS_L are the same peptide as V₆₈₁.

A control peptide (peptide C) designed to exhibit negligible secondary structure, *i.e.*, a random coil, was employed as a standard peptide for temperature profiling during RP-HPLC to monitor peptide dimerization. As shown in the previous study (Mant *et al.*, 2003a), this 18-residue peptide, with the sequence of Ac-ELEKGGLEGEKGGKELEK-amide, clearly exhibited negligible secondary structure, even in the presence of the strong α -helix inducing properties of 50% trifluoroethanol (TFE) and at the low temperature of 5 °C ($[\theta]_{222} = -3,950$).

IX-4-2 Structure of peptide diastereomers

To determine the secondary structure of peptides in different environments, circular dichroism (CD) spectra of the peptide analogs were measured under physiologically related pH and ionic strength (100 mM KCl, 50 mM *aq.* PO₄, pH 7 referred to as benign conditions) and also in 50% TFE to mimic the hydrophobic environment of the membrane. The native peptide, V₆₈₁, exhibited low α -helical content in benign conditions, *i.e.*, $[\theta]_{222}$ of -12,900 compared to -27,300 in 50% TFE, an increase in α -helical content from 45% to 94%, respectively (Table IX-1). From Table IX-1, in benign conditions, D-amino acid substituted peptides generally exhibited considerably less α -helical structure compared to their L-diastereomers. The negligible secondary structure characteristics of the D-peptides underlines the helix-disrupting properties of a single D-amino acid substitution, as demonstrated in our previous model α -helical peptide study (Chen *et al.*, 2002). On the non-polar face, the native L-Val residue was critical in maintaining α -helical structure. Substitution of L-Val with less hydrophobic amino acids (L-Ala, Gly, L-Ser and L-Lys) dramatically decreased the α -helical structure (NV_L, $[\theta]_{222}$ of -12,900 to values ranging from -1,300 to -3,450 for NS_L, NK_L, NG and NA_L) (Table IX-1). Even the substitution with L-Ala, which is known to have the highest α -helical propensity of all 20 amino acids (Zhou *et al.*, 1994b), could not stabilize the α -helical structure. *This shows the importance of hydrophobicity on the non-polar face in maintaining the α -helical structure.* In contrast, substitution with a more hydrophobic amino acid (L-Leu for L-Val) on the non-polar face significantly increased α -helical structure ($[\theta]_{222}$ for peptide NL_L of -20,600 compared to peptide NV_L of -12,900). It is noteworthy that, on the non-polar face, the magnitude of the helical content of L-peptides

in benign buffer was related to the hydrophobicity of the substituting amino acids, *i.e.*, $NL_L > NV_L > NA_L > NS_L, NK_L$, again showing the importance of hydrophobicity on the non-polar face in maintaining the α -helical structure. Due to their helix-disruptive ability, on the non-polar face, the D-amino acid substitutions D-Val and D-Leu dramatically decreased α -helical structure in benign medium compared to their L-counterparts. However, whether L- or D-substitutions were made on the non-polar face, high helical structure could be induced by the hydrophobic environment of 50% TFE, a mimic of the membrane's hydrophobicity and α -helix inducing ability (Table IX-1). From Table IX-1, it is clear that, although D-amino acid substituted peptides were strongly induced into helical structure in 50% TFE, they were still generally less helical than the L-diastereomers, indicating that D-substitutions were still destabilizing of α -helical structure compared to their L-diastereomers in a hydrophobic environment.

In this study, the L-substitutions on the polar face in benign medium had dramatically different effects on α -helical structure than the same substitutions on the non-polar face. For example, NL_L ($[\theta]_{222}$ of -20,600) differed from PL_L ($[\theta]_{222}$ -10,850), indicating that Leu stabilized α -helical structure on the non-polar face and destabilized α -helical structure on the polar face. Similarly, Val destabilized α -helical structure on the polar face; on the other hand, Ala and Ser destabilized helical structure on the non-polar face, whilst, Ala and Ser stabilized α -helical structure when substituted in the polar face, compared to the other amino acid substitutions. Taken together, even though Ala had the highest α -helical propensity of all amino acids (Zhou *et al.*, 1994b), its α -helical propensity could not overcome the need for hydrophobicity on the non-polar face ($[\theta]_{222}$ for peptides NA_L , -3,450 and NL_L , -20,600); whereas, on the polar face, peptide PA_L

exhibited high helical structure in benign ($[\theta]_{222} -13,600$) in contrast to peptide PL_L ($[\theta]_{222} -10,850$) (Table IX-1). It is noteworthy that Val and Leu substitutions on the polar face decreased the amphipathicity of the helix as well as increased the hydrophobicity; however, the lower helical content compared with the native PS_L indicated that there should be a balance of amphipathicity and hydrophobicity to enhance the helical content. Similar to the substitutions on the non-polar face, all D-amino acid substitutions on the polar face were destabilizing to α -helical structure in benign medium; however, high helical structure could be induced by adding 50% TFE. As shown in Table IX-1, non-polar face substitutions exhibited a greater range of molar ellipticity values in benign conditions than polar face analogs, *demonstrating that the amino acid residues on the non-polar face of the helix played a more important role in peptide secondary structure than those on the polar face*. As expected, Gly was destabilizing to α -helical structure whether on the non-polar or polar face due to its low α -helical propensity (Zhou *et al.*, 1994b).

Figure IX-2 shows the CD spectra of the most and the least hydrophobic substitutions on the non-polar face. In benign conditions, peptide NL_D showed much less helical structure than NL_L due to the helix-destabilizing ability of the D-amino acid; whilst, in 50% TFE, both peptides could be induced to a fully helical structure (Figure IX-2, Panel A). In contrast, in benign condition, peptides NK_L and NK_D were random coils, due to the combined effects of decreasing hydrophobicity and amphipathicity by replacing the native L-Val to D-/L-Lys on the non-polar face; again, in 50% TFE, both of them were induced into highly helical structures, albeit that peptide NK_L demonstrated slightly more helical content than peptide NK_D.

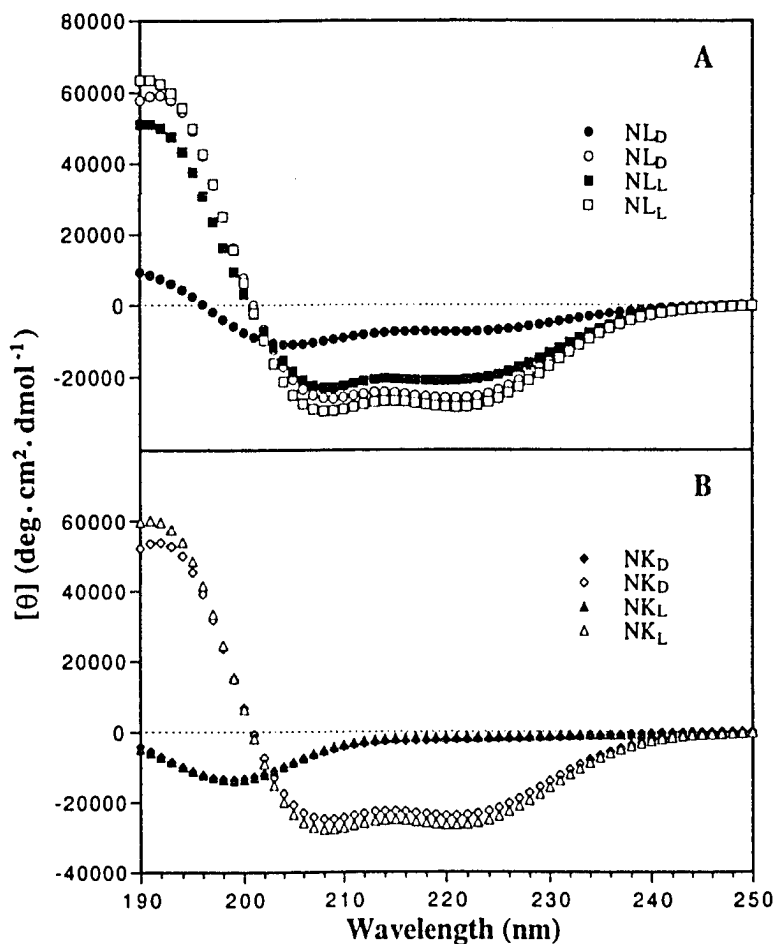


Figure IX-2 Circular dichroism (CD) spectra of peptides NL_D and NL_L (panel A) and peptides NK_D and NK_L (panel B) at pH 7 and 25°C, in 50mM *aq.* PO_4 containing 100mM KCl. In both Panel A and Panel B, solid symbols represent the CD spectra of peptide analogs in benign buffer without TFE, whilst open symbols represent CD spectra obtained in the presence of 50%TFE. The symbols used are: in Panel A, circle for NL_D and square for NL_L ; in Panel B, diamond for NK_D and triangle for NK_L .

Table IX-1 Circular dichroism data of V₆₈₁ peptide analogs

Peptides ^a	Benign ^b				50% TFE ^d			
	X _L ^c		X _D ^c		X _L ^c		X _D ^c	
	[θ] ₂₂₂	% helix ^c	[θ] ₂₂₂	% helix ^c	[θ] ₂₂₂	% helix ^c	[θ] ₂₂₂	% helix ^c
NL	-20,600	71	-7,350	25	-28,250	98	-25,750	89
NV ^f	-12,900	45	-2,800	10	-27,300	94	-26,000	90
NA	-3,450	12	-2,850	10	-28,950	100	-24,650	85
NS	-1,300	4	-1,700	6	-27,550	95	-22,200	77
NK	-1,450	5	-2,000	7	-26,250	91	-23,600	82
NG	-2,250	8			-24,350	84		
PL	-10,850	37	-2,950	10	-28,550	99	-26,100	90
PA	-13,600	47	-3,050	11	-27,600	95	-27,300	94
PS ^f	-12,900	45	-2,800	10	-27,300	94	-26,000	90
PV	-7,550	26	-2,400	8	-23,050	80	-20,800	72
PK	-5,950	21	-2,500	9	-27,350	94	-27,800	96
PG	-4,550	16			-25,950	90		

a. Peptides are ordered by relative hydrophobicity to the native analog V₆₈₁ at 5 °C. N denotes non-polar face; P denotes polar face (Figure IX-1)

b. The mean residue molar ellipticities, [θ]₂₂₂, (deg.cm².dmol⁻¹) at wavelength 222nm were measured at 25 °C in benign buffer (100mM KCl, 50mM PO₄ pH 7.0).

c. The helical content (in percentage) of a peptide relative to the molar ellipticity value of the peptide NA_L in 50% trifluoroethanol (TFE).

d. The mean residue molar ellipticities (deg.cm².dmol⁻¹) at wavelength 222nm were measured at 25 °C in the benign buffer diluted 1:1 (v/v) with trifluoroethanol (TFE).

e. X_L and X_D denote the L- and D-substitutions, respectively.

f. NV_L and PS_L are the same peptide, which is the native peptide V₆₈₁.

IX-4-3 Helix stability of peptide V_{681} in a hydrophobic environment

We wanted to use temperature profiling during RP-HPLC to determine the self-association ability of the various analogs of V_{681} which would occur through interaction of the non-polar faces of these amphipathic α -helices. Using model amphipathic α -helical peptides with all 20 amino acid substitutions in the center of the non-polar face, we showed previously that the model amphipathic peptides were maximally induced into an α -helical structure in 40% TFE and that the stability of the α -helix during temperature denaturation was dependent on the substitution (Chen *et al.*, 2002). In order to investigate the stability of V_{681} in a hydrophobic environment, we carried out a temperature denaturation study in solution, as monitored by circular dichroism spectroscopy. We used 50% aqueous TFE in 0.05% TFA to mimic the hydrophobic conditions in the reversed-phase column since the hydrophobic environment of a reversed-phase column (hydrophobic stationary phase and the hydrophobic organic solvent in the mobile phase) could induce α -helical structure in a similar manner to TFE. Figure IX-3, panel A shows the change of V_{681} helical conformation over the temperature range from 5 °C to 80 °C in the hydrophobic medium. At 5 °C, 50% TFE induced full α -helical structure of V_{681} . During the temperature denaturation the helical content of V_{681} decreased with increasing temperature and even at 80 °C V_{681} remained significantly α -helical. Figure IX-3, panel B shows the stability profile of V_{681} with a transition temperature T_m of 79.3 °C, where T_m is defined as the temperature when 50% of α -helical structure is denatured compared with the fully folded conformation of the peptide in 50% TFE at 5 °C. These data support the view, that during temperature profiling in RP-HPLC, the peptides are fully helical at low temperatures such as 5 °C and can remain at least partially α -helical at 80 °C in

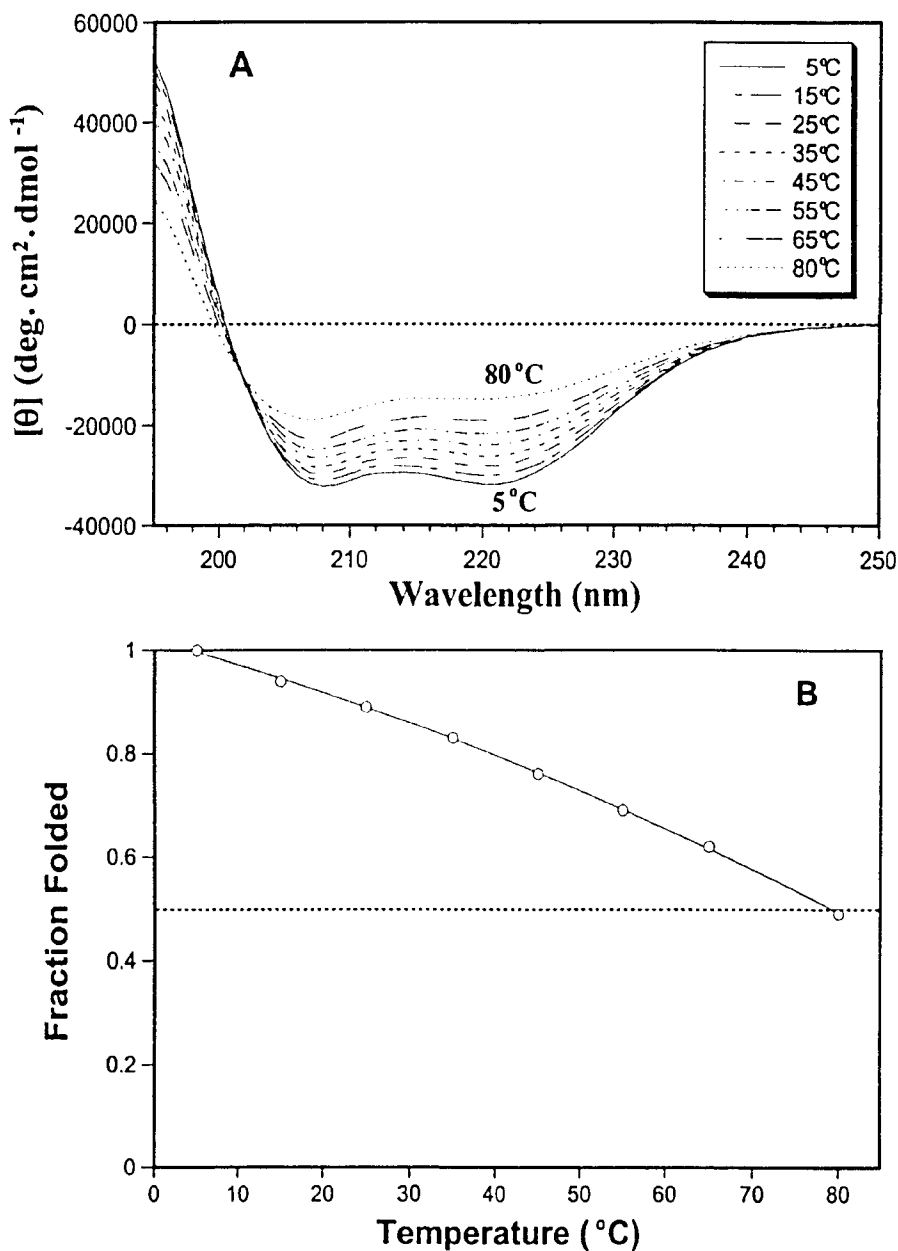


Figure IX-3 CD Temperature denaturation of peptide V₆₈₁. Panel A: the experiment was carried out in 0.05% *aq.* TFA (pH 2) in the presence of 50% TFE. CD spectra at different temperatures are shown as different lines in the figure; Panel B: stability plot of peptide V₆₈₁ during CD temperature denaturation.

solution during partitioning in RP-HPLC. In addition, due to their hydrophobic preferred binding domains, the peptides will remain α -helical when bound to the hydrophobic matrix. Overall, these results suggest that V₆₈₁ is a very stable α -helical peptide in a hydrophobic environment, whether it is in solution (such as 50% TFE), under the conditions of RP-HPLC or in the hydrophobic environment of the membrane.

IX-4-4 *Effect of L-/D-amino acid substitutions on RP-HPLC retention behavior of peptides*

It is well documented that the formation of a hydrophobic binding domain due to peptide secondary structure can affect peptide interactions with reversed-phase matrices, this effect having been observed especially for amphipathic α -helical peptides (Chen *et al.*, 2002; Mant *et al.*, 1993; Mant *et al.*, 2002b; Mant *et al.*, 2002c; Zhou *et al.*, 1990). Indeed, Zhou *et al.* (Zhou *et al.*, 1990) clearly demonstrated that, because of this preferred binding domain, amphipathic α -helical peptides are considerably more retentive than non-amphipathic peptides of the same amino acid composition. In addition, the chromatography conditions characteristic of RP-HPLC (hydrophobic stationary phase, nonpolar eluting solvent) are able to induce and stabilize helical structure in potentially helical polypeptides (Blondelle *et al.*, 1995; Purcell *et al.*, 1995c; Zhou *et al.*, 1990) in a manner similar to that of the helix-inducing solvent TFE. From Figure IX-1, it can be seen that the substitution site at position 13, in the center of the nonpolar face of the helix, ensures a maximal effect on the intimate interaction of the substituting side-chain with the reversed-phase stationary phase; thus, any differences in effective hydrophobicity via amino acid substitutions in the preferred binding domain can be readily monitored through consequent differences in RP-HPLC retention time. The

retention time data for the peptides is shown in Table IX-2 which records retention times at 5 °C, the maximal retention times and retention times at 80 °C during the temperature profiling. Temperatures of 5 °C and 80 °C were the lower and upper temperature limits of temperature profiling in RP-HPLC, representing dimerization of the peptides at 5 °C and the monomerization of peptides at 80 °C due to dissociation of the dimers. The maximal retention times represent the threshold points at which peptides transform from dimeric to monomeric form. The retention profiles from 5-80 °C are shown in Figure IX-4. Among the non-polar face substituted peptides, peptides with more hydrophobic substitutions (whether L- or D-amino acid substitutions) were more retained during RP-HPLC, *i.e.*, peptides were eluted in the order of Lys, Gly, Ser, Ala, Val and Leu (Table IX-2). In addition, on the non-polar face, the L-analogs were always more retained than the D-diastereomers (Table IX-2, Figure IX-4). Since the aforementioned preferred binding domain of amphipathic helices is actually the non-polar face of the helix, D-peptides had a smaller preferred binding domain compared with L-diastereomers, due to the helix disruptive ability of D-amino acids, resulting in lower retention times during RP-HPLC. In contrast, on the polar face, the elution order of peptides was not correlated with the order of amino acid side-chain hydrophobicity, *e.g.*, PA_L and PS_L were more retained than PV_L (Table IX-2); PS_D was the most retained peptide among the D-amino acid substituted analogs on the polar face (Table IX-2). Indeed, on the polar face, peptides PL_L and PA_L, with the replacement of L-Ser by L-Leu or L-Ala, had increased overall hydrophobicity as revealed by higher retention times compared with V₆₈₁. Although amino acid L-Val is much more hydrophobic than L-Ser, the observation that peptide PV_L was less retained than the native peptide V₆₈₁ (with L-Ser at position 11 of the polar

Table IX-2 Relative hydrophobicity and association ability of peptide analogs during RP-HPLC temperature profiling

Peptides ^a	t_R (min) ^b			Δt_R (X-NV _L) (min) ^c		P_A (min) ^d
	5 °C	Max	80 °C	5 °C	80 °C	
Non-polar ^e						
NL _L	48.16	50.45	47.02	0.06	1.19	4.22
NV _L ^f	48.10	49.99	45.83	0	0	3.63
NA _L	43.94	44.88	41.38	-4.16	-4.45	2.59
NS _L	40.72	41.08	37.62	-7.38	-8.21	1.82
NK _L	36.85	36.91	33.22	-11.25	-12.61	1.10
NG	39.96	40.22	36.74	-8.14	-9.09	1.64
NL _D	45.10	46.37	43.03	-3.00	-2.80	3.02
NV _D	42.55	43.43	40.15	-5.55	-5.68	2.63
NA _D	40.49	41.01	38.00	-7.61	-7.83	2.19
NS _D	37.02	37.12	34.08	-11.08	-11.75	1.46
NK _D	34.05	34.05	30.96	-14.05	-14.87	1.10
Polar ^e						
				Δt_R (X-PS _L) (min) ^c		
PL _L	48.78	51.23	47.51	0.68	1.68	4.33
PA _L	48.25	50.57	46.63	0.15	0.80	4.15
PS _L ^f	48.10	49.99	45.83	0	0	3.63
PV _L	47.83	49.93	46.18	-0.27	0.35	3.91
PK _L	46.38	47.90	43.89	-1.72	-1.94	3.17
PG	45.86	47.09	43.07	-2.24	-2.76	2.82
PS _D	45.47	46.60	42.59	-2.63	-3.24	2.73
PA _D	45.19	46.36	42.57	-2.91	-3.26	2.82
PL _D	44.73	45.85	42.14	-3.37	-3.69	2.82
PV _D	42.96	43.83	40.51	-5.14	-5.32	2.54
PK _D	42.20	42.87	39.29	-5.90	-6.54	2.23
C ^g	22.74	-	18.64	-	-	-

a. Peptides are ordered by relative hydrophobicity to the native L-Val substituted analog on the non-polar face and L-Ser substituted analog on the polar face.

b. denotes the retention times at 5 °C, the maximal retention times and the retention times at 80 °C during the temperature profiling.

c. denotes the difference of retention time relative to that of the native peptide V₆₈₁ (NV_L for the non-polar face substitutions and PS_L for the polar face substitutions), representing the relative hydrophobicity of the peptide analogs.

d. P_A denotes the association parameter of each peptide during the RP-HPLC temperature profiling, which is the maximal retention time difference of $((t_R^t - t_R^5)$ for peptide analogs) - $((t_R^t - t_R^5)$ for control peptide C)) within the temperature range, and $(t_R^t - t_R^5)$ is the retention time difference of a peptide at a specific temperature (t) compared with that at 5 °C.

e. denotes the amino acid substituted on either the non-polar face (N) or the polar face (P) of the amphipathic native peptide V₆₈₁ (see Figure IX-1).

f. NV_L and PS_L are the same peptide, which is the native peptide V₆₈₁.

g. Peptide C is a random coil control used to calculate P_A values, see footnote d.

face) could be attributed to the helix-disrupting characteristics of the β -branched Val residue (also see Table IX-1). In contrast, at 80 °C, PV_L became better retained than PS_L. Due to the unfolding of the helical structure at high temperature, the side-chain hydrophobicity of the substituting amino acid in the peptide plays a more important role in the overall hydrophobicity. In a similar manner to the non-polar face substituted peptides, peptides with D-amino acids substituted into the polar face were dramatically less retained than their L-diastereomers. Due to the effect of the preferred binding domain, peptides with substitutions on the non-polar face had a greater retention time range than those with polar face substitutions, *e.g.*, 11.31 min for the L-peptides with non-polar face substitutions *versus* 2.40 min for the L-peptides with polar face substitutions at 5 °C, and 11.05 min *versus* 3.27 min for the D-peptides with non-polar or polar face substitutions, respectively, at 5 °C (Table IX-2).

IX-4-5 Relative hydrophobicity

Elution times during RP-HPLC have frequently been utilized as a measure of relative hydrophobicity of peptide analogs (Chen *et al.*, 2002; Monera *et al.*, 1995). In the current study, peptide analogs differed only by a single amino acid substitution on either the non-polar face or the polar face of V₆₈₁; thus, the retention time data in Table IX-2 can be considered to reflect the hydrophobicity difference between peptide analogs. In order to more easily visualize the variation in hydrophobicity of the peptide analogs, the retention time data in Table IX-2 were normalized relative to that of the native peptide V₆₈₁ at 5 °C and 80 °C, respectively. Hydrophobicity relative to the native peptide V₆₈₁ indicates an increase or decrease of the apparent peptide hydrophobicity with the different amino acid substitutions on the polar or non-polar face. Again, from Table IX-2

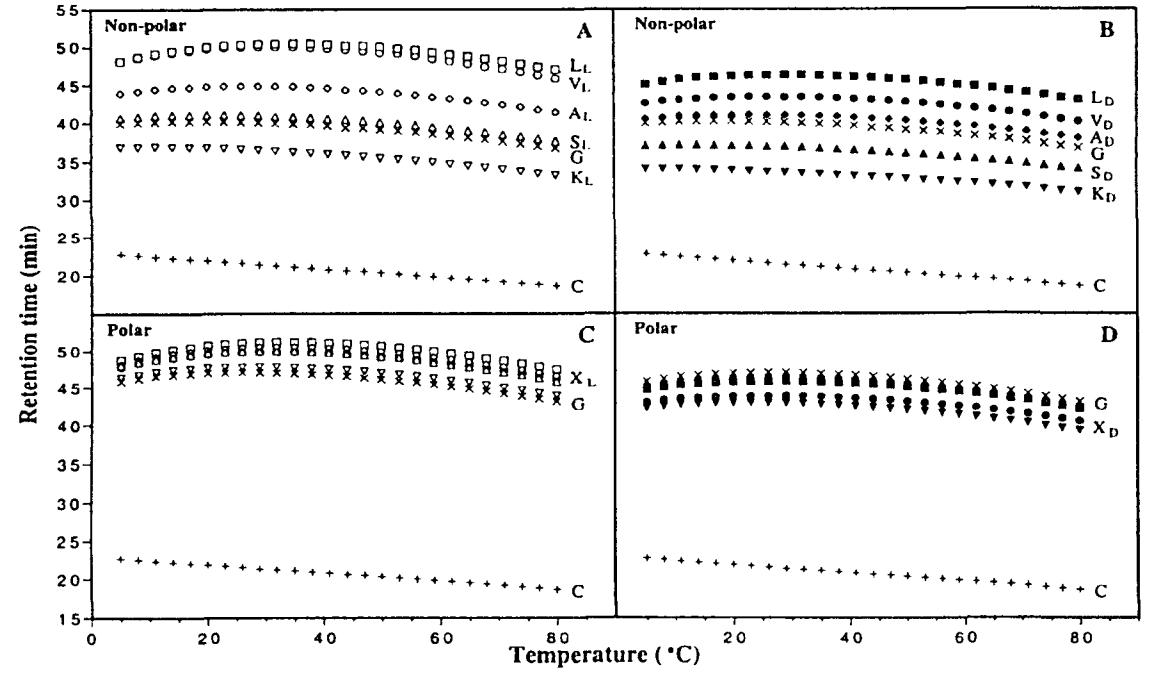


Figure IX-4 RP-HPLC temperature profiles of peptide V_{681} and its analogs. Conditions: RP-HPLC, narrow-bore SB- C_8 column (150x2.1 mm ID; 5 μ m particle size, 300 \AA pore size), linear A-B gradient (1% acetonitrile/min) at a flow-rate of 0.25 ml/min, where eluent A is 0.05% aqueous TFA and eluent B is 0.05% TFA in acetonitrile. Retention data has been collected in 3 $^{\circ}$ C increments within the temperature range from 5 $^{\circ}$ C to 80 $^{\circ}$ C. Open symbols represent the temperature profiles of L-amino acid substituted peptides on either the non-polar or polar face of V_{681} (panels A and C); whereas solid symbols represent the temperature profiles of D-amino acid substituted peptides on either the non-polar or polar face of V_{681} (panels B and D). In all panels, the substituting amino acids used in either the non-polar or polar face of V_{681} are Val (circle), Leu (square), Ala (diamond), Ser (triangle), Lys (inverted triangle) and Gly (X). The temperature profile of the random coil control peptide (C1) is shown in the figure (+).

and Figure IX-4, for non-polar face substituted peptides, there was a wide range of peptide hydrophobicity in the order L-Leu>L-Val>L-Ala>L-Ser>Gly>L-Lys at both 5 °C and 80 °C. On both the non-polar and polar faces, the relative hydrophobicities of the D-peptides was always less than their L-diastereomers, indicating the helix-disrupting characteristic of D-amino acids also leads to disruption of the preferred binding domain of the helices. On both non-polar and polar faces, peptides exhibited a greater retention time range at 80 °C than at 5 °C, also indicating that, due to the unfolding of the helical structures at 80°C, the side-chain hydrophobicity of the substituted amino acids played a more essential role in determining the overall hydrophobicity of the peptide analogs.

The hydrophobicity/hydrophilicity effects of substitutions on the non-polar face relative to the native peptide V₆₈₁ were large. For example, NV_L to NA_L, to NS_L, and to NK_L resulted in decreases in hydrophobicity of -4.45, -8.21 and -12.61 min at 80 °C, respectively (Table IX-2). In fact, the same substitutions, *i.e.*, PV_L to PA_L, to PS_L, and to PK_L, resulted in overall hydrophobicity changes of the peptide by +0.45, -0.35 and -2.29 min at 80 °C, respectively. This indicates that the polar face substitutions affected overall hydrophobicity of the peptide in a minor way relative to substitutions on the non-polar face. In fact, the effect was of 10 times less for Ala, >20 times less for Ser and >5 times less for Lys.

IX-4-6 *Determination of peptide self-association parameter by RP-HPLC temperature profiling*

Since its introduction, the technique of RP-HPLC temperature profiling has been applied on several types of molecules, including cyclic β -sheet peptides (Lee *et al.*, 2003b), monomeric α -helices and α -helices that dimerize (Mant *et al.*, 2003a), as well as

α -helices that dimerize to form coiled-coils (Mant *et al.*, 2003b). Although peptides are eluted from a reversed-phase column mainly by an adsorption/desorption mechanism (Mant *et al.*, 1991), even a peptide strongly bound to a hydrophobic stationary phase will partition between the matrix and the mobile phase when the acetonitrile content becomes high enough during gradient elution. The proposed mechanism of action for temperature profiling of α -helical peptides in RP-HPLC has been explained in detail by Mant, *et al.* (Mant *et al.*, 2003a). In summary, the mechanism is based on four assumptions: (i) at low temperature, just as an amphipathic α -helical peptide is able to dimerize in aqueous solution (through its hydrophobic, nonpolar face), it will dimerize in solution during partitioning in reversed-phase chromatography; (ii) at higher temperatures, the monomer-dimer equilibrium favors the monomer as the dimer is disrupted; (iii) at sufficiently high temperatures, only monomer is present in solution; and (iv) peptide is always bound in its monomeric helical form to the hydrophobic stationary phase, *i.e.*, the dimer can only be present in solution and disruption of the dimer is required for rebinding to the RP-HPLC matrix.

It is well accepted that the amphipathicity of antimicrobial peptides is necessary for their mechanism of action, since the positively-charged polar face will help the molecules reach the biomembrane through electrostatic interaction with the negatively-charged head groups of phospholipids, and then the nonpolar face of the peptides will allow insertion into the membrane through hydrophobic interactions, causing increased permeability and loss of barrier function of target cells (Duclohier *et al.*, 1989; Hancock *et al.*, 1998). Thus, we believe that peptide self-association (*i.e.*, the ability to dimerize) in aqueous solution is a very important parameter to understand antimicrobial activity. If

the self-association ability of a peptide in aqueous media is too strong (forming dimers and burying the non-polar face), it could decrease the ability of the peptide to dissociate and penetrate into the biomembrane and to kill target cells.

Figure IX-4 shows the temperature profiling of all L-/D-amino acid substituted peptide analogs during RP-HPLC from 5 °C and 80 °C. As mentioned above, the dimerization is temperature-dependent. At low temperatures, peptides exist in a dimer-monomer equilibrium during RP-HPLC partitioning, with the dimeric unbound state favored and dissociation required for rebinding; thus, the retention times are relatively low. With the increase of temperature, equilibrium is shifted toward the monomeric form in solution due to the disruption of the dimer. The higher solution concentration of monomer during partitioning increases the on-rate for the bound state, and the retention time therefore increases. It should be noted that the increased temperature also introduces other general effects on retention time because of lower mobile phase viscosity and a significant increase in mass transfer between the stationary phase and mobile phase. These effects decrease retention time with increasing temperature in a linear fashion, as shown for the random coil control peptide C (Figure IX-4). Conversely, for the dimerized peptides, at a given temperature dimers are disrupted and converted to monomers and the retention time reaches the maximal value. Above this critical temperature, one will observe a decrease in retention time with increasing temperature because of the low mobile phase viscosity and increase in mass transfer. In addition, the above described temperature-induced conformational changes, as monitored by CD, may also have an impact by decreasing the retention time with increasing temperature, largely due to the destabilization of peptide α -helical structure and loss of preferred binding domain at high

temperatures. To eliminate these general effects during RP-HPLC, the data from Figure IX-4 were normalized relative to the temperature profile of the random coil peptide standard C, and normalized to the retention time at 5 °C, the latter of which is presented as a dotted line in Figure IX-5.

It was observed that the peptide analogs in this study showed dramatic varying dimerization ability in solution (Figure IX-5). The maximal values of the change of retention times ($(t_R^1 - t_R^5)$ for peptide) - $(t_R^1 - t_R^5)$ for C) in Figure IX-5 were defined as the peptide association parameter (P_A) to quantify the association ability of peptide analogs in solution (Table IX-2). As seen from the data in Table IX-2, peptides with higher relative hydrophobicity generally showed stronger self-association ability in solution. The P_A values of the peptide with non-polar face substitutions were of the same order as their relative hydrophobicity, indicating that *the hydrophobicity on the hydrophobic face of the amphipathic helix was essential during dimerization*, since the dimers are formed by the binding together of the non-polar faces of two amphipathic molecules. In contrast, the different relationship between P_A and the relative hydrophobicity of the peptides with polar face substitutions demonstrated that the hydrophobicity on the polar face of the helices plays a less important role in peptide association. Generally speaking, the P_A values of L-peptides were significantly greater than those of their D-diastereomers, indicating the importance of helical structure during dimerization (Table IX-2). In Table IX-2, in most cases, the peptides with polar face substitutions had greater P_A values than the corresponding peptide analogs with the same amino acid substitutions on the non-polar face. This is exactly what one would expect since polar face substitutions have little

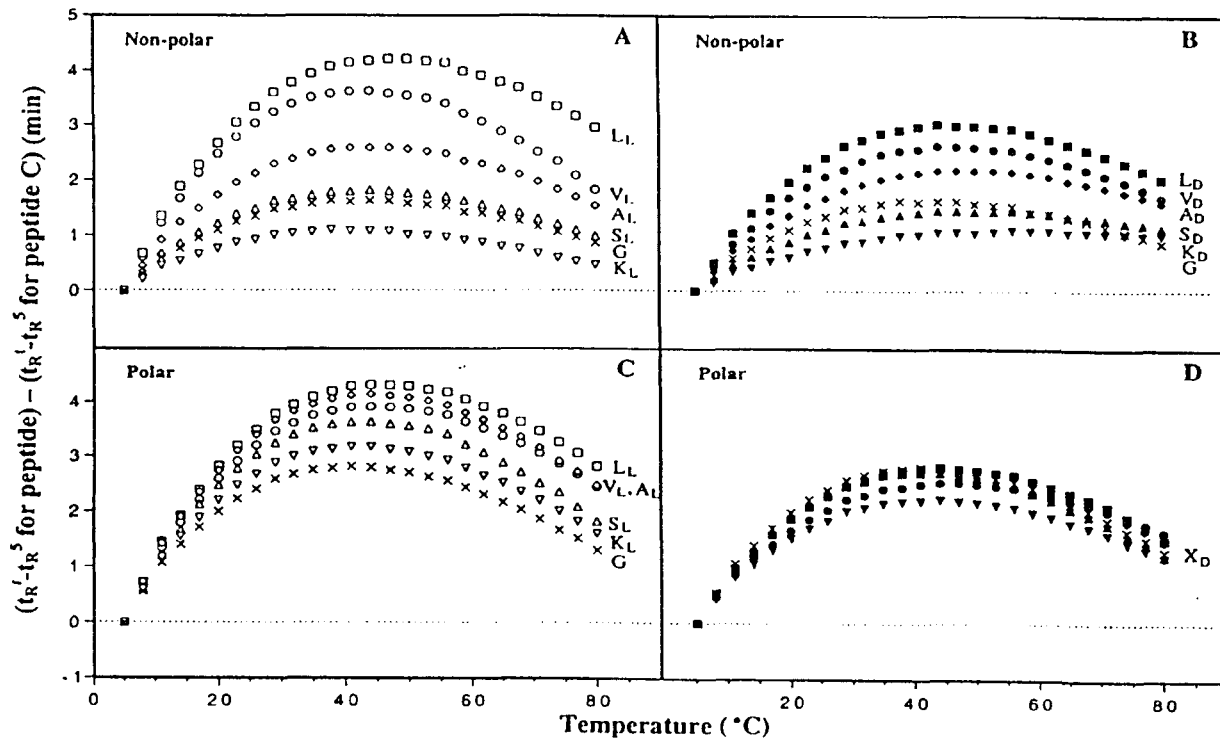


Figure IX-5 Normalized RP-HPLC temperature profiles of peptide V₆₈₁ and its analogs. Temperature profiles normalized to retention behavior of random coil peptide C1. Column and conditions: see Fig. 3. The retention behavior of the peptides was normalized to that of the random coil peptide C1 through the expression $(t_R^1 - t_R^5 \text{ for peptides}) - (t_R^1 - t_R^5 \text{ for C1})$, where t_R^1 are the retention times at a specific temperature of an antimicrobial peptide or the random coil peptide, and t_R^5 are the retention times at 5 °C. Open symbols represent the temperature profiling of L-amino acid substituted peptides on either the non-polar or polar face of V₆₈₁ (panels A and C); whereas solid symbols represent D-amino acid substituted peptides on either the non-polar or polar face of V₆₈₁ (panels B and D). In all panels, amino acids used for substitution in either the non-polar or polar face of V₆₈₁ are Val (circle), Leu (square), Ala (diamond), Ser (triangle), Lys (inverted triangle) and Gly (X).

effect on the preferred dimerization domain, whereas non-polar face substitutions would dramatically affect the hydrophobicity and dimerization ability of the peptide.

IX-4-7 Amphipathicity

Amphipathicity of the L-amino acid substituted peptides was determined by the calculation of hydrophobic moment (Eisenberg *et al.*, 1982) using the software package Jemboss version 1.2.1 (Carver *et al.*, 2003), modified to include the hydrophobicity scale determined in our laboratory (see Materials and Methods for details) (Table IX-3). Peptide amphipathicity, for the non-polar face substitutions, was directly correlated with side-chain hydrophobicity of the substituted amino acid residue, *i.e.*, the more hydrophobic the residue the higher the amphipathicity (values of 6.70 and 5.60 for NL_L and NK_L, respectively); in contrast, on the polar face, peptide amphipathicity was inversely correlated with side-chain hydrophobicity of the substituted amino acid residue, *i.e.*, the more hydrophobic the residue, the lower the amphipathicity (compare PK_L and PL_L with amphipathicity values of 6.62 and 5.45, respectively, Table IX-3).

The native sequence, V₆₈₁ was very amphipathic with a value of 6.35. To place this value in perspective, the sequence of V₆₈₁ can be shuffled to obtain an amphipathic value of 0.96 (KHAVIKWSIKSSVKFKISTAFKATTI) or a maximum value of 8.10 for the sequence of HWSKLLKSFTKALKKFAKAITSVVST.

The range of amphipathicity values achieved by single substitutions on the polar and non-polar faces varied from a low of 5.45 for PL_L to a high of 6.70 for NL_L (Table IX-3). Even though single substitutions changed the amphipathicity, all the analogs remained very amphipathic, *e.g.*, even with a lysine substitution on the non-polar face, NK_L has a value of 5.60.

Table IX-3 Amphipathicity of peptide analogs

Peptide	Amphipathicity ^a	Peptide	Amphipathicity ^a
NL _L	6.70	PL _L	5.45
NV _L ^b	6.35	PV _L	5.82
NA _L	5.98	PA _L	6.21
NG	5.85	PG	6.35
NS _L	5.85	PS _L ^b	6.35
NK _L	5.60	PK _L	6.62

a. Amphipathicity was determined by the calculation of hydrophobic moment using hydrophobicity coefficients determined by reversed-phase chromatography (see Experimental for details).

b. Peptides NV_L and PS_L are the same peptide as V₆₈₁.

IX-4-8 Relationships between peptide self-association and hydrophobicity, amphipathicity and helicity

From Table IX-2 and Table IX-3, peptides with higher relative hydrophobicity on their non-polar face created higher amphipathicity and generally showed stronger self-associating ability in solution; in contrast, for peptides with polar face substitutions, increasing hydrophobicity lowers amphipathicity yet the peptides still strongly self-associate, which indicates that peptide amphipathicity plays a less important role in peptide self-association when changes in amphipathicity are created on the polar face. In addition, self-associating ability is correlated with the secondary structure of peptides, *i.e.*, in this study, disrupting the peptide helical structure by replacing the L-amino acid with its D-amino acid counterpart decreases the P_A values (Table IX-1 and Table IX-2).

IX-4-9 Hemolytic activity

The hemolytic activity of the peptides against human erythrocytes was determined as a major measure of peptide toxicity toward higher eukaryotic cells (Table IX-4). As mentioned before, the native peptide V₆₈₁ (also named as NV_L or PS_L) had strong hemolytic activity, with a minimal hemolytic concentration (MHC value) of 15.6 µg/ml (Table IX-4). In this study, due to the alteration of hydrophobicity, amphipathicity and stability, the hemolytic activity of the best variants of peptide V₆₈₁ was significantly decreased to no detectable activity, a >32 fold decrease for NK_L (Table IX-6). From Table IX-4, it is clear that, *for the non-polar face substituted peptides, hemolytic activity was correlated with the side-chain hydrophobicity of the substituting amino acid residue, i.e., the more hydrophobic the substituting amino acid, the more hemolytic the peptide,* consistent with our previous study on the β-sheet antimicrobial peptide gramicidin S

Table IX-4 Antimicrobial (MIC) and hemolytic (MHC) activities of peptide analogs against gram-negative bacteria and human red blood cells

Peptides	MIC ^a (μg/ml)						MHC ^c (μg/ml)	Therapeutic Index ^d	
	<i>E. coli</i> UB1005 wt ^e	<i>E. coli</i> DC2 abs ^e	<i>S. typhimurium</i> C587 wt ^e	<i>S. typhimurium</i> C610 abs ^e	<i>P. aeruginosa</i> H187 wt ^e	<i>P. aeruginosa</i> H188 abs ^e	GM ^b hrBC		
NL _L	6.4	5.0	32.0	10.1	12.7	32.0	12.7	7.8	0.6
NV _L ^f	7.1	4.5	20.2	5.7	6.4	20.2	8.8	15.6	1.8
NA _L	2.5	2.5	6.4	2.5	5.0	6.4	3.8	31.2	8.1
NG	2.5	2.5	5.0	2.5	6.4	10.1	4.1	125.0	30.2
NS _L	2.5	2.5	6.4	2.0	6.4	10.1	4.2	125.0	30.1
NK_L^g	2.5	1.6	4.0	1.3	8.0	5.0	3.1	>250.0	163.0
NL _D	3.2	2.5	16.0	3.2	6.4	10.1	5.5	7.8	1.4
NV _D	2.5	1.6	5.0	2.0	4.0	8.0	3.3	62.5	19.0
NA_D^g	1.6	2.0	5.0	2.0	4.0	10.1	3.3	250.0	75.7
NS _D	3.2	2.0	12.7	2.0	18.3	20.2	6.3	>250.0	79.9
NK _D	3.2	2.5	32.0	1.0	32.0	25.4	7.7	>250.0	65.0
PL _L	16.0	5.0	32.0	12.7	20.2	32.0	16.6	4.0	0.2
PV _L	6.4	4.0	32.0	5.0	10.1	20.2	9.7	7.8	0.8
PA _L	6.4	4.0	20.2	4.0	10.1	16.0	8.3	15.6	1.9
PG	5.0	2.5	12.7	3.2	4.0	10.1	5.2	7.8	1.5
PS _L ^f	7.1	4.5	20.2	5.7	6.4	20.2	8.8	15.6	1.8
PK _L	10.1	4.0	25.4	8.0	25.4	32.0	13.7	4.0	0.3
PL _D	5.0	2.5	10.1	3.2	4.0	10.1	5.0	31.2	6.2
PV _D	5.0	2.5	10.1	4.0	6.4	16.0	6.1	125.0	20.5
PA _D	4.0	2.5	8.0	2.0	5.0	8.0	4.3	15.6	3.6
PS _D	2.5	1.6	5.0	1.6	2.0	10.1	2.9	15.6	5.3
PK _D	3.2	1.6	3.2	1.6	2.0	6.4	2.6	31.2	11.8

a. Antimicrobial activity (minimal inhibitory concentration) is given as the geometric mean of three sets of determinations.

b. GM denotes the geometric mean of MIC values from all 6 microbial strains in this table.

c. Hemolytic activity (minimal hemolytic concentration) was determined on human red blood cells (hrBC). When no detectable hemolytic activity was observed at 250 μg/ml, a value of 500 μg/ml was used for calculation of the therapeutic index.

d. Therapeutic index = MHC (μg/ml) / geometric mean of MIC (μg/ml). Larger values indicate greater antimicrobial specificity.

e. wt denotes the wild type strain and abs denotes the antibiotics sensitive strain.

f. NV_L and PS_L are the same peptide, which is the native peptide V₆₈₁.

g. The boxed results show the two best peptides with broad spectrum activity in terms of the therapeutic index against both Gram-negative and Gram-positive bacteria.

(Kondejewski *et al.*, 2002). For example, the MHC of peptide NL_L was 7.8 µg/ml; in contrast, the MHC was decreased, parallel with the reduction of hydrophobicity, to an undetectable level for peptide NK_L. Peptide hydrophobicity and amphipathicity on the non-polar face were also correlated with peptide self-associating ability, thus peptides with less self-association in benign conditions also exhibited less hemolytic activity against eukaryotic cells. In contrast, for polar face substituted peptides, the relationships between self-association, hydrophobicity/amphipathicity and hemolytic activity were less clear. Of course, the hydrophobic non-polar face remained very similar when L-substitutions were made on the polar face; thus, dimerization and hydrophobicity of the non-polar face would be less affected and hemolytic activity would remain relatively strong.

In addition to hydrophobicity/amphipathicity, peptide helicity seemed to have an additional effect on hemolytic activity. In general, on both the non-polar and polar faces, D-amino acid substituted peptides were less hemolytic than their L-diastereomers. For example, NA_L had a MHC value of 31.2 µg/ml compared to NA_D with a value of 250 µg/ml, an 8-fold decrease in hemolytic activity (Table IX-4). This phenomenon generally correlated with peptide self-associating ability, since D-diastereomeric analogs exhibited weaker self-associating ability than L-analogs (Table IX-2). Additionally, D-substitutions disrupt helicity which, in turn, disrupts hydrophobicity of the non-polar face. This result was also consistent with the data of Shai and coworkers (Oren *et al.*, 1997b; Shai *et al.*, 1996), who demonstrated that, through multiple D-amino acid substitutions, the helicity of peptides is substantially reduced leading to decreased hemolytic activity. Thus, peptide

structure is important in the cytotoxicity towards mammalian cells although these disturbed helices can still maintain antibacterial activity.

In the present study, peptide analogs with non-polar face substitutions exhibited a greater range of hemolytic activity (7.8 $\mu\text{g/ml}$ to not detectable) than the polar face substitutions (4 to 125 $\mu\text{g/ml}$), again indicating that the non-polar face of the helix may play a more essential role during the interaction with the biomembrane of normal cells (Table IX-4). As expected, the peptides with the polar face substitutions showed stronger hemolytic activity than the peptides with the same amino acid substitutions on the non-polar face, which may be attributed to the different magnitude of the hydrophobicity change by the same amino acid substitutions on different sides of the amphipathic helix. Interestingly, in this study, all polar face substituted peptides except PL_D , PV_D and PK_D showed stronger hemolysis of erythrocytes than V_{681} ; in contrast, on the non-polar face, only peptides NL_D and NL_L were more hemolytic than V_{681} (Table IX-4).

IX-4-10 Antimicrobial activity against gram-negative microorganisms

The antimicrobial activity of the peptides with either non-polar face or polar face amino acid substitutions against a range of Gram-negative microorganisms is shown in Table IX-4. The geometric mean MIC values from 6 microbial strains in this table were calculated to provide an overall evaluation of antimicrobial activity against Gram-negative bacteria. It is apparent that many peptide analogs showed considerable improvement in antimicrobial activity against Gram-negative bacteria over the native peptide V_{681} , as much as 3.4-fold (Table IX-6).

For Gram-negative bacteria, disruption of peptide helicity seemed to outweigh other factors in the improvement of antimicrobial activity; *i.e.*, in most cases, the peptides

with D-amino acid substitutions showed better antimicrobial activity than L-diastereomers. The exceptions were peptides NS_D and NK_D. The reason for the weaker activity of peptides NS_D and NK_D compared to NS_L and NK_L, respectively was possibly the combined effects of the destabilization of the helix, the decrease of hydrophobicity on the non-polar face and the disruption of amphipathicity, highlighting the importance of maintaining a certain magnitude of hydrophobicity and amphipathicity on the non-polar face of the helix for biological activity, *i.e.*, perhaps there is a combined threshold of helicity and hydrophobicity/amphipathicity required for biological activity of α -helical antimicrobial peptides. In this study, peptide self-associating ability (relative hydrophobicity) seemed to have no general relationship to MIC; however, interestingly, for peptides with L-hydrophobic amino acid substitutions (Leu, Val and Ala) in the polar and non-polar faces, the less hydrophobic the substituting amino acid, the more active the peptide against Gram-negative bacteria (Table IX-4).

IX-4-11 Antimicrobial activity against gram-positive microorganisms

Table IX-5 shows the antimicrobial activity of the peptides against Gram-positive microorganisms. By introducing D-/L-amino acid substitutions, we improved the antimicrobial activity of peptide V₆₈₁ against Gram-positive bacteria by as much as 2.7-fold (mean MIC values for V₆₈₁ were 6.3 μ g/ml compared to 2.3 μ g/ml for PS_D, Table IX-6). Compared with peptide V₆₈₁, most of the peptide analogs with increased antimicrobial activity against Gram-positive microorganisms were D-amino acid substituted peptides (7 D-peptides *versus* 1 L-peptide, Table IX-5). It was surprising to observe that peptides with polar face substitutions showed an overall greater improvement in MIC than those with non-polar face substitutions. Generally speaking,

Table IX-5 Antimicrobial (MIC) and hemolytic (MHC) activities of peptide analogs against gram-positive bacteria and human red blood cells

Peptides	MIC ^a (μg/ml)						GM ^b	MHC ^c (μg/ml)	Therapeutic Index ^d
	<i>S. aureus</i> 25923 wt ^e	<i>S. aureus</i> SAP0017 methR ^e	<i>S. epidermidis</i> C621 wt ^e	<i>B. subtilis</i> C971 wt ^e	<i>E. faecalis</i> C625 wt ^e	<i>C. xerosis</i> C875 wt ^e			
NL _L	32.0	25.4	8.0	3.2	32.0	2.5	10.9	7.8	0.7
NV _L ^f	16.0	9.0	5.0	2.2	16.0	2.5	6.3	15.6	2.5
NA _L	8.0	5.0	3.2	2.0	16.0	2.0	4.5	31.2	6.9
NG	25.4	10.1	3.2	2.0	50.8	2.0	7.4	125.0	16.8
NS _L	16.0	12.7	4.0	2.5	50.8	1.6	7.4	125.0	16.9
NK_L^g	64.0	64.0	5.0	1.6	64.0	1.3	11.8	>250.0	42.3
NL _D	5.0	4.0	2.5	2.5	6.4	1.6	3.3	7.8	2.4
NV _D	4.0	3.2	1.6	1.3	12.7	1.3	2.8	62.5	22.7
NA_D^g	8.0	5.0	2.0	1.6	32.0	1.6	4.3	250.0	57.8
NS _D	64.0	64.0	12.7	2.5	64.0	2.0	16.0	>250.0	31.3
NK _D	64.0	64.0	25.4	3.2	64.0	2.0	18.7	>250.0	26.8
PL _L	32.0	32.0	16.0	5.0	50.8	2.5	14.8	4.0	0.3
PV _L	16.0	12.7	8.0	2.5	20.2	1.3	6.9	7.8	1.1
PA _L	16.0	12.7	4.0	2.5	20.2	2.0	6.6	15.6	2.4
PG	8.0	5.0	4.0	2.0	12.7	2.0	4.5	7.8	1.7
PS _L ^f	16.0	9.0	5.0	2.2	16.0	2.5	6.3	15.6	2.5
PK _L	32.0	16.0	6.4	3.2	32.0	4.0	10.5	4.0	0.4
PL _D	8.0	5.0	4.0	2.0	16.0	2.0	4.7	31.2	6.7
PV _D	16.0	8.0	4.0	2.5	32.0	2.0	6.6	125.0	19.0
PA _D	6.4	5.0	2.5	2.0	12.7	1.6	3.8	15.6	4.1
PS _D	4.0	2.5	2.0	1.3	6.4	1.0	2.3	15.6	6.7
PK _D	4.0	2.5	2.0	2.0	12.7	1.0	2.8	31.2	11.0

a. Antimicrobial activity (minimal inhibitory concentration) is given as the geometric mean of three sets of determinations.

b. GM denotes the geometric mean of MIC values from all 6 microbial strains in this table.

c. Hemolytic activity (minimal hemolytic concentration) was determined on human red blood cells (hRBC). When no detectable hemolytic activity was observed at 250 μg/ml, a value of 500 μg/ml was used for calculation of the therapeutic index.

d. Therapeutic index = MHC (μg/ml)/geometric mean MIC (μg/ml). Larger values indicate greater antimicrobial specificity.

e. wt denotes the wild type strain and methR denotes the methicillin-resistant strain.

f. NV_L and PS_L are the same peptide, which is the native peptide V₆₈₁.

g. The boxed results show the two best peptides with broad spectrum activity in terms of the therapeutic index against both Gram-negative and Gram-positive bacteria.

Table IX-6 Effect of amino acid substitutions on the biological activity of V₆₈₁^a

Peptide	Gram-negative					Gram-positive				
	MIC ^b ($\mu\text{g/ml}$)	Fold ^e	Therapeutic index ^c	Fold ^e	MHC ^d ($\mu\text{g/ml}$)	Fold ^e	MIC ^b ($\mu\text{g/ml}$)	Fold ^e	Therapeutic index ^c	Fold ^e
V ₆₈₁	8.8	1.0	1.8	1.0	15.6	1.0	6.3	1.0	2.5	1.0
NA _L	3.8	2.3	8.1	4.5	31.2	2.0	4.5	1.4	6.9	2.8
NG	4.1	2.1	30.2	16.8	125.0	8.0	7.4	0.9	16.8	6.7
NS _I	4.2	2.1	30.1	16.7	125.0	8.0	7.4	0.9	16.9	6.8
NK _L ^f	3.1	2.8	163.0	90.6	>250.0	32.1	11.8	0.5	42.3	16.9
NV _D	3.3	2.7	19.0	10.6	62.5	4.0	2.8	2.3	22.7	9.1
NA _D ^f	3.3	2.7	75.7	42.1	250.0	16.0	4.3	1.5	57.8	23.1
NS _D	6.3	1.4	79.9	44.4	>250.0	32.1	16.0	0.4	31.3	12.5
NK _D	7.7	1.1	65.0	36.1	>250.0	32.1	18.7	0.3	26.8	10.7
PL _D	5.0	1.8	6.2	3.4	31.2	2.0	4.7	1.3	6.7	2.7
PV _D	6.1	1.4	20.5	11.4	125.0	8.0	6.6	1.0	19.0	7.6
PA _D	4.3	2.0	3.6	2.0	15.6	1.0	3.8	1.7	4.1	1.6
PS _D	2.9	3.0	5.3	2.9	15.6	1.0	2.3	2.7	6.7	2.7
PK _D	2.6	3.4	11.8	6.6	31.2	2.0	2.8	2.3	11.0	4.4

a. Only the peptide analogs with a therapeutic index greater than V₆₈₁ are included in this table.

b. Antimicrobial activity (minimal inhibitory concentration) was given as the geometric mean data of Tables IX-4 & IX-5.

c. Therapeutic index = MHC (in $\mu\text{g/ml}$) / MIC (in $\mu\text{g/ml}$). Larger values indicate greater antimicrobial specificity.

d. Hemolytic activity (minimal hemolytic concentration) was determined on human red blood cells (hRBC). When no detectable hemolytic activity was observed at 250 $\mu\text{g/ml}$, a value of 500 $\mu\text{g/ml}$ was used for calculation of the therapeutic index and fold increased.

e. denotes the fold improvement in activity compared with the corresponding data of the native peptide V₆₈₁.

f. The boxed results show the two best peptides with broad spectrum activity in terms of the therapeutic index against both Gram-negative and Gram-positive bacteria.

increasing the hydrophobicity of the native peptide V₆₈₁ by amino acid substitutions at either the polar or the non-polar face weakened the antimicrobial activity against Gram-positive bacteria, *e.g.*, peptides NL_L and PL_L (Table IX-5). Amino acid substitutions of D-Ser and D-Lys on the non-polar face significantly weakened the activity, in a similar manner to the anti-Gram-negative activity, indicating again the importance of maintaining a certain magnitude of helicity, hydrophobicity/amphipathicity on the non-polar face of the helix for peptide Gram-positive antimicrobial activity.

IX-4-12 Therapeutic index

Therapeutic index is a widely employed parameter to represent the specificity of antimicrobial reagents. It is calculated by the ratio of MHC (hemolytic activity) and MIC (antimicrobial activity); thus, larger values in therapeutic index indicate greater antimicrobial specificity. As mentioned above, the native peptide V₆₈₁ is a peptide with good antimicrobial activity coupled with strong hemolytic activity; hence, its therapeutic index is low (1.8 and 2.5 for Gram-negative and Gram-positive bacteria, respectively, Table IX-6) and comparable to general toxins like melittin. In this study, by altering peptide hydrophobicity/hydrophilicity, amphipathicity and helicity, we significantly increased the therapeutic index of peptide V₆₈₁ against Gram-negative bacteria by 90-fold (Table IX-6) and Gram-positive bacteria by 23-fold (Table IX-6). As indicated in Tables IX-4 and IX-5, there was a greater range of therapeutic indices for peptides with the non-polar face substitutions compared with the polar face substitutions, which was consistent with peptide self-association studies, indicating that the non-polar face of the helix may play a more important role in the mechanism of action.

Table IX-6 summarizes the data for these peptide analogs with improved therapeutic index values relative to the native peptide V₆₈₁. From Table IX-1 and Table IX-6, it is clear that all peptides with improved therapeutic indices are those showing less stable helical structure in benign medium (either the D-amino acid substituted peptides or the hydrophilic amino acid substituted peptides on the non-polar face). The two peptides with the best therapeutic indices among all the analogs were NK_L with a 90-fold and 17-fold improvement and NA_D with a 42-fold and 23-fold improvement compared with V₆₈₁ against all the tested Gram-negative and Gram-positive microorganisms, respectively. It is noteworthy that the hemolytic activity of these two peptides was extremely weak; in addition, peptides NK_L exhibited improved antimicrobial activity compared to peptide V₆₈₁ against Gram-negative bacteria and NA_D exhibited improved antimicrobial activity against Gram-negative and Gram-positive bacteria (Table IX-6).

IX-4-13 *Proposed mechanism of action of antimicrobial peptides in biomembranes*

The exact mechanism of action of cationic amphipathic antimicrobial peptides is not well understood (Blondelle *et al.*, 1999; Hancock *et al.*, 2002; Matsuzaki, 1999; Shai, 1999; Sitaram *et al.*, 1999; Zhang *et al.*, 2001), since their lethal action could be from membrane disruption solely or from translocation through the membrane to target receptors inside the cell. We believe that the main target for the peptides with the desired biological activities in this study is the cytoplasmic membrane. Many models have been proposed on how these peptides interact with the membrane. For example, the peptide may form transmembrane channels/pores by bundles of amphipathic α -helices, as their hydrophobic surfaces interact with the lipid core of the membrane and the hydrophilic surfaces point inward, producing an aqueous pore (“barrel-stave” mechanism)

(Ehrenstein *et al.*, 1977); or the peptides lie at the interface parallel with the membrane allowing their hydrophobic surface to interact with the hydrophobic component of the lipid and the positive charge residues can still interact with the negatively-charged headgroups of the phospholipid (“carpet” mechanism) (Pouny *et al.*, 1992). In support of interface model is the NMR study of the amphipathic cyclic β -sheet antimicrobial peptide of gramicidin S (Salgado *et al.*, 2001). In the latter model the peptides are not in the hydrophobic core of the membrane, and neither do they assemble the aqueous pore with their hydrophilic faces. Neither of these mechanisms alone can fully explain the data in this study. For example, the hemolytic activity is correlated to the peptide hydrophobicity and amphipathicity on the non-polar face, which may be consistent with the “barrel-stave” mechanism, *i.e.*, peptides interact with the hydrophobic core of the membrane by their non-polar face to form pores/channels. In contrast, the antimicrobial activity is not correlated with peptide hydrophobicity/amphipathicity, showing that the “barrel-stave” mechanism may not be suitable to explain the mechanism of antimicrobial action. Indeed, the “carpet” mechanism may best explain the interaction between the peptides and the bacterial membrane. Based on the above observations, we propose that both mechanisms are in operation for the peptides used in this study, *i.e.*, the mechanism depends upon the difference in membrane composition between prokaryotic and eukaryotic cells. If the peptides form pores/channels in the hydrophobic core of the eukaryotic bilayer, they would cause the hemolysis of human red blood cells; in contrast, for prokaryotic cells, the peptides lyse cells in a detergent-like mechanism as described in the “carpet” mechanism.

Indeed, it is known that the extent of interaction between peptide and biomembrane is dependent on the composition of lipid bilayer. For example, Liu, *et al.*

(Liu *et al.*, 2002a; Liu *et al.*, 2004a; Liu *et al.*, 2004b) utilized a polyleucine-based α -helical transmembrane peptide to demonstrate that the peptide reduced the phase transition temperature to a greater extent in phosphatidylethanolamine (PE) bilayers than in phosphatidylcholine (PC) or phosphatidylglycerol (PG) bilayers, indicating a greater disruption of PE organization. The zwitterionic PE is the major lipid component in prokaryotic cell membranes and PC is the major lipid component in eukaryotic cell membranes (Daum, 1985; Devaux *et al.*, 1985). In addition, although PE also exists in eukaryotic membranes, due to the asymmetry in lipid distribution, PE is mainly found in the inner leaflet of the bilayer while PC is mainly found in the outer leaflet of the eukaryotic bilayer. We draw the conclusion that, in a similar fashion to the results of transmembrane α -helical peptides, the antimicrobial specificity of the antimicrobial α -helical peptides is a result of the composition differences of the lipid bilayer between eukaryotic and bacterial cells.

In support of this proposal, we have selected two examples from our study. The results for peptide NK_I, the peptide with the highest therapeutic index against Gram-negative bacteria, can be explained using our combined model. For example, if hemolysis of eukaryotic cells requires insertion of the peptide into the hydrophobic core of the membrane, which depends on the composition of the bilayer, and interaction of the non-polar face of the amphipathic α -helix with the hydrophobic lipid core of the bilayers, it seems reasonable to assume that disruption of the hydrophobic surface with the Lys substitution (NK_I) would both disrupt dimerization of the peptide in aqueous solution allowing the peptide to more easily enter the interface region and prevent penetration into the hydrophobic core of the membrane. Thus, the peptide is unable to cause hemolysis.

On the other hand, if the mechanism for prokaryotic cells allows the interaction of monomeric peptides with the phospholipid headgroups in the interface region, then no insertion into the hydrophobic core of the membrane is required for antimicrobial activity.

In contrast, the observation that the antimicrobial activity of peptide NL_L (with Leu at the substitution site) was worse than that of NK_L, while its hemolytic activity was stronger (MIC values of 12.7 μg/ml for NL_L versus 3.1 μg/ml for NK_L against Gram-negative bacteria; hemolytic activity of 7.8 μg/ml for NL_L versus no detectable hemolytic activity for NK_L) can also be explained by our combined model. Thus, peptide NL_L has a fully accessible non-polar face required for insertion into the bilayer and for interaction with the hydrophobic core of the membrane to form pores/channels (“barrel-stave” mechanism), while the hemolytic activity of peptide NL_L is dramatically stronger than peptide NK_L. On the other hand, due to the stronger tendency of peptide NL_L to be inserted into the hydrophobic core of the membrane than peptide NK_L, peptide NL_L actually interacts less with the water/lipid interface of the bacterial membrane; hence, the antimicrobial activity is 4-fold weaker than the peptide NK_L against Gram-negative bacteria. This supports the view that the “carpet” mechanism is essential for strong antimicrobial activity and if there is a preference by the peptide for penetration into the hydrophobic core of the bilayer, the antimicrobial activity will actually decrease.

IX-5 Conclusions

Utilizing a structure-based rational approach to antimicrobial peptide design with single D-/L-amino acid substitutions in the center of peptide nonpolar/polar face, we

were able to develop antimicrobial peptides with improved activity and specificity and clinical potential as broad spectrum antibiotics. Systematically altering peptide hydrophobicity/ hydrophilicity, amphipathicity and helicity, we were able to optimize the specificity of the native peptide V₆₈₁ with significantly increased therapeutic indices of 90-fold against Gram-negative bacteria and 23-fold against Gram-positive microorganisms, respectively. Hemolytic activity of the peptides has been demonstrated to have close relationships with peptide hydrophobicity, amphipathicity and helicity. High peptide hydrophobicity, amphipathicity and helicity usually result in strong hemolytic activity. The controlled disruption of the α -helical structure (disruption under benign conditions and inducible in hydrophobic conditions) seems to be also related with the strong antimicrobial activity over a variety of Gram-negative and Gram-positive bacterial strains. Furthermore, the technique of temperature profiling in RP-HPLC appears to be a valuable tool to determine the self-association ability of molecules in solution, which, we believe, is an important property influencing the peptide biological activity.

CHAPTER X

Comparison of Reversed-Phase Chromatography and Hydrophilic Interaction/Cation-Exchange Chromatography for the Separation of Amphipathic α -Helical Peptides with L- And D-Amino Acid Substitutions in the Hydrophilic Face

A version of this chapter has been published: Hartmann, E., Chen, Y., Mant, C. T. Jungbauer, A. and Hodges, R. S. (2003) *J. Chromatogr. A* **1009**, 61-71. Only methods unique to this chapter are described in the **Experimental** section, the remaining general methods are described in Chapter III.

X-1 Abstract

Mixed-mode hydrophilic interaction/cation-exchange chromatography (HILIC/CEX) is a novel high-performance technique which has excellent potential for peptide separations. Separations by HILIX-CEX are carried out by subjecting peptides to linear increasing salt gradients in the presence of high levels of acetonitrile, which promotes hydrophilic interactions overlaid on ionic interactions with the cation-exchange matrix. In the present study, HILIC/CEX has been compared to reversed-phase chromatography (RP-HPLC) for separation of mixtures of diastereomeric amphipathic α -helical peptide analogues, where L- and D- amino acid substitutions were made in the centre of the hydrophilic face of the amphipathic α -helix. Unlike RP-HPLC, temperature had a substantial effect on HILIC/CEX of the peptides, with a rise in temperature from 25°C to 65°C increasing the retention times of the peptides as well as improving resolution. Our results again highlight the potential of HILIC-CEX as a peptide separation mode in its own right as well as an excellent complement to RP-HPLC.

X-2 Introduction

Although reversed-phase chromatography (RP-HPLC) is generally the method of choice for separation of peptide mixtures (Mant *et al.*, 1991; Mant *et al.*, 2002a), this laboratory has previously shown mixed-mode hydrophilic interaction/cation-exchange chromatography (HILIC/CEX) to be an excellent complement to RP-HPLC (Litowski *et al.*, 1999; Mant *et al.*, 1996; Mant *et al.*, 1997; Mant *et al.*, 1998a; Mant *et al.*, 1998b; Mant *et al.*, 2000; Zhu *et al.*, 1991; Zhu *et al.*, 1992). Indeed, HILIC/CEX, which combines the most advantageous aspects of two widely different separation mechanisms, *i.e.*, a separation based on hydrophilicity/hydrophobicity differences between peptides overlaid on a separation based on net charge, has rivalled or even exceeded RP-HPLC for specific peptide mixtures (Litowski *et al.*, 1999; Mant *et al.*, 1997; Zhu *et al.*, 1992). For example, for the separation of two synthetic peptides and their deletion impurities (serine and cysteine), HILIC/CEX was clearly superior to RP-HPLC (Mant *et al.*, 1997). In another study (Litowski *et al.*, 1999), a two-step protocol consisting of HILIC/CEX followed by RP-HPLC was required for the successful purification of a 21-residue synthetic amphipathic α -helical peptide from serine side-chain acetylated impurities, with HILIC/CEX proving to be highly sensitive to subtle differences in hydrophilicities between the acetylated peptides and the desired product. Mixed-mode HILIC/CEX has also been used for the separation of H1 histones (Lindner *et al.*, 1996; Lindner *et al.*, 1997), proteins notoriously difficult to separate by traditional high-performance liquid chromatography (HPLC) techniques.

In an earlier study (Mant *et al.*, 1998b), we examined the potential of both RP-HPLC and HILIC/CEX for the separation of amphipathic α -helical peptides. Such

peptides were represented by model α -helical peptides varying in amphipathicity and the nature of the side-chain substituted in the centre of the hydrophilic or hydrophobic face of the helix. Aside from clarifying the relative values of HILIC/CEX and RP-HPLC for specific model peptide separations, our results had wider implications for resolving complex peptide mixtures such as those characteristic of protein digests, where the occurrence of peptides with amphipathic α -helices is commonplace. In the present study, we now wished to examine further the relative effectiveness of RP-HPLC and HILIC/CEX in separating amphipathic α -helical peptides. Specifically, we looked to ascertain the ability of these techniques to separate mixtures of diastereomeric peptide analogues of a biologically active amphipathic α -helix denoted native (V_{681}) (Zhang *et al.*, 1998; Zhang *et al.*, 1999). Thus, diastereomeric peptide pairs were prepared with either an L-amino acid or its D-amino acid enantiomer in the centre of the polar face of the amphipathic α -helix. Thus, each diastereomeric peptide pair has the same inherent hydrophilicity/hydrophobicity but potentially different amphipathicity due to the helix-disrupting properties of D-amino acids when substituted into an α -helix made up entirely of L-amino acids (Aguilar *et al.*, 1993; Chen *et al.*, 2002; Krause *et al.*, 2000; Rothmund *et al.*, 1995; Rothmund *et al.*, 1996), providing a potent test for the resolving power of RP-HPLC and HILIC/CEX.

X-3 Experimental

X-3-1 Columns

Analytical RP-HPLC runs were carried out on a Zorbax SB-300-C₈ column (150 x 2.1 mm I.D., 5- μ m particle size; 300-Å pore size) from Agilent Technologies (Little

Falls, DE, USA). Mixed-mode HILIC/CEX runs were carried out on a poly(2-sulfoethyl aspartamide)-silica (PolySulfoethyl A) strong cation-exchange column (200 x 2.1 mm I.D., 5 μm , 300 Å) from PolyLC (Columbia, MD, USA).

X-4 Results and discussion

X-4-1 RP-HPLC versus HILIC/CEX: general principles

Although the general principles of HILIC/CEX have been described in detail previously (Mant *et al.*, 1998b; Mant *et al.*, 2000), a brief overview of this mixed-mode technique is useful for the present study. Thus, the term hydrophilic interaction chromatography was originally introduced to describe separations based on solute hydrophilicity (Alpert, 1990). Separation by HILIC, therefore, in a manner similar to normal-phase chromatography (to which it is related), depends on hydrophilic interactions between the solutes and a hydrophilic stationary phase, *i.e.*, solutes are eluted in order of increasing hydrophilicity (decreasing hydrophobicity). This is, of course, in direct contrast to RP-HPLC, where solutes are eluted from a hydrophobic stationary phase in order of increasing hydrophobicity (decreasing hydrophilicity).

Characteristic of HILIC separations is the presence of a high organic modifier concentration to promote hydrophilic interactions between the solute and the hydrophilic stationary phase. Taking this concept a step further, this laboratory (Zhu *et al.*, 1991; Zhu *et al.*, 1992) demonstrated how to take advantage of the inherent hydrophilic character of ion-exchange, specifically strong cation-exchange (CEX) columns, by subjecting peptide mixtures to linear salt gradients in the presence of high levels of organic modifier. Separations based on hydrophilicity are thus superimposed on separations based on

charge, *i.e.*, the overall separation is effected by a mixture of chromatographic modes, namely mixed-mode HILIC/CEX. Such an approach takes simultaneous advantage of both the charged character of peptides as well as any hydrophilic/ hydrophobic properties they possess.

X-4-2 Synthetic model peptides used in this study

Figure X-1 shows the sequences of the synthetic model peptides, based on the native V681 (denoted S_L), with L-Ser at position 11 of the sequence, *i.e.*, in the hydrophilic face of the amphipathic α -helix. This position (denoted as X11 in Figure X-1) was chosen for the substitution site since it was in the very centre of the hydrophilic face of the amphipathic α -helix and is, therefore, surrounded by a very hydrophilic environment comprised of Thr and Ser residues (classified as containing uncharged, polar side-chains) and Lys and His residues (classified as basic, potentially positively charged side-chains). In contrast, the hydrophobic face is comprised solely of non-polar residues: Ala (containing a small, slightly hydrophobic side-chain), Val (containing a larger, moderately hydrophobic side-chain), Leu and Ile (both containing bulky, strongly hydrophobic side-chains), and Phe and Trp (both containing aromatic, hydrophobic side-chains). Overall, the sizes of the hydrophilic and hydrophobic faces of the helix are essentially identical, enabling a good comparison of the relative efficacies of RP-HPLC and HILIC/CEX to separate different peptide analogues. It should be noted that the non-polar face of the amphipathic α -helix represents a preferred binding domain for RP-HPLC, *i.e.*, this face will bind preferentially to a reversed-phase hydrophobic stationary phase (Steiner *et al.*, 1998; Zhou *et al.*, 1990); conversely, the hydrophilic face should represent a preferred binding domain for a hydrophilic stationary phase such as the strong

cation-exchange matrix employed for HILIC/CEX in the present study. Evidence for such hydrophilic preferred binding domains has been described previously by our laboratory for both amphipathic α -helical peptides (Mant *et al.*, 1998b) as well as cyclic amphipathic β -sheet peptides (Mant *et al.*, 1998a).

For the present study, the L- and D-amino acids chosen for substitution at position 11 of the peptide sequence represented a range of side-chain properties. Thus, the three non-polar residues, Leu, Val and Ala, contain side-chains of increasing size and hydrophobicity: $A_L, A_D < V_L, V_D < L_L, L_D$; Ser (S_L, S_D) contains a small, polar (i.e., hydrophilic) side-chain; finally, Lys (K_L, K_D) contains a positively charged side-chain. The peptide analogue substituted with Gly at position 11 (G) represents the situation where no side-chain is present at the centre of the hydrophilic face of the helix.

The native sequence, V_{681} , is known to have a high potential to form an α -helix (Zhang *et al.*, 1998; Zhang *et al.*, 1999), as determined by circular dichroism spectroscopy. In addition, it has been shown that, even where helix-disrupting D-amino acids are substituted into α -helical peptides, high helicity may still be attained (generally comparable to their L-amino acid substituted analogues) in the presence of helix-inducing solvents such as trifluoroethanol (TFE) (Chen *et al.*, 2002). Such was also the case in the present study, with high helicities for all L- and D-peptide analogues being obtained in 50% (v/v) TFE (data not reported). The run conditions characteristic of RP-HPLC (hydrophobic stationary phase, increasingly non-polar mobile phase) are well known to induce helical structure in potentially helical molecules (Blondelle *et al.*, 1995; Purcell *et al.*, 1995c; Steer *et al.*, 1998; Zhou *et al.*, 1990). Thus, the peptides used in the present study will be eluted as single-stranded amphipathic α -helices during RP-HPLC,

interacting with the stationary phase through preferential binding with their hydrophobic faces. Further, it has also been previously shown that high concentrations of organic modifiers such as acetonitrile can induce helix formation in a potentially helical peptide (Lau *et al.*, 1984b; Zhou *et al.*, 1990). Thus, under characteristic conditions of HILIC/CEX (high acetonitrile concentration in the mobile phase; 70% (v/v) in the present study), the peptide analogues would also be expected to be α -helical, allowing interaction of the hydrophilic face with the ion-exchange matrix (Mant *et al.*, 1998b).

X-4-3 RP-HPLC of amphipathic α -helical diastereomeric peptides

Figure X-2 shows the elution reversed-phase elution profiles of two mixtures of diastereomeric peptide pairs at 25°C (top panels) and 65°C (bottom panels). From Figure X-2, the D-substituted analogues were consistently eluted faster than their corresponding diastereomers. This decrease in retention time of the D-analogues compared to the L-analogues can be rationalized as being due to disruption of the amphipathic α -helix due to the introduction of the D-amino acid (Aguilar *et al.*, 1993; Chen *et al.*, 2002; Krause *et al.*, 2000; Rothmund *et al.*, 1995; Rothmund *et al.*, 1996), this disruption affecting both the hydrophobic face of the helix as well as the hydrophilic face where the substitution has been made. The overall effect on the non-polar face would be a decrease in the apparent hydrophobicity of this face when the helix is substituted with a D-amino acid relative to its L-diastereomer and, hence, a decrease in retention time of the former compared to the latter. Also from Figure X-2, the elution order of the analogues is generally in order of increasing hydrophobicity of the substituted residues within the L-analogues, *i.e.*, $K_L < A_L < L_L$ (Figure X-2, left panels) and $S_L < V_L$ (Figure X-2, right panels). However, this is not necessarily true with the D-substituted analogues. Thus, A_D

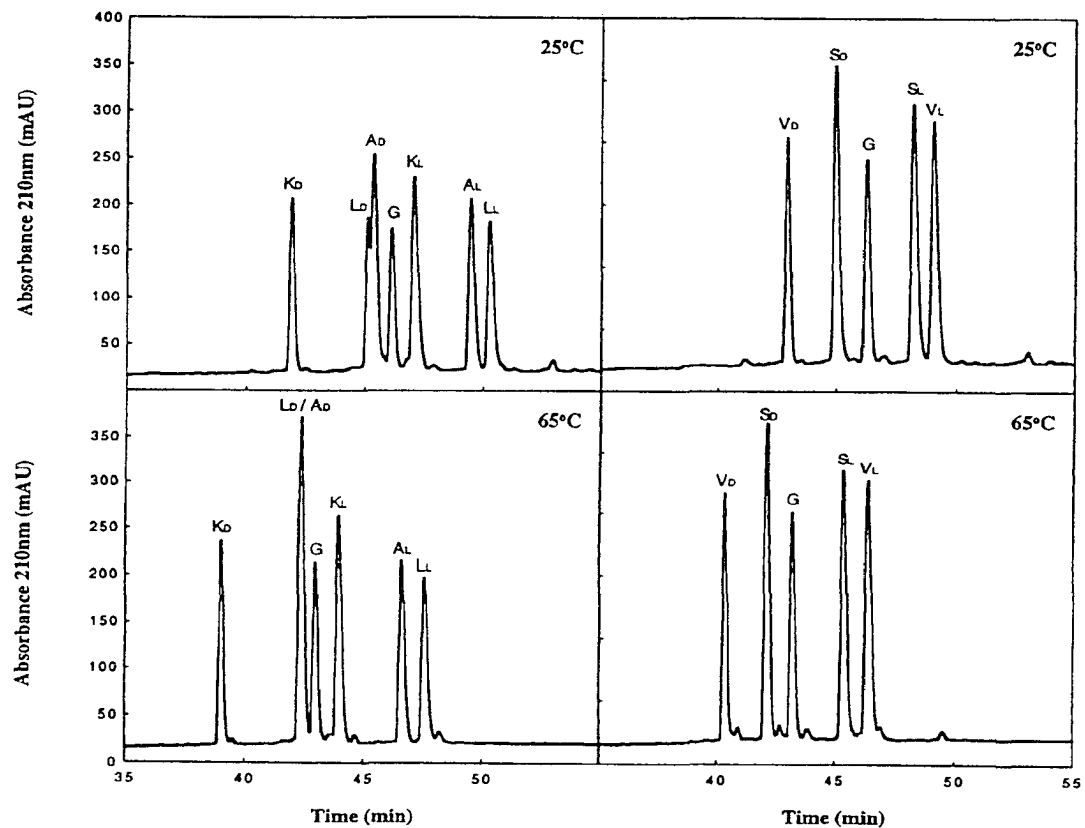


Figure X-2 RP-HPLC of diastereomeric amphipathic α -helical peptides. Column: reversed-phase Zorbax SB300-C₈ (150x2.1 mm I.D., 5 μ m particle size, 300 Å pore size). Conditions: linear AB gradient (1%B/min) at a flow rate of 0.3 ml/min, where eluent A is 0.05% *aq.* TFA, pH 2.0, and eluent B is 0.05% TFA in acetonitrile. The sequences of the peptides are shown in Figure X-1.

and L_D are almost co-eluted at 25°C (Figure X-2, top left panel), with L_D being eluted just prior to A_D at 25°C (top left panel); from Figure X-2, right panels, V_D, with a hydrophobic side-chain is eluted prior to S_D, which contains a polar, hydrophilic side-chain. This observation is likely due to the varying magnitude of disruption of the preferred non-polar binding domain of the peptide helix when different D-amino acids are substituted into the sequence, *i.e.*, different D-amino acids disrupt the non-polar face to differing extents, resulting in the RP-HPLC elution orders shown for the D-analogues. Considering the elution of V_D significantly prior to S_D, for instance, reflects the observation by Chen *et al.* (Chen *et al.*, 2002) that amino acids, such as Val, with β -branched side-chains showed the greatest reduction in apparent side-chain hydrophobicity due to D-amino acid substitutions into the centre of the non-polar face of an amphipathic α -helix.

The elution behavior of K_L (Figure X-2, left panels) relative to analogue G is of note, since it has been clearly shown in model random coil peptides (Guo *et al.*, 1986a; Guo *et al.*, 1986b) that substitution of a Gly residue by a positively charged Lys residue leads to a significant decrease in peptide retention time during RP-HPLC at pH 2.0. In contrast, from Figure X-2 (left panels) K_L is eluted after the G analogue. This observation is likely due to the L-Lys amino acid being in the centre of the hydrophilic face of the amphipathic α -helix, *i.e.*, on the opposite side of the hydrophobic face which binds preferentially to the reversed-phase matrix. Clearly, the overall hydrophilicity of the Lys side-chain still has an effect on peptide retention behavior (witness its elution prior to the A_L and L_L analogues containing non-polar groups at the substitution site); however, this effect is likely diminished compared to the situation where L-Lys was substituted into the

centre of the non-polar face of the helix and was therefore able to interact to a greater extent with the hydrophobic stationary phase. In other words, substitutions, whether hydrophobic or hydrophilic, when made in the hydrophilic face of an amphipathic α -helix, are not part of the preferred binding domain interacting with the hydrophobic matrix and have consequently lesser effects than if located in the centre of the hydrophobic face.

Concerning the effect of temperature on the RP-HPLC elution behavior of the peptides, all peptides showed a decrease in retention time at 65 °C (bottom panels) compared to 25 °C (top panels), with no significant effect on resolution. Indeed, the major effect of temperature on resolution was a further deterioration of the poor separation of L_D and A_D seen at 25 °C (Figure X-2, top left panel) when the temperature was raised to 65 °C (Figure X-2, bottom left panel), where the two peptides are now co-eluted.

X-4-4 HILIC/CEX of amphipathic α -helical diastereomeric peptides

Figure X-3 shows the HILIC/CEX elution profiles of the two mixtures of diastereomeric peptides at 25 °C (top panels) and 65 °C (bottom panels). In a similar manner to their RP-HPLC retention behavior (Figure X-2), the D-substituted analogues were again consistently eluted faster than their corresponding diastereomers (Figure X-3). As noted above for the RP-HPLC resolution of diastereomeric peptide pairs (Figure X-2), this separation by HILIC/CEX (Figure X-3) is probably a result of disruption of the preferred binding domain (in this case the hydrophilic preferred binding domain represented by the polar face of the amphipathic α -helix) by a D-amino acid substitution into the centre of the hydrophilic face of the helix. Interestingly, the observation that the

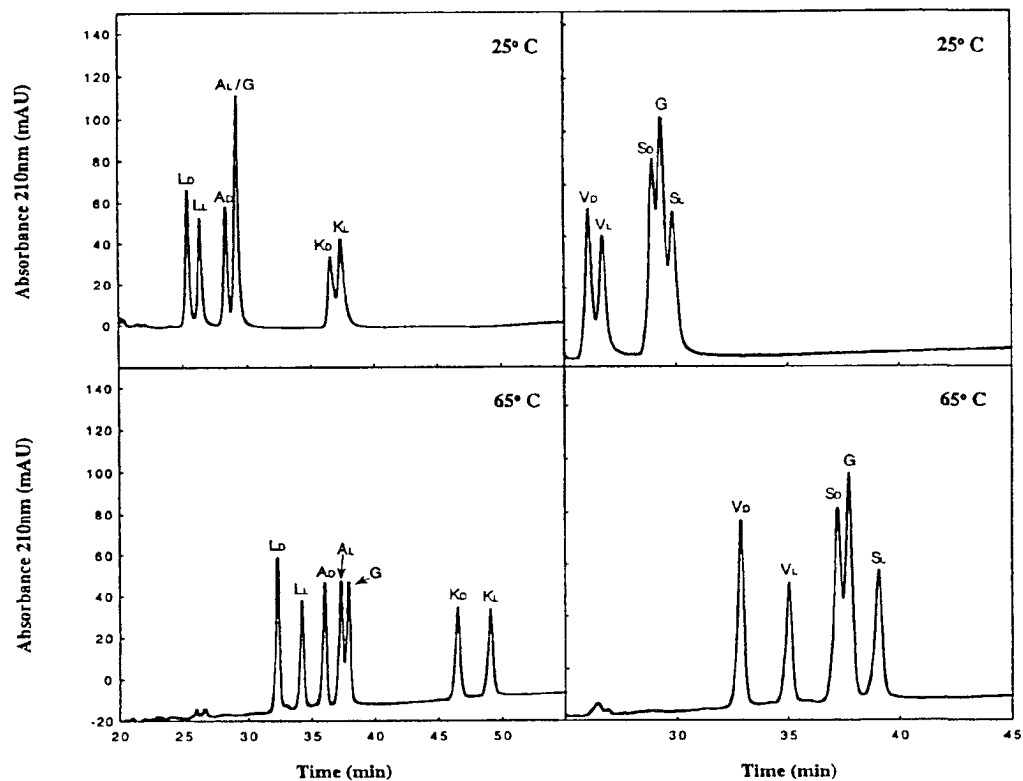


Figure X-3 HILIC/CEX of diastereomeric amphipathic α -helical peptides. Column: strong cation-exchange PolySulfoethyl A (200 \times 2.1 mm I.D., 5 μ m particle size, 300 \AA pore size). Conditions: linear AB gradient (5 mM NaClO₄ to 250 mM NaClO₄ in 50 min) at a flow rate of 0.3 ml/min, where eluent A is 5 mM *aq.* triethylammonium phosphate (TEAP), pH 4.5, containing 5 mM NaClO₄ and eluent B is 5 mM *aq.* TEAP, pH 4.5, containing 250 mM NaClO₄, both eluents also containing 70% (v/v) acetonitrile. The sequences of the peptides are shown in Figure X-1.

D-analogues are eluted prior to their respective L-analogues suggests that the apparent hydrophilicity of the preferred binding domain is reduced by an L- to D-amino acid substitution in the centre of the polar face of the α -helix. Also from Figure X-3, the elution order of the analogues is in order of increasing hydrophilicity of the substituted residues within both the L- and D-analogues, *i.e.*, $L < A < K$ (Figure X-3, left panels) and $V < S$ (Figure X-3, right panels).

The effect of temperature on the HILIC/CEX elution behavior of the peptides (Figure X-3) is quite distinct to that of its effect during RP-HPLC (Figure X-2), with the retention times of the peptides all increasing on raising the temperature from 25°C (top panels) to 65 °C (bottom panels). In addition, resolution of the peptides is greatly improved at the higher temperature. Thus, A_L and G are co-eluted at 25 °C (Figure X-3, top left) but mainly resolved at 65 °C (Figure X-3, bottom left); the L_L/L_D , A_L/A_D and K_L/K_D peptide pairs are also better separated at 65 °C (bottom left) compared to 25 °C (top left). From Figure X-3 (right panels), the improvement in separation of V_D and V_L at 65 °C (bottom right) compared to 25 °C (top right) is quite clear, as is the improvement in resolution of S_D , G and S_L .

X-4-5 Comparison of RP-HPLC and HILIC/CEX of amphipathic α -helical diastereomeric peptides at 25 °C and 65 °C

Table X-1 summarizes retention time data for the L- and D-peptide analogues during RP-HPLC (Figure X-2) and HILIC/CEX (Figure X-3) at temperatures of 25 °C and 65 °C. From Table X-1, the effect of raising the temperature of the separation from 25 °C to 65 °C has now been quantified by the expression $\Delta t_R(65\text{ °C} - 25\text{ °C})$, denoting the retention time change for each peptide with the temperature rise. As illustrated by the

Table X-1 Effect of temperature on peptide retention behavior in RP-HPLC and HILIC/CEX

Peptide ^a	RP-HPLC ^b			HILIC/CEX ^c		
	$t_{R25^{\circ}\text{C}}$	$t_{R65^{\circ}\text{C}}$	Δt_{R} (65°C-25°C)	$t_{R25^{\circ}\text{C}}$	$t_{R65^{\circ}\text{C}}$	Δt_{R}^{d} (65°C-25°C)
Mix 1						
L _L	50.3	47.6	-2.7	26.4	34.2	+7.8
L _D	45.1	42.4	-2.7	25.4	32.3	+6.9
A _L	49.5	46.6	-2.9	29.2	37.3	+8.1
A _D	45.3	42.4	-2.9	28.4	36.0	+7.6
G	46.1	43.0	-3.1	29.2	37.9	+8.7
K _L	47.1	43.9	-3.2	37.4	49.0	+11.6
K _D	41.9	39.0	-2.9	36.5	46.5	+10.0
Mix 2						
V _L	49.0	46.4	-2.6	26.8	35.1	+8.3
V _D	42.9	40.4	-2.5	26.1	33.0	+6.9
S _L	48.1	45.4	-2.7	29.9	39.2	+9.3
S _D	44.9	42.1	-2.8	29.0	37.3	+8.3
G	46.2	43.2	-3.0	29.3	37.7	+8.4

- a. Sequence and denotation of peptides shown in Figure X-1.
b. RP-HPLC conditions shown in Figure X-2. Column, reversed-phase Zorbax SB-300-C₈.
c. HILIC/CEX conditions shown in Figure X-3. Column, strong cation-exchange (PolySulfoethyl A).
d. Δt_{R} refers to the retention time of a peptide at 65°C ($t_{R65^{\circ}\text{C}}$) minus its retention time at 25°C ($t_{R25^{\circ}\text{C}}$).

elution profiles shown in Figure X-2, all peptides show a decrease in RP-HPLC retention time (*i.e.*, a negative ΔT_R value) as the temperature is increased. In addition, this negative value is very similar for all peptides shown in Table X-1: an average of $\Delta t_R = -2.8 \pm 0.4$ min. In contrast, and as illustrated in Figure X-3, all peptides show a quite significant increase in retention time with the temperature change from 25 °C to 65 °C. Points to note include the observation that the effect of the temperature rise is consistently greater for the L-substituted analogues compared to the D-substituted peptides. The Δt_R values for the L-analogues and D-analogues show an average of +8.4 min and +7.4 min, respectively, excluding G, K_L and K_D. Interestingly, the effect of the rise in temperature from 25 °C to 65 °C appeared to have a greater effect on K_L and K_D (Δt_R values of 11.6 min and 10.0 min, respectively) than the other peptide analogues, suggesting that the presence of an extra positive charge (which is concomitantly a significant increase in hydrophilicity of the polar face of the helix) enhances the effect of temperature during HILIC/CEX. Indeed, although subtle, the greater Δt_R values of S_L (+9.3 min) and S_D (+8.3 min) relative to the peptides substituted with non-polar Ala, Leu and Val residues (Δt_R ranges of +7.8 min to +8.3 min for the L-analogues and +6.9 min to +7.6 min for the D-analogues) support the conclusion that the effect of temperature during HILIC/CEX is related to the overall hydrophilicity of the polar face of the α -helix, *i.e.*, the more hydrophilic (less hydrophobic) the preferred binding domain, the greater the increase in retention time with increasing temperature.

This observation is illustrated graphically in Figure X-4 which plots the effect of raising the temperature from 25 °C to 65 °C on the retention times of L_L (representing an amphipathic helix with a bulky, hydrophobic side-chain substituted into the centre of the

hydrophilic face), S_L (substituted with a polar, uncharged side-chain), and K_L (substituted with a positively charged side-chain). Also included is the effect of temperature on a 10-residue random coil peptide standard, S5. From Figure X-4 (top), the small, and similar, effect of temperature on RP-HPLC of the three α -helical peptides is quite clear, with essentially parallel decreasing profiles as the temperature is raised from 25 °C to 65 °C. Indeed, the profiles of these three peptides were also similar to that of the random coil peptide standard, S5, albeit the latter had a slightly less steep profile. In contrast, the profiles for the three helical peptides during HILIC/CEX (Figure X-4, bottom) were somewhat more distinct from each other, as well as from the random coil S5, as the temperature was raised from 25 °C to 65 °C. Thus, the positive slopes of the three helical peptides increased in the order $L_L < S_L < K_L$, *i.e.*, in order of increasing hydrophilicity of the substituted side-chain at the centre of the hydrophilic face of the helix, as noted previously. Interestingly, the positive slope of S5 was considerably shallower than those of the three helical peptides, *i.e.*, the retention time of this peptide with negligible secondary structure increased little with a rise in temperature compared to the amphipathic α -helical peptides. It is also interesting to note that despite the reversal in retention time order between the two HPLC modes ($K_L < S_L < L_L$ for RP-HPLC (Figure X-4, top) and $L_L < S_L < K_L$ for HILIC/CEX (Figure X-4, bottom)), the random coil peptide S5 was eluted first in both modes. This again suggests a link between the retention behavior of peptides with a defined conformation (in this case α -helical peptides with defined hydrophilic and hydrophobic faces) during RP-HPLC and HILIC/CEX compared to a peptide with negligible secondary structure.

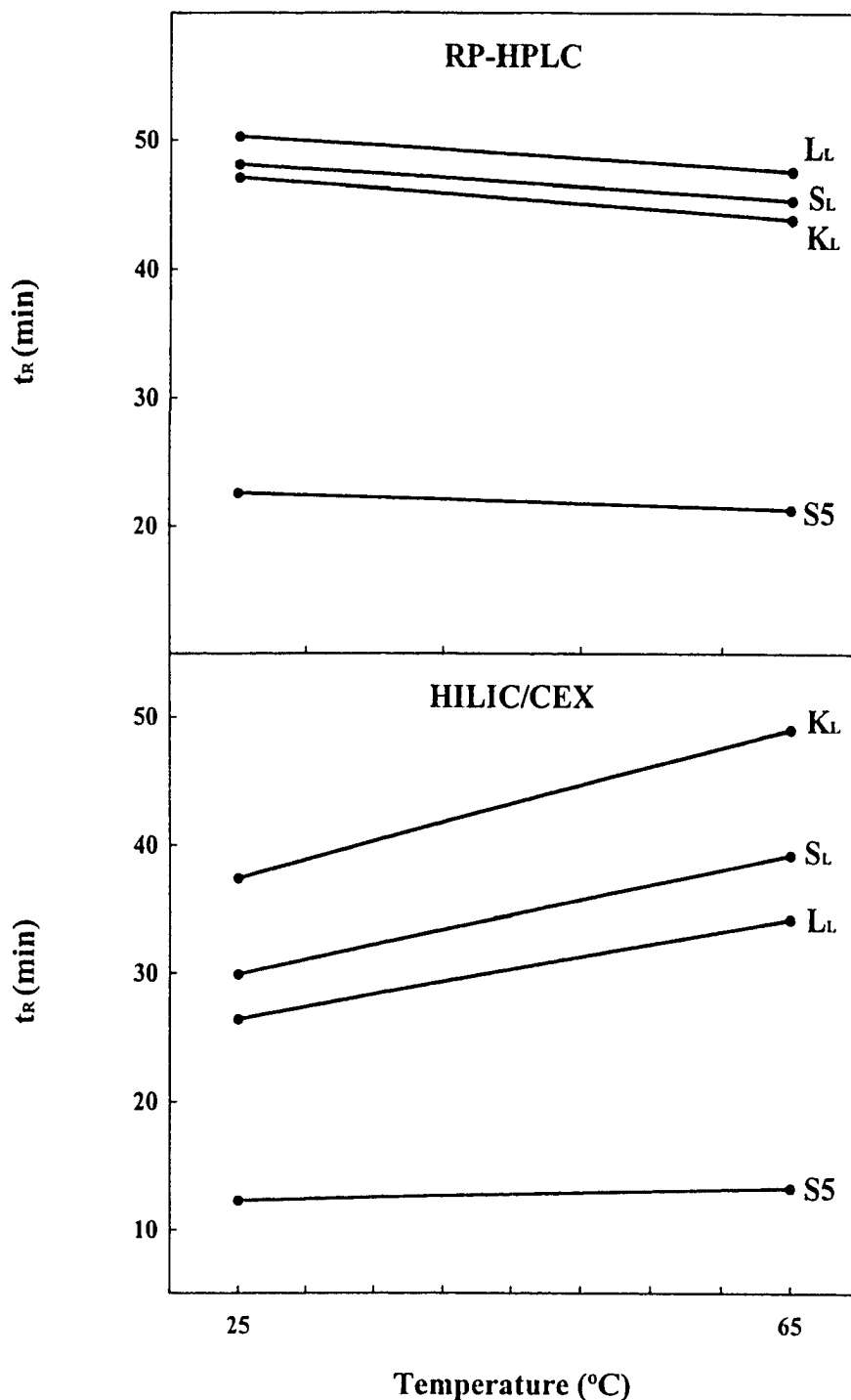


Figure X-4 Effect of temperature on retention behavior of diastereomeric amphipathic α -helical peptides in RP-HPLC (top) and HILIC/CEX (bottom). Columns: (top) reversed-phase Zorbax SB300-C₈ (150×2.1 mm I.D., 5 μ m particle size, 300 Å pore size) and (bottom) strong cation-exchange PolySulfoethyl A (200×2.1 mm I.D., 5 μ m particle size, 300 Å pore size). Conditions for RP-HPLC and HILIC/CEX as in Figures X-2 and X-3, respectively. The sequences of the peptides are shown in Figure X-1. The sequence of the random coil peptide standard, S5, is Ac-RGVVGLGLGK-amide.

Also from Figure X-4, it is important to note that, under the conditions employed for RP-HPLC and HILIC/CEX in this study, the three L-analogues were considerably better separated by HILIC/CEX (Figure X-4, bottom) compared to RP-HPLC (Figure X-4, top). These results reflect previous results from this laboratory (Mant *et al.*, 1998b) that amphipathic α -helical peptides with substitutions made in the hydrophilic face of the helix are likely to be better separated by HILIC/CEX compared to RP-HPLC. A more thorough investigation of this phenomenon for the present peptide analogues (where L- and D-amino acids are substituted into the hydrophilic and hydrophobic faces of the amphipathic α -helices) is the subject of a separate study (Hodges *et al.*, 2004).

Table X-2 now examines the effect of temperature on the separation of diastereomeric peptide pairs. From Table X-2, there is no clear link between the inherent hydrophobicity/hydrophilicity of a particular side-chain and the decrease in retention time in both HPLC modes ($\Delta t_{R25\text{ }^\circ\text{C}}$, $\Delta t_{R65\text{ }^\circ\text{C}}$) when the L-amino acid is substituted by its D-enantiomer. However, it can be seen that there is a smaller difference in Δt_R values between L- and D-peptide pairs during HILIC/CEX compared to RP-HPLC at both 25 °C and 65 °C. In contrast, the separation between such peptide pairs is enhanced during HILIC/CEX when raising the temperature ($\Delta\Delta t_R$ values ranging from +0.5 min to +1.6 min) compared to the negligible effect during RP-HPLC ($\Delta\Delta t_R$ values ranging from -0.3 min to +0.1 min, the negative values for V_L/V_D and K_L/K_D actually indicating a deterioration in the separation).

Table X-2 Effect of temperature on separation of diastereomeric peptide pairs by RP-HPLC and HILIC/CEX

Peptide Pair ^a	RP-HPLC ^b			HILIC/CEX ^c		
	Δt_R 25°C ^d	Δt_R 65°C ^d	$\Delta\Delta t_R$ ^e	Δt_R 25°C ^d	Δt_R 65°C ^d	$\Delta\Delta t_R$ ^e
L _L /L _D	5.2	5.2	0	1.0	1.9	0.9
V _L /V _D	6.1	6.0	-0.1	0.7	2.1	1.4
A _L /A _D	4.2	4.2	0	0.8	1.3	0.5
S _L /S _D	3.2	3.3	0.1	0.9	1.9	1.0
K _L /K _D	5.2	4.9	-0.3	0.9	2.5	1.6

a. Sequence and denotation of peptides shown in Figure X-1

b. RP-HPLC conditions are shown in Figure X-2. Column, reversed-phase Zorbax SB-300-C₈.

c. HILIC/CEX conditions are shown in Fig X-3. Column, strong cation-exchange (PolySulfoethyl A).

d. Δt_R refers to the retention time of the first peptide (L-analogue) shown in each pair of peptides minus the retention time of the second (D-analogue) peptide

e. $\Delta\Delta t_R$ is the Δt_R 65°C value minus the Δt_R 25°C value

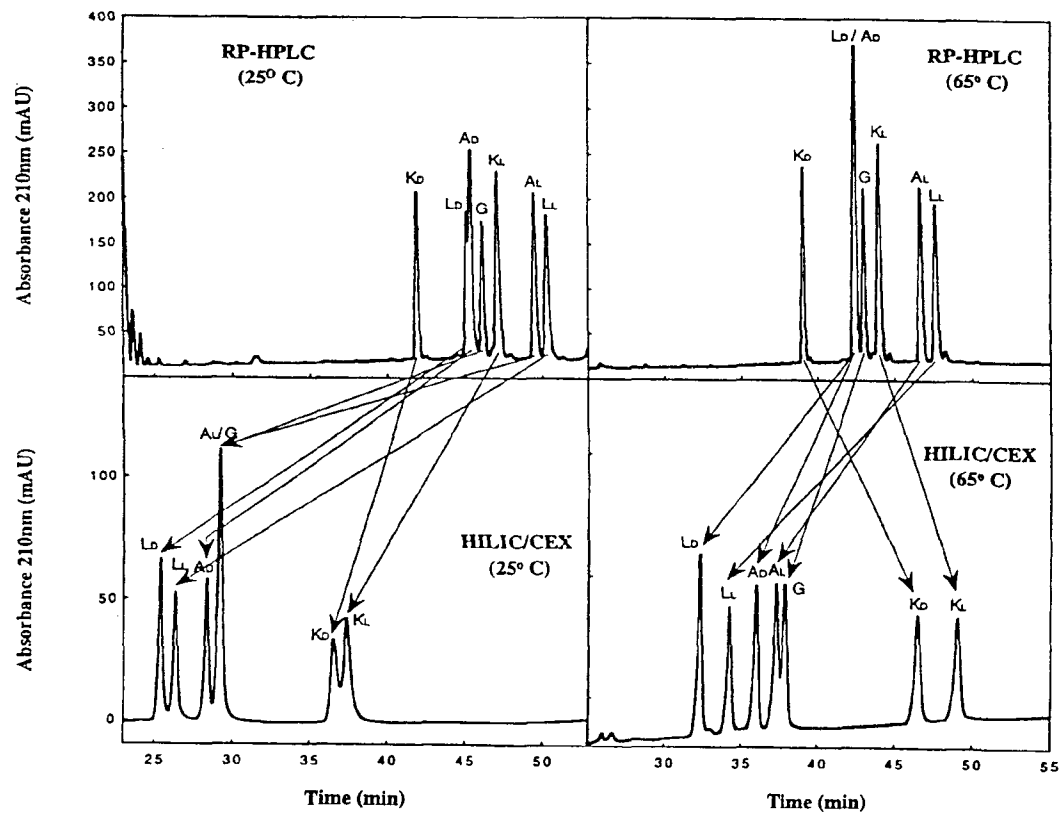


Figure X-5 Comparison of selectivity changes in the separation of diastereomeric amphipathic α -helical peptides by RP-HPLC (top) and HILIC/CEX (bottom) at 25 °C (left panels) and 65 °C (right panels). Columns: (top) reversed-phase Zorbax SB300-C₈ (150x2.1 mm I.D., 5 μ m particle size, 300 Å pore size) and (bottom) strong cation-exchange PolySulfoethyl A (200x2.1 mm I.D., 5 μ m particle size, 300 Å pore size). Conditions for RP-HPLC and HILIC/CEX as in Figures X-2 and X-3, respectively. The sequences of the peptides are shown in Figure X-1.

X-4-6 Comparison of selectivity of RP-HPLC and HILIC/CEX separation of amphipathic α -helical diastereomeric peptides

Figure X-5 compares the selectivity of RP-HPLC (top panels) and HILIC/CEX (bottom panels) for the separation of a mixture of seven amphipathic α -helical diastereomeric peptides at 25 °C (left panels) and 65 °C (right panels). As the arrows highlight for the 25 °C runs (Figure X-5, left panels), there is a considerable switch in elution order of the peptides between the two HPLC modes, underlining the useful complementary nature of RP-HPLC and HILIC/CEX. Of note here also is the clear illustration of the greater time required to elute the seven peptides during RP-HPLC (a range of 41.9 min for K_D to 50.2 min for L_L) compared to HILIC/CEX (25.4 min for L_D to 37.4 min for K_L) under the conditions employed for the two HPLC modes. However, this difference is strikingly diminished when the temperature is raised to 65 °C. Thus, from Figure X-5 (right panels), due to the small reduction in RP-HPLC retention times with the rise in temperature concomitant with the significant increase in HILIC/CEX retention times, the retention time range between the two modes is now more similar, allowing perhaps a more valid comparison of the complementary selectivity differences between RP-HPLC and HILIC/CEX of these peptides. In addition, the superior resolution of the peptides in this particular peptide mixture by HILIC/CEX at 65 °C compared to RP-HPLC at this temperature (and, indeed, to RP-HPLC at 25 °C) is well illustrated.

X-5 Conclusions

We have compared the ability of RP-HPLC and HILIC/CEX to separate mixtures of amphipathic α -helical diastereomeric peptides, with L- and D-amino acid substitutions

made in the centre of the hydrophilic face of the α -helix. While both methods proved to be effective for separating such peptides, they did so often with greatly different selectivities, underlining the useful complementary nature of the two HPLC methods. Interestingly, temperature had a substantial effect on HILIC/CEX of the peptides, more so than RP-HPLC, with a rise in temperature from 25 °C to 65 °C both increasing the retention times of the peptides, as well as improving peptide separation. These results again stress the potential of HILIC/CEX, both as a peptide separation mode in its own right as well as an excellent complement to RP-HPLC.

CHAPTER XI

Monitoring the Hydrophilicity/Hydrophobicity of Amino Acid Side-Chains in the Non-Polar and Polar Faces of Amphipathic α -Helices by Reversed-Phase and Hydrophilic Interaction/Cation-Exchange Chromatography

A version of this chapter has been published: Hodges, R. S., Chen, Y., Kopecky, E. and Mant, C. T. (2004) *J. Chromatogr. A.* **1053**, 161-172 Only methods unique to this chapter are described in the **Experimental** section, the remaining general methods are described in Chapter III.

XI-1 Abstract

The ability to monitor precisely the hydrophobicity/hydrophilicity effects of amino acid substitutions in both the non-polar and polar faces of amphipathic α -helical peptides is critical in such areas as the rational *de novo* design of more effective antimicrobial peptides. The present study reports our initial results of employing the complementary separation modes of reversed-phase high-performance chromatography (RP-HPLC) and hydrophilic interaction/cation-exchange chromatography (HILIC/CEX) to monitor the effect on apparent peptide hydrophilicity/hydrophobicity and amphipathicity of substituting single L- or D-amino acids into the centre of the non-polar or polar faces of a 26-residue biologically active amphipathic α -helical peptide, V₆₈₁. Our results clearly show that RP-HPLC and HILIC/CEX are best suited for resolving amphipathic peptides where substitutions are made in the non-polar and polar faces respectively. Further, RP-HPLC and HILIC/CEX were demonstrated to be excellent monitors of hydrophilicity/-hydrophobicity variations where amino acid substitutions were made in these respective faces. We believe these complementary high-performance

modes offer excellent potential for rational design of novel amphipathic α -helical biologically active peptides.

XI-2 Introduction

The ever-increasing development of bacterial resistance to traditional antibiotics has precipitated an urgent requirement for new antibiotics possessing novel modes of action as well as different cellular targets compared to existing antibiotics in order to decrease the likelihood of development of resistance. Antimicrobial peptides may represent such a new class of antibiotics and their design and structure-activity relationships have become an area of active research in recent years (Hancock, 1997; Hancock *et al.*, 1998). From numerous studies on both natural and synthetic α -helical and β -sheet cationic antimicrobial peptides (so-called due to their possession of a net positive charge resulting from the presence of excess arginine and/or lysine residues), factors believed to be important for antimicrobial activity have been identified: the presence of both hydrophobic and basic residues, as well as a defined secondary structure (α -helix or β -sheet), either preformed or inducible, and an amphipathic nature which segregates basic and hydrophobic residues to opposite sides of the molecule in lipid or lipid-mimicking environments (Blondelle *et al.*, 1999; Hancock, 1997; Hancock *et al.*, 1998; Houston *et al.*, 1998; Kondejewski *et al.*, 1996; Kondejewski *et al.*, 1999; Lee *et al.*, 2003a; Lee *et al.*, 2004; Oh *et al.*, 1999; Pathak *et al.*, 1995). This amphipathic structural feature is believed to play a critical role in the antimicrobial mechanism of action, with the hydrophilic (positively charged) domain of the peptide proposed to initiate peptide interaction with the negatively charged bacterial surface and the negatively charged head

groups of bilayer phospholipids. The hydrophobic domain of the amphipathic peptide would then permit the peptide to enter the interior of the membrane (Bechinger, 1997; Blondelle *et al.*, 1999; Epanand *et al.*, 1999; Wu *et al.*, 1999). Subsequent bilayer disruption or concomitant channel formation in, for example, the bacterial cytoplasmic membrane may lead to the leakage of cell contents and cell death (Bechinger, 1997; Epanand *et al.*, 1999; Sitaram *et al.*, 1999; Wu *et al.*, 1999).

For amphipathic α -helical peptides specifically, antimicrobial potency depends upon peptide amphipathicity, hydrophobicity and helicity, such features only coming into play when the helical structure is induced in a hydrophobic environment such as a bacterial cell membrane (Liu *et al.*, 1998) or, conversely, disrupted in an aqueous environment (Chen *et al.*, 2002). Clearly, the ability to monitor the hydrophilicity/hydrophobicity effects of amino acid substitutions in both the non-polar and polar faces of potentially useful antimicrobial amphipathic α -helical peptides is critical in the design process for such molecules. Reversed-phase high-performance liquid chromatography (RP-HPLC) has, in addition to being an effective separation tool for peptide separations, also proven to be a useful physicochemical probe of peptide and protein structure (Blondelle *et al.*, 1995; Blondelle *et al.*, 1996; Hodges *et al.*, 1994; Lazoura *et al.*, 1997; Mant *et al.*, 1993; Purcell *et al.*, 1995c; Sercda *et al.*, 1994; Steiner *et al.*, 1991; Zhou *et al.*, 1990). The latter use includes the monitoring by RP-HPLC of the hydrophilicity/hydrophobicity of the non-polar face of amphipathic α -helical molecules, due to the interaction of this non-polar face (the preferred binding domain) with the hydrophobic stationary phase. In an analogous manner, we propose that mixed-mode hydrophilic interaction/cation-exchange chromatography (HILIC/CEX) may

provide the required tool to monitor hydrophilicity/hydrophobicity of the polar face of amphipathic α -helical molecules, due to the interaction of this polar face with the hydrophilic/charged cation-exchange matrix. Although this novel high-performance mode was originally developed in the authors' laboratory strictly as a novel separation approach for peptide separations (Hartmann *et al.*, 2003; Litowski *et al.*, 1999; Mant *et al.*, 1998a; Mant *et al.*, 1998b; Mant *et al.*, 2000; Zhu *et al.*, 1991; Zhu *et al.*, 1992), subsequently adapted by other researchers for protein separations (Lindner *et al.*, 1996; Lindner *et al.*, 1997; Lindner *et al.*, 1998; Lindner *et al.*, 1999; Mizzen *et al.*, 2000), we believe that HILIC/CEX can transcend its original development as simply a complementary separation technique to RP-HPLC and aid in the rational design of potentially valuable amphipathic α -helical antibiotics.

Thus, the present study represents the first report describing the employment of these complementary separation modes to monitor the effect on apparent peptide hydrophilicity/hydrophobicity and amphipathicity of substituting single L- or D-amino acids into the centre of the non-polar or polar faces of a 26-residue biologically active amphipathic α -helical peptide denoted V₆₈₁ (Zhang *et al.*, 1998; Zhang *et al.*, 1999).

XI-3 Experimental

XI-3-1 Analytical HPLC columns and instrumentation

RP-HPLC runs were carried out on a Zorbax SB300-C₈ column (150 x 2.1 mm I.D., 5- μ m particle size; 300-Å pore size) from Agilent Technologies (Little Falls, DE, USA). Mixed-mode HILIC/CEX runs were carried out on a poly (2-sulfoethyl

aspartamide)-silica (PolySulfoethyl A) strong cation-exchange column (200 x 2.1 mm I.D., 5 μ m, 300 Å) from PolyLC (Columbia, MD, USA).

XI-3-2 HPLC run conditions

RP-HPLC: linear AB gradient elution (1% B/min) at a flow-rate of 0.3 ml/min, where eluent A is 0.05% *aq.* TFA, pH 2.0, and eluent B is 0.05% TFA in acetonitrile; temperature, 25°C.

HILIC/CEX: linear AB gradient elution of 5 mM NaClO₄ to 250 mM NaClO₄ in 60 min at a flow-rate of 0.3 ml/min, where buffer A is 5 mM triethylammonium phosphate (TEAP), pH 4.5, containing 5mM NaClO₄ and buffer B is 5 mM *aq.* TEAP, pH 4.5, containing 250 mM NaClO₄, both buffers containing 70% (v/v) acetonitrile at temperatures of 25°C or 65°C.

Samples injected onto the columns contained 5-10 nmol of each peptide. The gradient delay time for the HPLC system was 1.2 min. Samples were dissolved in the starting eluents for both HPLC modes. Peptide elution order was definitively established by spiking with individual peptides and individual injections. The reproducibility of the peptide separations in both HPLC modes was confirmed via duplicate (RP-HPLC) and triplicate (HILIC/CEX) runs.

XI-4 Results and discussion

XI-4-1 RP-HPLC versus HILIC/CEX of amphipathic α -helical peptides

RP-HPLC has proven to be an ideal system for measuring hydrophobicity, amphipathicity and association of α -helical and β -sheet peptides (Benedek, 1993; Chen *et al.*, 2002; Hodges *et al.*, 1994; Kondejewski *et al.*, 1999; Lee *et al.*, 2003b; Mant *et al.*,

1989; Mant *et al.*, 1998a; Mant *et al.*, 1998b; Mant *et al.*, 2002b; Mant *et al.*, 2002c; Mant *et al.*, 2003a; Mant *et al.*, 2003b; Richards *et al.*, 1994; Rosenfeld *et al.*, 1993; Sereda *et al.*, 1994; Tripet *et al.*, 2000; Yu *et al.*, 2000). The non-polar face of, for example, an amphipathic α -helix represents a preferred binding domain for RP-HPLC, *i.e.*, this face will bind preferentially to a reversed-phase hydrophobic stationary phase (Steiner *et al.*, 1991; Zhou *et al.*, 1990). Indeed, Zhou *et al.* (Zhou *et al.*, 1990) clearly demonstrated that, because of this preferred binding domain, amphipathic α -helical peptides are considerably more retentive than non-amphipathic peptides of the same amino acid composition. Thus, this preferential binding of the non-polar face of the amphipathic peptides to a reversed-phase matrix potentially makes RP-HPLC an effective monitor of the relative hydrophilicity/hydrophobicity of the non-polar face of such peptides. It should be noted that the potential for any non-specific, electrostatic interactions between negatively charged silanol groups on the hydrophobic stationary phase and positively charged lysine residues in the peptides should be negligible at the RP-HPLC run conditions used in this study (pH 2.0), where any such silanols will be protonated, *i.e.*, neutral (Mant *et al.*, 1987b; Regnier, 1983). Indeed, application of peptide standards designed specifically to detect/monitor such non-ideal behaviour confirmed the column exhibited only ideal hydrophobic interaction behaviour under the run conditions employed (Mant *et al.*, 1987b).

The term hydrophilic interaction chromatography (HILIC) was originally introduced to describe separations based on solute hydrophilicity (Alpert, 1990), with solutes being eluted from the HILIC column in order of increasing hydrophilicity, *i.e.*, the opposite of RP-HPLC elution behaviour. Our laboratory subsequently took this concept a

step further by taking advantage of the inherent hydrophilic character of ion-exchange, specifically strong cation-exchange (CEX), columns by subjecting peptide mixtures to linear salt gradients in the presence of high levels of organic modifier, specifically acetonitrile (Hartmann *et al.*, 2003; Litowski *et al.*, 1999; Mant *et al.*, 1998a; Mant *et al.*, 1998b; Mant *et al.*, 2000; Zhu *et al.*, 1991; Zhu *et al.*, 1992). The presence of high levels of organic modifier not only suppresses any undesirable hydrophobic interactions between the peptides and the cation-exchange matrix (Burke *et al.*, 1989), but also promotes desired hydrophilic interactions between the peptides and packing. Separations based on hydrophilicity are thus superimposed on top of those based on charge, resulting in mixed-mode HILIC/CEX, *i.e.*, such an approach takes simultaneous advantage of both the charged character of peptides as well as any hydrophilic/hydrophobic properties they possess. Note that, in an analogous manner to the non-polar face of an amphipathic α -helix representing a preferred binding domain for RP-HPLC, the hydrophilic face of the α -helix would represent a preferred binding domain for a hydrophilic stationary phase such as the strong cation-exchange matrix employed for HILIC/CEX in the present study. Evidence for such hydrophilic preferred binding domains has been reported previously by our laboratory for both amphipathic α -helical peptides (Mant *et al.*, 1998b) and cyclic amphipathic β -sheet peptides (Mant *et al.*, 1998a). Hence, we believe that HILIC/CEX has excellent potential for monitoring the relative hydrophilicity/hydrophobicity of the polar face of such peptides.

We believe it is important to distinguish the difference in using ion-exchange stationary phases in a non-HILIC *versus* a true HILIC mode, such a distinction depending on the level of organic modifier in the run solvents. Thus, in (1), a non-HILIC separation,

the presence of organic modifier may be simply required to eliminate non-specific hydrophobic interactions with the matrix, improve solubility of solutes being separated or perhaps enhance ionic interactions and hydrophilic effects to improve separation of some of the individual components of a solute mixture. Reports of non-HILIC mode separations in the presence of varying levels of organic solvent have been reported for various solutes including amino acids (Hodges *et al.*, 1975), peptides (Crimmins *et al.*, 1989; Doris, 1984), proteins (Bietz, 2002; McGregor *et al.*, 1985), and carbohydrates (Tiihonen *et al.*, 2002). However, our definition of, (2), a separation carried out on an ion-exchanger in HILIC mode is the point at which the minimum organic modifier concentration required to reverse the solute elution order of a particular solute mixture relative to RP-HPLC is reached. This minimum concentration will depend on the nature and hydrophilicity/hydrophobicity of the solute components under consideration. Below this minimum concentration, hydrophilic effects may be present that affect resolution of just some of the mixture components. However, above this minimum concentration, the resolution of all sample components is affected, with higher concentrations potentially able to improve the separation still further. In fact, at very high concentrations of organic modifier, the HILIC mode is so dominant over the ion-exchange mode that a peptide with a greater net positive charge can be eluted prior to a lesser charged peptide (Mant *et al.*, 2000; Zhu *et al.*, 1992).

XI-4-2 Synthetic peptide analogues based on V_{681}

V_{681} is a biologically active amphipathic α -helix with potent antimicrobial, as well as hemolytic, properties (Zhang *et al.*, 1998; Zhang *et al.*, 1999). Such a peptide represents an excellent model to investigate the effect of introducing D-amino acids into

the centre of its non-polar or polar face in an effort to modulate the hydrophilicity/hydrophobicity of the polar and non-polar faces of the peptide. The helix-disrupting properties of D-amino acids when substituted into an α -helix made up entirely of L-amino acids is well known (Aguilar *et al.*, 1993; Chen *et al.*, 2002; Krause *et al.*, 2000; Rothemund *et al.*, 1995; Rothemund *et al.*, 1996). Indeed, our laboratory determined a set of stereochemistry stability coefficients based on substitution D-amino acids into an 18-residue amphipathic α -helix otherwise made up entirely of L-amino acids (Chen *et al.*, 2002).

Figure XI-1 shows the sequences of the synthetic peptides, based on the native V₆₈₁, with substitution positions at position 11 (denoted S11X peptides, where Ser11 is being substituted) in the hydrophilic face of the amphipathic α -helix or position 13 (denoted V13X peptides, where Val13 is being substituted) in the hydrophobic face of the amphipathic α -helix. For the S11X peptides, the substitution position (denoted as X11 in the helical net and helical wheel presentations of Figure XI-1) was chosen as being as central as possible in the hydrophilic face of the amphipathic α -helix, this face being comprised solely of polar residues, *i.e.*, Thr and Ser residues (containing uncharged, polar side-chains) and Lys and His residues (containing basic, potentially positively charged side-chains). For the V13X peptides, the substitution position (denoted as X13 in the helical net and helical wheel presentations in Figure XI-1) was chosen as being as central as possible in the hydrophobic face of the amphipathic α -helix, this face being comprised solely of non-polar residues, *i.e.*, Ala (containing a small, slightly hydrophobic side-chain), Val (containing a larger, moderately hydrophobic side-chain), Leu and Ile (both containing bulky, strongly hydrophobic side-chains), and Phe and Trp (both containing

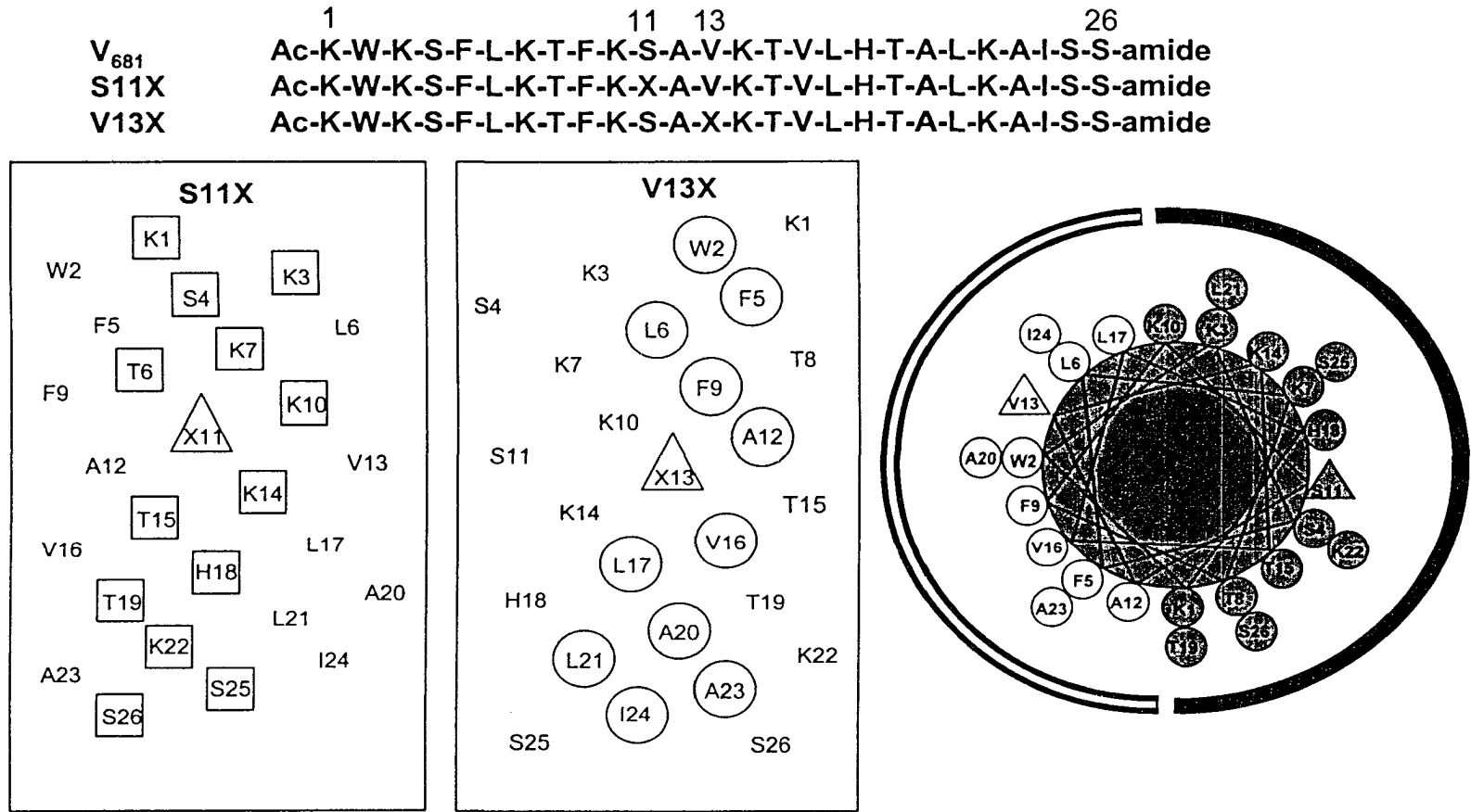


Figure XI-1 Synthetic amphipathic α -helical peptides. Top: sequence of “native” peptide, denoted V₆₈₁, and sequence of peptide analogs, where X at position 11 (S11X series) or X at position 13 (V13X series) is substituted by L-Leu (analog denoted L_L, etc. for other L-analogs), D-Leu (analog denoted L_D, etc. for other analogs), L-Val, D-Val, L-Ala, D-Ala, L-Ser, D-Ser, L-Lys, D-Lys or Gly (denoted G). Bottom left and middle: helical net representations of the peptide sequences, showing the hydrophilic face of the amphipathic α -helix of the S11X series and the hydrophobic face of the amphipathic α -helix of the V13X series; the substituted site at position 11 (S11X series) and position 13 (V13X series) is highlighted by triangles. Bottom right: helical wheel representation of the model peptide sequences; the substituted site at position 11 (S11X series) and position 13 (V13X series) is highlighted by triangles; residues in the hydrophilic face are shaded. The closed arc denotes the hydrophilic face; the open arc denotes the hydrophobic face.

aromatic, hydrophobic side-chains). Overall, the sizes of the polar and non-polar faces of the helix are essentially identical, enabling a good comparison of the effectiveness of HILIC/CEX and RP-HPLC, respectively, to monitor the hydrophilicity/hydrophobicity of these faces. In addition, these peptide analogues offer a concomitant opportunity to gauge the relative effectiveness of HILIC/CEX and RP-HPLC to separate amphipathic α -helical peptide analogues with substitutions made in the polar or non-polar faces of the amphipathic α -helix.

For the present initial study, L- and D-amino acids chosen for substitution at position 11 (polar face) or position 13 (non-polar face) of the peptide sequence (Figure XI-1) represented a range of side-chain properties: the three non-polar residues, Ala, Val and Leu contain side-chains of increasing size and hydrophobicity ($A_L, A_D < V_L, V_D < L_L, L_D$); Ser (S_L, S_D) contains a small, polar (*i.e.*, hydrophilic) side-chain; and Lys (K_L, K_D) contains a positively charged side-chain. Finally, the V_{681} analogues substituted with Gly at positions 11 or 13 (denoted G) represent the situations where no side-chain is present at the centre of the hydrophilic (position 11) or hydrophobic (position 13) faces of the helix.

Clearly, in order for both RP-HPLC and HILIC/CEX to be effective as monitors of hydrophilicity/hydrophobicity of the two faces of amphipathic α -helices, it is important that (1) the peptides under consideration must have a high potential to form α -helices; (2) this secondary structure must be present under the HPLC run conditions employed; and (3) the peptides must be eluted as single-stranded monomeric α -helices. V_{681} is known to have a high potential to form an α -helix (Zhang *et al.*, 1998; Zhang *et al.*, 1999), as determined by circular dichroism spectroscopy. The α -helix-inducing

properties of trifluoroethanol (TFE) are well documented (Cooper *et al.*, 1990; Nelson *et al.*, 1989). Indeed, Monera *et al* (Monera *et al.*, 1995), when carrying out temperature denaturation of α -helices in the presence of just 30% TFE, demonstrated that TFE not only induces α -helical structure but also stabilizes it. Chen *et al* (Chen *et al.*, 2002) demonstrated that, even where helix disrupting D-amino acids are substituted into α -helical peptides, high helicity (generally comparable to their L-amino acid substituted analogues) may still be attained in the presence of 50% TFE. This was also the case in the present study, with high helicities for all L- and D-peptide analogues being obtained in 50% (v/v) TFE (data not shown).

Since all the peptides with L- or D- substitutions are maximally induced into their α -helical conformation (with the exception of Pro) in the presence of a hydrophobic environment, CD spectroscopy cannot be used to measure the α -helix disrupting properties of the substitutions based on α -helical structure.

It is also well documented that non-polar solvents and hydrophobic matrices characteristic of RP-HPLC both induce and stabilize α -helical structure (Blondelle *et al.*, 1995; Blondelle *et al.*, 1996; Purcell *et al.*, 1995c; Steer *et al.*, 1998; Zhou *et al.*, 1990). For instance, a classic example reported by Blondelle *et al* (Blondelle *et al.*, 1995; Blondelle *et al.*, 1996) demonstrated an excellent correlation between the CD ellipticities of peptides bound to a set of C₁₈-coated quartz plates and their RP-HPLC retention times. Indeed there is no evidence that the hydrophobic matrix characteristic of RP-HPLC destabilizes α -helical structure, quite the opposite, in fact. In addition, the ability of acetonitrile, the organic modifier traditionally employed for the majority of peptide

separations by RP-HPLC (Mant *et al.*, 2002a), to induce α -helical structure in potentially helical molecules has also been demonstrated (Lau *et al.*, 1984a; Lau *et al.*, 1984b).

Excellent examples of the disruption of any tertiary/quaternary structure of amphipathic α -helical peptides by organic modifiers has been clearly demonstrated by size-exclusion chromatography of model amphipathic α -helical coiled-coil peptides by Lau *et al* (Lau *et al.*, 1984a) and Mant *et al* (Mant *et al.*, 1997). Coupled with similar disruption of such higher levels of peptide structure, or, indeed, any potential for peptide aggregation, by hydrophobic stationary phases (Lau *et al.*, 1984b; Mant *et al.*, 1989), the peptides used in the present study can be confidently expected to be eluted as single-stranded amphipathic α -helices during RP-HPLC.

In a similar manner to RP-HPLC, under characteristic conditions of HILIC/CEX [high acetonitrile concentration in the mobile phase; 70% (v/v) in the present study], the peptide analogues would also be expected to be α -helical, allowing interaction of the hydrophilic face with the ion-exchange matrix (Mant *et al.*, 1998b). Finally, it should be noted that the substitution sites at position 11 (hydrophilic face) and position 13 (hydrophobic face) of the peptides (Figure XI-1) ensures intimate interaction of the substituting side-chain with the ion-exchange or reversed-phase stationary phase, respectively; concomitantly, this is designed to maximize any observed effects on HILIC/CEX or RP-HPLC retention behaviour, respectively, when substituting different residues at these sites.

XI-4-3 *RP-HPLC of amphipathic α -helical peptide analogues of V_{681}*

Figure XI-2 shows the reversed-phase elution profiles of mixtures of the L-amino acid substituted analogues (Figure XI-2A and XI-2C) and D-amino acid substituted

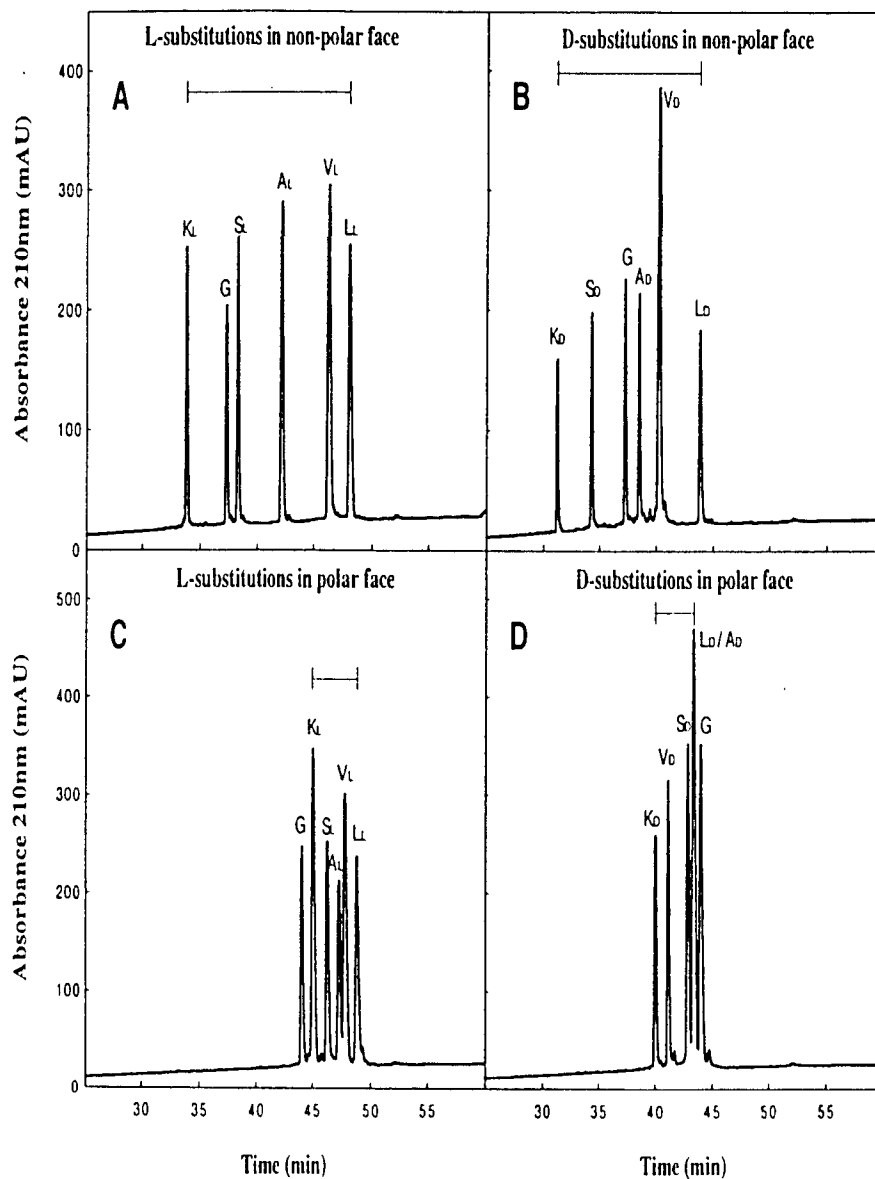


Figure XI-2 RP-HPLC of amphipathic α -helical peptides. Column: reversed-phase Zorbax SB 300-C₈ (150mm x 2.1 mm I.D.). Conditions: linear AB gradient (1% B/min) at a flow rate of 0.3 ml/min, where eluent A is 0.05% aq. TFA, pH 2.0, and eluent B is 0.05% TFA in acetonitrile; temperature, 25 °C. Bars denote elution ranges for the five L- or D-amino acid substituted peptides. The sequences of the peptides are shown in Figure XI-1.

analogues (Figure XI-2B and XI-2D) when substitutions were made in the non-polar face (Figure XI-2A and XI-2B) or polar face (Figure XI-2C and XI-2D) of the amphipathic α -helix. Clearly, for both the L- and D-amino acid substituted peptides, the peptide mixtures are better separated when substitutions are made in the non-polar face (the preferred binding domain for RP-HPLC; 2A and 2B, respectively) compared to the polar face (2C and 2D, respectively). Thus, for L-substitutions in the non-polar (2A) and polar (2C) faces, the elution ranges for the first and last eluted L- or D-peptides (*i.e.*, K_L to L_L) were 14.3 min and 3.8 min, respectively; for D-substitutions in the non-polar (2B) and polar (2D) faces, these values (*i.e.*, K_D to L_D) were 12.7 min and 3.4 min, respectively. In addition, the D-substituted analogues were consistently eluted faster than their L-amino acid counterparts when substituted into either the polar (Table XI-1; Figure XI-2) or non-polar (Table XI-2; Figure XI-2) faces of the α -helix, despite the fact that each L-/D-substituted peptide pair has the same inherent hydrophilicity/hydrophobicity. This observation can be rationalized as being due to disruption of the amphipathic α -helix following introduction of the D-amino acid (Aguilar *et al.*, 1993; Chen *et al.*, 2002; Krause *et al.*, 2000; Rothmund *et al.*, 1995; Rothmund *et al.*, 1996). The overall effect on the non-polar face would be a decrease in the apparent hydrophobicity of this face when the helix is substituted (on either face) with a D-amino acid compared to its L-diastereomer and, hence, a decrease in retention time of the former compared to the latter. From Tables XI-1 and XI-2, subtraction of the RP-HPLC retention time of the D-amino acid substituted analogues from their L-amino acid substituted counterparts produces a retention time difference (Δt_R) representing either the disruption of the polar face (Table

Table XI-1 RP-HPLC and HILIC/CEX Retention Data

Amino acid substitution ^b	Amino acid substitution in polar peptide face ^a					
	RP-HPLC (t_R , min) ^c		Δt_R (D-L) ^d (min)	HILIC/CEX (t_R , min) ^c		Δt_R (D-L) ^d (min)
	S11X _L	S11X _D		S11X _L	S11X _D	
L	48.8	43.4	-5.4	39.4	36.8	-2.6
V	47.8	41.1	-6.7	40.4	37.4	-3.0
A	47.3	43.4	-3.9	43.1	41.3	-1.8
S	46.3 ^e	42.9	-3.4	45.4 ^e	42.9	-2.5
K	45.0	40.0	-5.0	58.6	54.7	-3.9

a. Denotes that amino acid substitutions are made in the polar face (S11X series) of amphipathic α -helical peptides shown in Figure XI-1; X_L and X_D denote L- or D-amino acids are substituted at position X of this peptide series.

b. Denotes substitution of L-Ser with L-Leu, D-Leu, L-Val, D-Val, L-Ala, D-Ala, L-Ser, D-Ser, L-Lys or D-Lys.

c. Retention times of RP-HPLC and HILIC/CEX runs taken from Figures XI-2 and XI-3, respectively.

d. $\Delta t_R = t_R$, L-substituted analogue minus t_R , D-substituted analogues.

e. t_R values for native peptide which has three denotations: V₆₈₁ = S11S_L = V13V_L

Table XI-2 RP-HPLC and HILIC/CEX Retention Data

Amino acid substitution ^b	Amino acid substitution in non-polar peptide face ^a					
	RP-HPLC (t_R , min) ^c		Δt_R (D-L) ^d (min)	HILIC/CEX (t_R , min) ^c		Δt_R (D-L) ^d (min)
	V13X _L	V13X _D		V13X _L	V13X _D	
L	48.1	43.9	-4.2	45.5	42.0	-3.5
V	46.3 ^e	40.2	-6.1	45.4 ^e	40.2	-5.3
A	42.4	38.5	-3.9	44.3	41.5	-2.8
S	38.3	34.3	-4.0	44.3	42.0	-2.3
K	33.8	31.2	-2.6	49.5	49.0	-0.5

a. Denotes that amino acid substitutions are made in the non-polar face (V13X series) of amphipathic α -helical peptides shown in Figure XI-1; X_L and X_D denote L- or D-amino acids are substituted at position X of this peptide series.

b. Denotes substitution of L-Val with L-Leu, D-Leu, L-Val, D-Val, L-Ala, D-Ala, L-Ser, D-Ser, L-Lys or D-Lys.

c. Retention times of RP-HPLC and HILIC/CEX runs taken from Figures XI-2 and XI-3, respectively.

d. $\Delta t_R = t_{R,L}$ L-substituted analogue minus $t_{R,D}$ D-substituted analogues.

e. t_R values for native peptide which has three denotions: V₆₈₁ = S11S_L = V13V_L

XI-1; S11X series) or non-polar face (Table XI-2; V13X series) by substitution of D-amino acids into these respective faces of the amphipathic α -helix.

From Figure XI-2, peptides were eluted in order of increasing hydrophobicity of the substituted side-chain ($K < S < A < V < L$ (Guo *et al.*, 1986a)) in the non-polar face for both the L- and D-analogues, *i.e.*, the elution order for the two peptide mixtures was the same, except for the relative position of the Gly-analogue (eluted between K_L and S_L in Figure XI-2A and between S_D and A_D in Figure XI-2B). Also from Figure XI-2C, the elution order of the L-analogues is again in order of increasing hydrophobicity of the side-chain substituted into the polar face of the α -helix ($K_L < S_L < A_L < V_L < L_L$), with G now eluted prior to K_L . However, this elution order was not observed for the analogues with D-amino acids substituted into the polar face of the amphipathic α -helix (Figure XI-2D), where A_D and L_D are co-eluted and V_D , with a hydrophobic side-chain, is eluted prior to S_D , which contains a polar, hydrophilic side-chain. Such an observation is likely due to the varying magnitude of disruption of the preferred non-polar binding domain of the peptide helix when different D-amino acids are substituted into the sequence, *i.e.*, different D-amino acids disrupt the non-polar face to different extents, resulting in the RP-HPLC elution order shown in Figure XI-2D. It is interesting to note that the elution of V_D significantly prior to S_D reflects the observation by Chen *et al.* (Chen *et al.*, 2002) that amino acids, such as Val, with β -branched side-chains showed the greatest reduction in apparent side-chain hydrophobicity due to D-amino acid substitutions into the centre of the non-polar face of an amphipathic α -helix. Similarly, when substituted into the centre of the non-polar face of V_{681} in the present study, the presence of D-Val was the most disruptive of the hydrophobic preferred binding domain of the α -helix as measured by

RP-HPLC (Δt_R , $V_D - V_L = -6.1$ min) relative to other D-substituted analogues (Table XI-2). Interestingly, when D-Val is substituted in the center of the polar face of V_{681} , it remains the most disruptive D-amino acid with a Δt_R value even larger than that on the non-polar face (Δt_R , $V_D - V_L = -6.7$ min) (Table XI-1). This suggests that D-Val can disrupt the α -helix better on the polar face than on the non-polar face. This was also observed for D-Leu (Δt_R of -5.4 min on the polar face *versus* -4.2 min on the non-polar face) and D-Lys (Δt_R of -5.0 min on the polar face *versus* -2.6 min on the non-polar face) (Table XI-1). D-Ser was the only example where the α -helix disruption was better on the non-polar face (Δt_R of -4.0 min on the non-polar face *versus* -3.4 min on the polar face).

Non-polar face substitutions are replacing L-Val at position 13. Since L-Ala, L-Ser and L-Lys are all more hydrophilic than L-Val, it would be expected that such substitutions would decrease peptide retention time as observed (L-Val, $t_R = 46.3$ min; L-Ala, 42.4 min; L-Ser, 38.3 min; and L-Lys, 33.8 min). Similarly, L-Leu is more hydrophobic than L-Val and retention time increases to 48.1 min. For all polar face substitutions, the non-polar face remains the same, *i.e.*, with Val at position 13 (Figure XI-1) and polar face substitutions are replacing L-Ser at position 11. Since L-Ala, L-Val and L-Leu are more hydrophobic than L-Ser, it would be expected that such substitutions would increase peptide retention time (as, indeed, was observed in the elution order of Figure XI-2C), even though they do not involve the preferred binding domain for RP-HPLC. Note that an L-Val to L-Leu substitution on the polar face increases retention time and hydrophobicity by 1.0 min (Table XI-1), whereas the same substitution on the non-polar face increases retention time and hydrophobicity by 1.8 min (Table XI-2). This almost doubling of the effect of the addition of a single CH_2 group shows that

hydrophobicity is more easily affected by substitution in the non-polar face, i.e., the preferred binding domain for RP-HPLC. Further, when you increase hydrophobicity on the polar face from L-Ser to L-Ala, L-Val and L-Leu, the overall hydrophobicity of the peptide, as measured by RP-HPLC, is 46.3 min, 47.3 min, 47.8 min and 48.8 min, respectively, i.e., L-Leu increases overall hydrophobicity by 2.5 min relative to L-Ser (Table XI-1). By comparison, the same change on the non-polar face accounts for a significantly greater effect where L-Leu increases overall hydrophobicity by 9.8 min relative to L-Ser (Table XI-2).

It is also worth noting the elution behaviour of K_L relative to analogue G when L-Lys is substituted into the non-polar face of the α -helix (Figure XI-2A) compared to the polar face (Figure XI-2C). It has been clearly shown in model random coil peptides (Guo *et al.*, 1986a) that substitution of a Gly residue by a positively charged Lys residue leads to a significant decrease in peptide retention time during RP-HPLC at pH 2.0, exactly as observed in Figure XI-2A for the amphipathic peptides of the present study. However, from Figure XI-2C, K_L is eluted after the G analogue when L-Lys is substituted into the polar face of the α -helix. Such an observation is likely due to the L-Lys being in the centre of the hydrophilic face of the amphipathic α -helix, i.e., on the opposite side of the hydrophobic preferred binding domain for RP-HPLC. Although the positively charged Lys side-chain still affects peptide retention behaviour (note its elution in Figure XI-2C prior to A_L , V_L and L_L containing non-polar groups at the substitution site), this effect is likely diminished compared to the situation where L-Lys is substituted into the centre of the non-polar face of the helix and is, therefore, able to interact to a greater extent with the hydrophobic stationary phase. Indeed, the RP-HPLC retention behaviour of all of the

polar face-substituted analogues (with identical non-polar faces) relative to their non-polar face counterparts, in terms of the much narrower elution range of the former, as well as the severely diminished contribution to apparent peptide hydrophobicity of even hydrophobic side-chains such as Leu and Val when substituted in the polar face of the helix, clearly underlines the presence of a preferred binding domain for RP-HPLC and represented by the non-polar face of the amphipathic α -helix. A similar overall trend can also be seen for the D-substituted analogues, albeit interpretation is complicated somewhat by the helix-disrupting properties of D-amino acids (note, for example, the slight reduction in retention time for L_D when D-Leu is substituted in the polar face (Figure XI-2D; Table XI-1) compared to the non-polar face (Figure XI-2B; Table XI-2).

XI-4-4 *HILIC/CEX of amphipathic α -helical peptide analogues of V_{681}*

Figure XI-3 shows the HILIC/CEX profiles of mixtures of the L-amino acid substituted analogues (Figure XI-3A and XI-3C) and D-amino acid substituted analogues (Figure XI-3B and XI-3D) when substitutions were made in the polar face (Figure XI-3A and XI-3B) or non-polar face (Figure XI-3C and XI-3D) of the amphipathic α -helix. From Figure XI-3, for both the L- and D-amino acid substituted peptides, the peptide mixtures are better separated when substitutions are made in the polar face of the α -helix (the preferred binding domain for HILIC/CEX) compared to the non-polar face. Thus, for L-substitutions in the polar (Figure XI-3A; Table XI-1) and non-polar (Figure XI-3C; Table XI-2) faces, the elution range for the first eluted and last eluted L-substituted peptides were 19.2 min (L_L to K_L) and 5.2 min (S_L to K_L), respectively; for D-substitutions in the polar (Figure XI-3B; Table XI-1) and non-polar (Figure XI-3D; Table XI-2) faces, these values were 17.9 min (L_D to K_D) and 8.8 min (V_D to K_D), respectively.

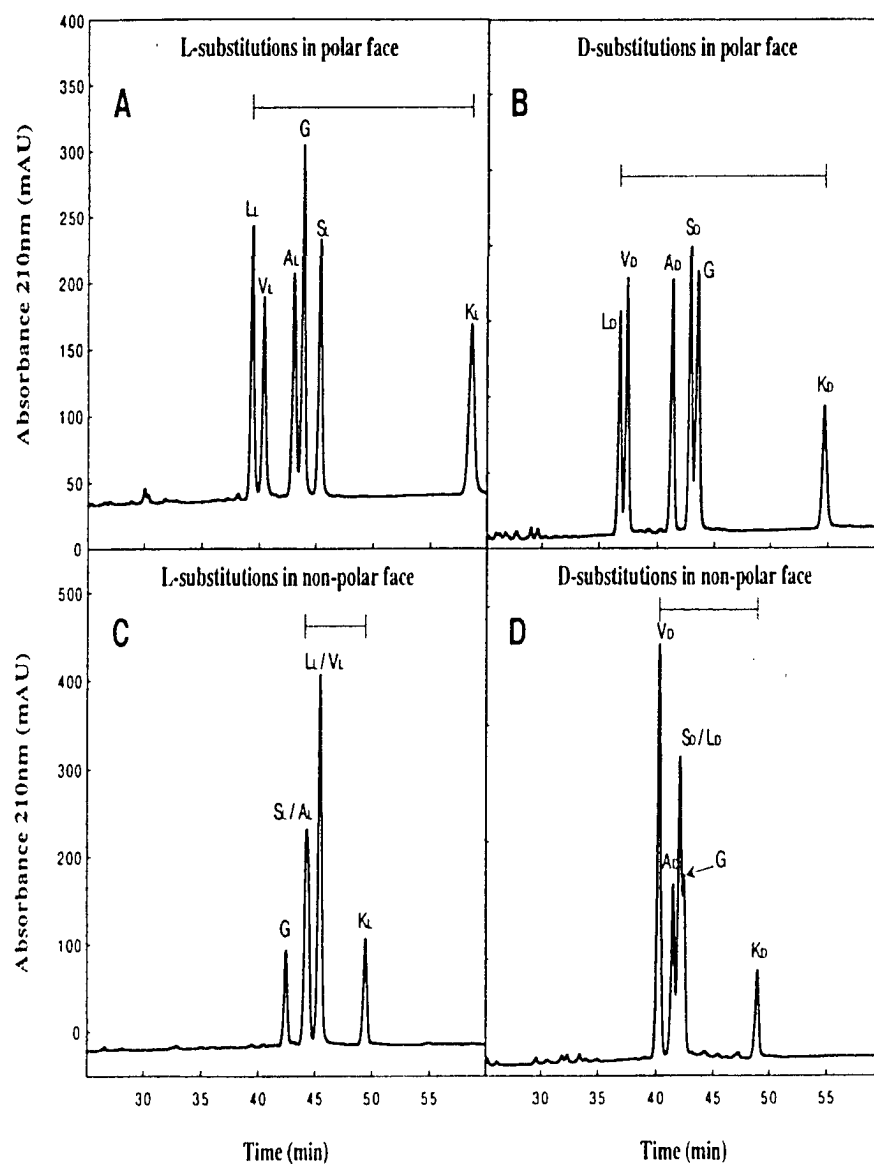


Figure XI-3 HILIC/CEX of amphipathic α -helical peptides. Column: strong cation-exchange Poly-Sulfoethyl A (200 mm \times 2.1 mm I.D.). Conditions: linear AB gradient (5 mM NaClO_4 to 250 mM NaClO_4 in 60 min) at a flow rate of 0.3 ml/min, where buffer A is 5 mM NaClO_4 and buffer B is 5 mM *aq.* TEAP, pH 4.5, containing 250 mM NaClO_4 , both buffers also containing 70% (v/v) acetonitrile; temperature, 65 $^\circ\text{C}$. Bars denote elution ranges for the five L- or D-amino acid substituted peptides. The sequences of the peptides are shown in Figure XI-1.

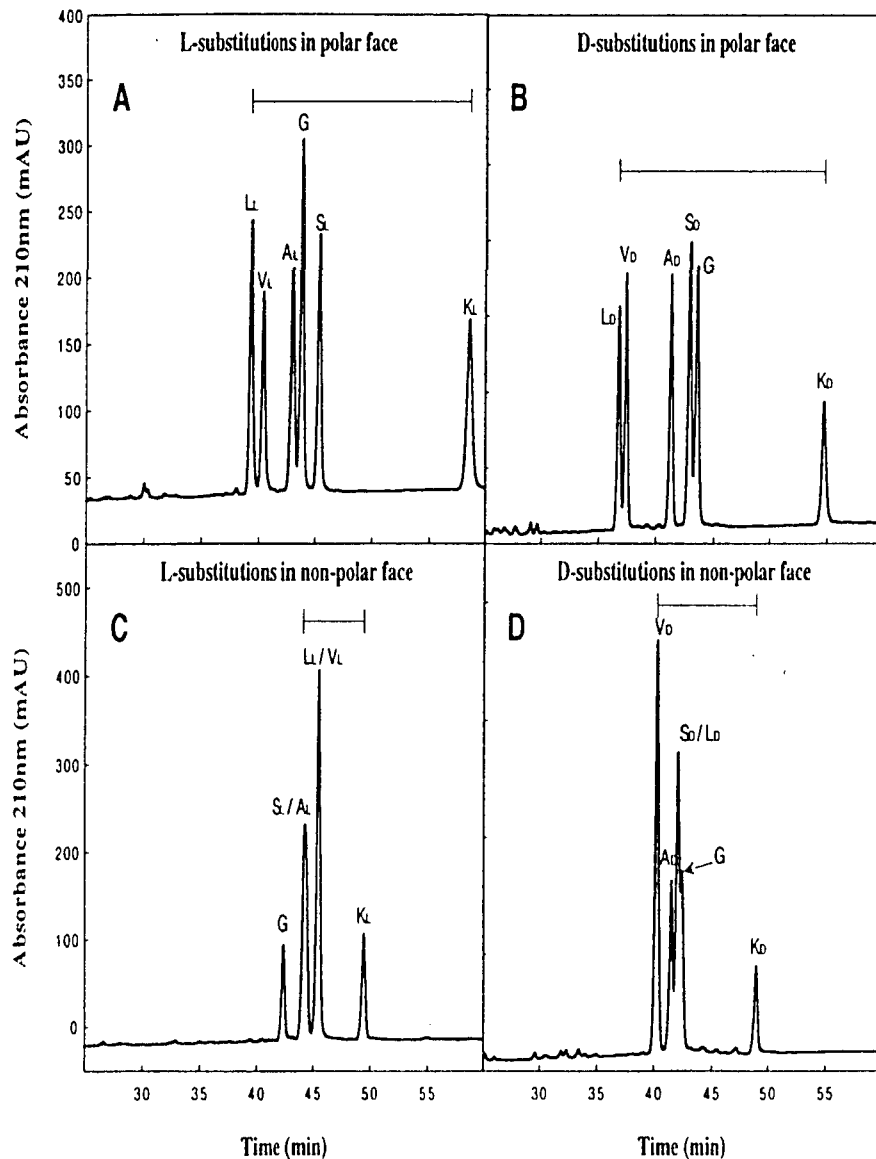


Figure XI-3 HILIC/CEX of amphipathic α -helical peptides. Column: strong cation-exchange Poly-Sulfoethyl A (200 mm \times 2.1 mm I.D.). Conditions: linear AB gradient (5 mM NaClO₄ to 250 mM NaClO₄ in 60 min) at a flow rate of 0.3 ml/min, where buffer A is 5 mM NaClO₄ and buffer B is 5 mM *aq.* TEAP, pH 4.5, containing 250 mM NaClO₄, both buffers also containing 70% (v/v) acetonitrile; temperature, 65 °C. Bars denote elution ranges for the five L- or D-amino acid substituted peptides. The sequences of the peptides are shown in Figure XI-1.

The Lys analogues, due to their extra positive charge, are clearly well separated from the remainder of the peptides in the mixtures. However, even if one were to exclude these analogues from the elution range comparison, *i.e.*, only compare peptides of identical net positive charge, the superior separation of the analogues with substitutions in the polar face of the α -helix is still clear: for L-substitutions in the polar (Figure XI-3A; Table XI-1) and non-polar (Figure XI-3C; Table XI-2) faces, the elution ranges were 6 min (L_L to S_L) and 1.2 min (L_L to S_L), respectively; for D-substitutions in the polar (Figure XI-3B; Table XI-1) and non-polar (Figure XI-3D; Table XI-2) faces, these values were 6.1 min (L_D to S_D) and 1.8 min (L_D to V_D), respectively. Concomitant with this larger elution range for peptide analogues substituted in their polar faces (Figures XI-3A and XI-3B) is improved peptide resolution compared to the analogues with substitutions made in their non-polar faces (Figures XI-3C and XI-3D). Thus, for both L- (Figure XI-3A) and D- (Figure XI-3B) amino acid substitutions in the polar face, all six peptides were satisfactorily separated. In contrast, for L-substitutions in the non-polar face (Figure XI-3C), S_L and A_L were coeluted as were L_L and V_L ; similarly, for D-substitutions in the non-polar face (Figure XI-3D), S_D and L_D were coeluted, these coeluted peptides also being only poorly resolved from A_D and G.

From Figure XI-3 and Tables XI-1 and XI-2, in a similar manner to the RP-HPLC results (Figure XI-2, Tables XI-1 and XI-2), the D-substituted analogues were again consistently eluted faster than their corresponding diastereomers in HILIC/CEX. As noted previously for the RP-HPLC results, this pattern of earlier elution for the D-substituted analogues is likely due to disruption of the preferred binding domain (in this case, the hydrophilic preferred binding domain represented by the polar face of the

amphipathic α -helix) by a D-amino acid substitution into the centre of either the polar or non-polar face of the helix. From Tables XI-1 and XI-2, in a similar manner to the RP-HPLC results, subtraction of the HILIC/CEX retention time of the D-amino acid substituted analogues from their L-amino acid substituted counterparts again produces Δt_R values representing either the disruption of the polar face (S11X series; Table XI-1) or non-polar face (V13X series; Table XI-2) by substitution of D-amino acids into these respective faces of the amphipathic α -helix. The D-amino acid that was most disruptive to the hydrophilic preferred binding domain of the α -helix as measured by HILIC/CEX was D-Val substituted on the non-polar face ($\Delta t_R, V_L - V_D = -5.3$ min; Table XI-2) and D-Lys substituted on the polar face ($\Delta t_R, K_L - K_D = -3.9$ min; Table XI-1). This contrasts with the RP-HPLC results where D-Val was most disruptive of the non-polar preferred binding domain whether the substitution was on the polar or non-polar face. HILIC/CEX could be more sensitive to the D-Lys substitution on the polar face because of the mixed mode effects. The lysine residue introduces an additional charge which affects both ion-exchange and hydrophilic interactions. Interestingly, D-Val was the second best substitution for disruption of the polar preferred binding domain when made on the polar face (Table XI-1).

Also from Figure XI-3, peptides are eluted in order of increasing hydrophilicity of the substituted amino acid side-chain in the polar face for both the L- (3A) and D- (3B) analogues, *i.e.*, $L < V < A < S < K$. There is no clear pattern to the elution order of the peptides when substitutions are made in the non-polar face (3C and 3D). In particular, the elution order of the D-substituted analogues is likely influenced by the degree of disruption of the polar face by different D-amino acid substitutions in the non-polar face.

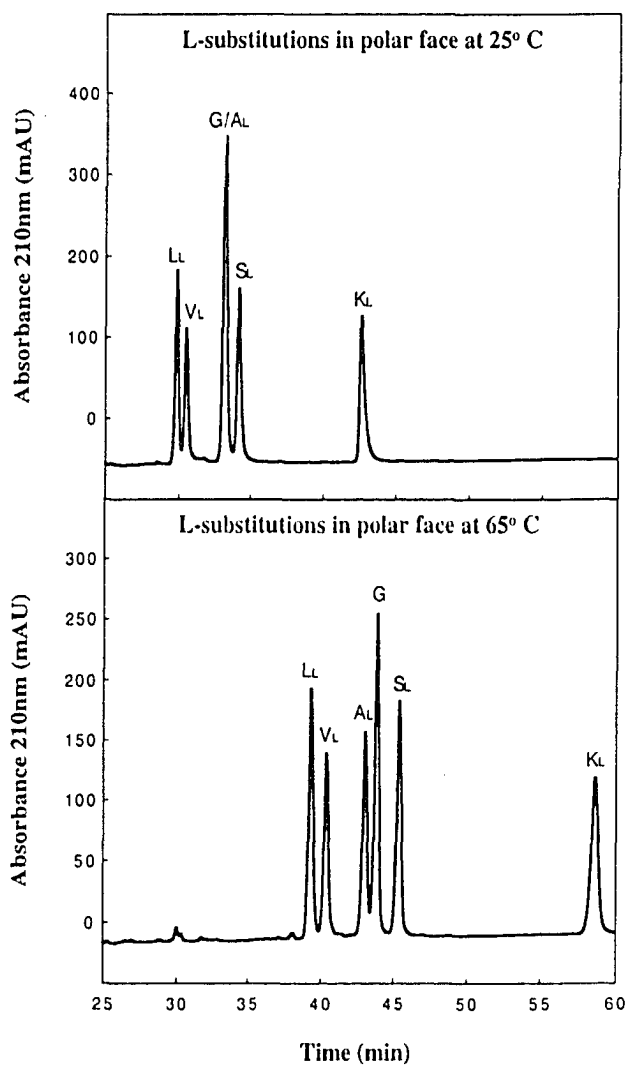


Figure XI-4 Effect of temperature on HILIC/CEX of amphipathic α -helical peptides, where substitutions are made in the polar face of the α -helix. Column: see Figure XI-3. Conditions: same as Figure XI-3 except temperature is now 25 °C (top panel) or 65 °C (bottom panel). The sequences of the peptides (SX11 series) are shown in Figure XI-1.

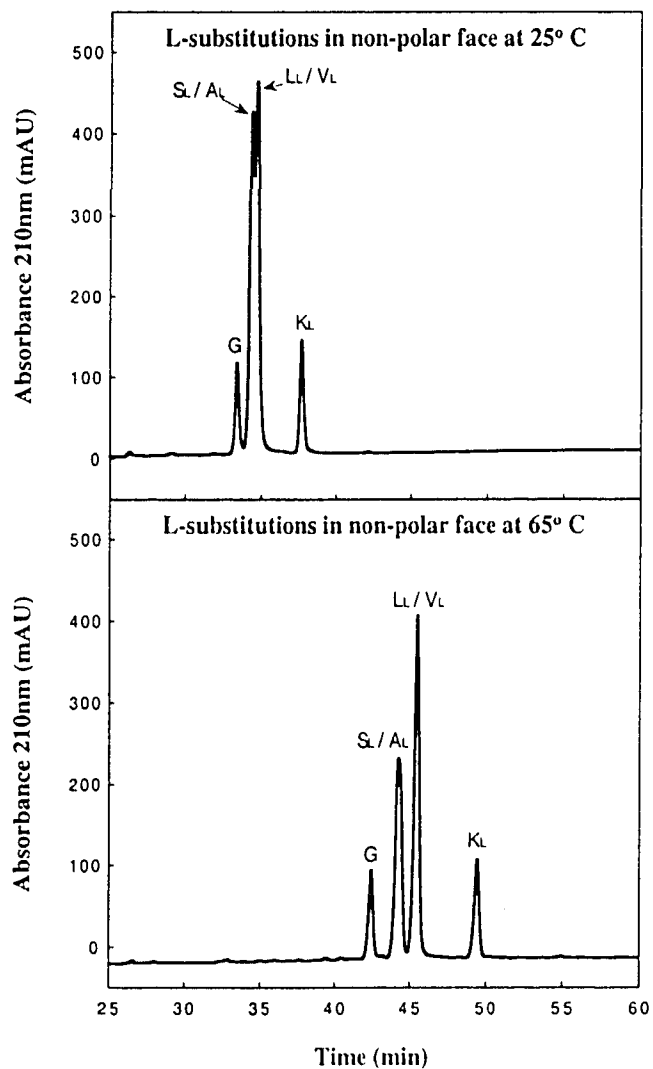


Figure XI-5 Effect of temperature on HILIC/CEX of amphipathic α -helical peptides, are made in the non-polar face of the α -helix. Column: see Figure XI-3. Conditions: : except temperature is now 25 °C (top panel) or 65 °C (bottom panel). The sequer (VX13 series) are shown in Figure XI-1.

Figures XI-4 and XI-5 now illustrate the effect of temperature on HILIC/CEX of peptide analogues with L-substitutions in the polar face (Figure XI-4) or the non-polar face (Figure XI-5). From Figure XI-4, the effect of a rise in temperature from 25°C to 65°C produced a dramatic improvement in the resolution of the L-substituted analogues, as well as a significant increase in retention time. A_L and G, in particular, illustrate this improvement, being coeluted at 25°C and resolved to baseline at 65°C. The greater the increase in retention time of K_L (with an extra positive charge) suggests that the more hydrophilic the substituted amino acid, the greater the effect of temperature on peptide retention time in HILIC/CEX, reflecting earlier observations by this laboratory (Hartmann *et al.*, 2003). From Figure XI-5, an improvement in resolution on raising the temperature from 25°C to 65°C can also be seen for the peptides where L-substitutions were made in the non-polar face, albeit not as dramatic as seen for the peptides substituted in the polar face (Figure XI-4). Retention times have also again increased. The major effect of raising the temperature was to improve the resolution of the coeluted peptide pairs of S_L/A_L and L_L/V_L.

Although not shown here, raising the temperature from 25°C to 65°C for RP-HPLC of these L-substituted peptides did not significantly improve the separation of the peptide mixtures achieved at the lower temperature (Figure XI-2A and XI-2C), particularly the already excellent resolution of the analogues with L-substitutions made in the non-polar face of the α -helix (Figure XI-2A). The major effect was a decrease in retention times of all peptides in the two mixtures. Thus, we believed that the similar retention time range of both the L- and D-substituted analogues at 25°C for RP-HPLC and 65°C for HILIC/CEX (as well as the clear advantage of employing the higher

temperature for HILIC/CEX; Figures XI-4 and XI-5) allowed a more valid comparison of the effectiveness of these two HPLC modes both for resolution of peptide mixtures and as monitors of hydrophilicity/hydrophobicity of the non-polar and polar faces, respectively, of amphipathic α -helical peptides.

XI-4-5 *RP-HPLC and HILIC/CEX as monitors of hydrophilicity/hydrophobicity of amphipathic α -helical peptides*

Table XI-3 summarizes the effect of amino acid substitutions on the retention behaviour of the native peptide, V₆₈₁ (also denoted as S11S_L and V13V_L). Of interest here is the relative range of Δt_R values as determined by RP-HPLC or HILIC/CEX when substitutions are made in the polar face (S11S_L series) or non-polar face (V13V_L) of V₆₈₁. Thus, when substitutions are made in the polar face, the Δt_R range as measured by RP-HPLC is just 8.8 min compared to 21.8 min for HILIC/CEX, highlighting the greater sensitivity of the latter HPLC mode for monitoring substitutions made in the polar face. In contrast, RP-HPLC (Δt_R range = 16.9 min) is clearly more sensitive to changes made in the non-polar face compared to HILIC/CEX (Δt_R range = 9.3 min). Such results again underline the complementary nature of these two HPLC modes.

From Figure XI-6, this opposing, if complementary, nature of RP-HPLC and HILIC/CEX is quite clear. Thus, with amino acid substitutions (whether L- or D-amino acids) made in the non-polar face of the amphipathic α -helix, peptides are eluted during RP-HPLC in order of increasing hydrophobicity of the non-polar preferred binding domain. In contrast, with substitutions made in the polar face of the α -helix (whether L- or D-amino acids), peptides are eluted during HILIC/CEX in order of increasing hydrophilicity (decreasing hydrophobicity) of the polar preferred binding domain. The

Table XI-3 Effects of Amino Acid Substitutions on the Retention Behavior of Peptide V₆₈₁

Amino acid ^a substitution	RP-HPLC ^b $\Delta t_R(\text{min})$	HILIC/CEX ^b $\Delta t_R(\text{min})$
S11 S _L ^c → L _L	+2.5	-6.0
S _L → V _L	+1.5	-5.0
S _L → A _L	+1.0	-2.3
S _L → K _L	-1.3	+13.2
S _L → L _D	-2.9	-8.6
S _L → V _D	-5.2	-8.0
S _L → A _D	-2.9	-4.1
S _L → S _D	-3.4	-2.5
S _L → K _D	-6.3	+9.3
V13 V _L ^c → L _L	+1.8	0
V _L → A _L	-3.9	-1.2
V _L → S _L	-8.0	-1.2
V _L → K _L	-12.5	+4.0
V _L → L _D	-2.4	-3.5
V _L → V _D	-6.1	-5.3
V _L → A _D	-7.8	-4.0
V _L → S _D	-12.0	-3.5
V _L → K _D	-15.1	+3.5

- a. Denotes that amino acid substitutions are made in the polar face (S11X series) or non-polar face (V13X series) of amphipathic α -helical peptides shown in Figure XI-1.
- b. Denotes change in retention time when an amino acid substitution is made in the polar face (*e.g.*, t_R of S11S_L minus t_R of S11L_L = +2.5 min and -6.0 min in RP-HPLC and HILIC/CEX, respectively) or non-polar face (*e.g.*, t_R of V13V_L minus t_R of V13L_L = +1.8 min and 0 min in RP-HPLC and HILIC/CEX, respectively) of the amphipathic α -helical peptides shown in Figure XI-1.
- c. Note that denotations S11S_L and V13V_L both represent the native V₆₈₁ peptide.

Table XI-4 Monitoring of Effects of the Same Substitutions on the Non-Polar *versus* the Polar Face by RP-HPLC and HILIC/CEX

Amino acid ^a substitution	RP-HPLC (pbd) ^b $\Delta t_R(\text{min})^c$	RP-HPLC (Non-pbd) ^b $\Delta t_R(\text{min})^c$	HILIC/CEX (pbd) ^b $\Delta t_R(\text{min})^c$	HILIC/CEX (Non-pbd) ^b $\Delta t_R(\text{min})^c$
S _L → L _L	+ 9.8	+ 2.5	- 6.0	+ 1.2
S _L → V _L	+ 8.0	+ 1.5	- 5.0	+ 1.2
S _L → A _L	+ 3.9	+ 1.0	- 2.3	0
S _L → K _L	- 4.5	- 1.3	+ 13.2	+ 5.2

a. Denotes L-Ser substitution with L-Leu, L-Val, L-Ala, or L-Lys.

b. pbd and non-pbd denote preferred binding domain and non-preferred binding domain, respectively.

c. Δt_R = retention time of S_L subtracted from denoted L-analogue with which it has been substituted; RP-HPLC and HILIC/CEX retention times taken from Figures XI-2 and XI-3, respectively, and Tables XI-1 and XI-2.

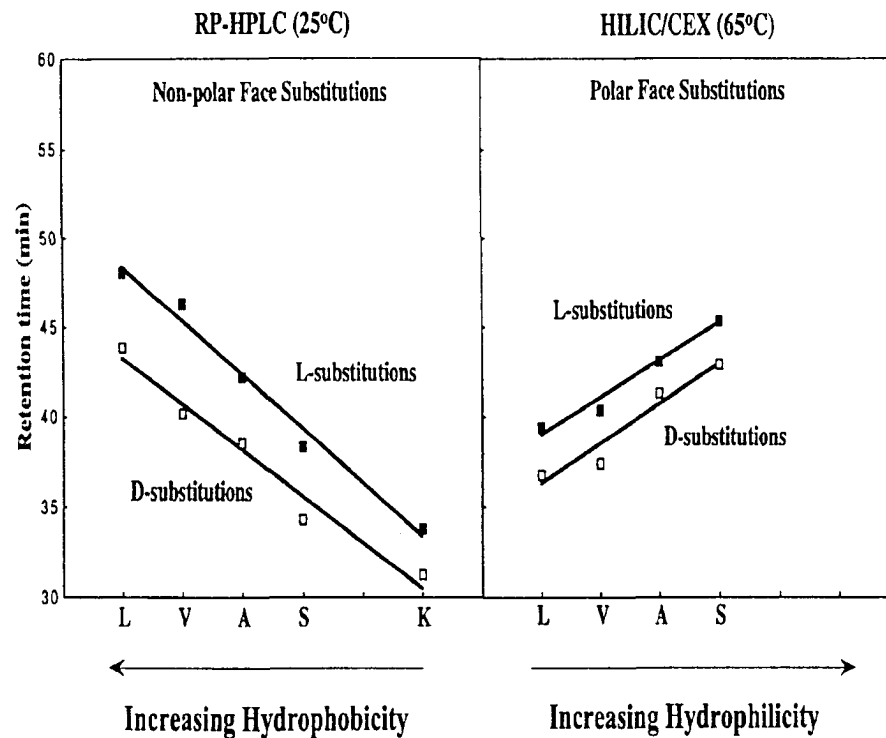


Figure XI-6 Selectivity of RP-HPLC versus HILIC/CEX of amphipathic α -helical peptides. Retention time data taken from Table XI-1 and Figure XI-2 (RP-HPLC) and Figure XI-3 (HILIC/CEX). The one-letter codes on the abscissa denote the L- or D-amino acid substituted into the non-polar face and separated by RP-HPLC at 25 °C (left panel) or polar face and separated by HILIC/CEX at 65 °C (right panel) of the V13X series or S11X series peptides, respectively (Figure XI-1).

results shown in Figure XI-6 indicate that RP-HPLC and HILIC/CEX are, indeed, potentially useful monitors of hydrophilicity/hydrophobicity of the non-polar and polar faces, respectively, of an amphipathic α -helical peptide.

Such potential is highlighted in Table XI-4 which compares the relative efficacy of RP-HPLC *versus* HILIC/CEX for monitoring hydrophilicity/hydrophobicity changes when substituting L-Ser with L-Ala, L-Val, L-Leu or L-Lys in the polar or non-polar face of V₆₈₁. L-substituted amino acids were chosen since replacement of an L-amino acid with another L-amino acid will have the least effect on helix conformation. In contrast, replacement of an L-amino acid with a D-amino acid will cause disruption of both the polar and non-polar faces of the helix, no matter which face the substitution is made, the extent of such disruption being dependent on the particular D-amino acid (Chen *et al.*, 2002). In addition, the Gly analogues were not included in Table XI-4 since glycine (which is also neither an L- or a D-amino acid) is a known α -helix disrupter, second only to proline in its helix-disruptive characteristics (Zhou *et al.*, 1994b). Thus, Table XI-4 represents the most valid demonstration of the potential effectiveness of RP-HPLC and HILIC/CEX for monitoring changes in the non-polar and polar faces, respectively, of V₆₈₁ through L-amino acid substitutions, *i.e.*, negligible effect on α -helix structure and a systematic increase in inherent hydrophobicity of either face through substitution of the polar uncharged Ser with non-polar side-chains (Ala < Val < Leu) (Lau *et al.*, 1984a) or a large increase in hydrophilicity through its substitution with positively charged Lys.

From Table XI-4, for the polar face substitutions on the preferred binding domain as measured by HILIC/CEX (S11X series; see Figure XI-1), as the hydrophobicity of the substitution is increased (Ala < Val < Leu), there is a decrease in retention time compared

to the Ser-substituted analogue (Δt_R of -2.3, -5.0 and -6.0 min, respectively); also, there is a large increase in retention time for the Lys-substituted analogue (+13.2 min). However, when these same polar face substitutions are measured by RP-HPLC (non-preferred binding domain), the Δt_R values are relatively small (ranging from just +1.0 min to +2.5 min for the non-polar side-chain substitutions and just -1.3 min for Lys), particularly when compared to the significantly larger substitution effects detected by HILIC/CEX. Clearly, and considering the overall similar retention time ranges of RP-HPLC (Figure XI-2) and HILIC/CEX (Figure XI-3) of these S11X series peptides (Table XI-1), Tables XI-3 and XI-4 demonstrate that *HILIC/CEX monitors changes in the polar face of V_{681} more effectively than RP-HPLC.*

From Table XI-4, for the non-polar face substitutions (V13X series; see Figure XI-1), as the hydrophobicity of the substitution is increased (Ala < Val < Leu), there is now a significant increase in RP-HPLC retention time compared to the Ser-substituted peptide, with Δt_R values ranging from +3.9 min for Ala up to +9.8 min for Leu when substituted into this preferred binding domain for RP-HPLC (compared to just +1.0 min for Ala and up to +2.5 min for Leu when substituted in the polar face and non-preferred binding domain). In addition, a Ser to Lys substitution now results in a Δt_R value of -4.5 min (compared to just -1.3 min for the polar face substitution). In contrast, HILIC/CEX is proving to be very insensitive to changes in hydrophobicity in the non-polar face (*i.e.*, its non-preferred binding domain), as witnessed by its inability to distinguish between the Ser- and Ala-substituted peptides ($\Delta t_R = 0$ min), as well as the Val- and Leu-analogues ($\Delta t_R = +1.2$ min for both peptides). The positive charge on Lys has enabled the Ser to Lys substitution in the non-polar face to be monitored by HILIC/CEX ($\Delta t_R = +5.2$ min),

albeit not as effectively as when this substitution is made in the polar face ($\Delta t_R = +13.2$ min). Thus, in contrast to the S11X series analogues, and again considering the overall similar analysis times for RP-HPLC (Figure XI-2) and HILIC/CEX (Figure XI-3) of the V13X series peptides (Table XI-2), Tables XI-3 and XI-4 also demonstrate that *RP-HPLC clearly monitors changes in the non-polar face of V₆₈₁ more effectively than HILIC/CEX.*

XI-5 Conclusions

The present study reports initial results of our approach to monitoring the effect on apparent peptide hydrophilicity/hydrophobicity and amphipathicity of substituting single L- or D-amino acids into the centre of the non-polar or polar faces of a 26-residue biologically active amphipathic α -helical peptide denoted V₆₈₁. Overall peptide hydrophobicity can be increased by amino acid substitutions in the polar or non-polar face of the amphipathic α -helix. However, our results show that, where substitutions have been made in the non-polar face, reversed-phase chromatography (RP-HPLC) is the best approach for monitoring such changes; conversely, for substitutions made in the polar face, mixed-mode hydrophilic interaction/cation-exchange chromatography (HILIC/CEX) which resolves peptides based substantially on their hydrophilic character, was best suited for monitoring the effect of such substitutions. Our results provide insights not only into the relative efficacy of RP-HPLC versus HILIC/CEX for resolution of specific peptide mixtures, but also for gauging the apparent hydrophilicity/hydrophobicity of L- and D-amino acids substituted into the non-polar or polar faces of an amphipathic α -helical peptide. We believe these complementary RP-HPLC and

HILIC/CEX methods offer excellent potential for rational design of novel amphipathic α -helical biologically active peptides, where modulation of the amphipathicity of such molecules may lead to the development of more effective antimicrobial agents.

CHAPTER XII

Future Studies

The research described in this thesis made significant advances in two important areas: HPLC methodology development for the separation of peptides and *de novo* design of antimicrobial peptides with enhanced activity and specificity.

HPLC of peptides:

Due to the emergence of the new field of proteomics, the development of novel separation protocols, especially in the area of multidimensional peptide/protein separations, has become essential. HPLC plays a critical role in the post-genomic era of proteomics, owing to its flexibility, reliability, reproducibility and capability to handle large amount of samples (Guttman *et al.*, 2004; Issaq, 2001; Liu *et al.*, 2002b; Wehr, 2002). In addition, the ability of HPLC to integrate with other major analytical instrumentations (such as mass spectroscopy, electrophoresis, *etc*) has greatly enhanced its application in proteomic practices. In order to fulfill the requirements of widely-employed multidimensional separations in proteomic studies, HPLC separation methodology needs to be further developed, especially the methods suitable for application to multidimensional peptide/protein separation/optimization systems. For example, as described in this thesis, HILIC/CEX may be an excellent complement to RP-HPLC for peptide separations and thus may also be a useful complementary HPLC mode for two-dimensional liquid chromatography separations, frequently required for complete resolution of complex peptide mixtures characteristic of proteomic separations.

Moreover, since it is well known that varying HPLC parameters, such as temperature, mobile phase conditions and stationary phase, may have dramatic influences on peptide/protein separations, the optimization of HPLC methodology will be extremely valuable for future proteomic studies. For example, since we have already proven the effect of temperature on the selectivity of peptide separations, temperature can be used as an additional parameter for proteomic separations of enzymatic digests of proteins during two-dimensional HPLC elutions. Thus, the use of high temperature to improve the separation of proteomic samples will be investigated. In addition, due to the superior effectiveness of the ion-pairing ability of the perchlorate ion, it could also be used in the proteomic elutions of protein digests to improve peptide selectivity and resolution. In a similar manner to work we have carried out to determine optimum TFA concentrations for RP-HPLC of peptides, the optimum concentration of perchlorate ion should be studied for routine usage for RP-HPLC peptide separation. The methods we developed to monitor the hydrophilicity/hydrophobicity of side-chains on both the polar and non-polar faces of amphipathic molecules will be applied to the development of new antimicrobial peptides.

Antimicrobial peptides:

Although there are a large number of antimicrobial peptides discovered or synthesized, only a few of them can be used in clinical practice. The main reasons are due to the toxicity of peptides to eukaryotic cells and the lack of understanding of antimicrobial mechanism of action. The antimicrobial peptides discovered in this thesis (*e.g.*, NK_L, NA_D in Chapter IX) are potential candidates for the development of peptide

therapeutics, because of their improved antimicrobial activity and the dramatic decrease in hemolytic activity compared with the native peptide V₆₈₁. As clinical therapeutics, *in vivo* efficacy is an extremely important element in the development of any peptide antibiotic. Ultimately many vertebrate animal model tests have to be carried out that are each representative of different infections by different organisms, *e.g.*, A.BY/SnJ mouse model (Pennington *et al.*, 1979) and chronic pulmonary infection model (Wilderman *et al.*, 2001) for *Pseudomonas* infection. Furthermore, in order to understand more about antimicrobial mechanism of action, peptide interactions with model and biological membranes have to be explored. Indeed, we will continue to collaborate with Dr. R. N. McElhaney and coworkers to do thorough studies on the interaction of V₆₈₁ and analogs with different lipid compositions of biomembrane including all of the major classes of phospho-, sphingo- and glyco-lipids found in prokaryotic and eukaryotic cell surface membranes. Many other studies will also be carried out to investigate the interactions of the peptides and membranes, such as liposaccharide (LPS) affinity studies, fluorescence quenching studies, and NMR studies, *etc.* Since the initial interaction of cationic antimicrobial peptides with the Gram-negative bacterial cells occurs via binding of the peptides to the anionic LPS, LPS affinity studies can help us to find out the relationship between peptide LPS affinity and biological activity. Moreover, it should be pointed out that, clinically, LPS and, in particular, lipid A play an important role in pathophysiology of Gram-negative bacterial sepsis which leads to endotoxic shock, often culminating in the death of the patient (Erand *et al.*, 1999). Hence, antimicrobial peptides may have a role in treating sepsis by binding LPS in circulation and thus neutralizing its toxic action, providing yet another important rationale for future studies in this area (Srimal *et al.*,

1996; Thomas *et al.*, 1999). Fluorescence quenching experiments may provide information on the orientation of the peptides after they interact with liposomes. NMR will allow us to have an insight into peptide structures when they interact with biomembranes. In addition, even more importantly, we can apply our *de novo* peptide design approach with single D-/L-amino acid substitutions in other peptides with antimicrobial potential to generalize the optimum way of developing antimicrobial peptides as clinical therapeutics.

- Aguilar, M. I., Mougos, S., Boublik, J., Rivier, J., and Hearn, M. T. (1993). High-performance liquid chromatography of amino acids, peptides and proteins. CXXVIII. Effect of D-amino acid substitutions on the reversed-phase high-performance liquid chromatography retention behaviour of neuropeptide Y[18-36] analogues. *J. Chromatogr.* **646**, 53-65.
- Aguilar, M. I. (2004). Reversed-phase high performance liquid chromatography. In *HPLC of peptides and proteins*, Aguilar, M. I., ed. (Totowa, NJ, Humana Press), pp. 9-22.
- Albericio, F., and Carpino, L. A. (1997). Coupling reagents and activation. *Methods Enzymol.* **289**, 104-126.
- Alpert, A. J., and Andrews, P. C. (1988). Cation-exchange chromatography of peptides on poly(2-sulfoethyl aspartamide)-silica. *J. Chromatogr.* **443**, 85-96.
- Alpert, A. J. (1990). Hydrophilic-interaction chromatography for the separation of peptides, nucleic acids and other polar compounds. *J. Chromatogr.* **499**, 177-196.
- Andreu, D., Ubach, J., Boman, A., Wahlin, B., Wade, D., Merrifield, R. B., and Boman, H. G. (1992). Shortened cecropin A-melittin hybrids. Significant size reduction retains potent antibiotic activity. *FEBS Lett* **296**, 190-194.
- Andreu, D., and Rivas, L. (1998). Animal antimicrobial peptides: an overview. *Biopolymers* **47**, 415-433.
- Antia, F. D., and Horvath, C. (1988). High-performance liquid chromatography at elevated temperatures: examination of conditions for the rapid separation of large molecules. *J. Chromatogr.* **435**, 1-15.
- Arthur, M., Brisson-Noel, A., and Courvalin, P. (1987). Origin and evolution of genes specifying resistance to macrolide, lincosamide and streptogramin antibiotics: data and hypotheses. *J Antimicrob Chemother* **20**, 783-802.
- Axen, A., Carlsson, A., Engstrom, A., and Bennich, H. (1997). Gloverin, an antibacterial protein from the immune hemolymph of *Hyalophora* pupae. *Eur J Biochem* **247**, 614-619.
- Barnidge, D. R., Dratz, E. A., Martin, T., Bonilla, L. E., Moran, L. B., and Lindall, A. (2003). Absolute quantification of the G protein-coupled receptor rhodopsin by LC/MS/MS using proteolysis product peptides and synthetic peptide standards. *Anal. Chem.* **75**, 445-451.

- Barry, E., Boyes, B. E., and Walker, D. G. (1995). Selectivity optimization of reversed-phase high-performance liquid chromatographic peptide and protein separations by varying bonded-phase functionality. *J. Chromatogr.* **691**, 337-347.
- Bateman, A., Singh, A., Congote, L. F., and Solomon, S. (1991). The effect of HP-1 and related neutrophil granule peptides on DNA synthesis in HL60 cells. *Regul Pept* **35**, 135-143.
- Bechinger, B. (1997). Structure and functions of channel-forming peptides: magainins, cecropins, melittin and alamethicin. *J. Membr. Biol.* **156**, 197-211.
- Benedek, K., Dong, S., and Karger, B. L. (1984). Kinetics of unfolding of proteins on hydrophobic surfaces in reversed-phase liquid chromatography. *J. Chromatogr.* **317**, 227-243.
- Benedek, K. (1993). Kinetics of recombinant human brain-derived neurotropic factor unfolding under reversed-phase liquid chromatography conditions. *J. Chromatogr.* **646**, 91-98.
- Bietz, J. A. (2002). HPLC of cereal endosperm storage proteins. In *HPLC of Biological Macromolecules*, Gooding, K. M., and Regnier, F. E., eds. (New York, Marcel Dekker), pp. 547-587.
- Bij, K. E., Horváth, C., Melander, W. R., and Nahum, A. (1981). Surface silanols in silica-bonded hydrocarbonaceous stationary phases : II. Irregular retention behavior and effect of silanol masking. *J. Chromatogr.* **203**, 65-84.
- Blondelle, S. E., Buttner, K., and Houghten, R. A. (1992a). Evaluation of peptide-peptide interactions using reversed-phase high-performance liquid chromatography. *J. Chromatogr.* **625**, 199-206.
- Blondelle, S. E., and Houghten, R. A. (1992b). Design of model amphipathic peptides having potent antimicrobial activities. *Biochemistry* **31**, 12688-12694.
- Blondelle, S. E., Ostresh, J. M., Houghten, R. A., and Perez-Paya, E. (1995). Induced conformational states of amphipathic peptides in aqueous/lipid environments. *Biophys. J.* **68**, 351-359.
- Blondelle, S. E., Forood, B., Perez-Paya, E., and Houghten, R. A. (1996). Evidence of conformational equilibria during the RP-HPLC elution process of peptides. *Int. J. Biochromatogr.* **2**, 133-144.
- Blondelle, S. E., Lohner, K., and Aguilar, M. (1999). Lipid-induced conformation and lipid-binding properties of cytolytic and antimicrobial peptides: determination and biological specificity. *Biochim. Biophys. Acta* **1462**, 89-108.

- Boman, H. C., Boman, I. A., Andreu, D., Li, Z. Q., Merrifield, R. B., Schlenstedt, G., and Zimmermann, R. (1989). Chemical synthesis and enzymic processing of precursor forms of cecropins A and B. *J. Biol. Chem.* **264**, 5852-5860.
- Boman, H. G. (1991). Antibacterial peptides: key components needed in immunity. *Cell* **65**, 205-207.
- Boman, H. G., Agerberth, B., and Boman, A. (1993). Mechanisms of action on *Escherichia coli* of cecropin P1 and PR-39, two antibacterial peptides from pig intestine. *Infect Immun* **61**, 2978-2984.
- Boyes, B. E., and Kirkland, J. J. (1993). Rapid, high-resolution HPLC separation of peptides using small particles at elevated temperatures. *Pept. Res.* **6**, 249-258.
- Brisson-Noel, A., Arthur, M., and Courvalin, P. (1988). Evidence for natural gene transfer from gram-positive cocci to *Escherichia coli*. *J. Bacteriol* **170**, 1739-1745.
- Browne, C. A., Bennett, H. P., and Solomon, S. (1982). The isolation of peptides by high-performance liquid chromatography using predicted elution positions. *Anal. Biochem.* **124**, 201-208.
- Burke, T. W., Mant, C. T., Black, J. A., and Hodges, R. S. (1989). Strong cation-exchange high-performance liquid chromatography of peptides. Effect of non-specific hydrophobic interactions and linearization of peptide retention behaviour. *J. Chromatogr.* **476**, 377-389.
- Burke, T. W., Black, J. A., Mant, C. T., and Hodges, R. S. (1991). Preparative reversed-phase shallow gradient approach to the purification of closely-related peptide analogs on analytical instrument. In *High-performance liquid chromatography of peptides and proteins: separation, analysis and conformation*, Mant, C. T., and Hodges, R. S., eds. (Boca Raton, FL, CRC Press, Inc), pp. 783-792.
- Burton, W. G., Nugent, K. D., Slattery, T. K., Summers, B. R., and Snyder, L. R. (1988). Separation of proteins by reversed-phase high-performance liquid chromatography. I. Optimizing the column. *J. Chromatogr.* **443**, 363-379.
- Calza, L., Manfredi, R., and Chiodo, F. (2004). Infective endocarditis: a review of the best treatment options. *Expert Opin Pharmacother* **5**, 1899-1916.
- Carver, T., and Bleasby, A. (2003). The design of Jemboss: a graphical user interface to EMBOSS. *Bioinformatics* **19**, 1837-1843.
- Chakrabarty, A., Kortemme, T., and Baldwin, R. L. (1994). Helix propensities of the amino acids measured in alanine-based peptides without helix-stabilizing side-chain interactions. *Protein Sci.* **3**, 843-852.

- Chen, Y., Mant, C. T., and Hodges, R. S. (2002). Determination of stereochemistry stability coefficients of amino acid side-chains in an amphipathic alpha-helix. *J. Pept. Res.* **59**, 18-33.
- Chen, Y., Mant, C. T., and Hodges, R. S. (2003). Temperature selectivity effects in reversed-phase liquid chromatography due to conformation differences between helical and non-helical peptides. *J. Chromatogr. A* **1010**, 45-61.
- Chloupek, R. C., Hancock, W. S., Marchylo, B. A., Kirkland, J. J., Boyes, B. E., and Snyder, L. R. (1994). Temperature as a variable in reversed-phase high-performance liquid chromatographic separations of peptide and protein samples. II. Selectivity effects observed in the separation of several peptide and protein mixtures. *J. Chromatogr. A* **686**, 45-59.
- Chou, P. Y., and Fasman, G. D. (1974). Prediction of protein conformation. *Biochemistry* **13**, 222-245.
- Christensen, B., Fink, J., Merrifield, R. B., and Mauzerall, D. (1988). Channel-forming properties of cecropins and related model compounds incorporated into planar lipid membranes. *Proc Natl Acad Sci U S A* **85**, 5072-5076.
- Clejan, S. (1998). HPLC analytical methods for the separation of molecular species of fatty acids in diacylglycerol and cellular phospholipids. *Methods Mol Biol* **105**, 255-274.
- Cohen, K. A., Schellenberg, K., Benedek, K., Karger, B. L., Grego, B., and Hearn, M. T. (1984). Mobile-phase and temperature effects in the reversed phase chromatographic separation of proteins. *Anal. Biochem.* **140**, 223-235.
- Cooper, T. M., and Woody, R. W. (1990). The effect of conformation on the CD of interacting helices: a theoretical study of tropomyosin. *Biopolymers* **30**, 657-676.
- Cornette, J. L., Cease, K. B., Margalit, H., Spouge, J. L., Berzofsky, J. A., and DeLisi, C. (1987). Hydrophobicity scales and computational techniques for detecting amphipathic structures in proteins. *J. Mol. Biol.* **195**, 659-685.
- Crimmins, D. L., Thoma, R. S., McCourt, D. W., and Schwartz, B. D. (1989). Strong-cation-exchange sulfoethyl aspartamide chromatography for peptide mapping of *Staphylococcus aureus* V8 protein digests. *Anal. Biochem.* **176**, 255-260.
- Cunico, R. L., Gooding, K. M., and Wehr, T., eds. (1998). HPLC and CE of Biomolecules (Richmond, Bay bioanalytical laboratory).
- Dathe, M., Wieprecht, T., Nikolenko, H., Handel, L., Maloy, W. L., MacDonald, D. L., Beyermann, M., and Bienert, M. (1997). Hydrophobicity, hydrophobic moment and angle subtended by charged residues modulate antibacterial and haemolytic activity of amphipathic helical peptides. *FEBS Lett* **403**, 208-212.
- Daum, G. (1985). Lipids of mitochondria. *Biochim. Biophys. Acta* **822**, 1-42.

- Devaux, P. F., and Seigneuret, M. (1985). Specificity of lipid-protein interactions as determined by spectroscopic techniques. *Biochim. Biophys. Acta* **822**, 63-125.
- Devine, D. A., and Hancock, R. E. (2002). Cationic peptides: distribution and mechanisms of resistance. *Curr Pharm Des* **8**, 703-714.
- Dolan, J. W. (2002). Temperature selectivity in reversed-phase high performance liquid chromatography. *J. Chromatogr. A* **965**, 195-205.
- Donovan, J. W. (1969). In *Ultraviolet Absorption in Physical Principles and Techniques of Protein Chemistry*, Leach, S. J., ed. (New York, Academic Press).
- Doris, P. A. (1984). Separation of biologically important angiotensin peptides by high-performance liquid chromatography on a weak cationic exchange bonded phase. *J. Chromatogr.* **336**, 392-396.
- Duclohier, H., Molle, G., and Spach, G. (1989). Antimicrobial peptide magainin I from *Xenopus* skin forms anion-permeable channels in planar lipid bilayers. *Biophys. J.* **56**, 1017-1021.
- Ehrenstein, G., and Lecar, H. (1977). Electrically gated ionic channels in lipid bilayers. *Q Rev Biophys* **10**, 1-34.
- Eisenberg, D., Weiss, R. M., and Terwilliger, T. C. (1982). The helical hydrophobic moment: a measure of the amphiphilicity of a helix. *Nature* **299**, 371-374.
- Eng, J., Huang, C. G., Pan, Y. C., Hulmes, J. D., and Yalow, R. S. (1987). Guinea pig pancreatic polypeptide: structure and pancreatic content. *Peptides* **8**, 165-168.
- Engelhardt, H., Ahr, G., and Hearn, M. T. (1981a). Experimental studies with a bonded N-acetylamino-propylsilica stationary phase for the aqueous high-performance exclusion chromatography of polypeptides and proteins. *J. Liq. Chromatogr.* **4**, 1361.
- Engelhardt, H., and Mathes, D. (1981b). High-performance liquid chromatography of proteins using chemically-modified silica supports. *Chromatographia* **14**, 325.
- Engstrom, P., Carlsson, A., Engstrom, A., Tao, Z. J., and Bennich, H. (1984). The antibacterial effect of attacins from the silk moth *Hyalophora cecropia* is directed against the outer membrane of *Escherichia coli*. *Embo J* **3**, 3347-3351.
- Epan, R. M., and Vogel, H. J. (1999). Diversity of antimicrobial peptides and their mechanisms of action. *Biochim. Biophys. Acta* **1462**, 11-28.
- Falla, T. J., Karunaratne, D. N., and Hancock, R. E. (1996). Mode of action of the antimicrobial peptide indolicidin. *J. Biol. Chem.* **271**, 19298-19303.

- Fausnaugh, J. L., Kennedy, L. A., and Regnier, F. E. (1984a). Comparison of hydrophobic-interaction and reversed-phase chromatography of proteins. *J. Chromatogr.* **317**, 141-155.
- Fausnaugh, J. L., Pfannkoch, E., Gupta, S., and Regnier, F. E. (1984b). High-performance hydrophobic interaction chromatography of proteins. *Anal. Biochem.* **137**, 464-472.
- Finland, M. (1979). Emergence of antibiotic resistance in hospitals, 1935-1975. *Rev Infect Dis* **1**, 4-22.
- Florin-Christensen, J., Suarez, C. E., Florin-Christensen, M., Wainszelbaum, M., Brown, W. C., McElwain, T. F., and Palmer, G. H. (2001). A unique phospholipid organization in bovine erythrocyte membranes. *Proc Natl Acad Sci U S A* **98**, 7736-7741.
- Gaertner, H., and Puigserver, A. (1985). Separation of some peptides and related isopeptides by high-performance liquid chromatography: structure—retention time relationships. *J. Chromatogr.* **350**, 279-284.
- Ganz, T., and Lehrer, R. I. (1994). Defensins. *Curr Opin Immunol* **6**, 584-589.
- Glajch, J. L., Kirkland, J. J., and Kohler, J. (1987). Effect of column degradation on the reversed-phase high-performance liquid chromatographic separation of peptides and proteins. *J. Chromatogr.* **384**, 81-90.
- Glajch, J. L., and Kirkland, J. J. (1990). *LC-GC* **8**, 140.
- Goldman, M. J., Anderson, G. M., Stolzenberg, E. D., Kari, U. P., Zasloff, M., and Wilson, J. M. (1997). Human beta-defensin-1 is a salt-sensitive antibiotic in lung that is inactivated in cystic fibrosis. *Cell* **88**, 553-560.
- Greenfield, N. J. (1996). Methods to estimate the conformation of proteins and polypeptides from circular dichroism data. *Anal. Biochem.* **235**, 1-10.
- Guo, D., Mant, C. T., Taneja, A. K., Parker, J. M. R., and Hodges, R. S. (1986a). Prediction of peptide retention times in reversed-phase high-performance liquid chromatography. I. Determination of retention coefficients of amino acid residues using model synthetic peptides. *J. Chromatogr.* **359**, 499-518.
- Guo, D., Mant, C. T., Taneja, A. K., Parker, J. M. R., and Hodges, R. S. (1986b). Prediction of peptide retention times in reversed-phase high-performance liquid chromatography. II. Correlation of observed and predicted peptide retention times and factors influencing retention times of peptides. *J. Chromatogr.* **359**, 519-532.
- Guo, D. C., Mant, C. T., and Hodges, R. S. (1987). Effects of ion-pairing reagents on the prediction of peptide retention in reversed-phase high-performance liquid chromatography. *J. Chromatogr.* **386**, 205-222.

- Gurley, L. R., Prentice, D. A., Valdez, J. G., and Spall, W. D. (1983). Histone fractionation by high-performance liquid chromatography on cyanoalkylsilane (CN) reverse-phase columns. *Anal. Biochem.* **131**, 465-477.
- Guttman, A., Varoglu, M., and Khandurina, J. (2004). Multidimensional separations in the pharmaceutical arena. *Drug Discov Today* **9**, 136-144.
- Hancock, R. E., Falla, T., and Brown, M. (1995). Cationic bactericidal peptides. *Adv Microb Physiol* **37**, 135-175.
- Hancock, R. E. (1997). Peptide antibiotics. *Lancet* **349**, 418-422.
- Hancock, R. E. (1998). The therapeutic potential of cationic peptides. *Exp. Opin. Invest. Drugs* **7**, 167-174.
- Hancock, R. E., and Lehrer, R. (1998). Cationic peptides: a new source of antibiotics. *Trends biotechnol.* **16**, 82-88.
- Hancock, R. E., and Rozek, A. (2002). Role of membranes in the activities of antimicrobial cationic peptides. *FEMS Microbiol Lett* **206**, 143-149.
- Hancock, W. S., Knighton, D. R., Napier, J. R., Harding, D. R., and Venable, R. (1986). Determination of thermodynamic parameters for the interaction of a lipid-binding peptide and insulin with a reversed-phase column. *J. Chromatogr.* **367**, 1-8.
- Hancock, W. S., Chloupek, R. C., Kirkland, J. J., and Snyder, L. R. (1994). Temperature as a variable in reversed-phase high-performance liquid chromatographic separations of peptide and protein samples. I. Optimizing the separation of a growth hormone tryptic digest. *J. Chromatogr. A* **686**, 31-43.
- Hartmann, E., Chen, Y., Mant, C. T., Jungbauer, A., and Hodges, R. S. (2003). Comparison of reversed-phase liquid chromatography and hydrophilic interaction/cation-exchange chromatography for the separation of amphipathic alpha-helical peptides with L- and D-amino acid substitutions in the hydrophilic face. *J. Chromatogr. A* **1009**, 61-71.
- Heinitz, M. L., Flanigan, E., Orlowski, R. C., and Regnier, F. E. (1988). Correlation of calcitonin structure with chromatographic retention in high-performance liquid chromatography. *J. Chromatogr.* **443**, 229-245.
- Henderson, D. E., and Mello, J. A. (1990). Physicochemical studies of biologically active peptides by low-temperature reversed-phase high-performance liquid chromatography. *J. Chromatogr.* **499**, 79-88.
- Hodges, R. S., and Merrifield, R. B. (1975). The role of serine-123 in the activity and specificity of ribonuclease. Reactivation of ribonuclease 1-118 by the synthetic COOH-terminal tetradecapeptide, ribonuclease 111-124, and its O-methylserine and alanine analogs. *J. Biol. Chem.* **250**, 1231-1241.

- Hodges, R. S., Zhu, B. Y., Zhou, N. E., and Mant, C. T. (1994). Reversed-phase liquid chromatography as a useful probe of hydrophobic interactions involved in protein folding and protein stability. *J. Chromatogr. A* **676**, 3-15.
- Hodges, R. S. (1996). Boehringer Mannheim award lecture 1995. La conference Boehringer Mannheim 1995. De novo design of alpha-helical proteins: basic research to medical applications. *Biochem. Cell Biol.* **74**, 133-154.
- Hodges, R. S., Chen, Y., Kopecky, E., and Mant, C. T. (2004). Monitoring the hydrophilicity/hydrophobicity of amino acid side-chains in the non-polar and polar faces of amphipathic α -helices by reversed-phase and hydrophilic interaction/cation-exchange chromatography. *J. Chromatogr. A* **1053**, 161-172.
- Hong, A., Brasseur, M. M., and Kesuma, D. (1991). Purification of histidine-rich hydrophilic peptides. In *HPLC of peptides and proteins: separation, analysis and conformation*, Mant, C. T., and Hodges, R. S., eds. (Boca Raton, FL, CRC Press), pp. 765.
- Horvath, C., Melander, W., and Molnar, I. (1976). Solvophobic interactions in liquid chromatography with nonpolar stationary phases. *J. Chromatogr.* **125**, 129-156.
- Horvath, C., Melander, W., Molnar, I., and Molnar, P. (1977). Enhancement of retention by ion-pair formation in liquid chromatography with nonpolar stationary phases. *Anal. Chem.* **49**, 2295-2305.
- Houghten, R. A., and DeGraw, S. T. (1987). Effect of positional environmental domains on the variation of high-performance liquid chromatographic peptide retention coefficients. *J. Chromatogr.* **386**, 223-228.
- Houston, M. E., Jr., Kondejewski, L. H., Karunaratne, D. N., Gough, M., Fidai, S., Hodges, R. S., and Hancock, R. E. (1998). Influence of preformed alpha-helix and alpha-helix induction on the activity of cationic antimicrobial peptides. *J. Pept. Res.* **52**, 81-88.
- Imanari, T., Toida, T., Koshiishi, I., and Toyoda, H. (1996). High-performance liquid chromatographic analysis of glycosaminoglycan-derived oligosaccharides. *J. Chromatogr. A* **720**, 275-293.
- Ingraham, R. H., Lau, S. Y., Taneja, A. K., and Hodges, R. S. (1985). Denaturation and the effects of temperature on hydrophobic-interaction and reversed-phase high-performance liquid chromatography of proteins : Bio-gel tsk-phenyl-5-pw column. *J. Chromatogr.* **327**, 77-92.
- Issaq, H. J. (2001). The role of separation science in proteomics research. *Electrophoresis* **22**, 3629-3638.
- Iwanaga, S., Muta, T., Shigenaga, T., Seki, N., Kawano, K., Katsu, T., and Kawabata, S. (1994). Structure-function relationships of tachyplesins and their analogues. *Ciba Found Symp* **186**, 160-174; discussion 174-165.

Jacob, L., and Zasloff, M. (1994). Potential therapeutic applications of magainins and other antimicrobial agents of animal origin. *Ciba Found Symp* **186**, 197-216; discussion 216-123.

Jacqueline, C., Asseray, N., Batard, E., Mabecque, V. L., Kergueris, M. F., Dube, L., Bugnon, D., Potel, G., and Caillon, J. (2004). In vivo efficacy of linezolid in combination with gentamicin for the treatment of experimental endocarditis due to methicillin-resistant *Staphylococcus aureus*. *Int J Antimicrob Agents* **24**, 393-396.

Johnson, W. C., Jr. (1990). Protein secondary structure and circular dichroism: a practical guide. *Proteins* **7**, 205-214.

Kelly, S. M., and Price, N. C. (1997). The application of circular dichroism to studies of protein folding and unfolding. *Biochim. Biophys. Acta* **1338**, 161-185.

Kennedy, L. A., Kopaciewicz, W., and Regnier, F. E. (1986). Multimodal liquid chromatography columns for the separation of proteins in either the anion-exchange or hydrophobic-interaction mode. *J. Chromatogr.* **359**, 73-84.

Kentsis, A., and Sosnick, T. R. (1998). Trifluoroethanol promotes helix formation by destabilizing backbone exposure: desolvation rather than native hydrogen bonding defines the kinetic pathway of dimeric coiled coil folding. *Biochemistry* **37**, 14613-14622.

Khaled, M. A., Urry, D. W., Sugano, H., Miyoshi, M., and Izumiya, N. (1978). Hydrogen-deuterium substitution and solvent effects on the nitrogen-15 nuclear magnetic resonance of gramicidin S: evaluation of secondary structure. *Biochemistry* **17**, 2490-2494.

Kirkland, J. J., Glajch, J. L., and Farlee, R. D. (1989). Synthesis and characterization of highly stable bonded phases for high-performance liquid chromatography column packings. *Anal. Chem.* **61**, 2-11.

Kirkland, J. J., and Dilkes, C. H. J. (1993). *LC-GC* **11**, 290.

Kirkland, J. J., Henderson, J. W., DeStefano, J. J., van Straten, M. A., and Claessens, H. A. (1997). Stability of silica-based, endcapped columns with pH 7 and 11 mobile phases for reversed-phase high-performance liquid chromatography. *J. Chromatogr. A* **762**, 97-112.

Kirkland, J. J., van Straten, M. A., and Claessens, H. A. (1998). Reversed-phase high-performance liquid chromatography of basic compounds at pH 11 with silica-based column packings. *J. Chromatogr.* **797**, 111-120.

Kissinger, P. T. (1977). Reverse-phase ion-pair partition chromatography. Comments. *Anal. Chem.* **49**, 883-883.

- Koizumi, K. (1996). High-performance liquid chromatographic separation of carbohydrates on graphitized carbon columns. *J. Chromatogr. A* **720**, 119-126.
- Kondejewski, L. H., Farmer, S. W., Wishart, D. S., Kay, C. M., Hancock, R. E., and Hodges, R. S. (1996). Modulation of structure and antibacterial and hemolytic activity by ring size in cyclic gramicidin S analogs. *J. Biol. Chem.* **271**, 25261-25268.
- Kondejewski, L. H., Jelokhani-Niaraki, M., Farmer, S. W., Lix, B., Kay, C. M., Sykes, B. D., Hancock, R. E., and Hodges, R. S. (1999). Dissociation of antimicrobial and hemolytic activities in cyclic peptide diastereomers by systematic alterations in amphipathicity. *J. Biol. Chem.* **274**, 13181-13192.
- Kondejewski, L. H., Lee, D. L., Jelokhani-Niaraki, M., Farmer, S. W., Hancock, R. E., and Hodges, R. S. (2002). Optimization of microbial specificity in cyclic peptides by modulation of hydrophobicity within a defined structural framework. *J. Biol. Chem.* **277**, 67-74.
- Kopaciewicz, W., and Regnier, F. E. (1982). Nonideal size-exclusion chromatography of proteins: effects of pH at low ionic strength. *Anal. Biochem.* **126**, 8-16.
- Kopaciewicz, W., Rounds, M. A., Fausnaugh, J., and Regnier, F. E. (1983). Retention model for high-performance ion-exchange chromatography. *J. Chromatogr.* **266**, 3-21.
- Koppelman, C. M., Den Blaauwen, T., Duursma, M. C., Heeren, R. M., and Nanninga, N. (2001). *Escherichia coli* minicell membranes are enriched in cardiolipin. *J. Bacteriol.* **183**, 6144-6147.
- Kraak, J. C., Jonker, K. M., and Huber, J. K. (1977). Solvent-generated ion-exchange systems with anionic surfactants for rapid separations of amino acids. *J. Chromatogr.* **142**, 671-688.
- Krause, E., Bienert, M., Schmieder, P., and Wenschuh, H. (2000). The Helix-Destabilizing Propensity Scale of D-Amino Acids: The Influence of Side Chain Steric Effects. *J. Am. Chem. Soc.* **122**, 4865-4870.
- Lau, S. Y., Taneja, A. K., and Hodges, R. S. (1984a). Synthesis of a model protein of defined secondary and quaternary structure. Effect of chain length on the stabilization and formation of two-stranded alpha-helical coiled-coils. *J. Biol. Chem.* **259**, 13253-13261.
- Lau, S. Y. M., Taneja, A. K., and Hodges, R. S. (1984b). Effects of HPLC solvents and hydrophobic supports on the secondary and quaternary structure of a model protein: Reversed-phase and size-exclusion high performance liquid chromatography. *J. Chromatogr.* **317**, 129-140.
- Lazoura, E., Maidonis, I., Bayer, E., Hearn, M. T., and Aguilar, M. I. (1997). Conformational analysis of neuropeptide Y-[18-36] analogs in hydrophobic environments. *Biophys. J.* **72**, 238-246.

- Lee, D. L., and Hodges, R. S. (2003a). Structure-activity relationships of de novo designed cyclic antimicrobial peptides based on gramicidin S. *Biopolymers* **71**, 28-48.
- Lee, D. L., Mant, C. T., and Hodges, R. S. (2003b). A novel method to measure self-association of small amphipathic molecules: temperature profiling in reversed-phase chromatography. *J. Biol. Chem.* **278**, 22918-22927.
- Lee, D. L., Powers, J. P., Pfliegerl, K., Vasil, M. L., Hancock, R. E., and Hodges, R. S. (2004). Effects of single D-amino acid substitutions on disruption of beta-sheet structure and hydrophobicity in cyclic 14-residue antimicrobial peptide analogs related to gramicidin S. *J. Pept. Res.* **63**, 69-84.
- Lee, T. H., Thompson, P. E., Hearn, M. T., and Aguilar, M. I. (1997). Conformational stability of a type II' beta-turn motif in human growth hormone [6-13] peptide analogues at hydrophobic surfaces. *J. Pept. Res.* **49**, 394-403.
- Leem, J. Y., Nishimura, C., Kurata, S., Shimada, I., Kobayashi, A., and Natori, S. (1996). Purification and characterization of N-beta-alanyl-5-S-glutathionyl-3,4-dihydroxyphenylalanine, a novel antibacterial substance of *Sarcophaga peregrina* (flesh fly). *J. Biol. Chem.* **271**, 13573-13577.
- Li, J., and Carr, P. W. (1997a). Estimating diffusion coefficients for alkylbenzenes and alkylphenones in aqueous mixtures with acetonitrile and methanol. *Anal. Chem.* **69**, 2550-2553.
- Li, J., and Carr, P. W. (1997b). Evaluation of temperature effects on selectivity in RPLC separations using polybutadiene-coated zirconia. *Anal. Chem.* **69**, 2202-2206.
- Lindner, H., Sarg, B., Meraner, C., and Helliger, W. (1996). Separation of acetylated core histones by hydrophilic-interaction liquid chromatography. *J. Chromatogr. A* **743**, 137-144.
- Lindner, H., Sarg, B., and Helliger, W. (1997). Application of hydrophilic-interaction liquid chromatography to the separation of phosphorylated H1 histones. *J. Chromatogr. A* **782**, 55-62.
- Lindner, H., Sarg, B., Hoertnagl, B., and Helliger, W. (1998). The microheterogeneity of the mammalian H1(0) histone. Evidence for an age-dependent deamidation. *J. Biol. Chem.* **273**, 13324-13330.
- Lindner, H., Sarg, B., Grunicke, H., and Helliger, W. (1999). Age-dependent deamidation of H1(0) histones in chromatin of mammalian tissues. *J Cancer Res Clin Oncol* **125**, 182-186.
- Lindner, H., and Helliger, W. (2004). Hydrophilic interaction chromatography. In *HPLC of peptides and proteins*, Aguilar, M. I., ed. (Totowa, NJ, Humana Press), pp. 75-88.

- Link, A. J., Eng, J., Schieltz, D. M., Carmack, E., Mize, G. J., Morris, D. R., Garvik, B. M., and Yates, J. R., 3rd (1999). Direct analysis of protein complexes using mass spectrometry. *Nat. Biotechnol.* **17**, 676-682.
- Litowski, J. R., Semchuk, P. D., Mant, C. T., and Hodges, R. S. (1999). Hydrophilic interaction/cation-exchange chromatography for the purification of synthetic peptides from closely related impurities: serine side-chain acetylated peptides. *J Pept Res* **54**, 1-11.
- Liu, F., Lewis, R. N., Hodges, R. S., and McElhaney, R. N. (2002a). Effect of variations in the structure of a polyleucine-based alpha-helical transmembrane peptide on its interaction with phosphatidylcholine bilayers. *Biochemistry* **41**, 9197-9207.
- Liu, F., Lewis, R. N., Hodges, R. S., and McElhaney, R. N. (2004a). Effect of variations in the structure of a polyleucine-based alpha-helical transmembrane peptide on its interaction with phosphatidylglycerol bilayers. *Biochemistry* **43**, 3679-3687.
- Liu, F., Lewis, R. N., Hodges, R. S., and McElhaney, R. N. (2004b). Effect of variations in the structure of a polyleucine-based alpha-helical transmembrane peptide on its interaction with phosphatidylethanolamine bilayers. *Biophysical Journal*, in press.
- Liu, H., Lin, D., and Yates, J. R., 3rd (2002b). Multidimensional separations for protein/peptide analysis in the post-genomic era. *Biotechniques* **32**, 898, 900, 902 passim.
- Liu, L. P., and Deber, C. M. (1998). Guidelines for membrane protein engineering derived from de novo designed model peptides. *Biopolymers* **47**, 41-62.
- Loft, S., Deng, X. S., Tuo, J., Wellejus, A., Sorensen, M., and Poulsen, H. E. (1998). Experimental study of oxidative DNA damage. *Free Radic Res* **29**, 525-539.
- Lork, D. K., Unger, K. K., Bruckner, H., and Hearn, M. T. (1989). Retention behaviour of paracelsin peptides on reversed-phase silicas with varying n-alkyl chain length and ligand density. *J. Chromatogr.* **476**, 135-145.
- Lu, X. M., Figueroa, A., and Karger, B. L. (1988). Intrinsic fluorescence and HPLC measurement of the surface dynamics of lysozyme adsorbed on hydrophobic silica. *J. Am. Chem. Soc.* **110**, 1978-1979.
- Ludtke, S. J., He, K., Heller, W. T., Harroun, T. A., Yang, L., and Huang, H. W. (1996). Membrane pores induced by magainin. *Biochemistry* **35**, 13723-13728.
- Maa, Y. F., and Horvath, C. (1988). Rapid analysis of proteins and peptides by reversed-phase chromatography with polymeric micropellicular sorbents. *J. Chromatogr.* **445**, 71-86.
- Mabuchi, H., and Nakahashi, H. (1981). Systematic separation of medium-sized biologically active peptides by high-performance liquid chromatography. *J. Chromatogr.* **213**, 275-286.

- Majors, R. E. (2004). New Chromatography Columns and Accessories at the 2004 Pittcon Conference, Part I. *LC-GC* **22**, 230-242.
- Mant, C. T., Parker, J. M. R., and Hodges, R. S. (1986). On-line derivatization to restore reserved-phase column performance in peptide separations. *LC-GC* **4**, 1004-1009.
- Mant, C. T., Burke, T. W. L., and Hodges, R. S. (1987a). Optimization of peptide separations in reversed-phase HPLC: isocratic versus gradient elution. *Chromatographia* **24**, 565-572.
- Mant, C. T., and Hodges, R. S. (1987b). Monitoring free silanols on reversed-phase supports with peptide standards. *Chromatographia* **24**, 805-814.
- Mant, C. T., and Hodges, R. S. (1987c). On-line derivatization of silica supports for regeneration and preparation of reversed-phase columns. *J. Chromatogr.* **409**, 155-173.
- Mant, C. T., Parker, J. M., and Hodges, R. S. (1987d). Size-exclusion high-performance liquid chromatography of peptides. Requirement for peptide standards to monitor column performance and non-ideal behaviour. *J. Chromatogr.* **397**, 99-112.
- Mant, C. T., Burke, T. W., Black, J. A., and Hodges, R. S. (1988). Effect of peptide chain length on peptide retention behaviour in reversed-phase chromatography. *J. Chromatogr.* **458**, 193-205.
- Mant, C. T., Zhou, N. E., and Hodges, R. S. (1989). Correlation of protein retention times in reversed-phase chromatography with polypeptide chain length and hydrophobicity. *J. Chromatogr.* **476**, 363-375.
- Mant, C. T., and Hodges, R. S. (1990). HPLC of peptides. In *HPLC of biological macromolecules: methods and applications*, Gooding, K. M., and Regnier, F. E., eds. (New York, NY, Marcel Dekker, Inc.), pp. 301-332.
- Mant, C. T., and Hodges, R. S., eds. (1991). *HPLC of peptides and proteins: separation, analysis and conformation* (Boca Raton, FL, CRC Press).
- Mant, C. T., Zhou, N. E., and Hodges, R. S. (1992). Amino acids and peptides. In *Chromatography*, Heflmann, E., ed. (Amsterdam, Elsevier), pp. B75-B150.
- Mant, C. T., Zhou, N. E., and Hodges, R. S. (1993). The role of amphipathic helices in stabilizing peptide and protein structure. In *The Amphipathic Helix*, Epanand, R. M., ed. (Boca Raton, CRC Press), pp. 39-64.
- Mant, C. T., Burke, T. W., and Hodges, R. S. (1994). A rapid, simple approach to predicting effects of varying run parameters on reversed-phase gradient elution profiles of peptides. *LC-GC* **12**, 396-404.
- Mant, C. T., and Hodges, R. S. (1996). Analysis of peptides by high-performance liquid chromatography. *Methods Enzymol.* **271**, 3-50.

- Mant, C. T., Kondejewski, L. H., Cachia, P. J., Monera, O. D., and Hodges, R. S. (1997). Analysis of synthetic peptides by high-performance liquid chromatography. *Methods Enzymol.* **289**, 426-469.
- Mant, C. T., Kondejewski, L. H., and Hodges, R. S. (1998a). Hydrophilic interaction/cation-exchange chromatography for separation of cyclic peptides. *J. Chromatogr. A* **816**, 79-88.
- Mant, C. T., Litowski, J. R., and Hodges, R. S. (1998b). Hydrophilic interaction/cation-exchange chromatography for separation of amphipathic alpha-helical peptides. *J. Chromatogr. A* **816**, 65-78.
- Mant, C. T., and Hodges, R. S. (2000). Hydrophilic interaction/cation-exchange chromatography of peptides. In *Encyclopedia of Separation Science*, Wilson, I. D., Adland, T. R., Poole, C. F., and Cook, M., eds. (Academic Press), pp. 3615-3626.
- Mant, C. T., and Hodges, R. S. (2002a). Analytical HPLC of Peptides. In *HPLC of biological macromolecules*, Gooding, K. M., and Regnier, F. E., eds. (New York, Marcel Dekker), pp. 433-511.
- Mant, C. T., and Hodges, R. S. (2002b). Reversed-phase liquid chromatography as a tool in the determination of the hydrophilicity/hydrophobicity of amino acid side-chains at a ligand-receptor interface in the presence of different aqueous environments. II. Effect of varying peptide ligand hydrophobicity. *J. Chromatogr. A* **972**, 61-75.
- Mant, C. T., and Hodges, R. S. (2002c). Reversed-phase liquid chromatography as a tool in the determination of the hydrophilicity/hydrophobicity of amino acid side-chains at a ligand-receptor interface in the presence of different aqueous environments. I. Effect of varying receptor hydrophobicity. *J. Chromatogr. A* **972**, 45-60.
- Mant, C. T., Chen, Y., and Hodges, R. S. (2003a). Temperature profiling of polypeptides in reversed-phase liquid chromatography. I. Monitoring of dimerization and unfolding of amphipathic alpha-helical peptides. *J. Chromatogr. A* **1009**, 29-43.
- Mant, C. T., Tripet, B., and Hodges, R. S. (2003b). Temperature profiling of polypeptides in reversed-phase liquid chromatography. II. Monitoring of folding and stability of two-stranded alpha-helical coiled-coils. *J. Chromatogr. A* **1009**, 45-59.
- Marchylo, B. A., Hatcher, D. W., Kruger, J. E., and Kirkland, J. J. (1992). Reversed-phase high performance liquid chromatographic analysis of wheat proteins using a new, highly stable column. *Cereal Chem.* **69**, 371-378.
- Matsuzaki, K. (1998). Magainins as paradigm for the mode of action of pore forming polypeptides. *Biochim Biophys Acta* **1376**, 391-400.
- Matsuzaki, K. (1999). Why and how are peptide-lipid interactions utilized for self-defense? Magainins and tachyplesins as archetypes. *Biochim. Biophys. Acta* **1462**, 1-10.

- McGregor, J. L., Clezardin, P., Manach, M., Gronlund, S., and Dechavanne, M. (1985). Tandem separation of labelled human blood platelet membrane glycoproteins by anion-exchange and gel fast protein liquid chromatography. *J. Chromatogr.* **326**, 179-190.
- McInnes, C., Kondejewski, L. H., Hodges, R. S., and Sykes, B. D. (2000). Development of the structural basis for antimicrobial and hemolytic activities of peptides based on gramicidin S and design of novel analogs using NMR spectroscopy. *J. Biol. Chem.* **275**, 14287-14294.
- McNeff, C., Zigan, L., Johnson, K., Carr, P. W., Wang, A., and Weber-Main, A. M. (2000). *LC-GC* **18**, 514.
- Meek, J. L. (1980). Prediction of peptide retention times in high-pressure liquid chromatography on the basis of amino acid composition. *Proc. Natl. Acad. Sci.* **77**, 1632-1636.
- Meek, J. L., and Rossetti, Z. L. (1981). Factors affecting retention and resolution of peptides in high-performance liquid chromatography. *J. Chromatogr.* **211**, 15-28.
- Milatovic, D., and Braveny, I. (1987). Development of resistance during antibiotic therapy. *Eur J Clin Microbiol* **6**, 234-244.
- Mizzen, C. A., Alpert, A. J., Levesque, L., Kruck, T. P., and McLachlan, D. R. (2000). Resolution of allelic and non-allelic variants of histone H1 by cation-exchange-hydrophilic-interaction chromatography. *J Chromatogr B Biomed Sci Appl* **744**, 33-46.
- Monera, O. D., Sereda, T. J., Zhou, N. E., Kay, C. M., and Hodges, R. S. (1995). Relationship of side-chain hydrophobicity and α -helical propensity on the stability of the single-stranded amphipathic α -helix. *Journal of peptide science* **1**, 319-329.
- Mootz, H. D., and Marahiel, M. A. (1997). The tyrocidine biosynthesis operon of *Bacillus brevis*: complete nucleotide sequence and biochemical characterization of functional internal adenylation domains. *J Bacteriol* **179**, 6843-6850.
- Morse, S. A., Johnson, S. R., Biddle, J. W., and Roberts, M. C. (1986). High-level tetracycline resistance in *Neisseria gonorrhoeae* is result of acquisition of streptococcal tetM determinant. *Antimicrob Agents Chemother* **30**, 664-670.
- Nelson, J. W., and Kallenbach, N. R. (1989). Persistence of the α -helix stop signal in the S-peptide in trifluoroethanol solutions. *Biochemistry* **28**, 5256-5261.
- Neu, H. C. (1992). The crisis in antibiotic resistance. *Science* **257**, 1064-1073.
- Novabiochem (2004). *Novabiochem Catalog and Peptide Synthesis Handbook '2004/2005* (San Diego, CA, Novabiochem).
- Nugent, K. D. (1991). Commercially available columns and packings for reversed-phase HPLC of peptides and proteins. In *HPLC of peptides and proteins: separation, analysis*

and conformation, Mant, C. T., and Hodges, R. S., eds. (Boca Raton, FL, CRC Press), pp. 279-287.

Oh, J. E., Hong, S. Y., and Lee, K. H. (1999). Structure-activity relationship study: short antimicrobial peptides. *J. Pept. Res.* **53**, 41-46.

Oren, Z., Hong, J., and Shai, Y. (1997a). A repertoire of novel antibacterial diastereomeric peptides with selective cytolytic activity. *J. Biol. Chem.* **272**, 14643-14649.

Oren, Z., and Shai, Y. (1997b). Selective lysis of bacteria but not mammalian cells by diastereomers of melittin: structure-function study. *Biochemistry* **36**, 1826-1835.

Oyler, A. R., Armstrong, B. L., Cha, J. Y., Zhou, M., X., Yang, Q., Robinson, R. I., Dunphy, R., and Burinsky, D. J. (1996). Hydrophilic interaction chromatography on amino-silica phases complements reversed-phase high-performance liquid chromatography and capillary electrophoresis for peptide analysis. *J. Chromatogr.* **724**, 378-383.

Pathak, N., Salas-Auvert, R., Ruche, G., Janna, M. H., McCarthy, D., and Harrison, R. G. (1995). Comparison of the effects of hydrophobicity, amphiphilicity, and alpha-helicity on the activities of antimicrobial peptides. *Proteins* **22**, 182-186.

Patton, G. M., and Robins, S. J. (1998). Separation and quantitation of phospholipid classes by HPLC. *Methods Mol Biol* **110**, 193-215.

Pennington, J. E., and Williams, R. M. (1979). Influence of genetic factors on natural resistance of mice to *Pseudomonas aeruginosa*. *J Infect Dis* **139**, 396-400.

Pfannkoch, E., Lu, K. C., Regnier, F. E., and Barth, H. G. (1980). Characterization of some commercial high performance size-exclusion chromatography columns for water-soluble polymers. *J. Chromatogr. Sci.* **18**, 433.

Piers, K. L., and Hancock, R. E. (1994). The interaction of a recombinant cecropin/melittin hybrid peptide with the outer membrane of *Pseudomonas aeruginosa*. *Mol Microbiol* **12**, 951-958.

Pouny, Y., Rapaport, D., Mor, A., Nicolas, P., and Shai, Y. (1992). Interaction of antimicrobial dermaseptin and its fluorescently labeled analogues with phospholipid membranes. *Biochemistry* **31**, 12416-12423.

Purcell, A. W., Aguilar, M. I., and Hearn, M. T. (1989). High-performance liquid chromatography of amino acids, peptides and proteins. XCI. The influence of temperature on the chromatographic behaviour of peptides related to human growth hormone. *J. Chromatogr.* **476**, 125-133.

- Purcell, A. W., Aguilar, M. I., and Hearn, M. T. (1993). High-performance liquid chromatography of amino acids, peptides, and proteins. 123. Dynamics of peptides in reversed-phase high-performance liquid chromatography. *Anal. Chem.* **65**, 3038-3047.
- Purcell, A. W., Aguilar, M. I., and Hearn, M. T. (1995a). Conformational effects in reversed-phase high-performance liquid chromatography of polypeptides. II. The role of insulin A and B chains in the chromatographic behaviour of insulin. *J. Chromatogr. A* **711**, 71-79.
- Purcell, A. W., Aguilar, M. I., and Hearn, M. T. (1995b). Conformational effects in reversed-phase high-performance liquid chromatography of polypeptides. I. Resolution of insulin variants. *J. Chromatogr. A* **711**, 61-70.
- Purcell, A. W., Aguilar, M. I., Wettenhall, R. E., and Hearn, M. T. (1995c). Induction of amphipathic helical peptide structures in RP-HPLC. *Pept. Res.* **8**, 160-170.
- Regnier, F. E. (1983). High-performance liquid chromatography of proteins. *Methods Enzymol.* **91**, 137-190.
- Richards, K. L., Aguilar, M. I., and Hearn, M. T. W. (1994). A comparative study of the retention behaviour and stability of cytochrome c in reversed-phase high-performance liquid chromatography. *J. Chromatogr.* **676**, 17-31.
- Rivier, J., McClintock, R., Galyean, R., and Anderson, H. (1984). Reversed-phase high-performance liquid chromatography: preparative purification of synthetic peptides. *J. Chromatogr.* **288**, 303-328.
- Rosenfeld, R., and Benedek, K. (1993). Conformational changes of brain-derived neurotrophic factor during reversed-phase high-performance liquid chromatography. *J. Chromatogr.* **632**, 29-36.
- Rothmund, S., Beyermann, M., Krause, E., Krause, G., Bienert, M., Hodges, R. S., Sykes, B. D., and Sonnichsen, F. D. (1995). Structure effects of double D-amino acid replacements: a nuclear magnetic resonance and circular dichroism study using amphipathic model helices. *Biochemistry* **34**, 12954-12962.
- Rothmund, S., Krause, E., Beyermann, M., Dathe, M., Bienert, M., Hodges, R. S., Sykes, B. D., and Sonnichsen, F. D. (1996). Peptide destabilization by two adjacent D-amino acids in single-stranded amphipathic alpha-helices. *Pept. Res.* **9**, 79-87.
- Rounds, M. A., Rounds, W. D., and Regnier, F. E. (1987). Poly(styrene-divinylbenzene)-based strong anion-exchange packing material for high-performance liquid chromatography of proteins. *J. Chromatogr.* **397**, 25-38.
- Sagliano, N., Floyd, T. R., Hartwick, R. A., Dibussolo, J. M., and Miller, N. T. (1988). Studies on the stabilization of reversed-phases for liquid chromatography. *J. Chromatogr.* **443**, 155-172.

- Sahl, H. G. (1994). Gene-encoded antibiotics made in bacteria. *Ciba Found Symp* **186**, 27-42; discussion 42-53.
- Sakamoto, Y., Kawakami, N., and Sasagawa, T. (1988). Prediction of peptide retention times. *J. Chromatogr.* **442**, 69-79.
- Salgado, J., Grage, S. L., Kondejewski, L. H., Hodges, R. S., McElhaney, R. N., and Ulrich, A. S. (2001). Membrane-bound structure and alignment of the antimicrobial beta-sheet peptide gramicidin S derived from angular and distance constraints by solid state 19F-NMR. *J Biomol NMR* **21**, 191-208.
- Sarin, V. K., Kent, S. B., Tam, J. P., and Merrifield, R. B. (1981). Quantitative monitoring of solid-phase peptide synthesis by the ninhydrin reaction. *Anal. Biochem.* **117**, 147-157.
- Sasagawa, T., Okuyama, T., and Teller, D. C. (1982). Prediction of peptide retention times in reversed-phases high-performance liquid chromatography during linear gradient elution. *J. Chromatogr.* **240**, 329-340.
- Schaberg, D. R., Rubens, C. E., Alford, R. H., Farrar, W. E., Schaffner, W., and McGee, Z. A. (1981). Evolution of antimicrobial resistance and nosocomial infection. Lessons from the Vanderbilt experience. *Am J Med* **70**, 445-448.
- Scholtz, J. M., Qian, H., Robbins, V. H., and Baldwin, R. L. (1993). The energetics of ion-pair and hydrogen-bonding interactions in a helical peptide. *Biochemistry* **32**, 9668-9676.
- Segrest, J. P., De Loof, H., Dohlman, J. G., Brouillette, C. G., and Anantharamaiah, G. M. (1990). Amphipathic helix motif: classes and properties. *Proteins* **8**, 103-117.
- Sereda, T. J., Mant, C. T., Quinn, A. M., and Hodges, R. S. (1993). Effect of the alpha-amino group on peptide retention behaviour in reversed-phase chromatography. Determination of the pK(a) values of the alpha-amino group of 19 different N-terminal amino acid residues. *J. Chromatogr.* **646**, 17-30.
- Sereda, T. J., Mant, C. T., Sonnichsen, F. D., and Hodges, R. S. (1994). Reversed-phase chromatography of synthetic amphipathic alpha-helical peptides as a model for ligand/receptor interactions. Effect of changing hydrophobic environment on the relative hydrophilicity/hydrophobicity of amino acid side-chains. *J. Chromatogr. A* **676**, 139-153.
- Sereda, T. J., Mant, C. T., and Hodges, R. S. (1995). Selectivity due to conformational differences between helical and non-helical peptides in reversed-phase chromatography. *J. Chromatogr. A* **695**, 205-221.
- Sereda, T. J., Mant, C. T., and Hodges, R. S. (1997). Use of sodium perchlorate at low pH for peptide separations by reversed-phase liquid chromatography. Influence of perchlorate ion on apparent hydrophilicity of positively charged amino acid side-chains. *J. Chromatogr. A* **776**, 153-165.

- Shai, Y., and Oren, Z. (1996). Diastereoisomers of cytolysins, a novel class of potent antibacterial peptides. *J. Biol. Chem.* **271**, 7305-7308.
- Shai, Y. (1999). Mechanism of the binding, insertion and destabilization of phospholipid bilayer membranes by alpha-helical antimicrobial and cell non-selective membrane-lytic peptides. *Biochim. Biophys. Acta* **1462**, 55-70.
- Shibue, M., Mant, C. T., and Hodges, R. S. (2005). The perchlorate anion is more effective than the trifluoroacetate anion as an ion-pairing reagent for reversed-phase chromatography of peptides. *J. Chromatogr. A*, in press.
- Shin, S. Y., Lee, M. K., Kim, K. L., and Hahm, K. S. (1997). Structure-antitumor and hemolytic activity relationships of synthetic peptides derived from cecropin A-magainin 2 and cecropin A-melittin hybrid peptides. *J. Pept. Res.* **50**, 279-285.
- Shoemaker, K. R., Kim, P. S., York, E. J., Stewart, J. M., and Baldwin, R. L. (1987). Tests of the helix dipole model for stabilization of alpha-helices. *Nature* **326**, 563-567.
- Sitaram, N., and Nagaraj, R. (1999). Interaction of antimicrobial peptides with biological and model membranes: structural and charge requirements for activity. *Biochim. Biophys. Acta* **1462**, 29-54.
- Sitaram, N., and Nagaraj, R. (2002). Host-defense antimicrobial peptides: importance of structure for activity. *Curr Pharm Des* **8**, 727-742.
- Sitrin, R., DePhillips, P., Dingerdissen, J., Erhard, K., and Filan, J. (1986). Preparative liquid chromatography, a strategic approach. *LC-GC* **4**, 530.
- Snider, R. H., Moore, C. F., Nylen, E. S., and Becker, K. L. (1988). Improved HPLC separation of radiolabelled hormonal peptides. *Horm. Metab. Res.* **20**, 254-255.
- Sonnichsen, F. D., Van Eyk, J. E., Hodges, R. S., and Sykes, B. D. (1992). Effect of trifluoroethanol on protein secondary structure: an NMR and CD study using a synthetic actin peptide. *Biochemistry* **31**, 8790-8798.
- Srimal, S., Surolia, N., Balasubramanian, S., and Surolia, A. (1996). Titration calorimetric studies to elucidate the specificity of the interactions of polymyxin B with lipopolysaccharides and lipid A. *Biochem J* **315 (Pt 2)**, 679-686.
- Steer, D. L., Thompson, P. E., Blondelle, S. E., Houghten, R. A., and Aguilar, M. I. (1998). Comparison of the binding of alpha-helical and beta-sheet peptides to a hydrophobic surface. *J. Pept. Res.* **51**, 401-412.
- Stein, G. M., Schaller, G., Pfuller, U., Wagner, M., Wagner, B., Schietzel, M., and Bussing, A. (1999). Characterisation of granulocyte stimulation by thionins from European mistletoe and from wheat. *Biochim. Biophys. Acta* **1426**, 80-90.

Steinberg, D. A., Hurst, M. A., Fujii, C. A., Kung, A. H., Ho, J. F., Cheng, F. C., Loury, D. J., and Fiddes, J. C. (1997). Protegrin-1: a broad-spectrum, rapidly microbicidal peptide with in vivo activity. *Antimicrob Agents Chemother* **41**, 1738-1742.

Steiner, H., Hultmark, D., Engstrom, A., Bennich, H., and Boman, H. G. (1981). Sequence and specificity of two antibacterial proteins involved in insect immunity. *Nature* **292**, 246-248.

Steiner, V., Schar, M., Bornsen, K. O., and Mutter, M. (1991). Retention behaviour of a template-assembled synthetic protein and its amphiphilic building blocks on reversed-phase columns. *J. Chromatogr.* **586**, 43-50.

Steiner, V., Schar, M., Bornsen, K. L., and Mutter, M. (1998). *Trends Biochem. Sci.* **13**, 360.

Tally, F. P., and Cuchural, G. J., Jr. (1988). Antibiotic resistance in anaerobic bacteria. *J Antimicrob Chemother* **22 Suppl A**, 63-71.

Tarr, G. E., and Crabb, J. W. (1983). Reverse-phase high-performance liquid chromatography of hydrophobic proteins and fragments thereof. *Anal. Biochem.* **131**, 99-107.

Thomas, C. J., and Surolia, A. (1999). Kinetics of the interaction of endotoxin with polymyxin B and its analogs: a surface plasmon resonance analysis. *FEBS Lett* **445**, 420-424.

Tiihonen, J., Sainio, T., Karki, A., and Paatero, E. (2002). Co-eluent effect in partition chromatography. Rhamnose-xylose separation with strong and weak cation-exchangers in aqueous ethanol. *J. Chromatogr. A* **982**, 69-84.

Titani, K., Sasagawa, T., Resing, K., and Walsh, K. A. (1982). A simple and rapid purification of commercial trypsin and chymotrypsin by reverse-phase high-performance liquid chromatography. *Anal. Biochem.* **123**, 408-412.

Torres, O. R., Korman, R. Z., Zahler, S. A., and Dunny, G. M. (1991). The conjugative transposon Tn925: enhancement of conjugal transfer by tetracycline in *Enterococcus faecalis* and mobilization of chromosomal genes in *Bacillus subtilis* and *E. faecalis*. *Mol Gen Genet* **225**, 395-400.

Tosteson, M. T., Holmes, S. J., Razin, M., and Tosteson, D. C. (1985). Melittin lysis of red cells. *J. Membr. Biol.* **87**, 35-44.

Travis, J. (1994). Reviving the antibiotic miracle? *Science* **264**, 360-362.

Tripet, B., Wagschal, K., Lavigne, P., Mant, C. T., and Hodges, R. S. (2000). Effects of side-chain characteristics on stability and oligomerization state of a de novo-designed model coiled-coil: 20 amino acid substitutions in position "d". *J. Mol. Biol.* **300**, 377-402.

- Van de Venne, J. L. M., Hendriks, J. L. H. M., and Deedler, R. S. (1978). Retention behaviour of carboxylic acids in reversed-phase column liquid chromatography. *J. Chromatogr.* **167**, 1-16.
- van 't Hof, W., Veerman, E. C., Helmerhorst, E. J., and Amerongen, A. V. (2001). Antimicrobial peptides: properties and applicability. *Biol Chem* **382**, 597-619.
- Velasco, M., Diaz-Guerra, M. J., Diaz-Achirica, P., Andreu, D., Rivas, L., and Bosca, L. (1997). Macrophage triggering with cecropin A and melittin-derived peptides induces type II nitric oxide synthase expression. *J Immunol* **158**, 4437-4443.
- Wagenlehner, F. M., and Naber, K. G. (2004). New drugs for Gram-positive uropathogens. *Int J Antimicrob Agents* **24 Suppl 1**, 39-43.
- Wagner, K., Racaityte, K., Unger, K. K., Miliotis, T., Edholm, L. E., Bischoff, R., and Marko-Varga, G. (2000). Protein mapping by two-dimensional high performance liquid chromatography. *J. Chromatogr. A* **893**, 293-305.
- Wagner, K., Miliotis, T., Marko-Varga, G., Bischoff, R., and Unger, K. K. (2002). An automated on-line multidimensional HPLC system for protein and peptide mapping with integrated sample preparation. *Anal. Chem.* **74**, 809-820.
- Washburn, M. P., Wolters, D., and Yates, J. R., 3rd (2001). Large-scale analysis of the yeast proteome by multidimensional protein identification technology. *Nat. Biotechnol.* **19**, 242-247.
- Wehr, T. (2002). Multidimensional liquid chromatography in proteomics studies. *LC-GC* **20**, 954-963.
- Wilderman, P. J., Vasil, A. I., Johnson, Z., and Vasil, M. L. (2001). Genetic and biochemical analyses of a eukaryotic-like phospholipase D of *Pseudomonas aeruginosa* suggest horizontal acquisition and a role for persistence in a chronic pulmonary infection model. *Mol Microbiol* **39**, 291-303.
- Williams, R. C., Vasta-Russell, J. F., Glajch, J. L., and Golebiowski, K. (1986). Separation of proteins on a polymeric fluorocarbon high-performance liquid chromatography column packing. *J. Chromatogr.* **371**, 63-70.
- Wilson, K. J., Honegger, A., Stotzel, R. P., and Hughes, G. J. (1981). The behaviour of peptides on reverse-phase supports during high-pressure liquid chromatography. *Biochem J* **199**, 31-41.
- Woody, R. W. (1995). Circular dichroism. *Methods Enzymol.* **246**, 34-71.
- Wu, M., and Hancock, R. E. (1999). Interaction of the cyclic antimicrobial cationic peptide bactenecin with the outer and cytoplasmic membrane. *J. Biol. Chem.* **274**, 29-35.

- Yoo, Y. C., Watanabe, R., Koike, Y., Mitobe, M., Shimazaki, K., Watanabe, S., and Azuma, I. (1997). Apoptosis in human leukemic cells induced by lactoferricin, a bovine milk protein-derived peptide: involvement of reactive oxygen species. *Biochem. Biophys. Res. Commun.* **237**, 624-628.
- Yu, Y. B., Wagschal, K. C., Mant, C. T., and Hodges, R. S. (2000). Trapping the monomeric alpha-helical state during unfolding of coiled-coils by reversed-phase liquid chromatography. *J. Chromatogr. A* **890**, 81-94.
- Zasloff, M. (1987). Magainins, a class of antimicrobial peptides from *Xenopus* skin: isolation, characterization of two active forms, and partial cDNA sequence of a precursor. *Proc Natl Acad Sci U S A* **84**, 5449-5453.
- Zhang, L., Falla, T., Wu, M., Fidai, S., Burian, J., Kay, W., and Hancock, R. E. (1998). Determinants of recombinant production of antimicrobial cationic peptides and creation of peptide variants in bacteria. *Biochem. Biophys. Res. Commun.* **247**, 674-680.
- Zhang, L., Benz, R., and Hancock, R. E. (1999). Influence of proline residues on the antibacterial and synergistic activities of alpha-helical peptides. *Biochemistry* **38**, 8102-8111.
- Zhang, L., Rozek, A., and Hancock, R. E. (2001). Interaction of cationic antimicrobial peptides with model membranes. *J. Biol. Chem.* **276**, 35714-35722.
- Zhao, C., Liaw, L., Lee, I. H., and Lehrer, R. I. (1997). cDNA cloning of three cecropin-like antimicrobial peptides (Styelins) from the tunicate, *Styela clava*. *FEBS Lett* **412**, 144-148.
- Zhou, N. E., Mant, C. T., and Hodges, R. S. (1990). Effect of preferred binding domains on peptide retention behavior in reversed-phase chromatography: amphipathic alpha-helices. *Pept. Res.* **3**, 8-20.
- Zhou, N. E., Mant, C. T., Kirkland, J. J., and Hodges, R. S. (1991). Comparison of silica-based cyanopropyl and octyl reversed-phase packings for the separation of peptides and proteins. *J. Chromatogr.* **548**, 179-193.
- Zhou, N. E., Zhu, B. Y., Sykes, B. D., and Hodges, R. S. (1992). Relationship between amide proton chemical shifts and hydrogen bonding in amphipathic alpha-helical peptides. *J. Am. Chem. Soc.* **114**, 4320-4326.
- Zhou, N. E., Kay, C. M., Sykes, B. D., and Hodges, R. S. (1993). A single-stranded amphipathic alpha-helix in aqueous solution: design, structural characterization, and its application for determining alpha-helical propensities of amino acids. *Biochemistry* **32**, 6190-6197.
- Zhou, N. E., Kay, C. M., and Hodges, R. S. (1994a). The role of interhelical ionic interactions in controlling protein folding and stability. De novo designed synthetic two-stranded alpha-helical coiled-coils. *J. Mol. Biol.* **237**, 500-512.

- Zhou, N. E., Monera, O. D., Kay, C. M., and Hodges, R. S. (1994b). Alpha-helical propensities of amino acids in the hydrophobic face of an amphipathic α -helix. *Protein Peptide Lett.* **1**, 114-119.
- Zhu, B. Y., Mant, C. T., and Hodges, R. S. (1991). Hydrophilic-interaction chromatography of peptides on hydrophilic and strong cation-exchange columns. *J. Chromatogr.* **548**, 13-24.
- Zhu, B. Y., Mant, C. T., and Hodges, R. S. (1992). Mixed-mode hydrophilic and ionic interaction chromatography rivals reversed-phase chromatography for the separation of peptides. *J. Chromatogr.* **594**, 75-86.
- Zhu, P. L., Dolan, J. W., and Snyder, L. R. (1996a). Combined use of temperature and solvent strength in reversed-phase gradient elution II. Comparing selectivity for different samples and systems. *J. Chromatogr.* **756**, 41-50.
- Zhu, P. L., Dolan, J. W., Snyder, L. R., Hill, D. W., Van Heukelem, L., and Waeghe, T. J. (1996b). Combined use of temperature and solvent strength in reversed-phase gradient elution III. Selectivity for ionizable samples as a function of sample type and pH. *J. Chromatogr.* **756**, 51-62.

APPENDIX I

Capillary Zone Electrophoresis (CZE) of α -Helical Diastereomeric Peptide Pairs Using Anionic Ion-Pairing Reagents

A version of this chapter has been published: Popa, T. V., Mant, C. T., Chen, Y., and Hodges, R. S. (2004) *J. Chromatogr. A* **1043**, 113-122.

Abstract

The present study uses an unique capillary electrophoresis (CE) approach, that we have termed ion-interaction capillary zone electrophoresis (II-CZE), for the separation of diastereomeric peptide pairs where a single site in the centre of the non-polar face of an 18-residue amphipathic α -helical peptide is substituted by the 19 L- or D-amino acids. Through the addition of perfluorinated acids at very high concentrations (up to 400 mM), such concentration levels not having been used previously in chromatography or CE, to the background electrolyte (pH 2.0), we have been able to achieve baseline resolution of all 19 diastereomeric peptide pairs with an uncoated capillary. Since each diastereomeric peptide pair has the same sequence, identical mass-to-charge ratio and identical intrinsic hydrophobicity, such a separation by CZE has previously been considered theoretically impossible. Excellent resolution was achieved due to maximum advantage being taken of even subtle disruption of peptide structure/conformation (due to the presence of D-amino acids) of the non-polar face of the amphipathic α -helix and its interaction with the hydrophobic anionic ion-pairing reagents. In addition, due to the excellent resolution of diastereomeric peptide pairs by this novel CZE approach, we have also been able to separate a mixture of these closely-related α -helical peptides.

1. Introduction

The importance of efficient separation of peptide diastereomers should not be underestimated, since pharmaceutical applications of peptides are rapidly expanding, with approximately 35 peptides already being commercialized worldwide, 150-300 in the development stage and 20 in late development (Sutherland, 2003). Concerning regulation of stereochemistry issues, the detection (and quantitation) of diastereomeric and enantiomeric impurities are required by various regulatory agencies for pharmaceutical peptides. While reversed-phase high-performance liquid chromatography (RP-HPLC) is generally the favoured mode of separation for peptide mixtures (Mant *et al.*, 1991; Mant *et al.*, 2002), including peptide diastereomers (Chen *et al.*, 2002; Gazdag *et al.*, 1997; Koval *et al.*, 2003; Mant *et al.*, 1991), we believe that capillary electrophoresis (CE) may also have general utility for separation of such peptides.

In order to examine the ability of CE to resolve peptide diastereomers, we have now applied an unique capillary zone electrophoresis (CZE) approach, which we have termed ion-interaction CZE or II-CZE (Popa *et al.*, 2003; Popa *et al.*, 2004b), to the separation of 18-residue amphipathic α -helical diastereomeric peptide pairs employing aqueous solutions of perfluorinated acid ion-pairing reagents at high concentrations (up to 400 mM) as background electrolyte (BGE). This is in distinct contrast to their employment as anionic ion-pairing reagents for RP-HPLC, where acid concentrations are very low (generally *ca.* 10 mM; (Guo *et al.*, 1987; Mant *et al.*, 1991; Mant *et al.*, 2002)). The separation of such peptides with single diastereomeric substitutions of L- or D-amino acids in the centre of the non-polar face of the amphipathic α -helix is a challenging task for CE. Indeed, since each diastereomer not only has the same sequence but also

identical mass-to-charge ratio and intrinsic hydrophobicity, such a separation by conventional CZE has been considered theoretically impossible (Thorsteinsdottir *et al.*, 1995). Our results demonstrate the importance of this bidimensional separation mechanism we have proposed, whereby the CZE mode produced a separation of identically charged peptides with negligible secondary structure; within each charged group of peptides, the addition of perfluorinated acids at high concentration allowed resolution of the peptides through differences in peptide hydrophobicity (Popa *et al.*, 2003; Popa *et al.*, 2004b). Such a mechanism is unique to CZE, since the separations all occur within the mobile phase (BGE) in an uncoated capillary. We now wished to extend this novel CE approach to the separation of amphipathic α -helical peptide diastereomers. Although we have previously reported some success in separating such peptides with more traditional CE approaches (Popa *et al.*, 2004a), baseline resolution of all diastereomeric peptide pairs by a single CE approach was not achieved and was now a goal of the present study.

In addition to demonstrating the potential of this unique CE approach for separation of peptide diastereomers, we also wished to determine whether CE could, in a similar manner to RP-HPLC (Chen *et al.*, 2002; Kondejewski *et al.*, 1999; Lee *et al.*, 2003; Mant *et al.*, 2002; Mant *et al.*, 2003a; Mant *et al.*, 2003b), provide useful information for protein structure/function studies, *de novo* design of amphipathic α -helical antimicrobial peptides, and proteomics applications in general. For example, modulation of the amphipathicity/stability of α -helices by substitution of L/D amino acids into the centre of the hydrophobic face enables a quantitative assessment of the effects of such substitutions on such properties as molecular self-association, a key issue

both for structure/function (Kondejewski *et al.*, 2002; Lee *et al.*, 2003; Mant *et al.*, 2003a; Mant *et al.*, 2003b) and for the efficacy of potential peptide antimicrobials (Kondejewski *et al.*, 2002; Lee *et al.*, 2003; Mant *et al.*, 2003a; Mant *et al.*, 2003b). The peptide models described in the present study are particularly suited for such applications, as has already been demonstrated via their application in RP-HPLC (Chen *et al.*, 2002).

2. Experimental

2.1. Materials

Trifluoroacetic acid (TFA), pentafluoropropionic acid (PFPA) and heptafluorobutyric acid (HFBA) were obtained from Sigma/Aldrich. Lithium hydroxide was obtained from J.T. Baker (New Jersey, USA).

2.2. Solutions

Background electrolyte (BGE) solutions were prepared from the corresponding acids neutralized to pH 2.0 with lithium hydroxide.

2.3. Peptides

The amphipathic α -helical peptide diastereomers were synthesized by standard solid-phase synthesis methodology as described previously (Chen *et al.*, 2002). A synthetic peptide standard with the sequence Arg-Gly-Gly-Gly-Gly-Leu-Gly-Leu-Gly-Lys-amide (+3 net charge) (denoted S₂) was obtained from the Alberta Peptide Institute (University of Alberta, Edmonton, Alberta, Canada).

2.4. CE instrumentation and run conditions

All CE runs were carried out on a Beckman-Coulter P/ACE Capillary Electrophoresis System controlled by MDQ software (version 2.3). Uncoated capillaries

(50 μm I.D.) were provided by Beckman-Coulter; in all cases, the shorter aperture (100 x 200 μm) was used. The total capillary length, L_t , was 60.2 cm and the effective length (L_d , the length from the injection point to the detection point) was 50 cm. The capillary was thermostatted at 15°C, the lowest value allowed by the instrument. Peptides were detected at 195 nm by UV absorption with photodiode array (PDA).

Analyte apparent mobility was calculated by software according to Vigh's correction (Williams *et al.*, 1995) for voltage ramp (the time for the voltage to reach the programmed separation voltage; the voltage ramp time was 5 min). As a general rule, we recommend the increase of voltage ramp time until no further increase in current is registered at the end of ramp time. Resolution (R_s) was calculated according to USP (United States Pharmacopoeia) rules.

For sample preparation, peptides were dissolved in water and maintained at 6°C in the instrument storage compartment. Peptide concentration, injection time and pressure were adjusted to produce a signal of 10-30 mAU. The sample volume was 50-100 μl , with evaporation loss minimized by adding water to the vial supporting the sample PCR microvial. The sample plug was bracketed by a pre-sample plug of water (0.5 psi for 5 sec) and a post-sample plug of buffer (0.5 psi for 15 sec). The water plug implemented an on-line sample-preconcentration mechanism (Albin *et al.*, 1993) and the post-sample plug (together with the voltage ramp (Knox *et al.*, 1994)) prevented sample loss due to thermal expansion of the sample plug. High current and associated joule heat is generated during these separations, especially in the presence of perfluorinated acids. Bubble formation and subsequent loss of resolution is avoided by a suitable length of voltage ramp time and by a pressurized run, 50 psi generally being sufficient. In this way, we

were able to perform successful runs even at a current of 300 μ A (the maximum limit recommended by the instrument manufacturer). Injection conditions were always below 5 psi x 8s, such conditions already demonstrated to be well below conditions which may cause sample overloading effects (Popa *et al.*, 2003).

3. Results and discussion

3.1. Synthetic model peptides

The 18-residue model peptide used in the present study was based on the well-characterized sequence: Ac-EAEKAAKEAEKAAKEAEK-amide, known to exhibit a highly amphipathic α -helical structure (Sereda *et al.*, 1994; Zhou *et al.*, 1994) (Fig. 1). Alanine was selected to form the hydrophobic face of the helix since it contains the minimum side-chain hydrophobicity required to create an amphipathic α -helix and because of its high intrinsic helical propensity and stability contributions (Monera *et al.*, 1995; Zhou *et al.*, 1994). Lysine and glutamic acid allow a potential for α -helix stabilizing intrachain electrostatic attractions at the $i \rightarrow i+3$ and $i \rightarrow i+4$ positions at pH 7 (Scholtz *et al.*, 1993) (Fig. 1). All substituted model peptides were synthesized with N $^{\alpha}$ -acetylated and C $^{\alpha}$ -amidated termini to reduce the unfavourable dipole interactions of α -helical structure (Shoemaker *et al.*, 1987).

It has previously been shown (Zhou *et al.*, 1994) that this amphipathic α -helical model exhibits the following features: the helix is single-stranded and non-interacting, enabling determination of the effect of different amino acid substitutions in the non-polar face; there is a uniform environment created by alanine residues surrounding the substitution site in the centre of the non-polar face (position 9; denoted position X in Fig. 1); the small size of the alanine side-chain methyl group ensures minimal interactions

with the “guest” amino acid residues; and, finally, the small size of the peptide maximizes the effects of single amino acid substitutions. Two series of model peptide analogues were synthesized, where position 9 in the centre of the non-polar face was substituted either by each of the 19 L-amino acids (X_L series, *e.g.*, I_L denotes L-isoleucine substituted at position 9) or by the 19 D-amino acids (X_D series, *e.g.*, I_D denotes D-isoleucine substituted at position 9). It is important to note that the intrinsic hydrophobicity of the non-polar face of the amphipathic helix is identical for each enantiomeric peptide pair. Despite the inherent helix destabilizing properties of D-amino acids substituted into an α -helix made up entirely of L-amino acids (Aguilar *et al.*, 1993; Krause *et al.*, 2000; Rothmund *et al.*, 1995; Rothmund *et al.*, 1996), previous circular dichroism studies of the peptides used in the present study in both benign medium and in the presence of 50% trifluoroethanol (TFE; a helix-inducing solvent for peptides with potential α -helical conformation (Nelson *et al.*, 1989)) have shown that the presence of the D-amino acids still allows full folding in a hydrophobic environment (with the sole exception of L- or D-proline (Chen *et al.*, 2002)).

The 10-residue peptide standard (S2) described above represents a reference cationic peptide (+3 net charge) with negligible secondary structure (*i.e.*, a “random coil” peptide).

3.2. Approaches to CE separation of model diastereomeric peptide pairs

In a previous study (Popa *et al.*, 2004a), some success in separating these diastereomeric peptide pairs was achieved, particularly through the addition of CHAPS to the BGE and using an uncoated capillary (micellar electrokinetic chromatography; MEKC) or by using a C_8 -coated capillary in the presence of 25% TFE or 25% ethanol

(open-tubular capillary electrochromatography; OT-CEC). However, no one method was able to separate, to baseline, all 19 peptide pairs. Nonetheless, even the limited success of this previous study suggested an explanation for the separation of specific diastereomeric peptide pairs may lie in conformational differences in the analogues effected by a substitution of an L-amino acid by its D-amino acid counterpart (Chen *et al.*, 2002). Any disruption of the amphipathic α -helix in this way would also disrupt the hydrophobicity of the non-polar face, possibly allowing a separation of the peptide pair via the introduction of a hydrophobic mechanism.

An important observation from this previous study (Popa *et al.*, 2004a) was that the separation of specific diastereomeric peptide pairs in the absence of hydrophobic media (*e.g.*, CZE) showed the same general trend as their separations in the presence of hydrophobic media (*e.g.*, MEKC and OT-CEC), *i.e.*, diastereomers generated by hydrophobic amino acid substitutions were generally better separated than those generated by hydrophilic amino acids. In addition, the CE separation of cationic random coil peptide standards was practically the same in the presence or absence of organized hydrophobic media, the migration order being dictated by peptide hydrophobicity (Popa *et al.*, 2003; Popa *et al.*, 2004b). This separation of both helical (Popa *et al.*, 2004a) and random coil (Popa *et al.*, 2003; Popa *et al.*, 2004b) peptides in the absence of organized hydrophobic media (CZE), coupled with the lack of improvement of the separation of the cationic random coil peptides by the addition of alcohols (Popa *et al.*, 2003), supported the idea that an hitherto unidentified hydrophobically-mediated mechanism located in the BGE was operating in both cases. The possibility that such a mechanism may be introduced *via* the interaction of ions in the BGE arose from consideration of the

mechanism of phase transfer catalysis, where the ion-pairing strength of the catalyst depends on this reagent's hydrophobicity and/or polarizability. For example, hydrophobic quaternary ammonium salts (specifically the quaternary ammonium cation) transport anions from the aqueous to the organic phase; the more hydrophobic the ion-pairing quaternary ammonium salt (such as tetraoctylammonium > tetrabutylammonium > tetramethylammonium), the more efficient for specific catalyzed reactions. Adapting this concept to CE, if an ion-pairing (or, more generally, ion-ion interaction) effect was the unidentified hydrophobically-mediated mechanism which resulted in the aforementioned α -helical (Popa *et al.*, 2004a) and random coil (Popa *et al.*, 2003; Popa *et al.*, 2004b) separations, presumably it would be optimized by an increase in hydrophobicity and/or concentration of an ion-pairing reagent. We set out to test this speculation through the addition of perfluorinated acids to the BGE. Thus, trifluoroacetic acid (TFA), pentafluoropropionic acid (PFPA) and heptafluorobutyric acid (HFBA) represent a homologous series of increasingly hydrophobic (TFA < PFPA < HFBA) anionic ion-pairing reagents (Guo *et al.*, 1987; Mant *et al.*, 1991; Mant *et al.*, 2002).

3.3. CE of diastereomeric peptide pairs

Figs. 2 and 3 show the effect of increasing hydrophobicity and concentration of ion-pairing reagent on the separation of representative diastereomeric peptide pairs: A_D/A_L (Fig. 2) and D_D/D_L (Fig. 3). For these two peptide pairs, there is a general trend of improved separation of the peptide pairs with increasing hydrophobicity (TFA < PFPA < HFBA) and concentration of perfluorinated acid. Similar results were obtained, to a greater or lesser extent, with all pairs of peptide diastereomers (with the exception of the Pro analogues). The migration times of the peptides with L-substitutions were greater

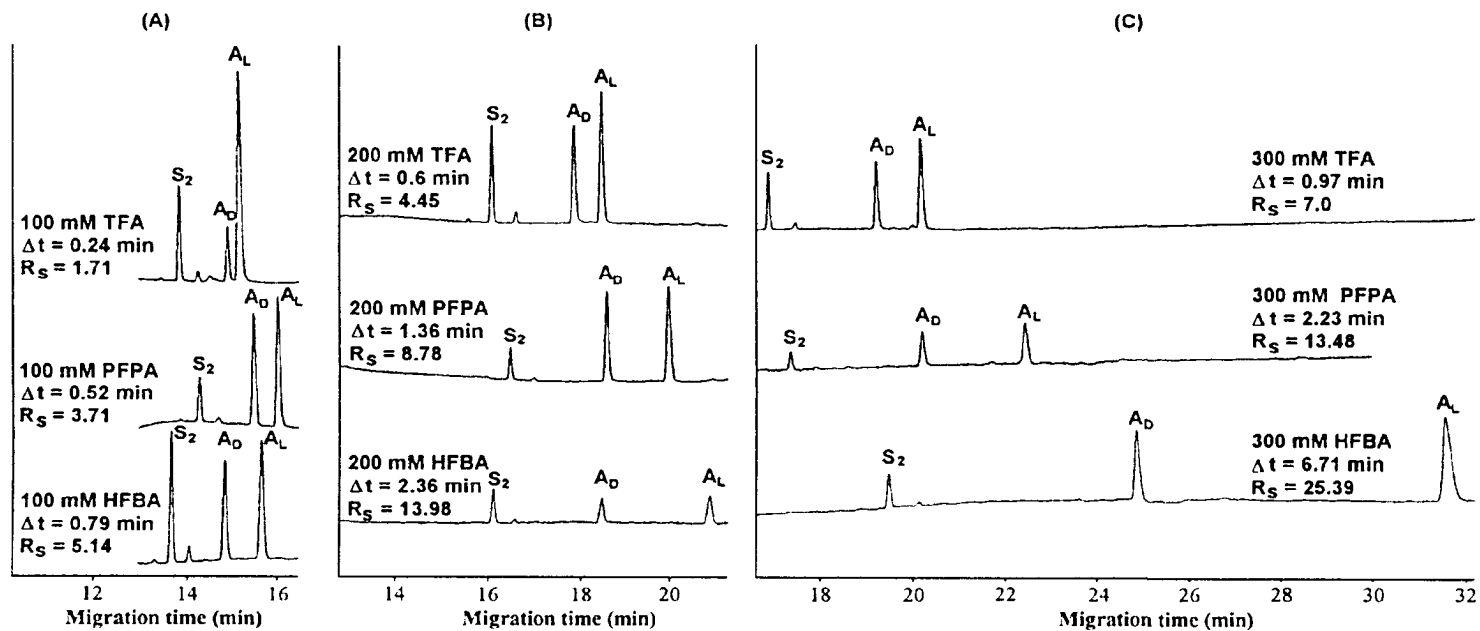


Figure 2 Effect of hydrophobicity and concentration of perfluorinated acids on CE separation of A_D/A_L diastereomeric peptide pair. Conditions: capillary, uncoated 60.2 cm (50 cm) \times 50 μ m i.d.; background electrolyte (BGE), various concentrations of *aq.* TFA, PFPA and HFBA, adjusted to pH 2.0 with lithium hydroxide; applied voltage, 25 kV (direct polarity) with 5 min voltage ramp; temperature, 15 $^{\circ}$ C; detection; UV absorption at 195 nm. The sequences of A_D and A_L are shown in Figure 1. S_2 represents a 10-residue random coil peptide standard. R_S and Δt denote resolution and difference in migration time, respectively, between the diastereomeric peptide pair.

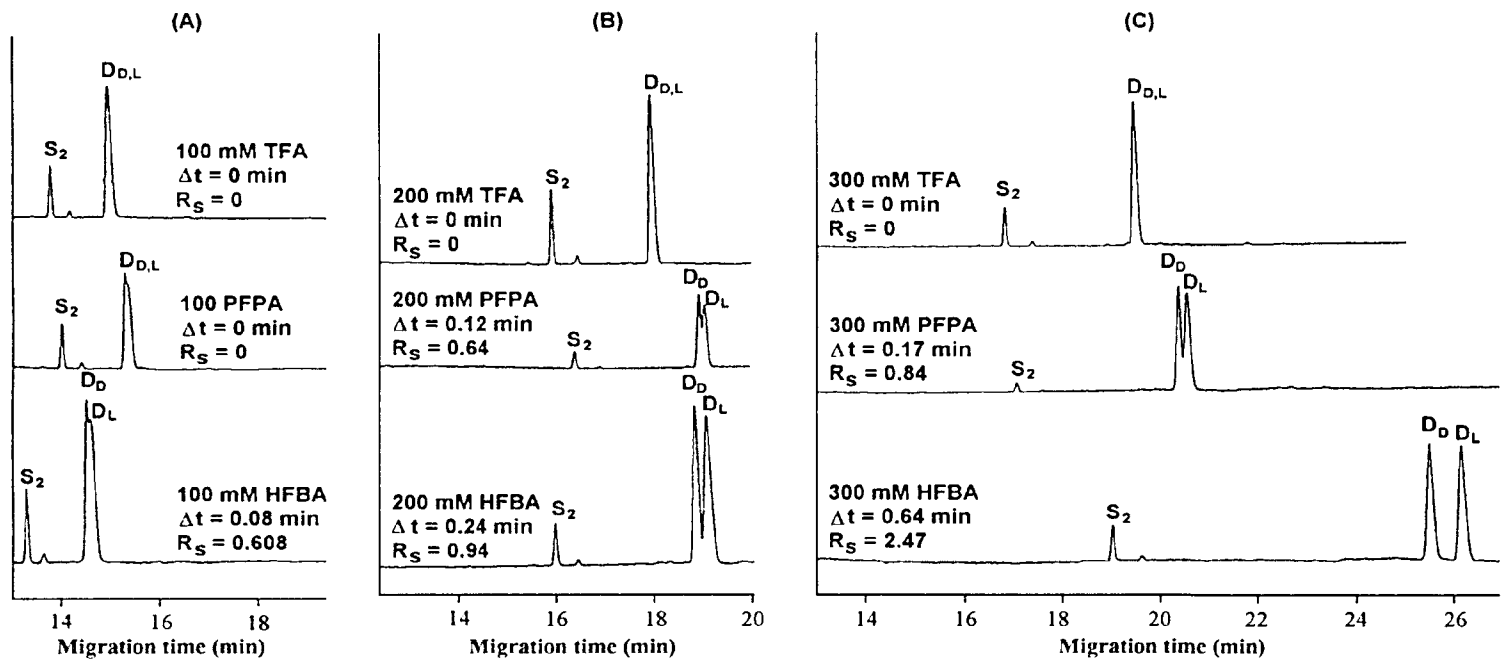


Figure 3 Effect of hydrophobicity and concentration of perfluorinated acids on CE separation of D_D/D_L diastereomeric peptide pair. Conditions and other details same as Figure 2. The sequences of D_D and D_L are shown in Figure 1.

than the peptides with the corresponding D-substitutions. In RP-HPLC, this can be explained by the disruption of the non-polar face by the D-amino acid substitution which decreases the retention time. Similarly, in CE the disruption of conformation likely affects BGE-analyte interactions, leading to a decrease in migration time. Under optimum conditions (300 mM HFBA), all 19 peptide pairs were separated to baseline (Table 1). Clearly the best results are obtained by the simultaneous increase in magnitude of both hydrophobicity and concentration. It should be noted that, at the concentrations used in the present study (100-400 mM), the perfluorinated acids are present essentially as salts, their pKa values being ~ 0.5 ; this is in contrast to RP-HPLC where the acid is traditionally employed at much lower concentrations (10 mM – 20 mM). It should also be noted that in a previous study (Popa *et al.*, 2004a), no significant differences in migration behaviour of these peptides was observed over a pH range of 2-4, indicating that intrachain ion-pairing did not play a role in the separation (due to protonation of the Glu side-chains). In the present study, we have chosen pH 2 to maximize the positive charge (and ion-ion interactions). In addition, this low pH also eliminates alternative explanations for our results, such as the aforementioned intrachain ion-pairing or variability in side-chain dissociation constants potentially caused by hydrophobically-induced peptide conformational changes.

Fig. 2, for the $A_{D,L}$ peptide pair, represents the best results which may be obtained for the majority of the peptide analogues generally and the substituted non-polar residues specifically. In contrast, Fig. 3 ($D_{D,L}$) and Fig. 4 ($P_{D,L}$) represent the most difficult peptide pairs to separate. For the $D_{D,L}$ peptide pair (Fig. 3), satisfactory resolution was only obtained with the most hydrophobic perfluorinated acid (HFBA) at a concentration

Table 1 Separation of X_{D,L} diastereomers by CZE using an uncoated capillary with 300mM HFBA as BGE

#	X _{D,L}	S ₂ reference		Migration time (min)		Migration time difference $\Delta t = (t_L - t_D)$ (min)	Resolution	Apparent selectivity $\times 100 = 2(t_L - t_D) / (t_L + t_D)$
		(t _R)	(t _L), X _L	Analyte (t _D), X _D	Analyte			
1	I	19.51	29.88	23.71		6.17	23.233	23.03
2	V	19.53	31.19	24.73		6.46	24.252	23.10
3	L	19.88	32.41	25.27		7.14	18.907	24.76
4	M	19.66	31.42	25.52		5.90	10.852	20.72
5	C	19.67	28.41	25.14		3.27	12.208	12.21
6	A	19.52	31.59	24.88		6.71	25.388	23.76
7	W	19.51	29.80	25.08		4.72	19.049	17.20
8	F	19.32	29.32	25.13		4.19	15.566	15.39
9	Y	19.42	29.22	25.02		4.20	11.005	15.49
10	T	19.27	26.95	24.39		2.56	9.016	9.97
11	S	19.16	27.16	24.32		2.84	8.757	11.03
12	Q	19.05	29.23	24.45		4.78	16.669	17.81
13	N	19.25	26.79	25.44		1.35	4.552	5.17
14	P	19.13	23.28	22.61		0.67	2.125	2.92
15	H	19.12	27.36	24.84		2.52	8.716	9.21
16	R	18.97	28.32	22.90		5.42	20.052	21.16
17	K	19.07	26.97	21.66		5.31	19.032	21.84
18	E	18.98	29.44	24.48		4.96	16.783	18.40
19	D	19.00	26.12	25.48		0.64	2.467	2.48

of 300 mM. The $P_{D,L}$ peptide pair (Fig. 4) represents an interesting phenomenon whereby the separation is practically independent of hydrophobicity and concentration of ion-pairing reagent. In order to examine whether peptide conformational changes potentially induced by the hydrophobic perfluorinated acids could be linked with this CE separation behaviour, circular dichroism (CD) spectra of peptides were measured in 150 mM HFBA at pH 2 and 15°C. For the peptide pairs shown in Figs. 2-4, absolute differences in mean molar ellipticity values between *L*- and *D*-diastereomers were in the order $A_{D,L} > D_{D,L} > P_{D,L}$ (both proline analogues exhibited random coil characteristics). Thus, even though some contribution from *D*- and *L*-analogue conformational differences may explain the difference in separation of the $A_{D,L}$ and $D_{D,L}$ and the other analogues shown in Table 1, this would be hard to reconcile with the behaviour of the P_D and P_L analogues (Fig. 4) which, although both exhibiting negligible secondary structure, are overall more easily separated than D_D and D_L (Fig. 3). However, as noted above, the behaviour of the Pro analogues appears to be the sole exception to the overall trend of effects of perfluorinated acids on the separation of the peptide pairs.

3.4. Effect of CE conditions on "apparent selectivity window" of diastereomeric peptide pairs

From Table 1, while the resolution represents a global characterization of separation quality, the selectivity of the separation is reflected in the difference in migration time of a particular diastereomeric peptide pair or, even better, by the apparent selectivity value. Apparent selectivity for the CE separations listed in Table 1 is defined as the ratio between the migration time difference to the mean migration time of the diastereomeric peptide pair (note that the values of apparent selectivity are multiplied by

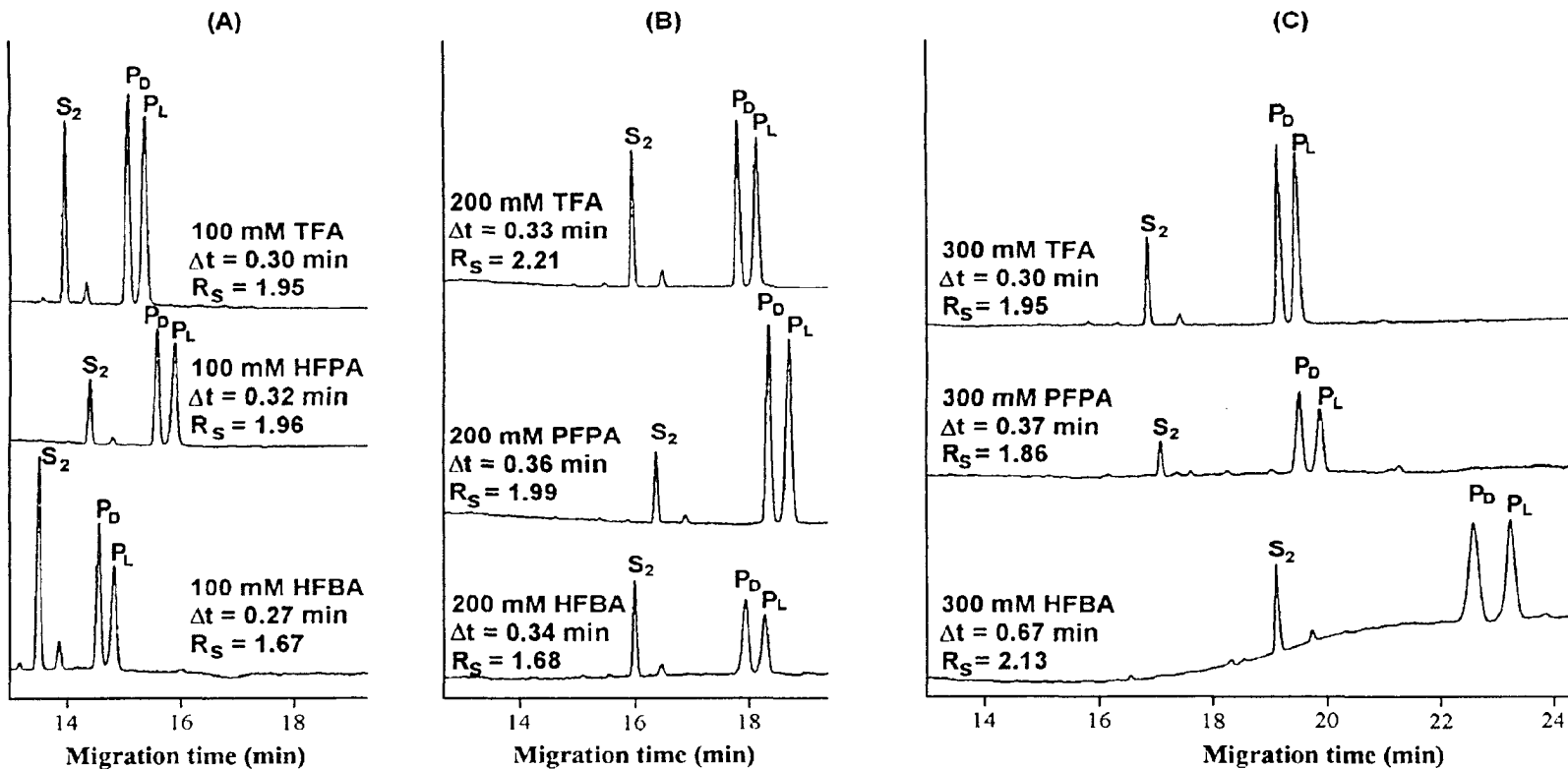


Figure 4. Effect of hydrophobicity and concentration of perfluorinated acids on CE separation of P_D/P_L diastereomeric peptide pair. Conditions and other details same as Figure 2. The sequences of P_D and P_L are shown in Figure 1.

100 for ease of comparison). Thus, an insight into the general trends of the effectiveness of the perfluorinated acids in the peptide separations may be obtained from a comparison of the apparent selectivities for the separation of all the peptide pairs under all conditions (Fig. 5). We are terming the range of apparent selectivity for all 19 peptide pairs under one set of experimental conditions as the “apparent selectivity window” for those conditions. From Fig. 5, it is clear that the selectivity window is expanding with increasing hydrophobicity and concentration of ion-pairing reagent, although this expansion is not linear, reflecting the different sensitivity of the peptide pairs to the twin optimization parameters. At first glance, the results of Fig. 5 reflect our earlier observation (Popa *et al.*, 2004a) that peptide pairs substituted with hydrophobic amino acids (e.g., Ile, Val, Leu, Met and Ala) are generally better resolved than hydrophilic residues (e.g., Ser, Thr, His, Asn). However, a closer examination shows that this is not a uniform observation, e.g., the hydrophilic (and charged) Lys and Arg residues exhibit apparent selectivities (21.84 and 21.16, respectively; Table 1) of a magnitude similar to hydrophobic amino acids listed above, whilst other hydrophobic residues, e.g., Trp, Tyr, Phe, exhibit more moderate, mid-range selectivities (17.2, 15.49, 15.39, respectively; Table 1). In addition, hydrophilic amino acids Gln and Glu also exhibit mid-range selectivities (17.81 and 18.4, respectively; Table 1). Interestingly, from Fig. 5, under optimum conditions (300 mM HFBA), there appear to be distinct groups of diastereomeric peptide pairs as expressed by the magnitude of their apparent selectivities and perhaps based on the character/structure of the side-chain and the ability as a D-amino acid to disrupt the non-polar face of the amphipathic α -helix :

Group 1: amongst side-chains with the highest selectivity are L, A, V, I and M, all non-polar amino acids containing alkyl side-chains; in addition, K and R are positively charged but also contain long, aliphatic side-chains.

Group 2: all three amino acids with aromatic side-chains (Y, W, F) are positioned in this group with the next highest selectivities; also, E and Q are polar, hydrophilic amino acids with aliphatic side-chains attached to the γ -carbon atom.

Group 3: this group is comprised of small, hydrophilic side-chains (C, S, T) or a bulky charged group close to the peptide backbone (H) (i.e., side chains attached to the β -carbon).

Group 4: the group with the lowest selectivities includes those amino acids containing polar, hydrophilic groups positioned close to the peptide backbone (N, D) and proline (P) with its cyclic, alkyl side-chain representing part of the peptide backbone.

Overall, it appears that a long n-alkyl side-chain should give the best possible separation. Any modification of this side-chain, such as branching or substitutions with charged, uncharged polar, or neutral groups, bulky or otherwise, decreases selectivity. Generally, the closer the modification to the peptide backbone, the more the decrease in selectivity. These observations remained constant even at higher concentrations (e.g., 350 mM – 400 mM) of HFBA (data not shown).

It is significant to note that there is a good general correlation between the magnitude of the apparent selectivity of the diastereomeric peptide pairs with the α -helical propensities of the L-analogues as determined by Zhou *et al.* (Zhou *et al.*, 1994).

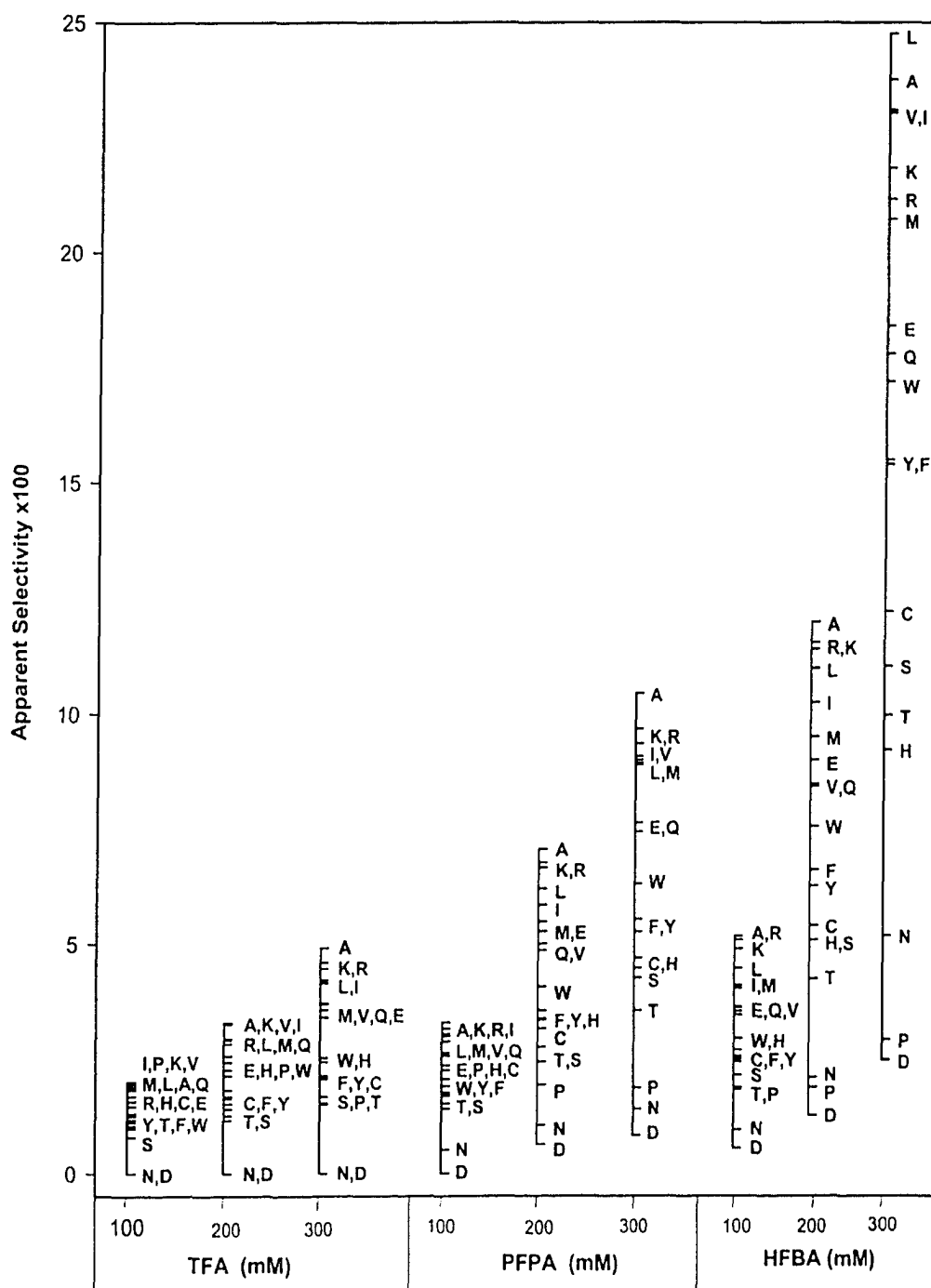


Figure 5 Effect of hydrophobicity and concentration of anionic ion-pairing reagents on apparent selectivity of CE of diastereomeric peptide pairs. Conditions described in Figure 2. Amino acid residues substituted into the centre of the hydrophobic face of the model peptides (Figure 1) are denoted by their one-letter code. Apparent selectivity between diastereomeric peptide pairs is expressed as $2(t_L - t_D)/(t_L + t_D)$, where t_L and t_D are the migration times of the l and d-amino acid substituted analogues, respectively.

For example, the L-analogues of A, R, L, K, M, I of Group 1 (highest selectivities) are amongst the strongest α -helix formers; in contrast, amino acids such as P and D of Group 4 (lowest selectivities) are α -helix disrupters. Thus, it seems reasonable to suggest that substitution of an L-amino acid with strong helix-inducing properties (e.g., alanine) with its D-amino acid counterpart would result in a much more significant disruption of secondary structure (and, hence, the apparent hydrophobicity of the non-polar face of the amphipathic α -helix) than that of a helix disrupter, e.g., D_L to D_D substitution, where the subsequent change in structure would be less. Overall, therefore, the difference in apparent hydrophobicity between the non-polar faces of such analogues as A_L and A_D would be significantly greater than between analogues such as D_L and D_D. Such observations support the view that conformational differences between diastereomeric peptide pairs do, indeed, contribute to the baseline separations presented in this study as well as the ability to resolve more complex mixtures of such peptides (shown below).

3.5. CE of a mixture of diastereomeric peptide pairs

Fig. 6 clearly illustrates the excellent CE separation of a mixture of peptide diastereomers which may be obtained through an increase in HFBA concentration. This particular peptide mixture is comprised of analogues substituted with potentially charged side-chains. However, at pH 2.0, the side-chains of Glu and Asp will be uncharged; (overall net charge of +5 on the peptides), while those of Lys, Arg and His will be charged (overall net charge of +6 on the peptides). In comparison with 300 mM HFBA (Table 1), apparent selectivities between diastereomeric peptide pairs are continuing to increase with increasing HFBA concentration to 400 mM HFBA. These values now are 2.49, 12.66, 25.55, 28.41 and 29.72 for D_D/D_L, H_D/H_L, E_D/E_L, R_D/R_L and K_D/K_L,

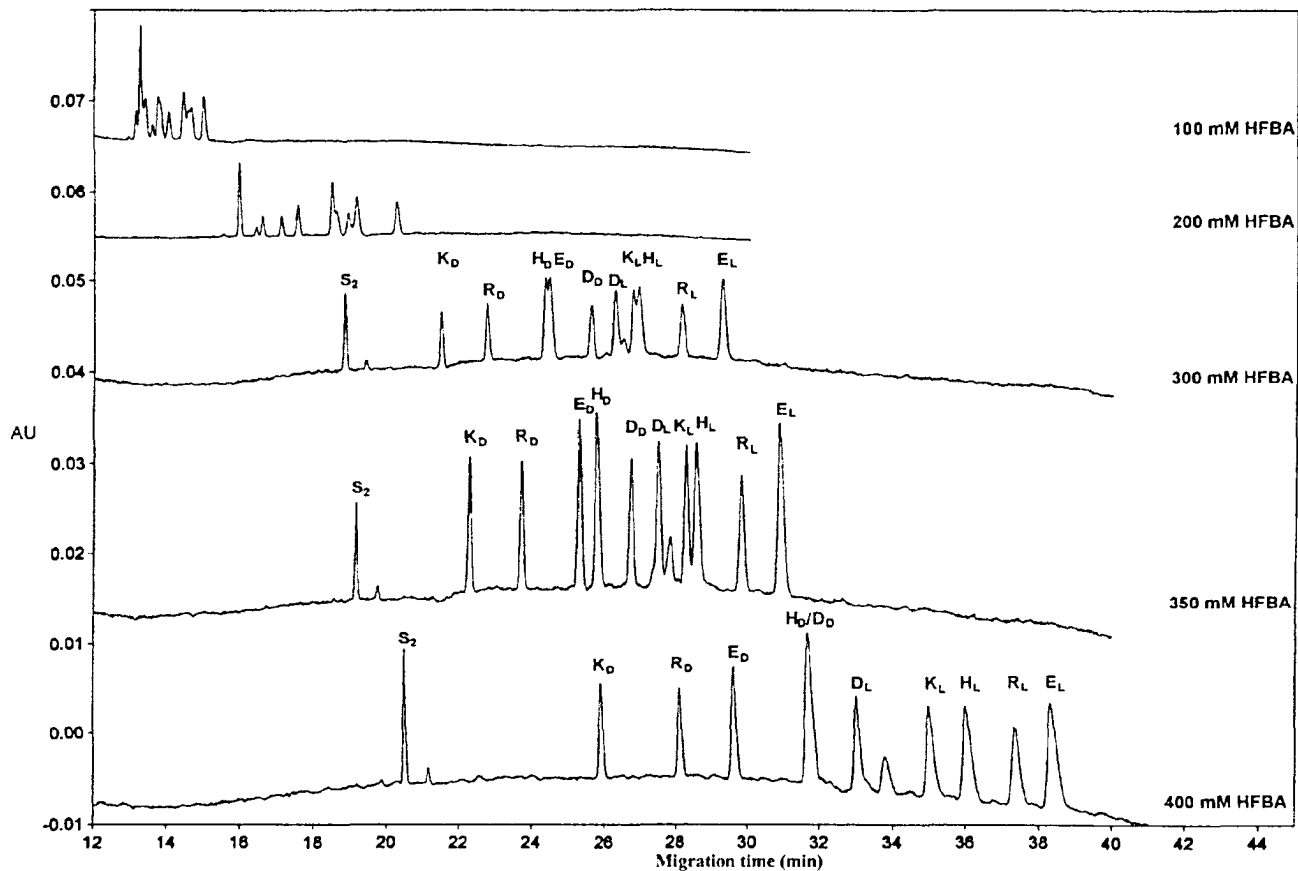


Figure 6 Effect of HFBA on CE separation of a mixture of diastereomeric peptide pairs. Conditions same as Figure 2, with BGE represented by various concentrations of *aq.* HFBA, adjusted to pH 2.0 with lithium hydroxide. The sequences of the peptide are shown in Figure 1. S2 represents a 10-residue random coil peptide standard. The peak between D_L and K_L is an impurity.

respectively, compared to 2.48, 9.21, 18.40, 21.16 and 21.84, respectively, in 300 mM HFBA (Table 1). An interesting observation from Fig. 6 is the difference in selectivity of the peptide separation at different HFBA concentrations due to the migration behaviour of the His-substituted analogues, which migrate relatively faster with increasing HFBA concentration relative to the other analogues. Thus, at 300 mM HFBA, H_D migrates just prior to E_D as a poorly separated doublet; at 350 mM HFBA, H_D is now baseline resolved from E_D and has a longer migration time than the latter analogue; finally, at 400 mM HFBA, H_D comigrates with D_D, albeit even better separated from E_D. Similarly, at 300 mM HFBA, H_L migrates a little longer than K_L, albeit as a poorly separated doublet; at 350 mM HFBA, H_L is almost baseline resolved from K_L; finally, at 400 mM HFBA, H_L is now well resolved from K_L, its migration time significantly longer than the latter analogue.

3.6 Differences in the mechanism of separation of peptides between RP-HPLC and ICZE in the presence of anionic ion-pairing reagents

Anionic ion-pairing reagents have seen widespread use for peptide separations in RP-HPLC for over two decades (Guo *et al.*, 1987; Mant *et al.*, 1991; Mant *et al.*, 2002). Aside from their high hydrophobicities, these reagents have the advantage of low pK_a values, enabling their use at low pH values (*e.g.*, pH 2.0), thus maximizing the positive charge on peptides. Their mode of action is via interactions between the negatively charged anions of these reagents (TFA⁻, PFPA⁻, HFBA⁻) and positively charged groups, in the peptide sequence (lysine, arginine, histidine side-chains; free α -amino group). The greater the net positive charge on the peptide, the greater the effect of a particular hydrophobic ion-pairing reagent, which subsequently translates into longer RP-HPLC

elution times (Guo *et al.*, 1987). Increasing concentrations of such ion-pairing reagents also serve to increase RP-HPLC retention times of positively charged peptides (Guo *et al.*, 1987). Note that such increases in peptide retention times via increasing hydrophobicity (TFA < PFPA < HFBA) and/or concentration of ion-pairing reagent reflect an increase in effective hydrophobicity of the peptides, *i.e.*, modulation of the overall hydrophobicity of the peptides through manipulation of the mobile phase. Thus peptides with a high number of positively charged groups become much more hydrophobic than peptides with few charged groups. However, although changes in ion-pairing reagent and/or concentration affects the relative elution order of peptides, it is the hydrophobicity of the reversed-phase matrix that separates the peptides based on differences in overall peptide hydrophobicity, *i.e.*, the more hydrophobic the peptide, the greater the affinity of the peptide for the stationary phase.

Note that, for RP-HPLC separations, two phases are required to achieve peptide separations based on differences in peptide hydrophobicity, *i.e.*, the aqueous mobile phase and the hydrophobic stationary phase. Here we are suggesting a quite distinct mechanism for II-CZE (which remains a working hypothesis for further studies), where we are able to exploit the hydrophobicity differences between peptides within a single phase, *i.e.*, the BGE, since CZE separations are taking place within an uncoated capillary. We believe the key to success of the II-CZE approach lies in providing a hydrophobic medium within the BGE substantial and uniform enough to separate peptides based on their different affinities for this hydrophobic environment. Thus, the use of hydrophobic anionic ion-pairing reagents such as HFBA increases the hydrophobic environment of the solution to a level where interaction of the peptides with this hydrophobic BGE is able to

separate the peptides based on just subtle differences in peptide hydrophobicity. In other words, the hydrophobicity of the high concentrations of ion-pairing reagents (approximately 40-fold higher than those used in RP-HPLC) replaces the hydrophobic matrix of RP-HPLC, *i.e.*, the separation in II-CZE is effected through the interaction or affinity of the peptides for the hydrophobic environment created in the BGE by the high concentrations of perfluorinated acids. It is important to note that, although we term this approach “ion-interaction” CZE, this does not imply that the ion-pairing property of the acids represent the critical factor in successful peptide separations by this method. Rather, it refers to interactions between the peptides and perfluorinated anions within the single phase BGE, albeit the critical interactions are between the hydrophobic groups in the peptides and the hydrophobic component of the anions. Certainly, the negatively charged anions are able to interact electrostatically with the positively charged cationic groups of the peptides; however, at the very high concentrations of acids used in II-CZE, this ion-pairing factor is negligible compared to the overwhelming influence of the hydrophobic environment of the BGE on peptide separations engendered by such concentrations. Support for this view lies in our previous success in using II-CZE to separate three groups (+1, +2 or +3 positive charges) of random coil peptides with identical substitutions of hydrophobic amino acids within their sequences (Popa *et al.*, 2004b). Thus, for example, a substitution of a Val for the less hydrophobic Ala produced the same increase in migration time for the former analogue compared to the latter no matter within what charged group of peptides such a substitution had been made, *i.e.*, the affinity for the hydrophobic solution phase produced by the high concentrations of anionic ion-pairing reagents is simply greater for the Val-substituted peptide compared to

the Ala-substituted analogue, with no or negligible impact of ion-pairing between the peptides and the ion-pairing reagents. In a similar fashion, in the present study, separations between diastereomeric peptide pairs are achieved by differing affinities of the non-polar faces of the amphipathic peptides (resulting from the change in apparent overall hydrophobicity of this face following an L- to D-amino acid substitution) for the hydrophobic environment of the BGE.

4. Conclusions

The present study demonstrates a novel CE approach to separate, in the absence of organic solvents, peptides of identical sequence, mass-to-charge ratio and inherent hydrophobicity, differing only in a single L- to D-amino acid substitution. We attribute this success primarily to a hydrophobic mechanism effected through the use of extremely high concentrations of perfluorinated acid anionic ion-pairing reagents and suggest terming this CE mode as ion-interaction capillary zone electrophoresis (II-CZE). In addition, we also believe that conformational differences between diastereomeric peptide pairs also contribute significantly to the successful separations, where the differences in hydrophobicity of the non-polar face of the amphipathic α -helix and its interaction with the hydrophobic anionic ion-pairing reagent is effecting the separation. Although small racemic or diastereomeric peptides have been previously separated by CE methodology, such approaches generally depend on additives to the BGE where bulky substituents form a complex with the peptides, such complexes then being separated, or where peptides are derivatized (i.e., chemically modified) prior to separation (references (Wan *et al.*, 1997; Wan *et al.*, 2000) represent useful introductions to such methods). In contrast, the present study represents the first instance where such manipulations are unnecessary, requiring

only a selective interaction of unmodified peptides with the counterion provided by the BGE. Indeed, we believe that the present results represent a starting point for developing CE methods for the pharmaceutical and life sciences fields, including proteomic applications. In addition, the separation of diastereomers allows a rigorous assessment of the resolving power of CE in general as well as that of specific CE instrumentation.

Acknowledgement

This work was supported by an NIH grant (RO1GM61855) to Robert S. Hodges.

References

- Aguilar, M. I., Mougos, S., Boublik, J., Rivier, J., and Hearn, M. T. (1993). High-performance liquid chromatography of amino acids, peptides and proteins. CXXVIII. Effect of D-amino acid substitutions on the reversed-phase high-performance liquid chromatography retention behaviour of neuropeptide Y[18-36] analogues. *J. Chromatogr.* **646**, 53-65.
- Albin, M., Grossman, P. D., and Moring, S. E. (1993). Sensitivity enhancement for capillary electrophoresis. *Anal. Chem.* **65**, 489A-496A.
- Chen, Y., Mant, C. T., and Hodges, R. S. (2002). Determination of stereochemistry stability coefficients of amino acid side-chains in an amphipathic alpha-helix. *J. Pept. Res.* **59**, 18-33.
- Gazdag, M., Mihályfi, K., and Görög, S. (1997). Ion-pair RP-HPLC separation of thymopietin fragments and related peptides. *Analytica Chimica Acta* **352**, 231-237.
- Guo, D. C., Mant, C. T., and Hodges, R. S. (1987). Effects of ion-pairing reagents on the prediction of peptide retention in reversed-phase high-performance liquid chromatography. *J. Chromatogr.* **386**, 205-222.
- Knox, J. H., and McCormack, K. A. (1994). Volume expansion and loss of sample due to initial self-heating in capillary electrophoresis (CES) systems. *Chromatographia* **38**, 279-282.
- Kondejewski, L. H., Jelokhani-Niaraki, M., Farmer, S. W., Lix, B., Kay, C. M., Sykes, B. D., Hancock, R. E., and Hodges, R. S. (1999). Dissociation of antimicrobial and hemolytic activities in cyclic peptide diastereomers by systematic alterations in amphipathicity. *J. Biol. Chem.* **274**, 13181-13192.
- Kondejewski, L. H., Lee, D. L., Jelokhani-Niaraki, M., Farmer, S. W., Hancock, R. E., and Hodges, R. S. (2002). Optimization of microbial specificity in cyclic peptides by

- modulation of hydrophobicity within a defined structural framework. *J. Biol. Chem.* **277**, 67-74.
- Koval, D., Kaika, V., Jiráek, J., and Collinsová, M. (2003). Separation of diastereomers of phosphinic pseudopeptides by capillary zone electrophoresis and reverse phase high-performance liquid chromatography. *J. Sep. Sci.* **26**, 653-660.
- Krause, E., Bienert, M., Schmieder, P., and Wenschuh, H. (2000). The Helix-Destabilizing Propensity Scale of D-Amino Acids: The Influence of Side Chain Steric Effects. *J. Am. Chem. Soc.* **122**, 4865-4870.
- Lee, D. L., Mant, C. T., and Hodges, R. S. (2003). A novel method to measure self-association of small amphipathic molecules: temperature profiling in reversed-phase chromatography. *J. Biol. Chem.* **278**, 22918-22927.
- Mant, C. T., and Hodges, R. S., eds. (1991). HPLC of peptides and proteins: separation, analysis and conformation (Boca Raton, FL, CRC Press).
- Mant, C. T., and Hodges, R. S. (2002). Analytical HPLC of Peptides. In *HPLC of biological macromolecules*, Gooding, K. M., and Regnier, F. E., eds. (New York, Marcel Dekker), pp. 433-511.
- Mant, C. T., Chen, Y., and Hodges, R. S. (2003a). Temperature profiling of polypeptides in reversed-phase liquid chromatography. I. Monitoring of dimerization and unfolding of amphipathic alpha-helical peptides. *J. Chromatogr. A* **1009**, 29-43.
- Mant, C. T., Tripet, B., and Hodges, R. S. (2003b). Temperature profiling of polypeptides in reversed-phase liquid chromatography. II. Monitoring of folding and stability of two-stranded alpha-helical coiled-coils. *J. Chromatogr. A* **1009**, 45-59.
- Monera, O. D., Sereda, T. J., Zhou, N. E., Kay, C. M., and Hodges, R. S. (1995). Relationship of side-chain hydrophobicity and α -helical propensity on the stability of the single-stranded amphipathic α -helix. *Journal of peptide science* **1**, 319-329.
- Nelson, J. W., and Kallenbach, N. R. (1989). Persistence of the alpha-helix stop signal in the S-peptide in trifluoroethanol solutions. *Biochemistry* **28**, 5256-5261.
- Popa, T. V., Mant, C. T., and Hodges, R. S. (2003). Capillary electrophoresis of synthetic peptide standards varying in charge and hydrophobicity. *Electrophoresis* **24**, 4197-4208.
- Popa, T. V., Mant, C. T., and Hodges, R. S. (2004a). Capillary electrophoresis of amphipathic alpha-helical peptide diastereomers. *Electrophoresis* **25**, 94-107.
- Popa, T. V., Mant, C. T., and Hodges, R. S. (2004b). *Electrophoresis*, submitted.
- Rothmund, S., Beyermann, M., Krause, E., Krause, G., Bienert, M., Hodges, R. S., Sykes, B. D., and Sonnichsen, F. D. (1995). Structure effects of double D-amino acid replacements: a nuclear magnetic resonance and circular dichroism study using amphipathic model helices. *Biochemistry* **34**, 12954-12962.
- Rothmund, S., Krause, E., Beyermann, M., Dathe, M., Bienert, M., Hodges, R. S., Sykes, B. D., and Sonnichsen, F. D. (1996). Peptide destabilization by two adjacent D-amino acids in single-stranded amphipathic alpha-helices. *Pept. Res.* **9**, 79-87.

- Scholtz, J. M., Qian, H., Robbins, V. H., and Baldwin, R. L. (1993). The energetics of ion-pair and hydrogen-bonding interactions in a helical peptide. *Biochemistry* **32**, 9668-9676.
- Sereda, T. J., Mant, C. T., Sonnichsen, F. D., and Hodges, R. S. (1994). Reversed-phase chromatography of synthetic amphipathic alpha-helical peptides as a model for ligand/receptor interactions. Effect of changing hydrophobic environment on the relative hydrophilicity/hydrophobicity of amino acid side-chains. *J. Chromatogr. A* **676**, 139-153.
- Shoemaker, K. R., Kim, P. S., York, E. J., Stewart, J. M., and Baldwin, R. L. (1987). Tests of the helix dipole model for stabilization of alpha-helices. *Nature* **326**, 563-567.
- Sutherland, L. (2003). *Gen. Eng. News* **13**, 1.
- Thorsteinsdottir, M., Beijersten, I., and Westerlund, D. (1995). Capillary electroseparations of enkephalin-related peptides and protein kinase A peptide substrates. *Electrophoresis* **16**, 564-573.
- Wan, H., and Blomberg, L. G. (1997). Enantiomeric and diastereomeric separation of di- and tripeptides by capillary electrophoresis. *J. Chromatogr. A* **758**, 303-311.
- Wan, H., and Blomberg, L. G. (2000). Chiral separation of amino acids and peptides by capillary electrophoresis. *J. Chromatogr. A* **875**, 43-88.
- Williams, B., and Vigh, G. (1995). Effect of the Initial Potential Ramp on the Accuracy of Electrophoretic Mobilities in Capillary Electrophoresis. *Anal. Chem.* **67**, 3079-3081.
- Zhou, N. E., Monera, O. D., Kay, C. M., and Hodges, R. S. (1994). Alpha-helical propensities of amino acids in the hydrophobic face of an amphipathic a-helix. *Protein Peptide Lett.* **1**, 114-119.